

**The Petrology of the Merensky Cyclic Unit and Associated Rocks
and their Significance in the Evolution of the
Western Bushveld Complex**

by

Floris Johan Kruger
B.Sc.(Hons) (Natal), M.Sc. (Rhodes).

Thesis submitted in fulfilment
of the requirements for the degree of

Doctor of Philosophy

in the Department of Geology at
Rhodes University
Grahamstown

December, 1982

The clearest statement on the new position was from Sir Henry:

"The person giving the exercise reasonable care that the information to another whom he knows will rely upon in circumstances in which it is reasonable for him to do so, is under a duty to information given is correct."

Punch "Country Life" 9th June, 1982.

TABLE OF CONTENTS

<u>CHAPTER ONE: Introduction and Review</u>	1
<u>Introduction</u>	1
<u>The Origin of the Bushveld Complex: A Thematic Review</u>	2
<u>Hypotheses Concerning the Merensky Cyclic Unit</u>	5
<u>Developments in the Interpretation of Layered Intrusions</u>	6
<u>Objectives of this Work</u>	8
<u>CHAPTER TWO: Field Relationships, Petrography and Petrochemistry</u>	9
<u>Introduction</u>	9
Petrographic Classification	9
Stratigraphic Nomenclature	11
<u>Field Relationships</u>	12
Introduction	12
The Footwall Unit	13
The Merensky Cyclic Unit	14
The Bastard Cyclic Unit	16
Potholes and Koppies	17
The Ultramafic Pegmatites	20
The Acid Pegmatites	21
<u>Petrography</u>	21
Introduction	21
Mottled Anorthosite	22
Norite	24
Pyroxenite	25
Pegmatoid	26
Ultramafic Pegmatite	26

<u>Chemistry of Rocks and Minerals</u>	27
Strontium Isotope Data of Rocks and Minerals	27
Whole Rock Chemistry of the Merensky Cyclic Unit	27
Electron Microprobe Analyses of Minerals	28
Chemistry of the Plagioclase Separates	33
Chemistry of the Pyroxene Separates	33
<u>A Qualitative Assessment of Equilibria and an Evaluation of</u>	
<u>Selected Samples in the Study Section</u>	37
General Discussion	37
M-8: Zoning of Orthopyroxene	40
F-13 & F-15: Disequilibrium and Equilibrium	41
B-15: Disequilibrium or Isolation of Interstitial	
Minerals or Liquids	42
B-26 & B-30: Disequilibrium with Exsolution	43
<u>Summary and Conclusion</u>	44
<u>CHAPTER THREE: Physical Processes</u>	45
<u>Introduction</u>	45
<u>Physical Processes of Magmatic Differentiation</u>	46
Introduction	46
Crystal Settling	46
In Situ Crystallization and Double-Diffusive Convection	48
Interrelationships Between the Liquidus, Subliquidus and	
Solidus Stages	54
Replenishment of a Differentiating Intrusion	55
Wallrock Assimilation and Contamination	58
Trace Element and Isotopic Mixing and Diffusion	59
Addition of Fluid Phases from Below	59

<u>Physical Processes in the Bushveld Magma Chamber Recorded in the</u>	
<u>Study section</u>	60
Introduction	60
Strontium Isotope Data and the Identification	
of a New Magma Influx	62
Other Magma Influxes into the Rustenburg Layered Suite	
Magma Chamber	68
Mineralization at the Base of the Merensky Cyclic Unit	69
<u>Summary</u>	70
<u>CHAPTER FOUR: The Subliquidus Stage</u>	72
<u>Introduction</u>	72
<u>The Initial Interstitial Liquid and Primocrysts:</u>	
<u>A Qualitative Discussion</u>	73
<u>The Determination of the Composition of the Liquidus Primocrysts</u>	
<u>and Associated Parental Liquids which Crystallized as a</u>	
<u>Closed System</u>	74
Introduction	74
Selection of Samples and the determination of Initial	
Primocryst and Liquid Compositions	76
Selection and use of Major Component Distribution Coefficients	77
Determination of Major Element Compositions and Proportions	
of Phases	79
Trace Element Partitioning Between Phases	80
<u>Application to the Merensky Cyclic Unit</u>	80
Conclusions	82
<u>Sintering and Infiltration Metasomatism</u>	83
Introduction and Discussion of Irvine's Model	83
Sintering as a Petrological Process	83
Sintering and Infiltration Metasomatism in the Study Section	85

<u>The Behavior of Volatile Components in the Crystal Mush</u>	87
Introduction	87
The Merensky Pegmatoid	87
The Origin of Potholes	88
The Origin of Ultramafic Pegmatites	89
Conclusion	90
<u>Summary</u>	90
<u>CHAPTER FIVE: The Liquidus Stage</u>	91
<u>Introduction</u>	91
<u>Fractional Crystallization in Layered Rocks: General Principles</u>	91
The General Principles	91
Estimating the Thickness of Double-Diffusive Convection Layers	93
Fractional Crystallization with Interstitial Liquid	94
<u>Applications to the Study Section</u>	96
The Merensky Cyclic Unit	96
The Bastard Cyclic Unit	99
<u>Limitations and Problems</u>	99
<u>Summary and Conclusions</u>	100
<u>CHAPTER SIX: Summary and Conclusions</u>	101
<u>The Evolution of the Study Section: a Resumé</u>	101
The Physical Processes	101
The Liquidus Processes	101
The Subliquidus Processes	102
Solidus and Subsolidus Processes	103
Conclusion	103

<u>The Formation of the Bushveld Complex: Unification of Models</u>	103
<u>The Composition and Origins of the Bushveld Complex Magmas</u>	104
The Composition of the Primary Magmas	105
<u>REFERENCES</u>	108

ACKNOWLEDGEMENTS

This thesis contains many things besides that which its title and contents suggest. It contains some three and a half years of trials and tribulations on the one hand and many hours of pleasure, inspiration and discussion to balance the equation on the other. Many individuals and organizations have contributed to this mixture of visible and invisible human experience.

Dr. J.S. Marsh supervised this work and I am grateful for his guidance and the time he could spare. His work on the strontium isotopes in the laboratory of Chris Hawkesworth in the Department of Earth Sciences at the Open University was particularly fruitful. Long hours of discussion over many cups of tea with Prof. H.V. Eales and Dr. I.M. Reynolds helped to clarify my thinking on many subjects. My fellow research students Mike Botha, Andrew Mitchell, Roger Scoon, and Mike and Teral Bowen also contributed to my tea-time experience. Other members of staff Prof. R.E. Jacob, Dr. N. Hiller and Prof. R. Mason have also helped me in various ways, not necessarily geological.

Dennis Gouws assisted me a great deal with the gathering of probe data, and his cheerful help with a sometimes fractious machine is gratefully acknowledged.

Drs. T.S. McCarthy and R.G. Cawthorn of the University of the Witwatersrand, Dr. D.L. Buchanan of the Imperial College, Mike Watkeys, Jay Hodges, Trevor Elworthy and the other participants of the "Great Geology Field Trip" of the Wits. Geology Department are thanked for a most enjoyable and useful experience.

The Geological staff of Rustenberg Platinum Mines (Rustenberg Section) contributed greatly to my knowledge of the Merensky unit and its environs, the peculiarities of potholes and mine stratigraphy. I would especially like to thank John Barry for giving me the benefit of his many years of experience and study of the platinum mines. I am also indebted to Dr. Chris Lee and Dr. M.J. Viljoen for many discussions of Bushveld Complex problems.

The Johannesburg Consolidated Investment Co. contributed access to their mines and financial support without which this work could not have been done.

A three year post MSc.(Doctoral) grant from the CSIR made this work possible and I gratefully acknowledge their contribution.

Bill van Graan and International Computers Ltd. in Cape Town allowed me to use their ICL 7700 word processor free of charge.

My wife Dianne who gave me encouragement in times of frustration and calmness in times of stress. I also thank her for typing this work and for helping to draft the figures.

ABSTRACT

A brief review of the various models proposed to account for the Bushveld Complex shows that there are two main hypotheses. These are the Multiple Intrusion hypothesis and the In Situ Crystallization hypothesis. The latter also allows for multiple additions to the crystallizing magma, and several variants involving the number of these inputs, their composition, volume and timing have been proposed.

To facilitate description and investigation of the study section, the stratigraphic nomenclature of this part of the Rustenberg Layered Suite is revised and clarified. It is proposed that the boundary between the Critical Zone and Main Zone be placed at the base of the Merensky cyclic unit, and thus the whole of the Merensky and Bastard cyclic units are included in the Main Zone.

Furthermore, the extremely confused terminology for smaller units within the Merensky and Bastard cyclic units is resolved by discarding the term Reef as a formal term and substituting lithological terms such as Merensky pegmatoid, Merensky pyroxenite, Bastard pyroxenite and Merensky mottled anorthosite etc. It is recommended that the term Reef be retained as an informal term to designate the mineralized horizon which may be mined, regardless of lithology. The term "pegmatoid" is restricted to stratiform or lensoid masses of coarse grained feldspathic pyroxenite or harzburgite which are part of the layered sequence. The transgressive vertical pipe-like, coarse-grained ultramafic iron-rich bodies are termed "ultramafic pegmatites".

The main features of the Merensky and Bastard cyclic units are the regular chemical and mineralogical changes that occur with respect to stratigraphic height in these units. In the Merensky cyclic unit there is a smooth iron enrichment in the orthopyroxenes upward in the succession and a transition from pyroxenite at the base to mottled anorthosite at the top of the unit. The Bastard cyclic unit is broadly similar to the Merensky cyclic unit. A variety of textures and chemical features are in disequilibrium in some samples but not in others, and great complexity is evident when individual samples are studied in detail.

The initial $^{87}\text{Sr}/^{86}\text{Sr}$ ratios of plagioclase separates and whole rocks from the study section show a distinct step-like increase in the ratio from .70661 at the base of the Merensky cyclic unit to .70806 at the base of the Bastard cyclic unit. In contrast, samples from below the

Merensky cyclic unit have a constant initial Sr-isotopic ratio, as do the samples from the Bastard cyclic unit.

These isotopic and chemical data, and available published geologic relationships suggest that a major new influx of basic magma occurred after the Footwall unit was deposited and that this mixed with the residual magma in the chamber and then precipitated the Merensky and Bastard cyclic units.

The crystal settling theory as outlined by Wager and Brown (1968) fails to account for the chemical and stratigraphic variations observed in the study section. The theory of bottom crystallization, initially proposed by Jackson (1961), more adequately explains the features observed. Applying a model outlined by Irvine (1980a & b), it has been established from chemical data, that the Merensky cyclic unit crystallized from a magma layer with a thickness roughly equivalent to the average thickness of the cyclic unit itself ($\pm 10\text{m}$). A similar exercise on the Bastard unit was not possible. The formation of the Footwall unit is still enigmatic.

Infiltration metasomatism and sintering can modify the petrographic and chemical characteristics of rocks and minerals after deposition at the liquidus stage. During the solidification of the crystal mush a separate vapour phase may form in the crystal mush, which could move up through the crystal pile. This process may ultimately be responsible for the generation of potholes and pegmatoidal horizons, such as the Merensky pegmatoid. The upward increase in the initial $87\text{Sr}/86\text{Sr}$ ratio within the Merensky cyclic unit is strong evidence that infiltration metasomatism has played an important part in the generation of the Merensky cyclic unit. This process, coupled with fluid enrichment, may also result in the formation of pegmatoid layers. Sintering appears to have been a common process in the mottled anorthosites of the study section and may have severely reduced the amount of trapped interstitial liquid in these rocks.

CHAPTER ONE: Introduction and Review

Introduction

The well known Bushveld Complex comprises a suite of ultramafic to granitic rocks, of diverse origins, intrusive through the Kaapvaal craton into the sediments and volcanics of the Transvaal Supergroup. This vast intrusion (65,000 km² in area) and its host rocks occupy an irregular basin-like depression surrounded by the basement rocks of the Kaapvaal craton (Fig. 1:1), and has been well described in numerous interpretative reviews (e.g. Hall, 1932; Willemse, 1964 & 1969; Wager & Brown, 1968; von Gruenewaldt, 1979 and Hunter & Hamilton, 1978).

The study section, which covers a short sequence of layered rocks in the vicinity of the platiniferous Merensky horizon near Rustenburg, Western Transvaal, is within the mafic layered portion of the complex, now known as the Rustenburg Layered Suite (South African Committee on Stratigraphy, 1980; hereafter referred to as SACS). This suite of mafic layered plutonic rocks occurs in four lobes which outcrop or suboutcrop in arcuate belts, one of which to the east of Johannesburg is obscured by younger cover. An extension to the western lobe occurs to the north of Zeerust. The eastern and western lobes have been further subdivided by SACS into units of formation status, an informal role being assigned to the more usual zonal nomenclature. The succession studied, which includes the Merensky and Bastard cyclic units, falls in the upper part of the Mathlagame norite-anorthosite, which is considered by SACS to be in the Critical Zone*.

Figure 1:2 shows the simplified stratigraphy of the Western Bushveld Complex, with the major zonal subdivisions after SACS and Willemse (1969), with additional information on disconformable contacts from Coertze (1974) and Vermaak (1976a). The boundary between the Main and Critical Zones does not correspond with that recommended by SACS. The Bastard and Merensky cyclic units are here considered to be part of the Main Zone (see Fig. 1:2). The reasons for this choice are presented and discussed in Chapter Two.

* SACS recommends that the zonal nomenclature not be capitalized, but capitals are retained, as the zonal terminology is used exclusively in this work.

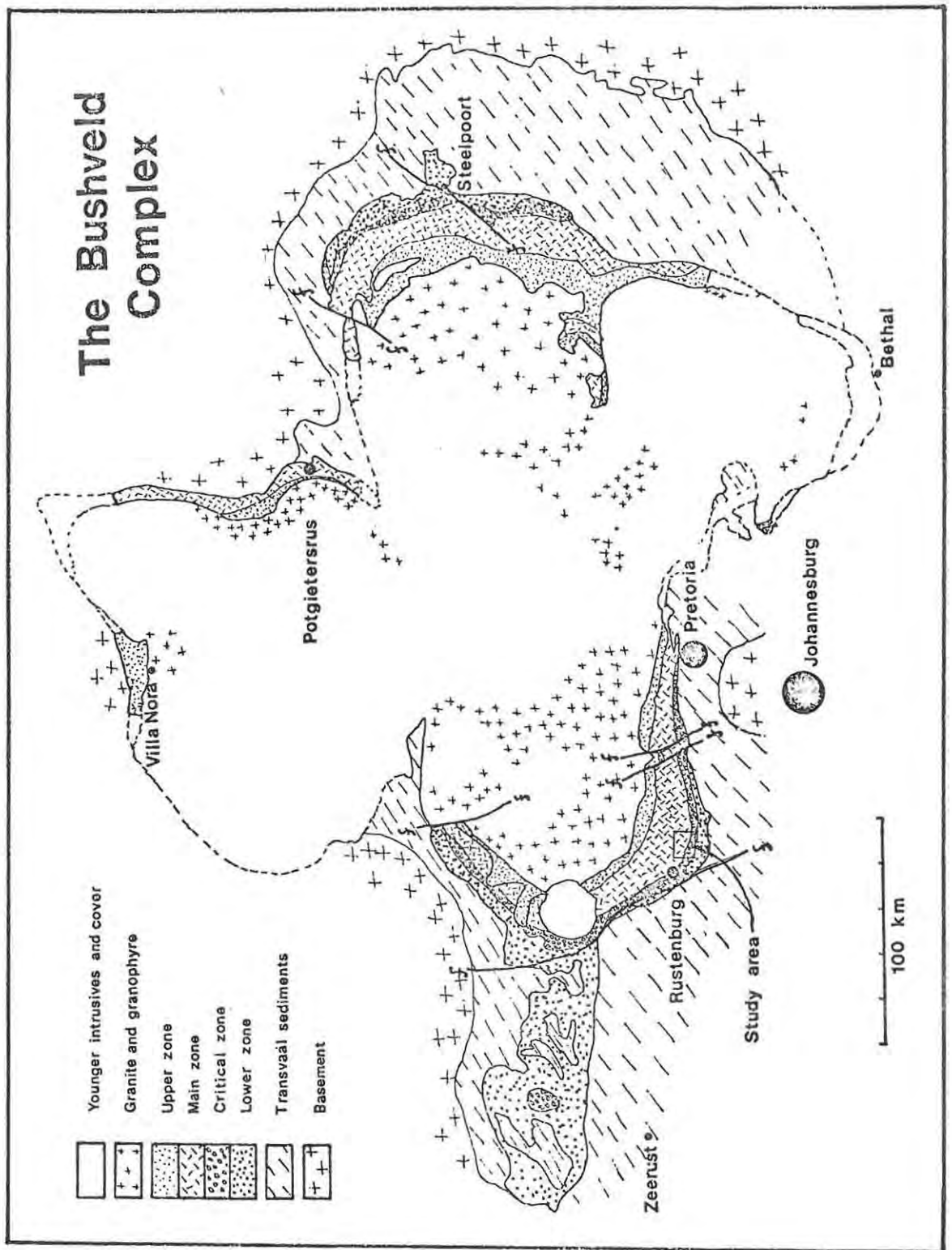


Fig. 1:1 Map of the Bushveld Complex and its environs, showing the major subdivisions of the layered suite and the locality of the study area near Rustenburg. Modified after Willemse (1969) and SACS (1980).

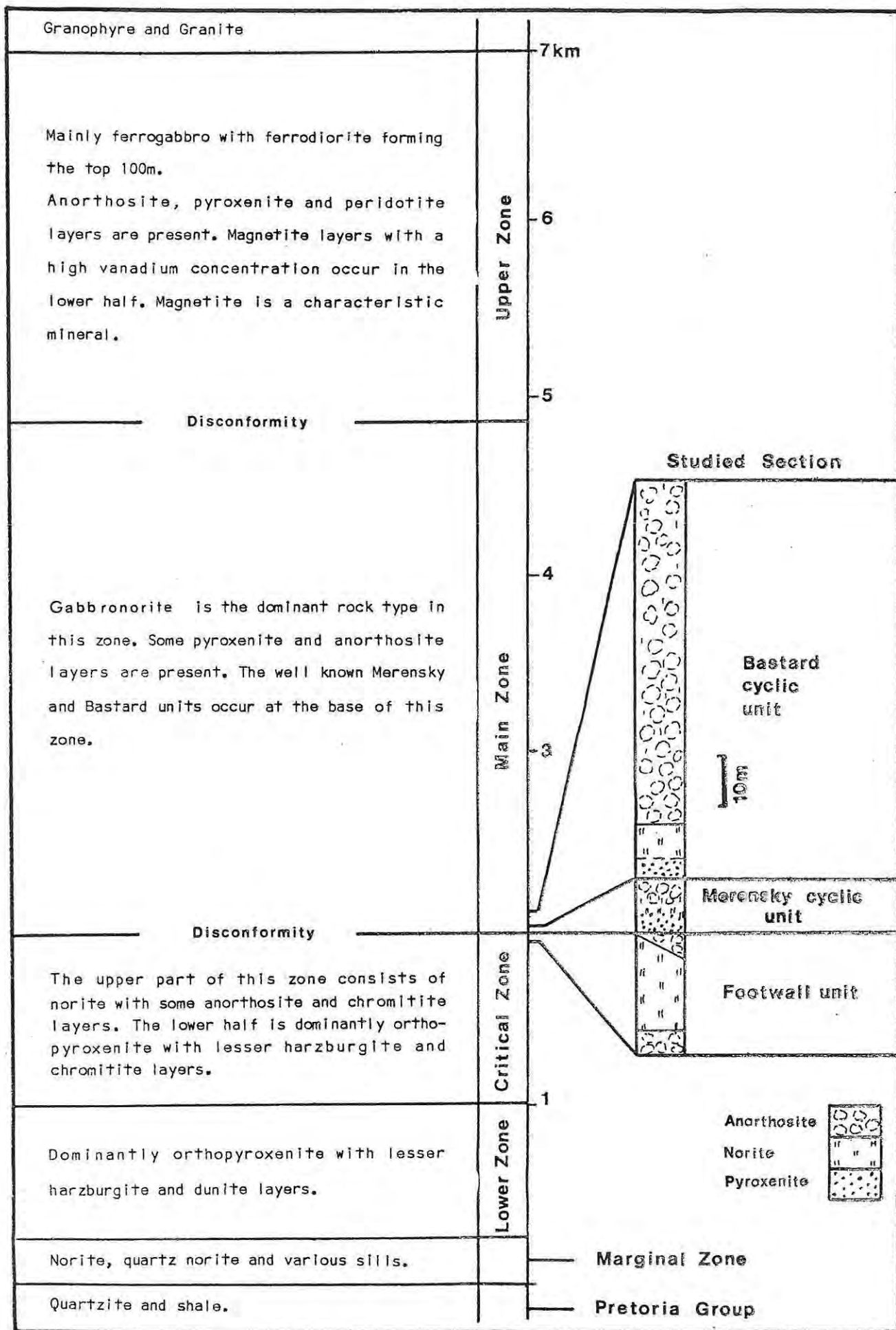


Fig. 1:2 Generalized stratigraphy of the Western Bushveld Complex, indicating the lithologies and the position of the studied section. Subdivisions after Willemsse (1969), SACS (1980) and Chapter Two of this work. Additional information from Coertze (1974) and Vermaak (1976).

The Origin of the Bushveld Complex: A Thematic Review

The first comprehensive model of the Bushveld Complex was presented by Molengraaff (1901), who described it as a vast laccolite (sic) with an initially flat floor, which then assumed a basin shape due to the superincumbent load. Following this early work, many papers of a more restricted scope appeared, and these were reviewed by Hall (1932). Publications of a more integrated nature were those of Daly & Molengraaff (1924) and Daly (1928). These works and that of Wagner (1929), on the platinum mineralization, form the basis of Hall's (op. cit.) holistic synthesis of the geology of the Bushveld Complex. These works delineated the basic tectonic framework of the complex, and established the concept of gravity differentiation of a basaltic magma to account for the variety of rock types and layering present. All the early workers, including Hall, believed that the structure of the Bushveld Complex was essentially lopolithic, and nearly all held the view that the basic rocks were derived from a single intrusive or extrusive event followed by in situ differentiation. A somewhat different view was expressed by Reuning (1927), who believed the different rock types to be sill-like intrusions of diverse magmas. Lombaard (1934) further developed the magmatic theory with the concept of multiple additions of evolving magma from a subcrustal chamber coupled with differentiation in situ. This concept to some extent unified the views of Reuning with the other magmatists.

Not all views concurred with those of the magmatists. Sandberg (1926) proposed that the various layers of the Bushveld Complex were formed by "transformation" of the earlier sediments such as shales, quartzites and dolomites by "magmatization", each sediment forming a different igneous rock type by in situ melting and later solidification. In 1949, S. van Biljon revived Sandberg's hypothesis in a controversial paper. He believed that the Transvaal Supergroup rocks were transformed into the rocks of the Bushveld Complex by heat and "emanations" without suffering any melting (van Biljon, 1949). This view has not found much favour despite further papers published by him in 1955, 1963 and 1974. However, due to their controversial nature, considerable discussion of the topic was generated, stimulating further research.

Truter (1955) revived Reuning's (1927) idea of multiple sill-like injections of different magmas to account for the different rock types in

the intrusion. He also proposed that there were four or five intrusive centres, forming a linear array extending from the eastern to the western parts of the complex, with a further centre to the north near Potgietersrus. He also gave some support to van Biljon's (1949) transformation hypothesis, but only for the granophyric rocks at the top of the mafic layered suite. Schwellnus (1956) and later Coertze (1958) further developed the idea of multiple intrusions for each rock type. The latter paper generated considerable discussion, and in subsequent works (Coertze, 1959, 1960a & b, 1962a & b, 1963, 1966, 1970 & 1974), he modified his views, and his current (1974) position is that several large heaves of magma were intruded with minor differentiation in place. However, no mixing of magmas is implied as each intrusion occurred after the previous one had solidified.

A significant advance in the understanding of the Bushveld Complex was made when Cousins (1959) showed that the mafic suite is not lopolithic as had been generally accepted, but that it forms arcuate, moat-like masses surrounding a core of felsic rocks. The possibility that the different lobes of the Bushveld Complex may have been separate intrusions with tenuous connections, was implied. In his paper Cousins also implied, and in a reply to a discussion by F. C. Truter on the paper stated, that he believed the mafic phase of the Bushveld Complex was extruded on surface into graben-like structures. This renewal of Daly's original hypothesis (Daly, 1928) has also been supported by Feringa (1959) and in subsequent papers and discussions by Cousins (e.g. the discussion and reply to Feringa's (op. cit.) paper).

Cousins' disagreement with Coertze (discussions of Coertze (1959, 1960, 1962 & 1970)) centred not so much on the concept of several inputs or heaves of magma, but on whether they were intruded as sills, or extruded as lavas. Cousins also believed that all the magmas were essentially basaltic and differentiated after extrusion.

Willemse (1964 & 1969) in reviews of the Bushveld Complex also endorsed the view that the mafic magmas intruded at separate centres, and suggested that processes of cone sheet formation and intrusion along fractures may have played an important part. This latter notion has been further developed by and Sharpe & Snyman (1980). In Willemse's view there were definitely several inputs of mafic basaltic magma, the earliest of which was ultramafic. In situ differentiation was nevertheless important

in generating the layering. In the later review paper Willemse (1969) suggested that although the different parts of the complex may have been separate, there must have been a connection between them to account for the similarity in stratigraphy.

Wager & Brown (1968) in an extensive review and interpretation of the Bushveld Complex geology, suggested that the lower part of the mafic layered suite, up to the Merensky unit, was the "integration stage" where tholeiite magma was added and mixed with that already in the chamber. The eastern and western lobes of the complex were postulated to have been separate unconnected intrusions up to the Merensky unit level. A further input of magma was invoked at the Merensky level, as had been suggested by Hess (1960), to account for the platinum mineralization. After this last influx, the complex continued to crystallize without interruption or further additions of magma. The position adopted by Wager & Brown is thus similar to that of Lombaard (1934) for the portion below the Merensky unit, but akin to Hall (1932) for the mafic part of the Bushveld Complex as a whole. Atkins (1969) proposed a similar model to that of Wager & Brown.

Gijbels et al. (1974), Vermaak (1976a), Cameron (1978) and von Gruenewaldt (1979) considered that the magmas introduced in pulses were initially very magnesian, later additions being less so. Hamilton (1977), using strontium isotope data, indicated that at least five pulses of magma, with different initial $^{87}\text{Sr}/^{86}\text{Sr}$ ratios, flowed into the magma chamber. The first of these magmas is postulated to have been of an unusual composition, having both high MgO (>21,5%) and high SiO_2 (50-55%). This latter conclusion was supported by Davies et al. (1980).

In a re-interpretation of Hamilton's (1977) data, McCarthy & Cawthorn (1980) postulate the occurrence of only two influxes of magma, the variation in the initial ratio being due to magmatic ageing during differentiation. This model requires the Rustenburg Layered Suite to have crystallized over some 40 to 60 my., which is not in agreement with calculations by Irvine (1970a) which indicated a solidification time of about 200,000 years. Cawthorn et al. (1981), in a study of the Bushveld sills, again suggest that only two magmas were involved. Sharpe (1981a) using detailed mapping and chemistry of the Marginal Zone and its associated sills, concludes that at least four magmas, with a range of compositions, were intruded. Sharpe's views correspond to some degree with those of Hamilton.

From the above discussion it is apparent that there is now wide acceptance that most of the rhythmic layering is due to in situ differentiation and that more than one input of magma occurred. Nevertheless, there is considerable disagreement as to the number of influxes that took place, their respective compositions and if the influxes occurred as intruding "sills" with no magma mixing implied, or as additions to an evolving magma.

A suggestion not fitting in with the otherwise smooth evolution of various models outlined above, is the astrobleme theory proposed by Dietz (1963), as this returns to the original proposal of Daly (1928) of a single, large magmatic event, the difference being only the source of energy. Dietz's hypothesis was later supported by W. Hamilton (1970) and Rhodes (1975).

Hypotheses Concerning the Merensky Cyclic Unit

As the question of the origin of the Merensky cyclic unit is to be dealt with in detail in later sections of this work, only a brief review of the various hypotheses to account for the Merensky pegmatoid and its associated mineralization will be given here.

Wagner (1929) suggested ^{that} the Merensky pegmatoid and its mineralization were due to normal magmatic processes coupled to volatile rich fluids. Reuning (1927) and Coertze (1958) proposed the pegmatoid to be a sill-like intrusive at the base of the Merensky cyclic unit, and thus totally independent of the processes occurring in the associated rocks. Lauder (1970) postulated that infiltration of interstitial liquid from below could account for most of the features of the pegmatoid. Hess (1960) and Wager & Brown (1968) suggested that the pegmatoid was an early (immiscible?) fraction forming from a new surge of magma. Brynard et al. (1976) concurred with this view, but emphasized that later hydrothermal alteration of the pegmatoid occurred (cf. Wagner, op. cit.). The Merensky and Bastard cyclic units were considered by Cousins (1964 & 1969) to have differentiated from separate heaves of magma, some time after the formation of the footwall rocks. The pegmatoid and its mineralization were thus derived from the Merensky magma by gravity differentiation and settling. He does, however, note that several unsolved problems exist.

In a comprehensive review of rocks of the Bushveld Complex occurring below and including the Merensky and Bastard cyclic units, Vermaak (1976a) suggested that an anorthosite mat (the Merensky mottled anorthosite, Fig. 2:2), formed due to the upward floating of plagioclase. The mat trapped volatile constituents and magma beneath it, and these then differentiated as a closed system. The volatile enriched environment resulted in pegmatoid boulders forming and sinking to the base of the trapped magma layer. The enrichment in platinoids was due, in part, to addition of enriched liquid from the footwall. Lee & Sharpe (1980) extended this hypothesis and invoked an immiscible bridging liquid to aggregate orthopyroxenes into boulders which sank to form the pegmatoid. McCarthy & Cawthorn (1980) considered that the Merensky pegmatoid precipitated from the residual liquid which had resulted from some 90% crystallization of the initial magma intruded into the Bushveld Complex chamber, before a second large influx of magma occurred above the Merensky cyclic unit.

Developments in the Interpretation of Layered Intrusions.

"A layered intrusion may be likened to a crucible, greatly magnified, of the experimental petrologist"

(Wager & Brown, 1968).

Layered intrusions have been extensively studied for many years, and it was soon appreciated that they provide clues to the understanding of processes occurring within magma chambers. The results of intrusion and differentiation can be directly observed, and compositions of successive liquids calculated. Investigations of layered complexes thus have much wider implications than a simple study of the rocks themselves and the ore deposits contained within them.

The first research into layered intrusions was that of Geikie (1894) and Geikie & Teall (1894). This was followed by those of Molengraaff (1901) and Harker (1904). At this early stage two schools of thought became apparent which are not yet completely reconciled. Geikie, Teall and Harker believed that the layered gabbros of the Isle of Skye were the result of multiple intrusions. Molengraaff (1901 & 1905), on the other hand, suggested that a single magma input into the Bushveld magma chamber differentiated, under the influence of gravity, to form the various rock

types. The idea of crystal settling under the influence of gravity to account for different rock types was proposed early in the 19th Century. For example, Darwin (1844) invoked the process to account for the diversity of rock types.

The two hypotheses continued in parallel until the work of Wager & Deer (1939) on the Skaergaard intrusion. The work on this intrusion has had a pervasive influence on our understanding of the differentiation of mafic igneous rocks. Using the Skaergaard intrusion as a type example, Wager and his associates developed a comprehensive model for the differentiation of layered intrusions, involving convection and crystal settling to account for the rhythmic and cryptic layering. This work culminated in the book by Wager & Brown (1968) in which many mafic layered intrusions, including the Bushveld Complex, were explained using this model. Some intrusions, such as at Rhum, are inferred in the book to be the result of crystal settling coupled with continuous injections of new magma pulses into the chamber (Wager & Brown, *op. cit.*).

Jackson (1961), using the Stillwater Complex as a basis, developed an alternative theory of bottom crystallization to account for the features of layered intrusions. He argued that a convecting magma, cooled from above, only nucleates and grows crystals when it reaches the floor of the magma chamber as opposed to near the roof of the intrusion.

The model developed by Wager and his co-workers (Wager & Brown, 1968) has, until recently, been more widely accepted as it apparently explained most features of layered rocks. McBirney & Noyes (1979) have revived Jackson's (1961) hypothesis and have presented a large body of evidence that tends to negate the crystal settling hypothesis. The basis of the McBirney & Noyes proposals is that the various layers develop by in situ crystallization on the floor, roof and sides of the Skaergaard Intrusion. The model invokes double-diffusive convection, a process induced by opposing temperature and concentration gradients. The theoretical background to this process is given by Turner (1973), and Rice (1981) has developed the concept as applied to magma chambers. The effects of the replenishment of a magma chamber have been investigated by Huppert & Turner (1981). These investigations into physical processes such as diffusion and convection are now in the vanguard of research into layered intrusions.

Studies of the intercumulus liquid present in the crystal pile (which in some cases may have constituted up to 50% of the crystal mush accumulated), has also received considerable attention. Irvine's (1980a) review of his and other investigations of the Muskox Intrusion, shows that a considerable amount of upward movement of interstitial liquid occurred. This synthesis of the cyclic units in the Muskox intrusion integrates the concept of double-diffusive convection, multiple intrusion and the upward migration of interstitial liquid.

This brief review is not intended to be exhaustive as further discussions of the concepts outlined above will be presented where appropriate in the text.

Objectives of this Work

The above reviews of the Bushveld Complex and evolution in the interpretation of layered intrusions, suggests that that the new concepts applied to, and current research on, other layered intrusions could be used to resolve some of the problems and controversies associated with the Bushveld Complex.

Thus, the object of this work is to present a comprehensive record of the chemistry of the various phases present in a 110m section through the Merensky unit in the vicinity of Rustenburg, Western Bushveld Complex. These data are supported by whole rock chemical analyses, relevant petrographic observations and a strontium isotope study of the Footwall, Merensky and Bastard units. With this information and data available in the literature I hope, firstly, to develop a model for the evolution of the studied section, secondly, to try and resolve the different views on the origin of these rocks and the rest of the Bushveld Complex and, thirdly, to relate the model to problems of layered rocks in general.

CHAPTER TWO: Field Relationships, Petrography and Petrochemistry

Introduction

The Merensky and Bastard cyclic units display a remarkable constancy in their chemical, mineralogical and stratigraphic relationships throughout most of the Bushveld Complex. This is shown by the work of Schmidt (1952), Van Zyl (1960), Cousins (1969), Meyer (1969) and De Klerk (1982). The compilation and review of Vermaak (1976a) in which he has summarized and collated published work, theses and internal company reports including a large amount of borehole information emphasizes this constancy of properties. The processes which gave rise to the Merensky and Bastard cyclic units were thus operative over extensive areas, and this work should thus be broadly applicable to most areas where these two units occur. The Footwall unit (as defined below) is less constant than the two overlying units, but nevertheless also displays lateral uniformity.

To facilitate discussion of this part of the Bushveld Complex the petrographic nomenclature and stratigraphy are revised and clarified.

Petrographic Classification

The mesoscopic petrographic classifications adopted in this work are based on the IUGS system (Streckeisen, 1973) but only primocryst* phases are considered, the interstitial phases being used only as modifiers of the basic name. The terminology is similar to that of Cameron (1980). This is not a modal classification system and accurate modes need not be known. It does, however, give an accurate idea of the primocryst (liquidus) mineralogy of the rock, and allows a clear representation of primocryst phase changes in the succession. It also has the advantage of being in common use by geologists working on the Bushveld Complex, although it has not previously been clearly defined.

* This term is used here to denote the initial presence of first generation (liquidus) crystals that initially grew without interference by other crystals.

A pyroxenite is here defined as a rock containing only pyroxene primocrysts. The modal volume of interstitial phases, notably plagioclase, is not considered. In cases where the proportion of plagioclase exceeds about 10% the modifier "feldspathic" is used. Similarly, an anorthosite contains only plagioclase primocrysts, but has a variable proportion of interstitial pyroxene which sometimes exceeds 10%, and therefore the rock could be termed a leuconorite in some cases if the IUGS system were used. Norite, gabbronorite and gabbro on the other hand contain both plagioclase and pyroxene primocrysts. Again this ignores the modal proportions and the interstitial phases. The modifiers "mela" and "leuco" indicate the overall colour of the rock. In some cases a leuconorite as defined here would be an anorthosite if the IUGS classifications were strictly applied. The terms used here thus tend to overlap in a modal sense, but give a clearer visualization of the nature of the layering present in the sequence. Furthermore, in practice the classifications generally correspond to those of the IUGS system.

The modifying terms "mottle" or "mottled" which are in common use in publications of Bushveld Complex geology are retained here. These terms indicate the presence of large, ovoid to irregular, sieve-like, poikilophitic pyroxene oikocrysts up to 10cm in diameter which are irregularly distributed and impart a mottled appearance to the anorthosite. The term "spotted (anorthosite)" is here abandoned as it is a synonym for leuconorite as defined above. Other non-standard terms such as "pyroxenitic" (for mela) and "anorthositic" (for leuco) are also discarded.

The term pegmatoid is used for the very coarse grained (pegmatitic) feldspathic pyroxenite or harzburgite occurring at the base of the Merensky cyclic unit and as discontinuous patches and ovoid masses in the Boulder Bed and below the basal contact of some chromitite layers. These rocks are usually considered part of the layered sequence. Ultramafic pegmatite is used for coarse-grained, cross-cutting intrusive or replacement bodies with an irregular and crudely pipe-like form, that are not necessarily directly related to the layering. Some of the cross-cutting bodies described by Willemse (1969) as "ultramafic pegmatoid" are in this category. This distinction is made as these two coarse grained rock types often occur in close proximity (cf. Irvine, 1982).

Stratigraphic Nomenclature

Although several attempts have been made to formalize the existing stratigraphic subdivisions of the Bushveld Complex, none has been completely successful (cf. Wagner, 1929; Feringa, 1959; Wager & Brown, 1968; Cousins, 1964 & 1969; Willemse, 1964 & 1969; Van Zyl, 1970; Coertze, 1974; Vermaak, 1976a;

von Gruenewaldt, 1973 & 1979 and SACS, 1980). For a succinct review of the different classifications, the reader is referred to Hunter & Hamilton (1978). The subdivisions and their names, adopted in this thesis, are summarised in Fig. 2:1 where they are compared to the existing terminology. The base of the Main Zone is taken to be the base of the Merensky cyclic unit as defined below (see also Fig. 1:2 & 2:1). This is in contrast to SACS (1980) who put the base of the Main Zone at the top of the Bastard mottled anorthosite (referred to by them as the Giant mottled anorthosite (Fig 2:1)). The reasons for the choice made here are threefold. Firstly, there is good evidence for a disconformity at the base of the Merensky cyclic unit (Vermaak, 1976a). Secondly, the contact between the Merensky cyclic unit and its footwall rocks is sharp as opposed to the gradational top contact of the Bastard mottled anorthosite as observed in the study section, and the position of the base of the Merensky unit is very well known from extensive exploration and mining operations. Finally, a variety of mineralogical, chemical and isotopic evidence presented and discussed in this work indicate that a new magma with markedly different isotopic characteristics flowed into the Bushveld Complex magma chamber immediately prior to the formation of Merensky cyclic unit. The Sr-isotope evidence of Hamilton (1977) and Kruger & Marsh (1982) especially suggests that the Merensky and Bastard units can not be regarded as a continuation of the differentiation of the Critical Zone, but should be regarded as part of the Main Zone.

The formally defined Mathlagame norite-anorthosite unit as defined by (SACS, 1980) extends upward from where primocryst plagioclase makes its first appearance about 400m below the study section to the top of the Bastard mottled anorthosite. The above discussion suggests that the upper boundary of this unit should be changed to coincide with the boundary between the Critical Zone and Main Zone as defined here, (i.e. the base of the Merensky cyclic unit).

The nomenclature developed here for smaller subdivisions of the Main and Critical Zones of the study section is based on the cyclic unit concept of Jackson (1961 & 1970) and Irvine (1970b, 1982). Wager & Brown (1968) termed the same cycle a rhythmic unit, and the term macrorhythmic unit was applied by them to Feringa's (1959) data, and this subdivision into mapable macrorhythmic units was accepted by Vermaak (1976a). The term cyclic unit does, however, have priority and is more generally acceptable (T. N. Irvine, 1982 & written communication, 1980).

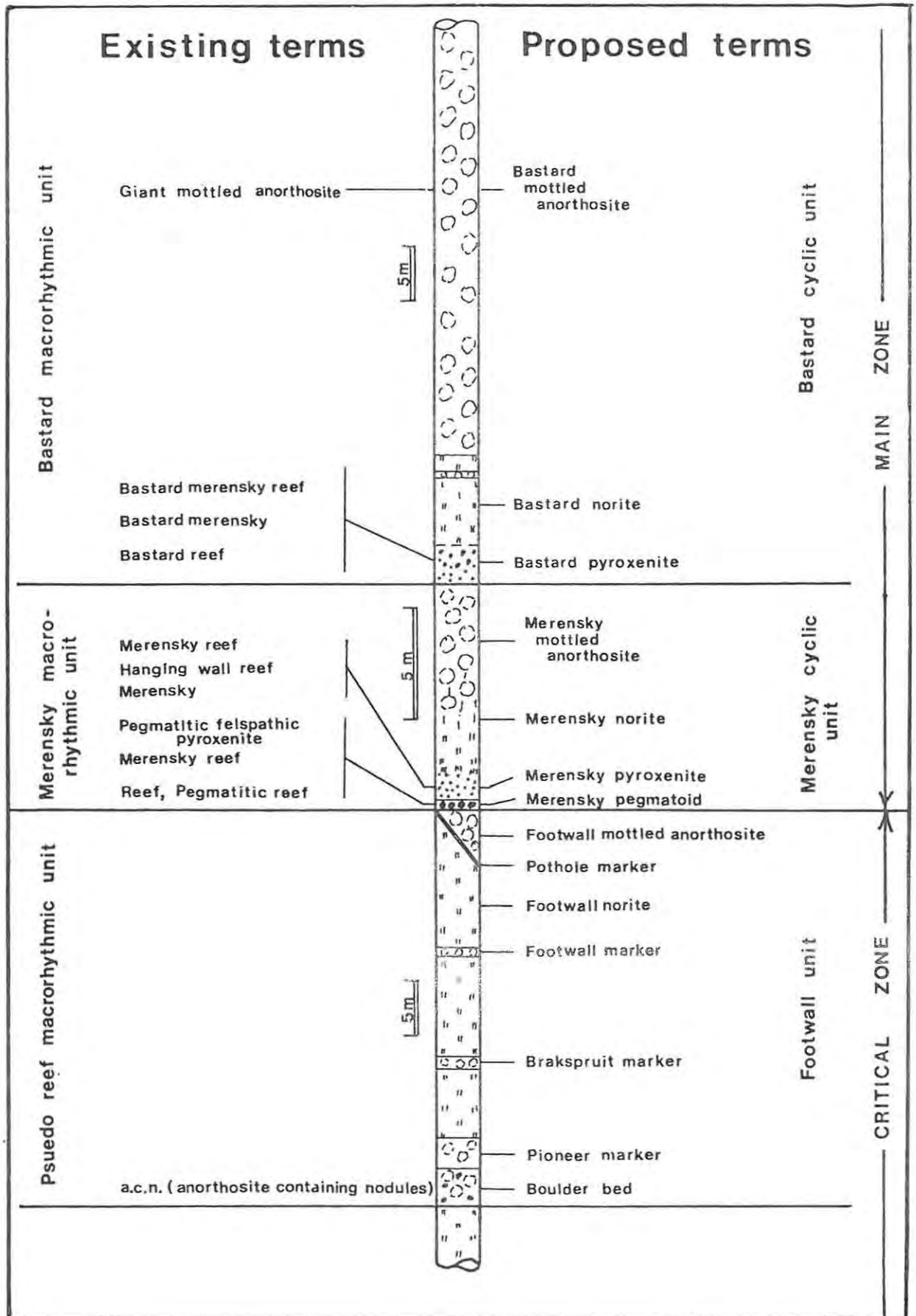


Fig. 2:1 The existing and proposed terminology for the sequence in the vicinity of the Merensky cyclic unit, Western Bushveld Complex. The ornamentation indicating the rock type in this and other diagrams is indicated by the proposed terminology of the Merensky and Bastard cyclic units.

The Merensky and Bastard cyclic units are laterally extensive and can be traced over large distances. This is, however, not true of the units in the immediate footwall to the Merensky cyclic unit. Correlation here is by no means certain (as yet), and different units may displace each other laterally in this stratigraphic position. In this work the footwall rocks are loosely termed the Footwall unit (which is defined in Fig. 2:1) even though, in the section studied, more than one cyclic unit may be present. Within the area of Rustenburg Platinum Mines the layers constituting the Footwall unit are easily recognised over a strike of more than thirty kilometers and the nomenclature used by the mine geologists has been adopted (see Fig. 2:1 and the section on the Footwall unit below).

There is more confusion in the naming of the individual layers within the cyclic units than the cyclic units per se, and this is due to the inconsistent use of the terms "Reef", "Merensky" and "Bastard". The confusing current terminology is illustrated on the left side of Fig. 2:1. The term "Reef" is here abandoned for formal use, and is reserved only for the informal description of whatever mineralized part of the Merensky cyclic unit is being mined. In this I concur with von Gruenewaldt (1979), although he retains the term for formal use. "Merensky" and "Bastard" are reserved as identifiers to the lithological terms defined above, and to identify the cyclic unit referred to.

Field Relationships

Introduction

The study section is within the Rustenburg Platinum Mines (Rustenburg section). The details of sampling are outlined in Appendix 5. The study section has a vertical dimension of some 120m straddling the boundary between the Main and Critical Zones as defined above. The Merensky cyclic unit is about 400m above the first norite layer and 460m above the LG6 (Main or Magazine) chromitite horizon. The Platinum group element (PGE) bearing UG2 and the UG1 chromitite layers are about 140m and 210m below the Merensky cyclic unit respectively. Above the Bastard cyclic unit the Main Zone is poorly known, but is composed of relatively uniform gabbronorite. The Upper Zone is heralded by the appearance of magnetite about 3000m above the Merensky cyclic unit.

From the paleomagnetic work of Gough & van Niekerk (1959) it is apparent that the Rustenburg layered suite was deposited in a horizontal position and that the dips now measured ($\pm 10^\circ$) were imposed by structural reajustment

below the Curie point. The bedding plane faults such as occur at the base of the Bastard and Merensky cyclic units and at other marked stratigraphic and compositional discontinuities could possibly be ascribed to this readjustment process, as could the common occurrence of strained crystals in many of the samples studied.

The normal stratigraphy of the study section is illustrated in Fig. 2:1. It remains here to discuss the three units defined in detail and also variations encountered. Other features described here are "potholes", "koppies" and cross-cutting, late-stage ultramafic pegmatite bodies.

The study section is considered to be representative of the Merensky and Bastard units in the Western Bushveld Complex as the work of Vermaak (1976) and the work of de Klerk (1982) indicate these horizons to be laterally continuous and also mineralogically similar. The Merensky pyroxenite was studied in several localities ⁱⁿ with Rustenburg Platinum Mines by Schmidt (1982) and confirms this lateral similarity on a smaller scale.

The Footwall Unit

The base of the Footwall unit is defined as the base of the Boulder Bed (see Jones, 1976 and Lee & Sharpe, 1980 for a description) where a very thin (1-3mm) chromitite layer is present. Below this chromitite layer is a laterally continuous (5mm) layer of large orthopyroxene crystals that include small, rounded, partly resorbed olivine grains. This very thin harzburgite layer in turn overlies a norite (~10m thick) which was not included in the rocks studied. The actual boundary (plane) between the Footwall unit and the underlying rocks is taken to be the lower contact of the chromitite layer.

The Boulder Bed consists of a mottled anorthosite, about 2.5m thick, which encloses scattered spheroidal pegmatoid "boulders" about 20cm in diameter. Photographs of this layer are presented by Jones (1976). The "boulders" are round in plan and ovoid in section with rounded bases and flattened tops. The "boulders" are surrounded by a zone between 5mm and 10mm thick consisting of anorthosite devoid of interstitial pyroxene (termed a "bleached zone" by Lee & Sharpe, 1980). To the northwest of the study area the "boulders" tend to coalesce and form pegmatoid lenses and disrupted layers (Jones, 1976). Jones also notes that the Boulder Bed is variable in thickness from 1m to 9m, thinning northward. At Rustenburg it is more constant at 2m to 5m thick, and Brynard (1976) records a thickness of 1m roughly 20km to the east of the study area. Descriptions of the Boulder Bed with models for its genesis are presented

by Jones (1976), Vermaak (1976a) and Lee & Sharpe (1980). The Boulder Bed grades upward, above the last line of "boulders", into the Pioneer marker, a darker mottled anorthosite some 4m thick. Above the Pioneer marker, and separated from it by a sharp contact, is a 9m thick layer of fine-grained norite which varies from a leuconorite near the base to a norite at the top. This in turn is overlain by the Brakspruit marker comprising a double band of mottled anorthosite (116cm thick), sandwiching a 22cm thick norite layer. Above the Brakspruit marker a further layer of norite 9m thick is developed, the base which has two rows of elongate mottles about 2cm apart (colloquially termed the "tramlines") which are traceable over many kilometres of strike and down dip. Above this norite is the Footwall marker which is about 80cm thick and also consists of two mottled anorthosite layers sandwiching a norite layer. The Footwall marker has sharp basal and upper contacts. This unit changes its appearance and thickness laterally, and in the northwest of the study area is about half as thick. Above the Footwall marker is a layer of norite (the Footwall norite) some 15m thick, ranging from a norite at the base to a mottled leuconorite near the contact with the overlying Merensky cyclic unit. In the northwest of the area this layer is thinner and is capped by the Pothole marker, a thin (5cm) coarse-grained pyroxenite layer at the base of the Footwall mottled anorthosite. The latter unit is some five metres thick and has sharp top and bottom contacts, and appears to pinch out laterally against the Merensky cyclic unit to the southeast, although this is not well established. The exact nature of this transition is crucial to the understanding of the genesis of the Footwall and Merensky units as the Pothole marker may merge into and become part of the Merensky pegmatoid. The Pothole marker widens to a maximum of about 80cm to the northwest of the study area, and with the overlying Footwall mottled anorthosite could be regarded as cyclic unit (C.D. Beater, personal communication 1982).

The Merensky Cyclic Unit

The Merensky cyclic unit which is about 10m thick in the study area, has a sharp but dimpled basal contact with the underlying Footwall anorthosite or norite. The top contact of the Footwall unit has a thin pure anorthosite layer 1cm to 2cm thick, similar to those described surrounding the "boulders" of the Boulder Bed. The dimples (domes and basins with a wavelength of 5cm to 7cm and an amplitude of 1cm to 5cm (Cousins, 1969)) have a pattern similar to that attributed by Lee (1981) to post accumulation plastic deformation in other layers of the Bushveld Complex. A thin (1cm to 4cm thick) chromitite layer

immediately overlies the dimpled contact. This is in turn followed by the Merensky pegmatoid, a very coarse-grained feldspathic orthopyroxenite or harzburgite. Besides plagioclase, interstitial phases include clinopyroxene, biotite, and base metal sulphides (BMS). The BMS may sometimes be concentrated in the depressions (Cousins, 1969). Other phases present include chromite and the platinum group minerals (PGM) (see Vermaak & Hendricks, 1976). This unit is about 30cm thick in general, but widens to about 1m thick in the centre of the area. The top contact of the pegmatoid is usually demarcated by a further chromitite layer less than 1cm thick. This chromitite layer is not as persistent as that at the base, and in some cases two or more chromitite stringers may be present at this level. Cousins (1969) noted that the platinum group element (PGE) mineralisation in the western Bushveld Complex is concentrated around the upper and lower chromite layers on either side of the Merensky pegmatoid. However, in the eastern Bushveld Complex the mineralization is associated with two chromitite layers above a pegmatoid which is itself barren. In places in the eastern lobe the pegmatoid overlies a basal layer of pyroxenite (Cousins, 1969; Von Gruenewaldt, 1979). J. Barry (personal communication 1979) notes that the upper chromitite layer at Rustenburg has a greater abundance of PGM compared to the lower chromitite, and that the pegmatoid per se is relatively poorly mineralized although it contains significant amounts of BMS.

The pegmatoid is overlain by the finer grained Merensky pyroxenite, which may be feldspathic and averages about 1m in thickness. This grades upward with the development of primocryst plagioclase into a melanorite (part of the Merensky norite). The basal part of the pyroxenite sometimes has pegmatoidal patches of limited extent and the mineralogy of this unit (especially the basal portion) is similar to that of the Merensky pegmatoid. Occasional large oikocrysts of clinopyroxene enclosing orthopyroxene give the rock a pseudo-porphyrific appearance. The base of the pyroxenite contains significant concentrations of PGM and BMS, and where the pegmatoid is absent (over koppies and at the edges of potholes) contains all the economically important minerals. The Merensky norite which overlies the Merensky pyroxenite, grades from a melanorite at the base to a mottled leuconorite at the top. The leuconorite grades upward into the Merensky mottled anorthosite with the disappearance of pyroxene as a primocryst phase. The Merensky mottled anorthosite is 3m to 4m thick in the study area and has a sharp upper contact with the base of the

overlying Bastard cyclic unit.

The Bastard Cyclic Unit

In the study section the Bastard cyclic unit is between 64m and 74m thick. The unit has a well defined lower contact and a poorly defined upper boundary as the Bastard mottled anorthosite is gradational into the Main Zone gabbro-norite. No attempt is made here to assign a precise upper contact as more detailed work is needed.

At the base of the cyclic unit there is an intermittent stringer of chromitite up to 5mm thick, and this is followed by the Bastard pyroxenite (3m thick), which is very similar to the Merensky pyroxenite and also has occasional small pegmatoidal patches developed near its base. This layer has very little interstitial plagioclase (much less than the Merensky pyroxenite) at the base, but is feldspathic towards the top. The upper boundary of this pyroxenite is sharp (in contrast to the boundary between the Merensky pyroxenite and norite) the transition being less than 5cm wide. The overlying Bastard norite which is some 7m to 10m thick is a fine grained rock grading up into a thin (50cm thick), dark, mottled anorthosite layer, which in turn has a sharp top contact with a 1.5m thick norite layer. The latter layer also has a sharp contact with the overlying Bastard mottled anorthosite, a major unit about 50m to 70m thick, with large mottles up to 10cm in diameter. The top contact is not well defined as there is some interlayering of anorthosite with the overlying gabbro-norite.

In the study section, the Bastard mottled anorthosite has a leuconorite layer developed which is defined by the presence primocryst orthopyroxene some 10m above the base of the Bastard mottled anorthosite. If this unit is laterally continuous, a further cyclic unit comprising the upper part of the Bastard mottled anorthosite should be defined in the Main Zone.

Potholes and Koppies*

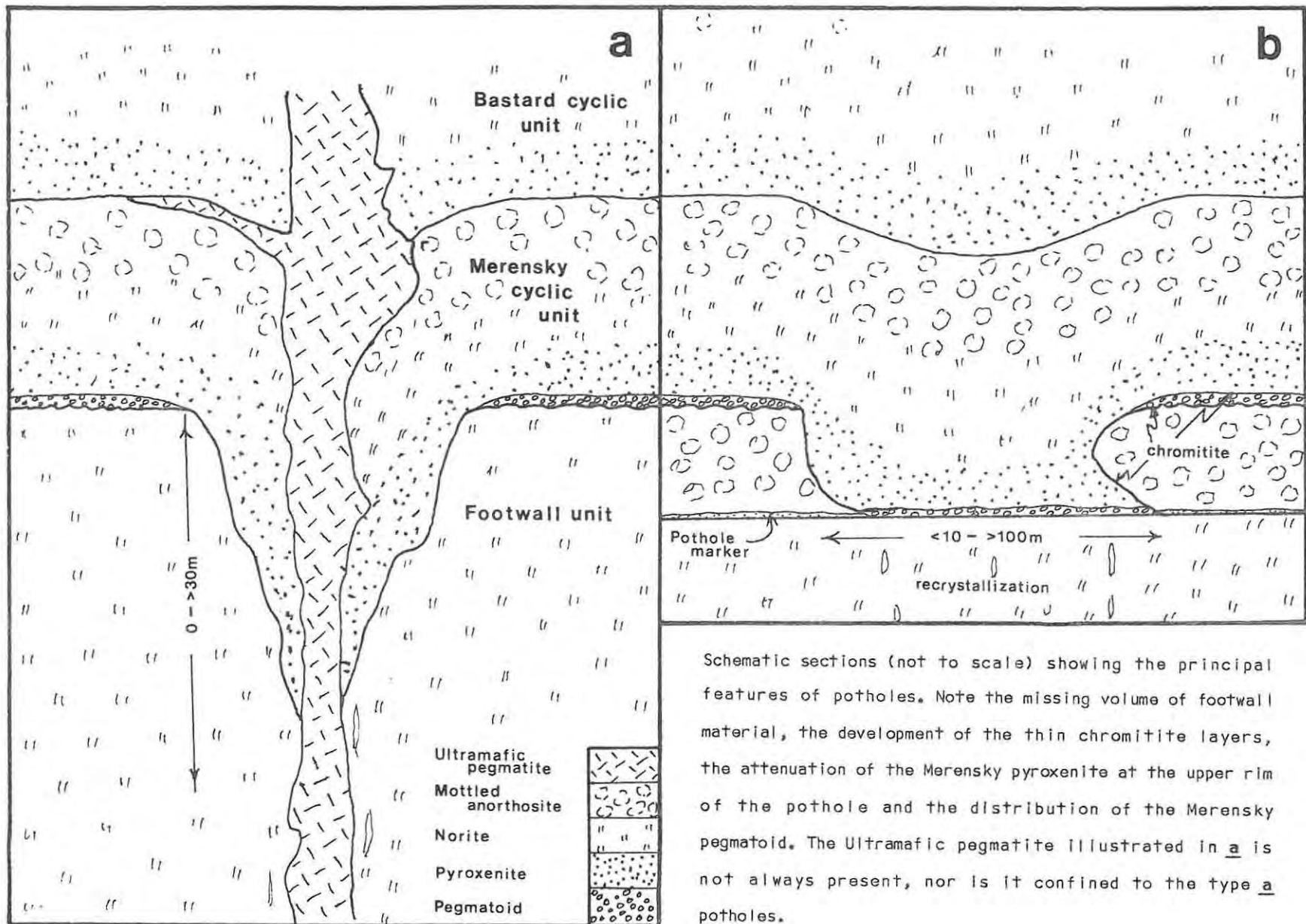
Potholes are enigmatic features that have been described by many workers who have also proposed a variety of hypotheses to account for them (Schmidt, 1952; Ferguson & Botha, 1963; Coertze, 1963; Cousins, 1964 & 1969; Vermaak, 1976a and Lee & Sharpe, 1980). Potholes are common at the base of the Merensky cyclic unit, but also frequently occur at other stratigraphic horizons. As the geologic relationships are central to understanding the morphology and genesis of potholes, a detailed

description is given. Fig. 2:2a & b illustrates the salient features of potholes that have been mapped in detail by Mr. J. Barry, and these illustrations also conform to descriptions and diagrams of potholes in the works referenced above, as well as the observations of the author.

The most striking feature of the potholes (as shown by Fig. 2:2) is that a part of the normal footwall stratigraphic succession below the Merensky pegmatoid is missing. This missing portion is very variable in size, shape and lateral extent, and is dependent on the original footwall stratigraphy. In parts where the relatively homogeneous Footwall norite forms the footwall to the Merensky unit the depth of the pothole is roughly proportional to the diameter and is funnel-shaped (Fig. 2:2a). In areas where there is strongly contrasting layering such as when the Footwall mottled anorthosite is present above the Footwall norite, the missing portion is confined to this unit, and thus the pothole has a depth equal to the thickness of the anorthosite (Fig. 2:2b) regardless of the lateral extent of the pothole. In some areas potholes are numerous and extensive, often appearing in plan view to coalesce. Potholes are also extremely variable in areal extent and have diameters that range from less than 10m to more than 100m. The funnel shaped types described above (Fig. 2:2a) may extend down to the Boulder Bed level and deeper (i.e. greater than 30m deep). Mining is possible in the case of the flat-bottomed pothole illustrated in Fig. 2:2b, although stoping has to be done on two levels. Mechanized mining methods are very difficult to apply in extensively potholed areas.

* The terms "potholes" for circular depressions and "koppies" for domes in the footwall to the Merensky and other units are retained as they are in widespread use and unambiguous in this context.

Fig. 2:2 Schematic illustrations of potholes from areas with contrasting Footwall unit successions. For explanation and sources of information see text.



Schematic sections (not to scale) showing the principal features of potholes. Note the missing volume of footwall material, the development of the thin chromitite layers, the attenuation of the Merensky pyroxenite at the upper rim of the pothole and the distribution of the Merensky pegmatoid. The Ultramafic pegmatite illustrated in a is not always present, nor is it confined to the type a potholes.

The footwall rocks immediately below potholes are characterized by the presence of occasional vertical veinlets of felsic material (P Coetser, personal communication 1979). Similar features have been described by Wagner (1929) in the Merensky pegmatoid and were interpreted by him as segregation veins. These veinlets consist predominantly of quartz and biotite, with some sodic plagioclase and orthoclase (Wagner, 1929). In some cases fine scale layering in the footwall succession is obliterated below potholes and larger crystals of pyroxene are developed possibly as a result of in situ recrystallization. This process appears to have occurred at high temperature as there are no obvious lower temperature phases such as serpentine present in the footwall rocks, although this has not been established (definitely).

Where the Merensky pegmatoid is developed in the potholes it is usually slightly different to the normal type described above. The pegmatoid is similar to the normal variety where the base of the pothole is flat (as in Fig. 2:2a), except that the lower chromitite layer is not always developed, and the chromite is disseminated throughout the pegmatoid. The upper chromitite layer appears to be more consistently developed (Cousins, 1969). In some cases several chromitite stringers are developed within the pegmatoid in potholes as illustrated by Ferguson & Botha (1963). The basal contact of the pegmatoid in a pothole is not dimpled, nor is the thin pure anorthosite band developed at the top of the footwall rocks (Cousins, 1969). The Pothole marker appears to merge laterally into the pegmatoid but this is not well documented, and furthermore the pegmatoid layer is thinner within the pothole (J. Barry, personal communication 1979).

The Merensky and Bastard successions, above the Merensky pegmatoid in the potholes, are the same as those of the undisturbed areas, except that they are displaced downward into the pothole relative to "normal" areas. This displacement decreases with height in the succession (Fig. 2:2). As the Merensky pegmatoid in a normal area is traced along strike towards a pothole the pegmatoid sandwiched between the two chromitite layers starts to thin as a pothole is approached (Fig. 2:2). The upper chromitite layer starts to dip down towards the basal chromitite layer and the two finally merge at the edge of the pothole where the pegmatoid pinches out. The distance from the edge of the pothole at which the thinning of the pegmatoid starts appears to be a function of the thickness of the

pegmatoid and the size of the pothole. Where the potholes are larger and the pegmatoid is thicker, the farther away from the pothole edge the thinning effect starts (M.J. Viljoen, personal communication 1979). The merged chromitite layer continues down and is developed on the walls of the pothole in which case it may dip down vertically, or even be overturned (Fig. 2:2b). De Klerk (1982) has documented some very significant and detailed observations of potholes in the Union Section of Rustenburg Platinum Mines near Northam some 85km NNE of the study area. He illustrates a very large pothole of the type shown in Fig. 2:2b which has a remnant lens of part of the footwall succession attached to the floor of the pothole. He notes that there is no major pegmatoid developed over this lens despite there being marked irregularities in the top of the lens. The merged chromitite layer, however, continues over the top of this remnant and, notably, has high concentrations of PGE's. The pegmatoid developed at the base of the pothole has high concentrations of PGE's where it is not covered by remnant footwall material, but has lower concentrations where it is covered. This pegmatoid also changes character laterally being coarser where underlying the Merensky unit in the pothole (De Klerk, 1982).

The downward displacement of the Merensky pyroxenite and anorthosite illustrated in Figs. 2:2a & b is not due to ring faulting as implied by Coertze (1963) as this cannot account for the section of missing footwall succession. The hangingwall layers have a centripetal dip toward the centre of the pothole, and usually only the Merensky pyroxenite is significantly attenuated at the edges of the potholes. The Bastard succession is also displaced downward but not as markedly so that over the centre of the pothole the Merensky cyclic unit is slightly thicker than normal. In large potholes of the type illustrated in Fig. 2:2a, the Bastard succession may be displaced below the level of the normal Merensky pegmatoid and in this case miners may confuse the Bastard pyroxenite with the Merensky pyroxenite and pegmatoid, hence the name.

In places layers above and below the footwall to the Merensky unit may also be potholed, this producing a stacked arrangement of potholes. This is especially noticeable in the case of larger potholes and implies the process responsible for pothole formation may have operated over an extended period in the same position.

Potholes are unlike any of the features that could be attributed to intraformational slumping such as illustrated by Hess (1960), Ferguson &

Botha (1963) and Irvine (1967) from various layered intrusions. In all these cases there is considerable folding and disruption of the rock, and all the material is accounted for, there being no significant "missing" volume of rock.

Potholes are concentrated in what are referred to as "disturbed areas" by mine geologists, with only scattered occurrences in "undisturbed" areas. Dawson (unpublished report 1968), showed that in "disturbed" areas the direction of greatest pothole frequency was 150° , which is parallel to other major structural features of the Bushveld Complex such as the Rustenberg fault. Lee (personal communication 1979) has shown that there is a good correlation of joint density with pothole density. All this field evidence suggests that there is a marked structural control to pothole distribution. Further support for this contention is the greater abundance ultramafic pegmatites in "disturbed areas", as discussed below.

Koppies are domes of limited extent, at the top of the Footwall unit, often associated with potholes in disturbed areas, against which the Merensky pegmatoid thins and pinches out. The two chromitite layers merge and continue as one layer over the top of the koppie. The Merensky pyroxenite, norite and mottled anorthosite are in their normal positions. These have been described by and Ferguson & Botha (1963) and Cousins (1964), and the reader is referred to these works for a more detailed description as the author has not been able to study any examples of these features.

The Ultramafic Pegmatites

Irregular pipe-like bodies of ultramafic pegmatite consisting largely of iron-rich clinopyroxene are frequently found in "disturbed areas". These bodies often transgress potholes, as illustrated in Fig 2.2a and clearly post-date both the potholes and the surrounding rocks. Ultramafic pegmatite is however, not associated with all potholes. These observations imply that the ultramafic pegmatite does not have a direct causal relationship to the potholes, but that the areas where potholes occur represent zones of weakness favourable for the movement of material which formed the ultramafic pegmatite pipes.

These pegmatites extend from a presently unknown depth through the whole succession up into the Main Zone above the Bastard cyclic unit. The pipes appear to be partly metasomatic in character as there appears to have been passive replacement of the layered rocks in some cases, but in other cases there has been considerable disruption of the layered host rocks (~~intruded~~) (J. Barry, personal communication 1979 and R. Scoon, research in progress). The ultramafic pegmatites are similar to those described by Cameron and Desborough (1964), Ferguson and McCarthy (1970), and Willemse (1969), and are similar in relative age and morphology to the nickel-rich sulphide pipes (the Vlakfontein pipes) described by Vermaak (1976b). Similar mafic pegmatites have been observed in other intrusions such as the stratiform Fiskenaesset Anorthosite Complex of Southwest Greenland (Myers, 1978).

The Acid Pegmatites

Thin vertical veinlets of acid pegmatite comprising quartz, alkali feldspar and biotite are found in the Footwall unit. Similar veins have been described by De Klerk (1982), and he notes that they strike in a northeasterly direction parallel to other major lineaments in the western Bushveld Complex. Wagner (1929) described these as segregation veins filled with magmatic residua rich in volatiles. This hypothesis is consistent with the observed mineralogy. The relative frequency of the veins in disturbed and normal areas is not certain, but they do appear to be more common beneath potholes (Coertzer, personal communication 1979). Their age relative to that of the ultramafic pegmatites is unknown.

Petrography

Introduction

The terminology used here for the microscopic description of the rocks of the study section as far as possible avoids any genetic connotations. For this reason the terminology of Wager et al. (1960) and Jackson (1970), is avoided as far as possible. However as this terminology is well known and has acquired some descriptive validity through use, the terms are used where necessary, but no genetic process is implied (see Irvine, 1982). The stratigraphic positions and lithology of the samples described in the text are illustrated in Fig. 2:3 which also shows the

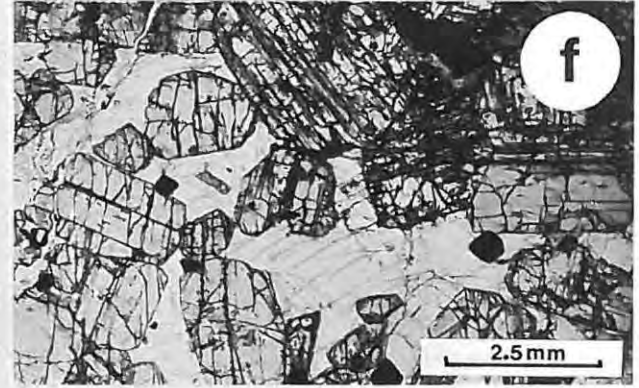
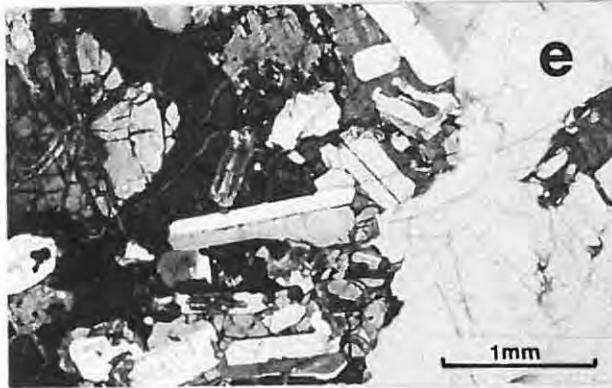
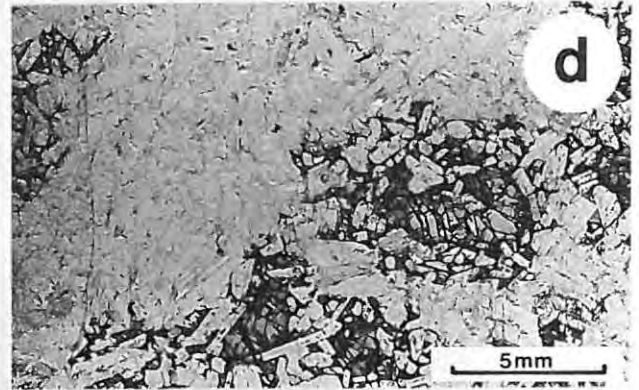
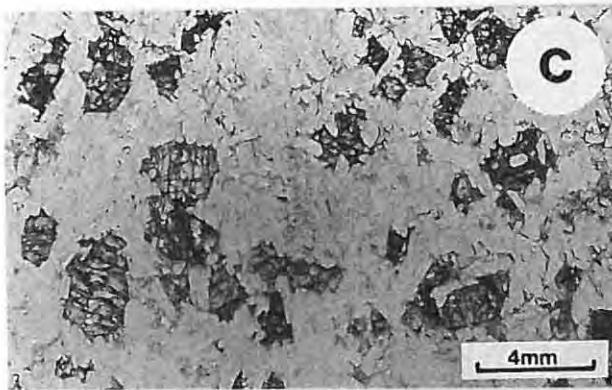
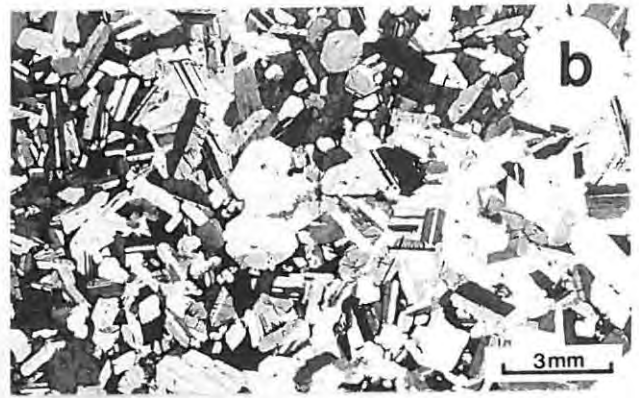
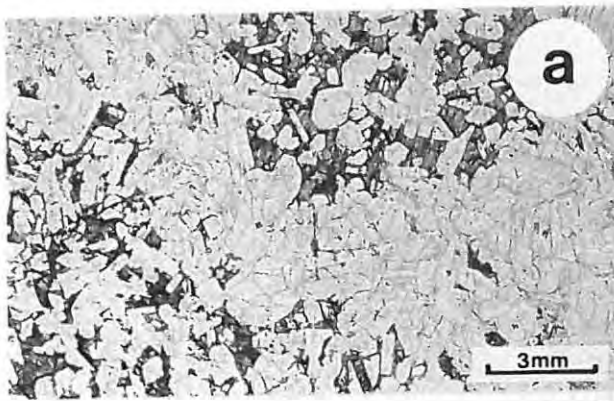


Plate 2:1 **a & b** B-15 anorthosite with opx mottles and small plag crystals enclosed. Large plag crystals where opx absent. **c** F-15 an average norite. **d** M-8 leuconorite showing plag crystals enclosed around the fringes of the opx. **e** F-13 norite with remnant olivine in top right corner rimmed by opx. an outer rim of exsolved opx enclosing plag is also present. **f** M-4 pyroxenite with textures discussed in text. **g** B-26 a large pigeonite crystal is successively surrounded by exsolved opx and then cpx. The latter minerals are interstitial to the plagioclase. **h** B-30 similar texture to B-26 but in this case earlier opx is surrounded by later exsolved opx in a different orientation. For further discussion of **a** to **h** see text.

major compositional variation of the minerals as determined by electron microprobe. The analyses used to compile the diagrams are listed in Appendix Two.

Mottled Anorthosite

The only primocryst phase in the mottled anorthosite is plagioclase which is often zoned and displays a range of grain sizes and a variety of textural features (Pl. 2:1). Where large pyroxene oikocrysts mantle the plagioclase primocrysts (heteradcumulate texture) the plagioclase grains are much smaller (0.3mm in diameter) and more euhedral although some overgrowth is visible. Where pyroxene is replaced by plagioclase as the interstitial phase (adcumulate texture), the size of the crystals, which are usually anhedral or subhedral, increases dramatically (1 to 1.5mm in diameter) and in some cases very large crystals up to 5mm in diameter are present. The volume occupied by these large crystals is similar to that occupied by several of the smaller poikilitically enclosed plagioclase crystals and their pyroxene host. The inference drawn from this observation is that if there initially were many smaller plagioclase crystals of the size enclosed in the mottles, these have subsequently been absorbed, or replaced by the larger grains. Similar features have been noted by Reynolds (1979) in oxide ores of the Bushveld Complex and other layered intrusions and are attributed by him to sintering and grain growth in the solid state. Willemse (1969) and McBirney and Noyes (1979) have also described this phenomenon. Zoning is common in the plagioclase crystals and is of various types. In some cases multiple oscillatory zoning of large crystals is present possibly indicating a rapidly changing environment. The euhedral outlines of the zones suggest that the crystals grew in a liquid without interference by other crystals. In other cases the zoning is more smoothly oscillatory and individual zones may be truncated by adjacent crystals. In this case the zones number about three or four. The outer zone is often discontinuous and very limited in extent. The range in the composition of plagioclase from a single thin section, which includes the zoning, is An₆₄ to An₇₄ in sample B-30 and the minimum An₇₆ to An₇₉ in B-10. In general, the range in An content of plagioclase from samples of mottled anorthosite is greater than that of the norites, but less than the interstitial plagioclase of the pyroxenite and pegmatoid.

The interstitial (intercumulus) material is dominantly plagioclase (dealt with above), ortho- and clinopyroxene. Other interstitial phases usually intimately associated with the pyroxene are biotite and ilmenite. Very small amounts of amphibole are occasionally present. The texture of the interstitial pyroxene is extremely variable. Where there is only orthopyroxene present it occurs as large ovoid to irregular oikocrysts ("mottles") up to several centimetres in diameter. These oikocrysts enclose numerous small plagioclase crystals less than one millimetre in diameter. These large orthopyroxenes are usually clear and show very little exsolution. At the outer fringes of these large orthopyroxene plates some small clinopyroxene crystals may be present as a discontinuous mantle of interstitial material similar in morphology to the orthopyroxene. Where more clinopyroxene is present this peripheral mantle on the orthopyroxene plates may be more continuous, but in some cases a separate large clinopyroxene oikocryst adjacent to the orthopyroxene may be present.

Clinopyroxene is usually associated with other interstitial phases like biotite and ilmenite. The biotite is variable in colour and composition ranging from a fox-red titanium-rich type to a green titanium-poor variety (Table 2:6). The mica occurs as discrete interstitial crystals and as fringes on both ortho- and clinopyroxene within the large oikocrysts. The red and green varieties may be present in a single thin section indicating short range chemical disequilibrium or isolation when these phases crystallized. The presence of ilmenite and mica indicate an enrichment in incompatible components (Ti, K & H₂O) in the anorthosite containing these phases. Where mica and more abundant clinopyroxene are present in a thin section, there is a suggestion that both the pyroxenes are more exsolved. Occasionally minute platelets of biotite occur parallel to the exsolution lamellae within the pyroxene crystals. This phenomenon is especially noticeable in the clinopyroxene at the top of the Bastard mottled anorthosite.

Within the Bastard mottled anorthosite, some leuconorite may be present which has some distinctive features as exhibited by sample B-22 and B-26. In the former specimen orthopyroxene primocrysts (2mm in diameter) are surrounded by small plagioclase primocrysts (.25mm in diameter) set in a zone of interstitial orthopyroxene 2mm to 3mm wide that is optically continuous with the primocryst orthopyroxene. All the orthopyroxene is clear and unexsolved. Where there is no interstitial orthopyroxene present, the plagioclase primocrysts are about 1.5mm in diameter. Higher up

in the Bastard mottled anorthosite, sample B-26 Pl.2:1g displays a similar gross texture to B-22 but the surrounding interstitial pyroxene is strongly exsolved and consists of inverted pigeonite with a markedly more iron-rich character. The core has a composition of about $Wo_2:En_{65}:Fs_{33}$ and the exsolved rim $Wo_1:En_{58}:Fs_{41}$. This is in turn surrounded by small plagioclase primocrysts (similar to sample B-22). The interstitial phases associated with the plagioclase primocrysts consist largely of strongly exsolved clinopyroxene ($Wo_{41}:En_{39}:Fs_{20}$) together with smaller amounts of ilmenite and biotite. Farther up in the succession (B-30 Pl.2:1h) remnant orthopyroxene is surrounded by exsolved orthopyroxene in a different crystallographic orientation but the composition is constant ($Wo_2:En_{58}:Fs_{40}$).

Norite

The orthopyroxene and plagioclase primocrysts of the norites display a wide range of grain sizes and textures Pl.2:1c. In most cases the norite sensu stricto has an equigranular texture Pl.2:1c. The plagioclase of the leuconorites and mottled leuconorites has a similar appearance to that in the mottled anorthosites described above. The scattered pyroxene primocrysts acted as nuclei for further pyroxene growth and the outer zones of these grains become interstitial to small plagioclase primocrysts as in the mottled anorthosites Pl.2:1d. This phenomenon was noted by McBirney & Noyes (1979) in their study of the Skaergaard intrusion. In some cases the outer mantle to the orthopyroxene enclosing the plagioclase is clinopyroxene. Enrichment in interstitial mica, clinopyroxene and ilmenite is fairly common in leuconorite samples but less so in norite sensu stricto.

Three samples of norite from the Footwall unit (F-1, F-13 & F-27) show minor relict olivine which has largely been replaced by orthopyroxenes Pl.2:2c. The rocks may thus initially have been troctolites or olivine norites following the petrographic nomenclature convention used here. The olivine occurs as isolated rounded remnant grains which may be quite large in some cases. Sample F-13 (Pl.2:1c) has features indicating disequilibrium. Olivine is surrounded by orthopyroxene and magnetite. Clinopyroxene and biotite are additional phases. This rock is discussed in detail in a later section in this chapter.

Pyroxenite

Euhedral to subhedral pyroxene primocrysts make up the bulk of the rock and the interstitial minerals are largely plagioclase with subor-

dinate amounts of clinopyroxene, biotite and sulphide in order of decreasing abundance. At the base of the pyroxenite layers some primocryst chromite may become a significant additional phase. The structural contacts between mutually impinging orthopyroxene primocrysts are relatively straight, but not necessarily rational crystal faces Pl.2:1f. However, where a different phase (clinopyroxene, plagioclase or biotite) is in contact the crystals have a euhedral outline. The interstitial plagioclase often occurs as very large plates (sometimes more than 10mm in diameter) enclosing the primocrysts in a way reminiscent of pyroxene mottles in the anorthosite. Clinopyroxene is an interstitial phase and where large oikocrysts of this mineral enclose euhedral to subhedral orthopyroxene chadacrysts, the rock has a pseudo-porphyrific appearance on a hand specimen or outcrop scale. Biotite occurs as platelets on orthopyroxene grain boundaries and mantling interstitial sulphide grains. Biotite also occurs as an interstitial phase similar to the plagioclase and in this case may be associated with very small amounts of orthoclase and quartz. The larger biotite crystals often enclose zircon crystals with pleochroic haloes surrounding them. Most of the biotite in the pyroxenite is the red titanium-rich variety, which in some cases contains significant amounts of chromium (Appendix Two F).

A very detailed petrofabric study of the Merensky pyroxenite (referred to as the "Merensky reef") by Schmidt (1952) established the fact that the pyroxene was aligned with its largest face parallel to the layering. This was also shown to be true of the Merensky mottled anorthosite. The average grain size (as seen in hand specimen) appears to be distinctly coarser for the pyroxenite and mottled anorthosite while the norite is finer grained. Maaløe (1978) noted similar grain size variations in the Skaergaard intrusion. Irvine (1980b) records vertical and horizontal fabrics in the layering of the Muskox intrusion but this is not obvious in the rocks of the study section except for the igneous lamination noted above. Schmidt (op. cit.) also noted an upward increase in the Fs content of orthopyroxene and the Ab content of interstitial plagioclase. The former is confirmed by the present study. Other features noted by Schmidt are the elongation of pyroxene crystals of the Merensky pyroxenite parallel to pothole walls which he attributed to current action. An

analysis of the histograms provided by Schmidt by this author using the techniques of Sinclair (1976), revealed that the orthopyroxene grain sizes are log normally distributed with an average of 5.8mm^2 . Schmidt noted that there is little difference in the grain size between normal and disturbed areas, but that the elongation of the pyroxenes (also lognormal) is greater in the potholes.

Pegmatoid

Detailed descriptions of the Merensky pegmatoid, and the pegmatoid boulders in the Boulder Bed are given by Vermaak & Hendricks (1976), Vermaak (1976a) and Lee & Sharpe (1980). Briefly, the pegmatoids are essentially very coarse feldspathic orthopyroxenites which sometimes contain significant amounts of olivine and are thus harzburgites in some cases. The texture is similar to that of the pyroxenite described above, the difference being the large grain size. Vermaak & Hendricks (op. cit.) note that the rock has a bimodal grain size distribution of the primocryst orthopyroxene, with ovoid masses of large crystals surrounded by smaller grains. The interstitial plagioclase also has a large grain size and zoning is common, but not ubiquitous. The maximum grain size of the normal Merensky pegmatoid is still in dispute, but Vermaak & Hendricks quote a figure of 1.29cm for large orthopyroxenes. The very large grain sizes quoted by Wagner (1929), Schmidt (1952) and Van Zyl (1960 & 1970) were attributed by Vermaak & Hendricks (op. cit.) to volatile-induced growth in potholes. Vermaak & Hendricks also state that the Merensky pegmatoid (referred to by them as the "Merensky reef") has a distinctly higher clinopyroxene content than the overlying Merensky pyroxenite, and that an unpublished petrofabric study of orthopyroxene failed to reveal any preferred orientation (cf. the Merensky pyroxenite).

Ultramafic pegmatite

These rocks are normally composed almost entirely of a relatively iron-rich clinopyroxene ($\text{Wo}_{44}:\text{En}_{54}:\text{Fs}_{16}$) with a mosaic texture. There is a large grain size variation between samples from the same occurrence ($\sim 1\text{cm}$ to $\pm 5\text{cm}$). Interstitial minerals include biotite, plagioclase, magnetite and sulphide (largely pyrrhotite). The pyroxene shows extensive alteration at the grain boundaries which could possibly be attributed to fluid action.

Chemistry of Rocks and Minerals

Strontium Isotope Data of Rocks and Minerals

A selection of whole rock and plagioclase samples were analysed for their $^{87}\text{Sr}/^{86}\text{Sr}$ ratios by J.S. Marsh at the Open University. Sr and Rb were determined by the author using high precision WD-XRF at Rhodes University (Appendix Three). These results and calculated initial $^{87}\text{Sr}/^{86}\text{Sr}$ ratios assuming an age of 2.1Ga for the Rustenburg Layered Suite (Hamilton, 1977) have been published (Kruger & Marsh, 1982) but are presented here in Table 2:1 and in Fig. 3:1.

The main features to be noted are the dramatic difference in the initial ratio of the Footwall unit samples as opposed to those of the Bastard cyclic unit (F- and B- samples respectively). The Merensky cyclic unit has variable initial ratios recorded in the mineral separates and whole rocks. The interstitial plagioclase (IPL samples) from the Merensky pegmatoid and pyroxenite have initial ratios close to those of the Footwall unit, whereas plagioclase that is dominantly primocrystic from the Merensky mottled anorthosite has initial ratios approaching those of the Bastard cyclic unit. The interpretation of these results is presented in Chapter Three.

Whole Rock Chemistry of the Merensky Cyclic Unit

A suite of whole rock samples from the Merensky cyclic unit and the pegmatoid were analysed to give an indication of their composition for comparison with the mineral data obtained with the electron probe.

All the analytical results are presented in Table 2:2. These were determined using the methods briefly outlined in Appendix Three. Inspection of this table reveals several features. Firstly, the major and some of the minor elements reflect the mineralogy of the rocks. Pyroxenite and pegmatoid samples have high MgO, Fe (expressed as Fe_2O_3) and SiO_2 concentrations, while the anorthosites have high Al_2O_3 , CaO, Na_2O , and SiO_2 . The norite (M-6) has intermediate characteristics. The only parameter not directly linked to the modal proportions of minerals is the Mg# (Mg-number) of the samples, which shows a steady upward decrease from 0.77 at the base to 0.55 at the top of the cyclic unit. The Merensky pegmatoid has an average Mg# of 0.78. The Mg# of the rock is directly linked to the MMF* ratio of the pyroxenes (discussed below), as these are the dominant Mg- and Fe-bearing phases.

* The ionic ratio $\text{Mg}^{2+}/(\text{Mg}^{2+} + \text{Fe}^{2+})$ of minerals is abbreviated to MMF in this work.

Table 2:1 Strontium Isotope Data of Rocks and Minerals

	$^{87}\text{Sr}/^{86}\text{Sr}\#$	Rb ppm \S	Sr ppm \S	Rb/Sr	R_0^\dagger
B-30 Cpl*	.70872±4	4.7	398	.0118	.70771
B-25 Cpl	.70849±4	2.2	403	.0054	.70803
B-20 Cpl	.70819±4	2.7	392	.0070	.70760
B-10 Cpl	.70787±3	1.7	407	.0041	.70752
B-5 Pl	.70806±2	2.4	416	.0059	.70756
B-1 Ipl	.70806±4	2.6	385	.0067	.70749
M-12 WR	.70776±3	1.7	403	.0042	.70740
M-12 Cpl	.70757±3	1.2	419	.0029	.70732
M-10 WR	.70789±2	2.9	386	.0075	.70725
M-9 Cpl	.70765±4	1.4	425	.0033	.70737
M-8 WR	.70699±2	1.9	394	.0047	.70659
M-7 Cpl	.70731±4	1.2	392	.0030	.70705
M-6 WR	.70696±2	1.4	322	.0044	.70655
M-5 Ipl	.79723±4	4.4	469	.0094	.70643
M-4 Ipl	.79733±2	4.9	457	.0108	.70641
P-6 Ipl	.70665±2	1.7	497	.0033	.70637
RR-6 Cpl	.70661±3	1.3	477	.0027	.70638
RR-5 Cpl	.70672±4	2.1	483	.0044	.70634
F-27 Cpl	.70653±5	1.1	482	.0022	.70634
F-12 Cpl	.70663±4	1.3	486	.0027	.70640
F-4 Cpl	.70665±4	1.6	479	.0034	.70636

Present day $^{87}\text{Sr}/^{86}\text{Sr}$ ratio ± 2 s.e.m. NBS-987 = .71026±2 during this study. This ratio was determined by J.S. Marsh in the laboratory of C.J. Hawkesworth at the Open University, Milton Keynes.

§ Rb and Sr concentrations determined using high precision Wd-XRF, by the Author.

† Initial $^{87}\text{Sr}/^{86}\text{Sr}$ ratio (R_0) calculated using an age of 2.1Ga and Decay Constant of $1.42 \times 10^{-11} \text{ yr}^{-1}$ for ^{87}Rb .

* Cpl = plagioclase primocrysts enclosed in pyroxene; WR = whole rock; Ipl = interstitial plagioclase.

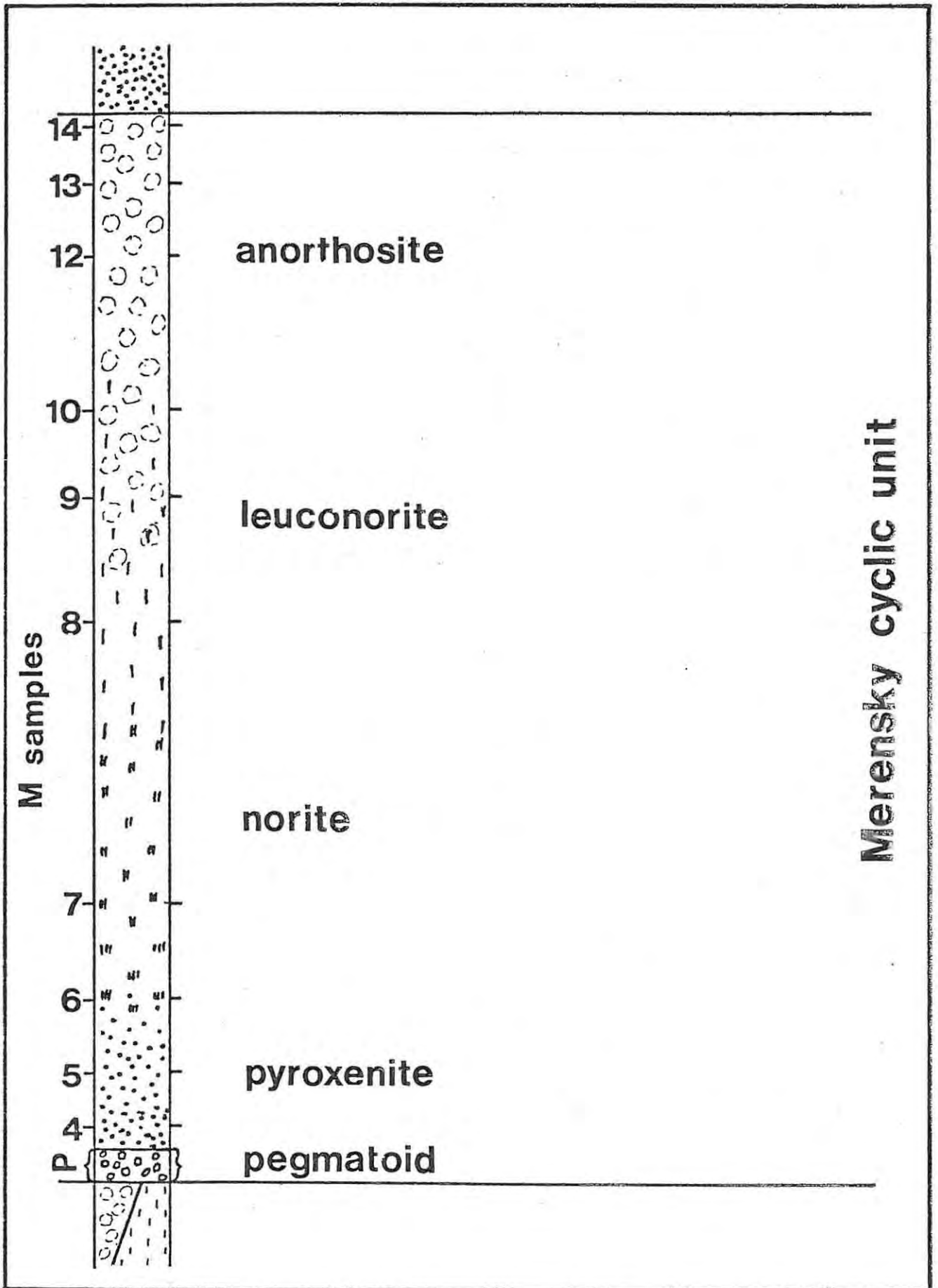


Diagram illustrating the rock types and relative positions of samples in Table 2.2 on the following page.

Table 2:2 Whole Rock Major and Trace Elements

	Major Elements									Total
	SiO ₂	TiO ₂	Al ₂ O ₃	Fe ₂ O ₃	MnO	MgO	CaO	Na ₂ O	K ₂ O	
M-4	52.59	0.235	5.57	13.48	0.21	22.49	4.64	0.67	0.11	100.00
M-6	50.31	0.109	22.46	5.45	0.09	7.90	11.61	1.94	0.13	100.00
M-7	49.39	0.068	28.87	2.26	0.05	2.61	14.36	2.19	0.16	100.00
M-8	49.30	0.076	27.90	2.64	0.47	3.04	14.32	2.10	0.16	100.00
M-10	49.33	0.075	29.54	1.93	0.04	1.98	14.73	2.19	0.19	100.00
M-12	48.69	0.041	31.06	1.28	0.03	0.94	15.68	2.13	0.15	100.00
M-13	48.86	0.048	31.25	1.19	0.02	0.74	15.56	2.15	0.19	100.00
P-3†	52.73	0.197	7.01	12.07	0.18	21.61	5.23	0.80	0.17	100.00
P-6	50.79	0.139	10.24	11.14	0.18	20.85	5.67	0.88	0.12	100.00
P-8	47.83	0.137	5.98	15.63	0.19	26.11	3.65	0.41	0.06	100.00
P-10	52.81	0.157	9.71	10.82	0.18	18.84	6.26	1.11	0.11	100.00
FEP-3†	49.77	0.407	4.57	12.80	0.21	13.54	18.35	0.35	----	100.00

	Trace Elements											
	Zn	Cu	Ni	Co	Cr	V	Rb	Sr	Y	Zr	Sc	Ba
M-4*	69.-	1663	3161	126.-	3046	139.-	4.9	68	10.2	22.-	30.-	45
M-6	34.-	274	556	46.-	827	64.-	1.4	322	5.2	5.9	13.-	72
M-7	13.5	76	147	16.4	228	26.7	1.5	394	1.8	2.9	5.6	89
M-8	15.3	56	128	18.7	336	35.-	1.9	394	3.8	7.0	7.1	72
M-10	10.6	45	96	12.5	175	24.-	2.9	386	4.4	7.3	5.3	85
M-12	7.0	32	41	7.7	39	14.3	1.7	403	2.2	2.6	2.8	69
M-13	13.0	97	168	8.4	26	11.6	3.2	417	3.1	5.7	2.5	88
P-3§	59.-	1068	4369	127.-	3474	128.-	9.7	87	53.3	26.-	27.-	43
P-6	62.-	665	2738	116.-	2757	94.-	5.5	132	4.9	15.6	ND	46
P-8	68.-	2396	7088	180.-	3744	98.-	3.9	71	4.7	12.0	17.-	30
P-10	60.-	1153	2197	97.-	2473	126.-	3.8	121	4.6	16.-	25.-	34
FEP-3†	367.-	576	413	91.-	926	883.-	--	31	16.6	10.7	87.-	ND

§ Analyses of the Merensky pegmatoid are not truly representative of of the whole rock due to the coarse-grained nature and small samples.

† Analysis of Ultramafic pegmatite from the Brakspruit area of the mine.

* M-4 contains 1.3ppm Nb. All the other samples had a lower concentration than the lower limit of determination.

The trace and minor elements determined fall in several groups with some overlap. The incompatible trace elements (Zr, Nb, Y) which are largely excluded from all the major phases are concentrated in the pyroxenite and pegmatoid possibly indicating a greater proportion of trapped interstitial liquid or later enrichment. Ba is more concentrated in the anorthosites by a factor of two indicating a greater affinity for plagioclase or the presence of small quantities of alkali feldspar. Sr is highly concentrated in the anorthosites due to its high affinity for plagioclase. Almost all the Sr is contained in plagioclase where the mineral occurs as an interstitial or as a primocryst phase.

Potassium and rubidium are closely linked and are contained in different phases in different rock types. In the pyroxenite and pegmatoid mica and a small amount of alkali feldspar are the main hosts for these elements, although some is contained in the major phases. In the anorthosites, however, these elements are contained mainly in plagioclase, although some is contained in accessory alkali feldspar and mica.

The mafic minerals of the rocks are hosts for Ni, Co, Cr, V, Sc, Zn, Ti and Mn, and for this reason the concentrations of these elements are high in the mafic rocks. Cr is strongly influenced by the presence of chromite in the pyroxenite and pegmatoid samples.

The chalcophile elements (Ni, Cu, Co) are strongly influenced by the presence of sulphide in the lower part of the pyroxenite and the pegmatoid. For this reason the concentrations of these elements are abnormally high in the rocks containing sulphide.

A comparison of cross-cutting ultramafic pegmatite (FEP-3) with the Merensky pegmatoid indicates that there are very significant differences.

CaO content is very high in the ultramafic pegmatite, but MgO is distinctly lower. In the concentrations of the trace elements Zn, V and Sc are strongly enriched in the ultramafic pegmatite relative to the pegmatoid.

Electron Microprobe Analyses of Minerals

It is not possible to describe and discuss all the parameters of all the minerals in all the samples that have been determined in this study.

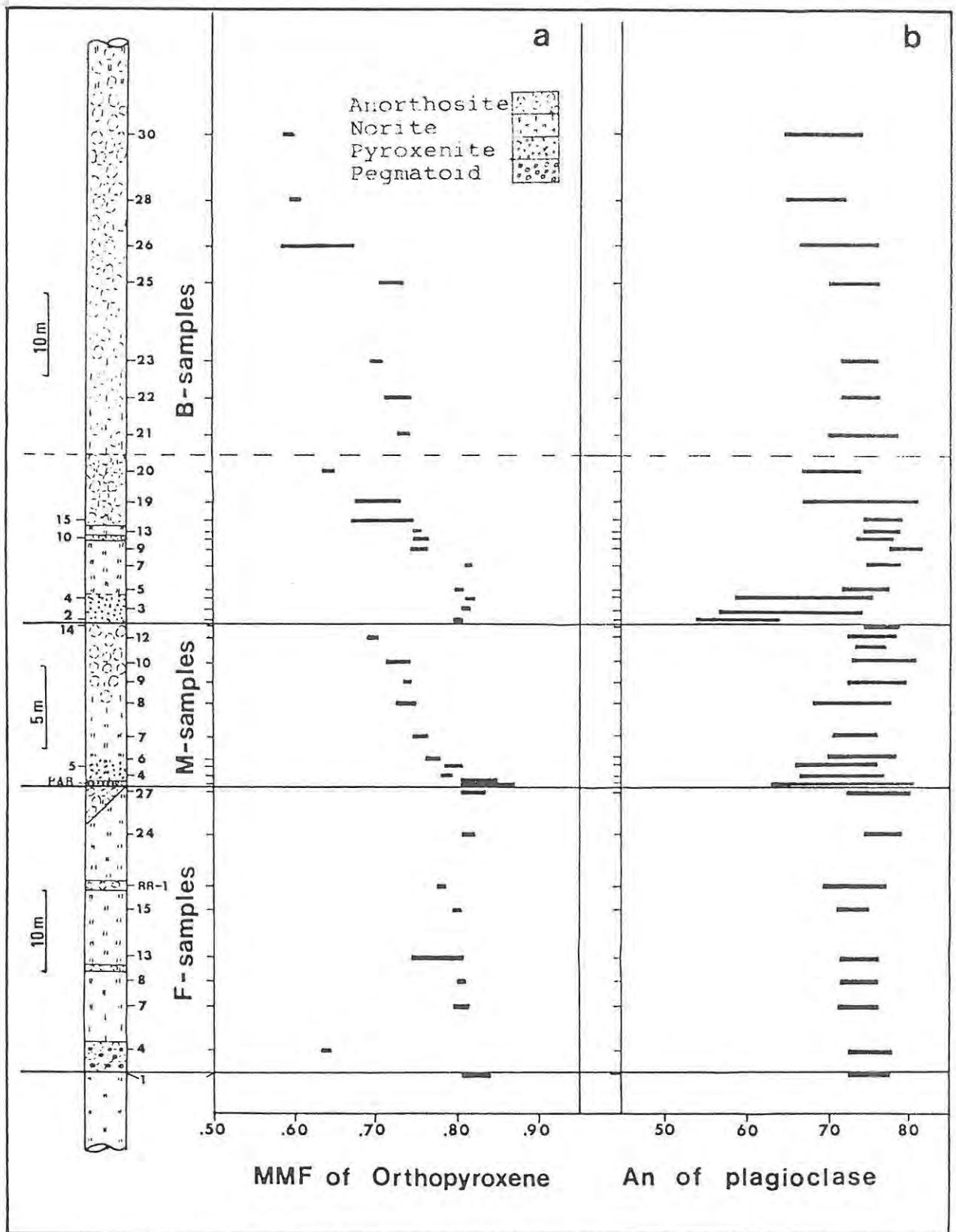


Fig. 2:3 This diagram shows the variation with respect to height of a the MMF ratio of orthopyroxene and b the An content (%) of plagioclase determined using the electron microprobe. Each horizontal bar of a represents the range of between 4 and 8 point analyses, and each bar of b between 8 and 16 analyses. For detailed discussion see text.

The chemical variations in the minerals plagioclase and orthopyroxene are discussed in detail as these minerals are the dominant phases in the study section. The analyses of all the minerals are listed in Appendix Two A (Plagioclase), B (Orthopyroxene), C (Clinopyroxene), D (Chromite), E (Olivine), F (Biotite), G (Other). Details of analytical procedures and standards are presented in Appendix 1.

The MMF ratio of Orthopyroxene (Fig. 2:3a)

Examination of the MMF_{opx} versus height diagram (Fig. 2:3a) reveals several features. Firstly, the Footwall unit has sparsely distributed data points considering the lithological variations. If only primocryst orthopyroxenes in the norites are considered, there is a general upward increase in the MMF ratio, (except for sample F-1 at the base of the unit, the analyses of which are from below the thin chromitite layer and thus are strictly speaking outside the Footwall unit). The data available do not allow the identification of any trends within the norites. The interstitial orthopyroxene of sample F-4 is very much more iron-rich than the orthopyroxene primocrysts from sample F-1, but it is unknown whether the interstitial orthopyroxenes changes composition with height in the Boulder Bed. It is also unknown whether there are any trends in the Footwall mottled anorthosite.

There is a general upward decrease in the MMF ratio of orthopyroxenes in the Merensky cyclic unit. This feature is not only related to the lithology, as the trends are well established within each of the rock types of the cyclic unit (pyroxenite, norite, anorthosite). This decrease in the enstatite content of orthopyroxene within the Merensky pyroxenite was also established by Schmidt (1952).

The orthopyroxenes of the Bastard cyclic unit also display an upward decrease in the MMF ratio, but there is a distinct break between samples B-20 and B-21. This break coincides with the reappearance of some primocryst orthopyroxene. If this leuconorite is laterally persistent, a new cyclic unit should be defined, the base of which should be marked by the first appearance of primocryst orthopyroxene. The Bastard mottled anorthosite would then be only $\pm 10\text{m}$ thick in the Rustenburg area. Orthopyroxenes from the Bastard pyroxenite show an upward increase in their MMF ratio, and in this aspect differ from those in the Merensky pyroxenite. Within the Bastard norite, sample B-7 contains anomalously Mg-rich ortho-

pyroxenes, but above this position there is a general upward iron-enrichment of the orthopyroxenes. Similarly, from sample B-21 upward, there is also a general decrease in the MMF ratio of the orthopyroxenes.

Within the study section some samples display an anomalous spread in the MMF ratio of the orthopyroxenes, notably F-13, B-15 and B-26. These samples are discussed further below. In general the average spread in the MMF ratio of the pyroxenes from a single sample is less than 3% (e.g. .74 to .76). In Chapter 4 it is shown that most primocrysts have undergone sub-liquidus re-equilibration with the interstitial liquid to more iron rich compositions than those initially present. It is also shown that the presently most magnesium primocrysts were associated with the most interstitial liquid and were thus changed to a greater degree. The trends now displayed would thus have been emphasized at the liquidus stage.

The Anorthite content of Plagioclase (Fig. 2:3b)

The zoning within the plagioclase of the study section produces a wide spread in the anorthite content of plagioclase of individual samples. This spread normally averages about 5mol percent, but can be considerably greater especially in the interstitial plagioclase of the pyroxenite where a range of more than 15mol percent is recorded (e.g. B-3 and B-4). In general the interstitial plagioclase of the Merensky pyroxenite and pegmatoid and the Bastard pyroxenite is more sodic than the plagioclase from the norites and anorthosites. This effect is very marked in the Bastard pyroxenite and more subdued in the Merensky pyroxenite and pegmatoid.

The zoning of plagioclase in the norites and anorthosites is of a smoothly oscillatory type with a suggestion that only three zones are dominantly present. The cores of the crystals are not necessarily more calcic or the rims more sodic. A true "core" or "rim" composition is difficult to discern. The zoning patterns need very careful study on a limited number of sections and this data is not available for this work. For this reason only an overall variation has been determined.

There is little between sample variation in the anorthite content of plagioclase of the Footwall unit and no marked trends can be discerned. There is however a suggestion of a decrease in the anorthite content of plagioclase from the base of the Boulder Bed (An₇₅) to the Footwall marker (An₇₂). In samples above the Footwall marker the plagioclase

crystals have an average composition of $\pm\text{An}_{76}$.

Within the Merensky cyclic unit, (M-6 to M-14) there is a suggestion of an upward increase in the An content of plagioclase as suggested by van Zyl (1960; 1970), and Meyer (1969) and later used by Vermaak (1976a). This is however not clear as there is a very wide scatter due to zoning.

Within the Bastard norite there is more definite evidence for an upward increase in the An content of plagioclase from sample B-5 (An_{75}) to sample B-9 (An_{79}), but a definite upward decrease in the anorthite content of plagioclase above sample B-9 to sample B-20 (An_{72}). Thus there is no unequivocal evidence for an upward increase in the anorthite content of plagioclase of the mottled anorthosites of either the Merensky or Bastard cyclic units.

Between samples B-20 and B-21 there is a break in the upward decrease of the anorthite content of plagioclase. Plagioclase from B-21 has an average composition of An_{75} . From B-21 to B-30 there is a steady upward increase in the anorthite content of plagioclase to An_{69} . There is also an increase in the spread of anorthite contents of plagioclase to 10 mol percent at B-30. The break between B-20 and B-21 is also reflected in the reappearance of primocryst orthopyroxene, the MMF ratio of the orthopyroxene discussed previously, and also the minor element content of orthopyroxene discussed below.

The Manganese content of Orthopyroxene (Fig. 2:4a)

The MnO content of orthopyroxene has trends that are inverse to the MMF ratio. This is due to the close association of MnO with FeO. In the Footwall unit there is little variation in the MnO content of the orthopyroxene although there is a suggestion of an upward decrease from 0.32% in F-7 to 0.24% in F-27. The interstitial orthopyroxenes of sample F-4 are strongly enriched in MnO.

Within the Merensky cyclic unit the MnO concentration in orthopyroxene rises from about 0.25% at the base to about 0.42% in the interstitial orthopyroxene at the top of the Merensky mottled anorthosite.

In the Bastard cyclic unit the MnO concentration of orthopyroxene shows a slight decrease from the base of the unit (0.28%) to sample B-7 (0.26%). Above sample B-7 there is an increase to 0.48% in the orthopyroxene of sample B-20. Between samples B-21 and B-22 there is a distinct break, the primocryst orthopyroxenes of the latter sample having a MnO

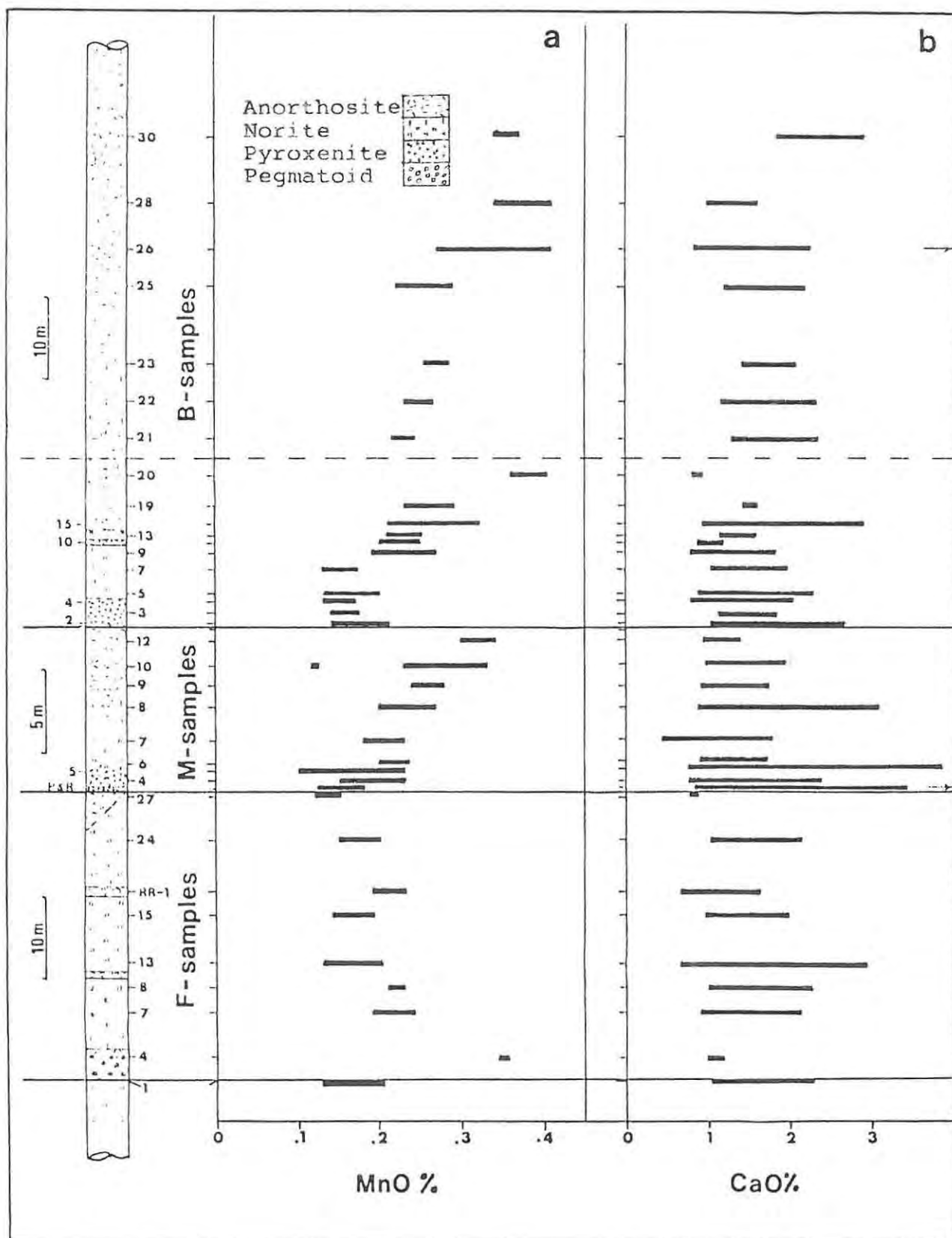
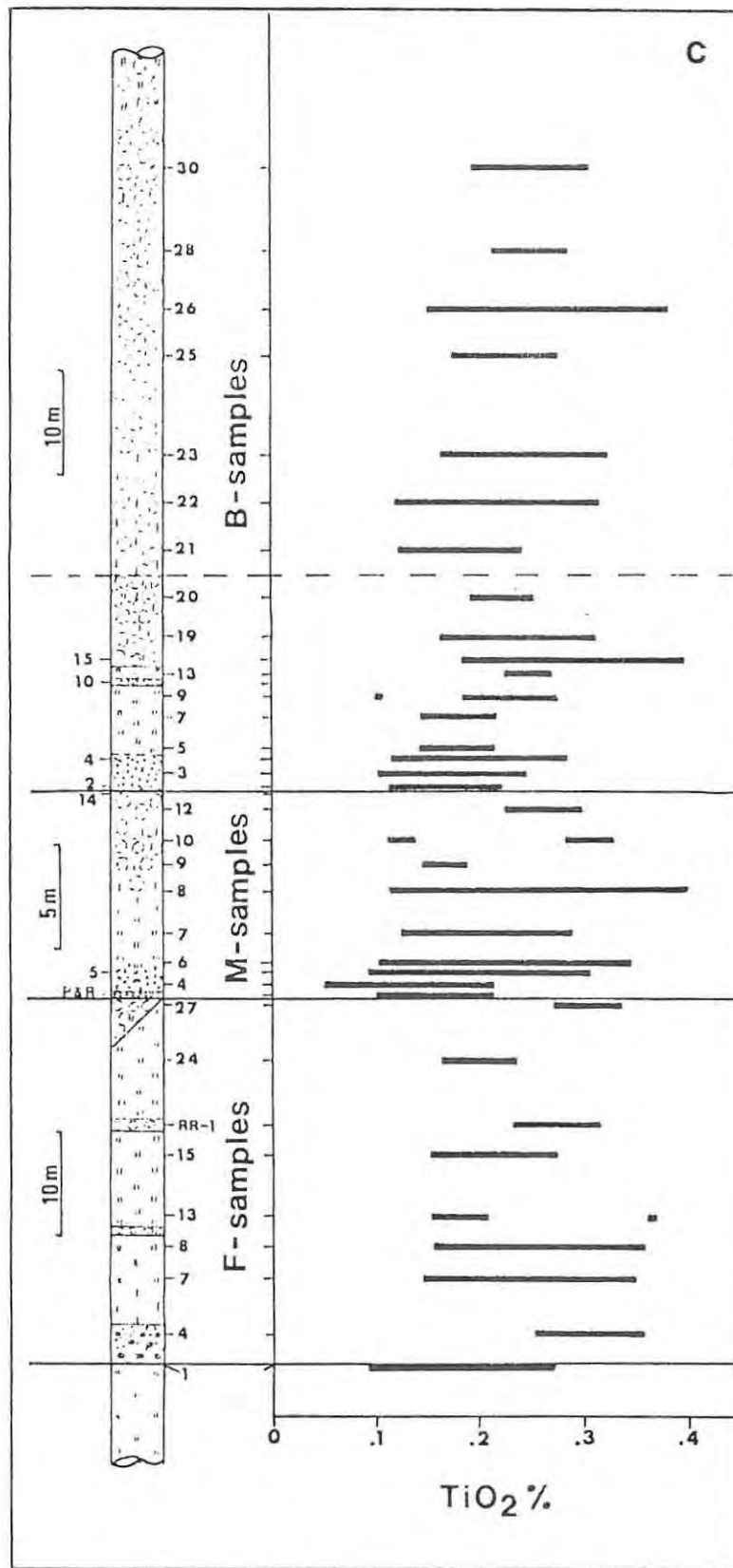
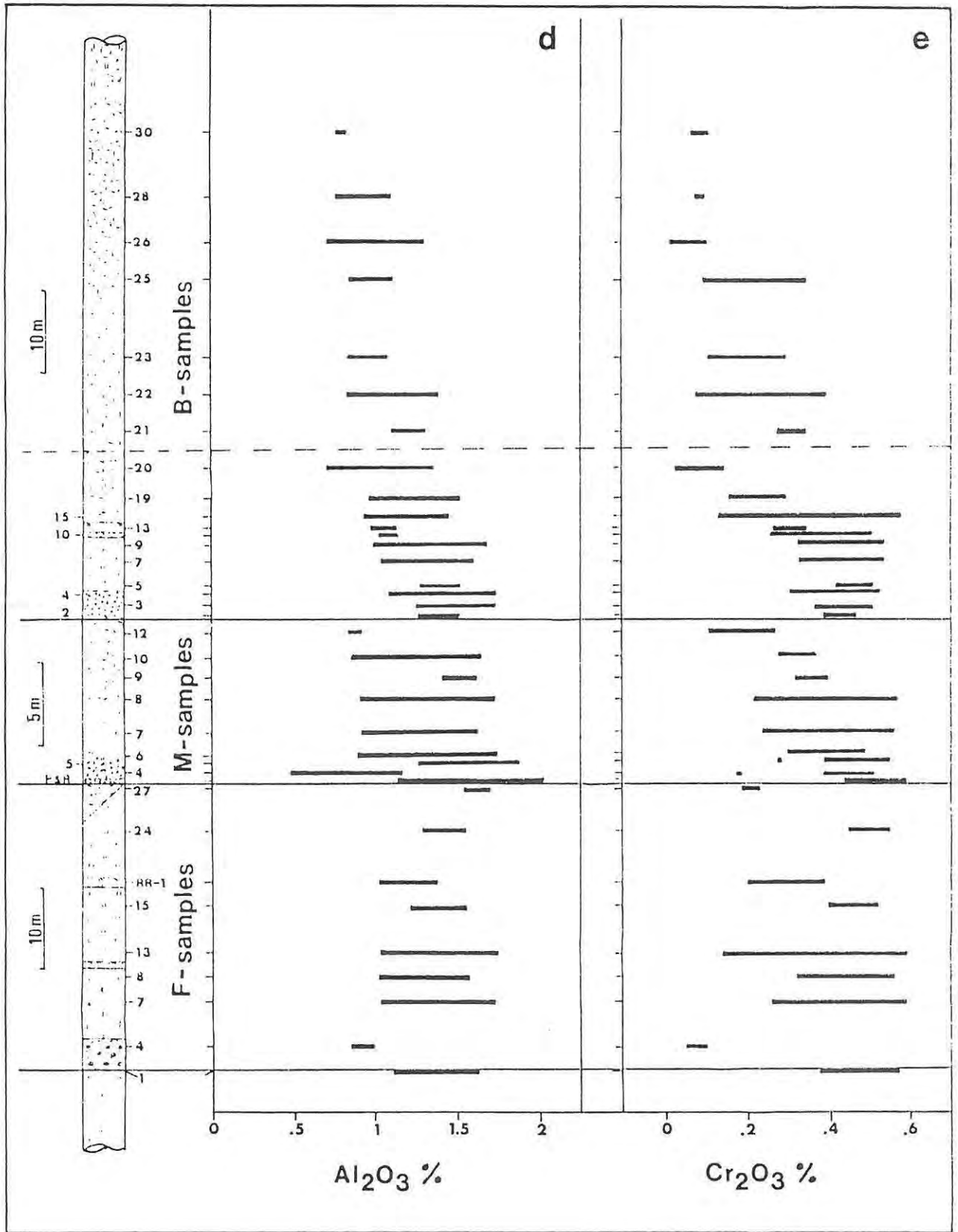


Fig. 2:4 These diagrams a, b, c, d & e (on this and the following two pages) represent the variation in the concentrations of the minor components (MnO, CaO, TiO₂, Al₂O₃ & Cr₂O₃) in orthopyroxene with respect to height in the succession. Each horizontal bar indicates the compositional range encountered in a single section. Where a single analyses falls well away from the main group, it has been plotted as a single point. The two small arrows on the right of b indicate pyroxenes with more than 4% CaO. The dashed line between B-20 and B-21 indicates the possible upper boundary for the Bastard cyclic unit. For detailed discussion of these diagrams see text.





concentration of 0.33%. Above sample B-21 there is a general upward increase in the MnO concentration to 0.46% in the orthopyroxene of sample B-30. There are some irregularities in this overall increase shown by samples B-25 and B-26.

The Calcium content of Orthopyroxene (Fig. 2:4b)

There is a considerable scatter of CaO concentrations of orthopyroxene displayed by individual samples of the study section. There are also no clearly discernable trends with respect to height in the succession displayed by the data. Much of the scatter is probably due to inhomogeneity produced by exsolution of the crystals, but some zoning is also present (see discussion of sample M-8 below). Inhomogeneity is emphasized as analyses were obtained with a focussed beam, and exsolution lamellae were avoided.

The Titanium content of Orthopyroxene (Fig. 2:4c)

There is a great deal of scatter in the TiO₂ concentrations of orthopyroxenes from individual samples. This is partly due to the poor precision of determination at very low concentrations, but probably mostly due to inhomogeneity due to zoning (see the discussion of sample M-8 below). Within the Footwall unit there are no clearly defined trends, and more work is needed. The TiO₂ concentration of orthopyroxene appears to increase with height in the Merensky cyclic unit, but this is not clearly defined.

The Bastard cyclic unit as defined for this work displays two possible trends of upward TiO₂ enrichment in orthopyroxene, with the break between the two situated between samples B-20 and B-21.

The Aluminium content of Orthopyroxene (Fig. 2:4d)

A considerable scatter of the Al₂O₃ concentrations of the orthopyroxenes from individual samples is evident in Fig. 2:4d. In the Footwall unit no consistent trends with respect to height in the succession are present. The orthopyroxenes of the Merensky cyclic unit also do not show any well defined pattern, but there is a suggestion of an upward decrease in the Al₂O₃ concentration of the orthopyroxene. Within the Bastard cyclic unit there is a consistent decrease in the Al₂O₃ concentration of orthopyroxene upward in the succession. The distinct break between samples B-20 and B-21 exhibited by other elements is not clear in this case.

The Chromium content of Orthopyroxene (Fig. 2:4e)

As with Al_2O_3 discussed above the orthopyroxenes from individual samples are very heterogeneous with respect to Cr_2O_3 . However, distinct overall trends in the Cr_2O_3 concentrations are evident in the Merensky and Bastard cyclic units. There is no consistent trend displayed by the available data in the Footwall unit.

In the Merensky cyclic unit, the average Cr_2O_3 concentrations of the orthopyroxenes decrease from $\pm 0.5\%$ at the base of the cyclic unit to $\pm 0.15\%$ at the top of the unit. This is clearly a generalization as considerable zoning is present and the "core" compositions may indicate contrary trends (cf. samples M-5 and M-8).

The Bastard cyclic unit again displays a break between samples B-20 and B-21 (average Cr_2O_3 concentrations are .1% and .3% respectively). In the lower portion of the Bastard cyclic unit (the section below and including B-20), there is an increase in the Cr_2O_3 concentration of orthopyroxene from the base of the Bastard pyroxenite ($\pm .45\%$) to sample B-7 ($\pm .47\%$) and then a steady decline in the concentration to sample B-20. This is not a clearly defined trend due to the range in the compositions determined in each sample. The upper portion of the Bastard mottled anorthosite (sample B-21 upward), also shows a general decrease in the Cr_2O_3 content of orthopyroxene upward in the succession.

Chemistry of the Plagioclase Separates

The trace element concentrations of the mineral separates are presented in Table 2:3. The separations and analyses were carried out as outlined in Appendices Four and Three respectively. The elements of major importance are Sr which is concentrated in plagioclase and the group comprising K, Rb and Ba. The concentration of Sr in the plagioclase is relatively uniform in the mottled anorthosites and norites within the major units, where plagioclase is a primocryst phase, although there are differences between the units. Where plagioclase is an interstitial phase, the concentrations of Sr in the plagioclase are more variable. This is illustrated by Fig. 2:5. A further feature revealed by Fig. 2:5 is that the Sr concentration in plagioclase from the Footwall unit (excluding interstitial plagioclase) is distinctly higher than that from the Bastard cyclic unit. The Sr concentrations in plagioclase are more variable in the Merensky cyclic unit, and are generally intermediate between those of the

Table 2:3 Trace Elements in Plagioclase Separates

		Zn	Cu	Ni	Co	Cr	V	Rb	Sr	K	Ba
F-4	CPI	3.9	11.1	5.0	4.5	9.6	4.3	1.6	478	839	87
F-4	NMP	6.7	12.4	8.2	4.0	3.7	3.8	7.2	463	1629	96
F-3	PI	3.7	11.0	3.5	4.1	11.6	3.2	1.0	501	919	90
F-9	PI	2.8	11.1	8.7	3.1	6.5	2.6	1.1	486	830	91
F-12	CPI	4.4	10.1	8.7	3.7	17.9	4.3	1.3	486	785	73
F-12	NMP	5.2	9.7	5.8	3.3	--	3.1	2.7	482	1067	80
F-13	PI	3.5	13.0	15.4	4.4	12.5	2.7	2.3	517	876	103
F-19	PI	1.7	21.7	26.-	6.7	16.3	3.6	1.3	493	1368	105
F-24	PI	4.0	16.1	25.5	4.0	38.-	4.7	3.8	470	1307	115
F-27	CPI	3.1	190.-	129.-	5.8	12.-	2.7	1.1	482	722	66
F-27	NMP	5.9	147.-	165.-	8.1	61.8	8.8	2.3	466	1186	98
RR-5	CPI	3.1	13.9	8.3	3.4	3.3	3.0	2.1	483	930	74
RR-5	NMP	3.7	10.6	14.2	3.9	7.8	8.3	4.8	479	1389	84
RR-6	CPI	8.7	36.-	11.9	3.7	7.7	3.2	1.3	477	746	71
RR-6	NMP	4.6	14.2	6.4	3.7	--	6.9	2.1	471	957	76
P-3	IPI	3.2	8.1	9.3	2.7	101.-	4.2	1.0	496	1292	83
P-6	IPI	3.4	7.4	7.4	3.0	107.-	4.9	1.7	497	1242	96
P-11	IPI	8.2	46.-	24.-	4.0	--	2.5	3.5	471	1902	140
M-4	IPI	4.4	89.-	27.-	2.9	9.0	--	5.0	457	2562	151
M-5	IPI	3.3	124.-	71.-	4.0	14.1	3.0	4.4	469	2417	154
M-7	CPI	2.1	38.-	11.1	3.8	6.7	3.5	1.2	392	838	89
M-7	NMP	4.7	65.-	65.-	5.5	18.9	5.3	2.4	434	1031	94
M-8	CPI	4.6	28.-	10.3	3.1	14.6	5.9	1.5	462	848	63
M-8	NMP	4.1	45.-	47.-	4.7	7.7	6.3	2.1	451	1041	90
M-9	CPI	3.1	30.-	12.6	3.2	17.0	5.7	1.4	425	790	70
M-9	NMP	4.0	49.-	44.-	4.8	12.0	5.1	2.8	418	1074	75
M-10	CPI	3.8	27.-	12.9	2.7	8.8	3.9	1.2	422	827	81
M-10	NMP	4.5	35.-	44.-	4.5	3.7	7.6	3.3	419	1334	93
M-11	CPI	6.2	24.3	13.2	3.7	9.0	4.8	1.0	422	737	78
M-11	NMP	4.8	22.-	21.-	4.0	1.4	6.1	3.4	424	1489	92
M-12	CPI	3.9	23.3	12.4	4.0	4.2	4.3	1.2	419	605	66
M-12	NMP	5.7	17.5	14.7	4.3	9.3	6.9	1.9	419	850	80
M-13	CPI	30.-	265.-	151.-	7.6	9.3	4.0	2.8	451	1270	85
M-13	NMP	5.7	26.-	32.-	3.6	6.2	4.8	2.4	434	1056	74
M-14	CPI	6.1	378.-	112.-	5.8	6.1	2.7	4.6	445	1552	108
M-14	NMP	7.1	60.-	61.-	5.4	5.9	9.7	9.7	433	2812	135
B-1	IPI	8.0	69.-	31.-	4.2	9.9	2.6	2.6	385	1786	144
B-2	IPI	16.3	225.-	86.-	10.6	49.-	4.1	7.2	442	3661	222
B-3	IPI	3.7	81.-	32.-	5.5	42.-	4.2	9.0	414	3975	213
B-4	IPI	3.0	14.4	13.6	8.8	27.-	2.3	3.8	481	2686	202
B-5	PI	3.4	33.-	13.2	2.7	9.2	2.6	2.4	416	1113	92
B-10	CPI	3.3	24.-	15.3	4.0	16.-	4.4	1.7	407	611	71
B-10	NMP	3.9	9.0	7.7	3.9	6.7	8.0	2.2	404	1049	71
B-13	PI	2.7	14.0	11.2	4.0	29.-	4.9	--	390	864	70
B-15	CPI	4.3	18.3	13.4	3.4	19.-	5.6	0.6	401	572	73
B-15	NMP	3.4	10.9	10.3	4.5	6.8	4.9	4.7	400	1503	106
B-20	CPI	5.2	14.4	9.6	4.0	9.2	6.1	2.7	392	810	72
B-20	NMP	6.2	11.4	25.-	4.1	--	6.4	2.7	389	1105	78
B-25	CPI	10.0	16.6	11.9	4.8	9.6	6.4	2.2	403	1539	101
B-25	NMP	6.8	10.9	9.3	4.2	4.2	9.4	6.7	392	2133	103
B-30	CPI	6.4	18.3	5.8	3.4	--	5.7	4.7	398	2235	121
B-30	NMP	13.6	31.-	20.4	4.9	13.4	13.2	13.1	392	3942	170

Details of IPL, CPI and NMP separates are listed in Appendix 4

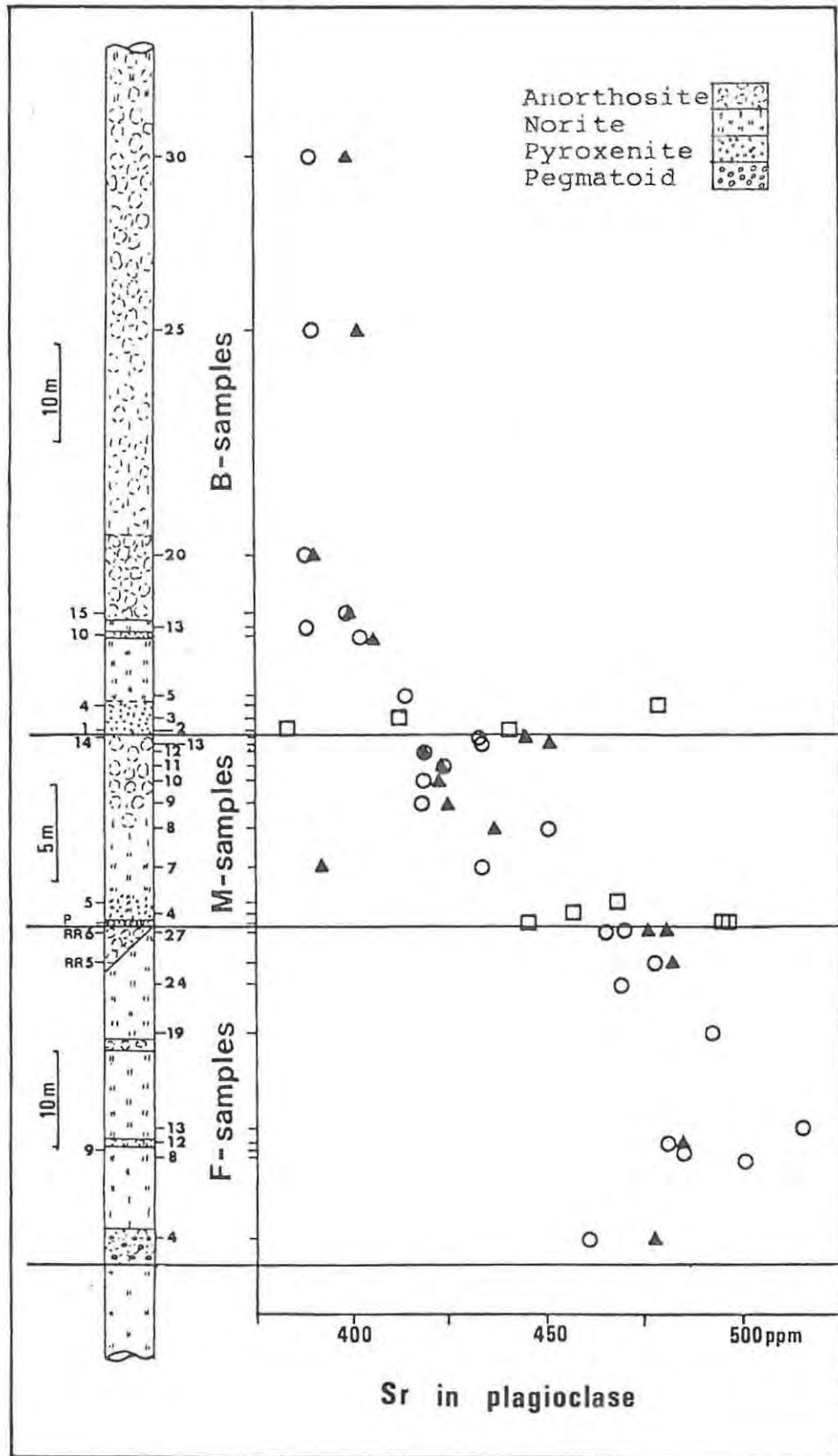


Fig. 2:5 Sr concentration of plagioclase separates with respect to height in the succession. NMP ○ ; CPL ▲ ; IPL □ . Note the differences in the concentrations of Sr in NMP & CPL separates from the Bastard, Merensky and Footwall units. The interstitial plagioclase (IPL) has a range of concentrations. For discussion see text.

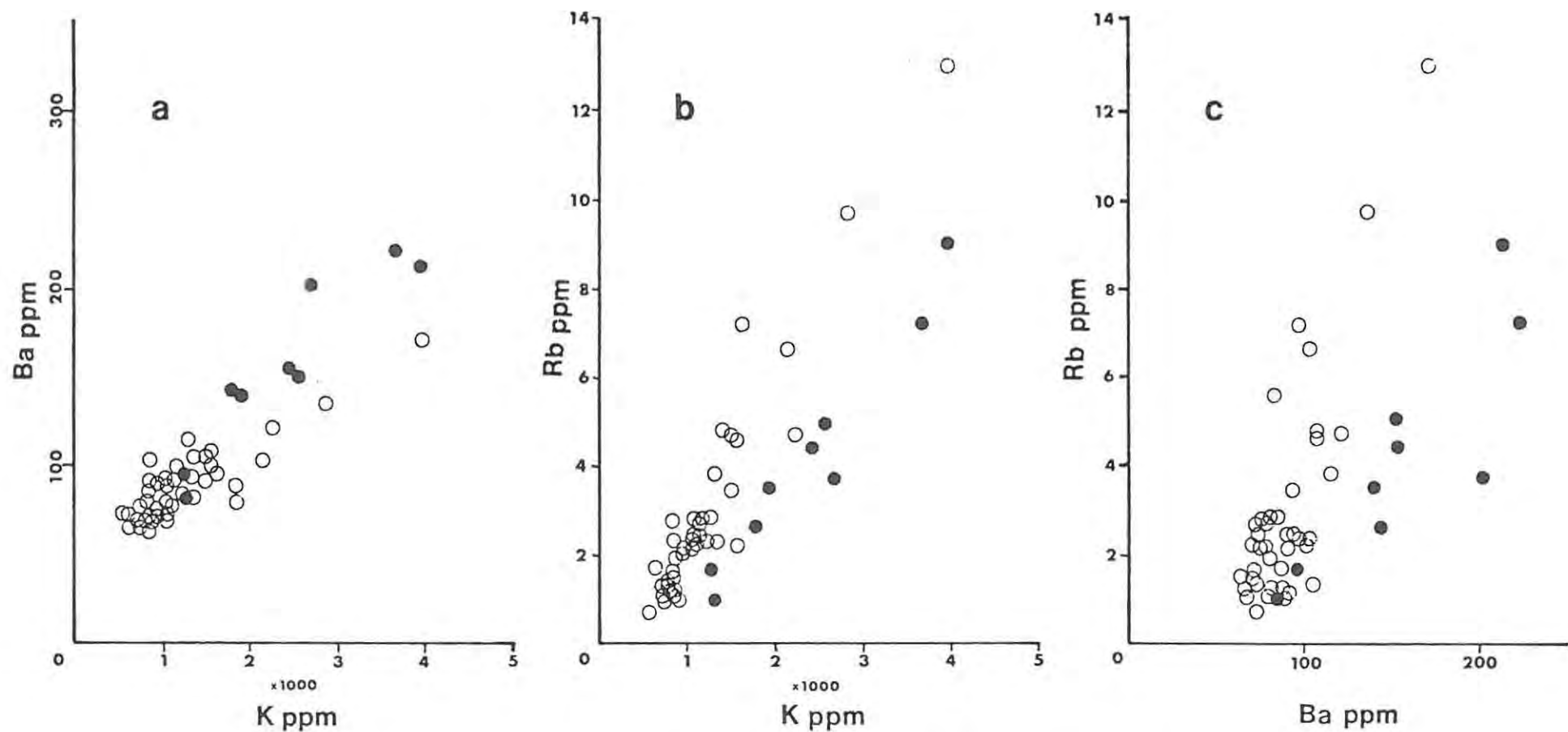


Fig. 2:6 These three diagrams (a, b & c) indicate the positive correlation among K, Rb and Ba in plagioclase separates. The high concentrations may be due to contamination by small quantities of alkali feldspar in the plagioclase separates. The reason for the apparent differences between interstitial plagioclase from pyroxenites (filled circles) and material (NMP & CPL) from the norites and anorthosites is still unclear. The precision of determination of each point (± 1 sigma) generally falls within the symbol.

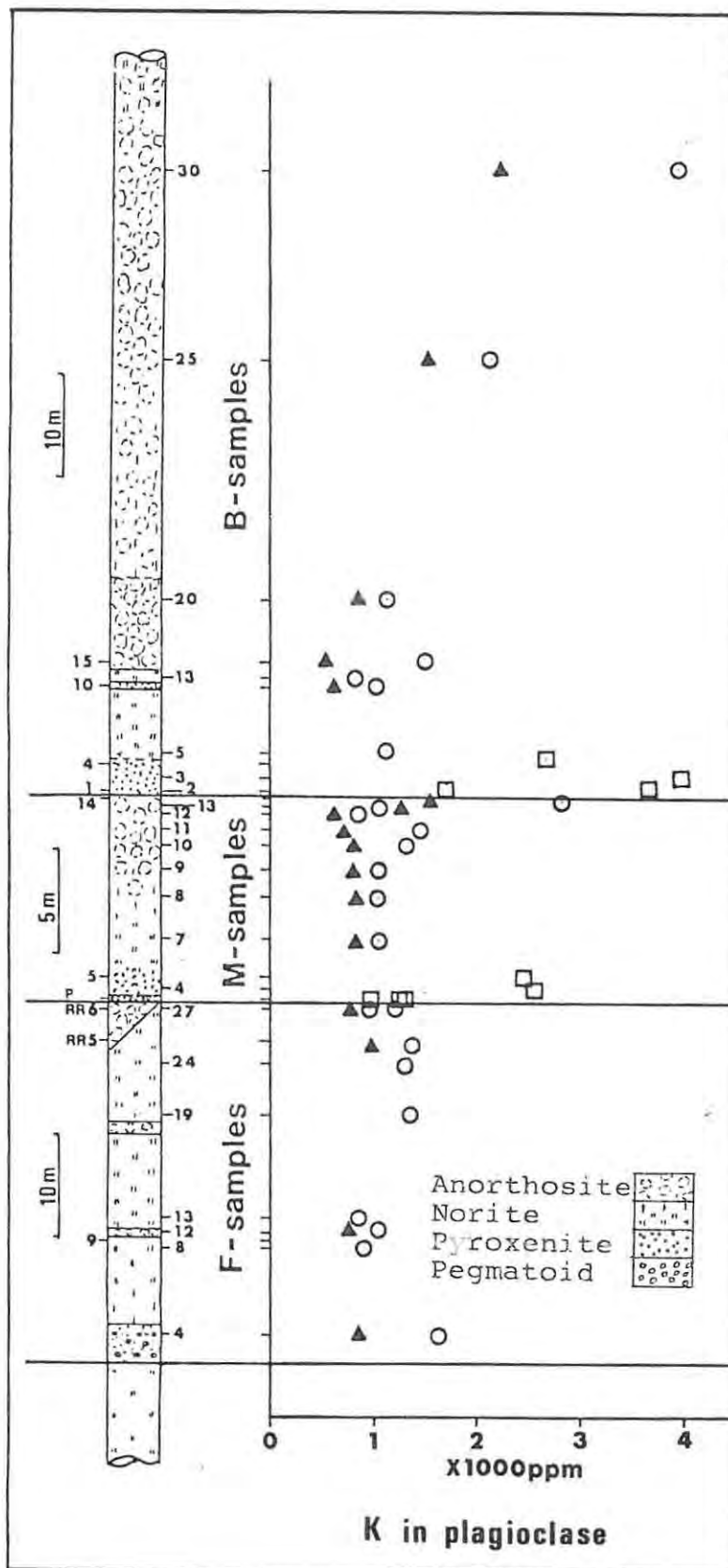


Fig. 2:7 A diagram of the concentration of K in plagioclase separates vs. height in the succession. Rb and Ba have a similar distribution. Note the relatively constant concentration in CPL (▲) and NMP (○) samples in the Footwall and Merensky units, and the upward increase within the Bastard unit. The interstitial plagioclase (□) is enriched in K. Precision (1 sigma) falls within the symbols. For further discussion see text.

Table 2:4 Trace Element Chemistry of Pyroxene Separates**a) Orthopyroxene**

	Zn	Cu	Ni	Co	Cr	V	Rb	Sr	Y	Zr	Sc
F-8 Opx	124	11.8	473	121	2716	181	2.5	7.5	8.5	13.1	34
F-9 Opx	123	14.1	378	117	2407	169	0.9	13.5	7.9	11.5	30
F-12 Opx	135	13.3	346	116	1806	150	---	11.5	6.2	8.5	31
F-13 Opx	109	11.4	566	110	2486	143	0.7	7.1	7.8	11.0	29
F-19 Opx	86	8.2	660	105	3285	145	---	2.2	7.1	12.6	34
F-24 Opx	85	11.5	616	100	2991	148	2.2	2.0	7.4	13.6	29
RR-5 Opx	114	19.-	359	108	2196	170	---	5.7	6.8	5.7	31
RR-6 Opx	119	24.-	610	123	1631	183	1.6	4.6	7.0	6.2	35
P-3 Opx	76	45.-	941	104	3686	138	---	---	5.0	5.5	30
P-10 Opx	85	98.-	896	103	3303	167	---	---	5.4	6.2	31
M-4 Opx	85	195.-	993	100	3029	142	1.3	4.4	8.0	7.0	30
M-5 Opx	91	124.-	987	106	3138	144	1.0	---	6.0	7.0	29
M-7 Opx	114	27.-	660	114	2534	197	---	3.7	8.4	5.7	35
M-8 Opx	114	24.-	592	112	2540	198	---	8.3	9.0	9.3	37
M-9 Opx	120	44.-	557	117	2568	199	---	7.5	8.0	8.8	37
M-10 Opx	119	24.-	605	114	2499	199	0.7	2.1	7.0	6.6	32
M-11 Opx	110	37.-	550	107	1167	219	---	29.6	9.1	13.1	38
M-12 Opx	129	36.-	549	118	1044	195	1.2	15.6	9.1	9.3	35
B-2 Opx	87	61.-	743	103	2775	131	1.1	1.6	7.3	15.8	29
B-4 Opx	86	101.-	898	99	2855	134	2.6	5.4	8.1	12.8	29
B-5 Opx	90	13.0	620	103	3109	149	---	4.3	7.4	9.4	34
B-10 Opx	123	14.4	450	113	2361	164	2.1	4.9	5.5	5.3	33
B-13 Opx	116	11.9	421	109	2026	181	1.5	3.6	6.8	16.6	32
B-15 Opx	125	8.1	367	110	2167	185	1.8	2.8	8.3	6.0	33
B-20 Opx	122	12.6	402	120	1761	221	---	0.9	5.7	3.1	35
B-25 Opx	134	15.4	344	117	1323	248	0.7	7.8	7.4	7.8	38

b) Clinopyroxene

F-13 Cpx	41	19.-	410	64	2488	266	5.4	99.-	34.-	74.-	60
M-8 Cpx	42	40.-	396	53	2558	346	1.4	49.-	32.-	48.-	64
M-9 Cpx	43	45.-	390	61	2910	376	1.5	54.-	29.-	45.-	70
B-2 Cpx	35	484.-	1067	76	4557	300	8.5	26.-	32.-	55.-	80
B-4 Cpx	38	445.-	1345	71	4764	291	8.1	33.-	32.-	57.-	75
B-13 Cpx	42	19.7	313	58	3436	367	5.4	43.-	31.-	66.-	72
B-20 Cpx	51	13.5	291	72	1640	469	0.9	37.-	23.-	28.-	71
B-30 Cpx	75	14.0	249	77	1539	511	1.6	15.-	33.-	42.-	82

Footwall and Bastard units.

K, Rb and Ba behave sympathetically in plagioclase separates. This is revealed by plots of K vs Rb, Rb vs Ba and K vs Ba (Fig. 2:6a, b & c). The interstitial plagioclase has generally higher concentrations of these elements than the plagioclase from the norites and anorthosites, which have generally lower and fairly constant concentrations of these elements. However, the plagioclase of the Bastard mottled anorthosite is an exception as the concentration of these elements increases upward in the succession. This is illustrated by a plot of K vs height (Fig. 2:7).

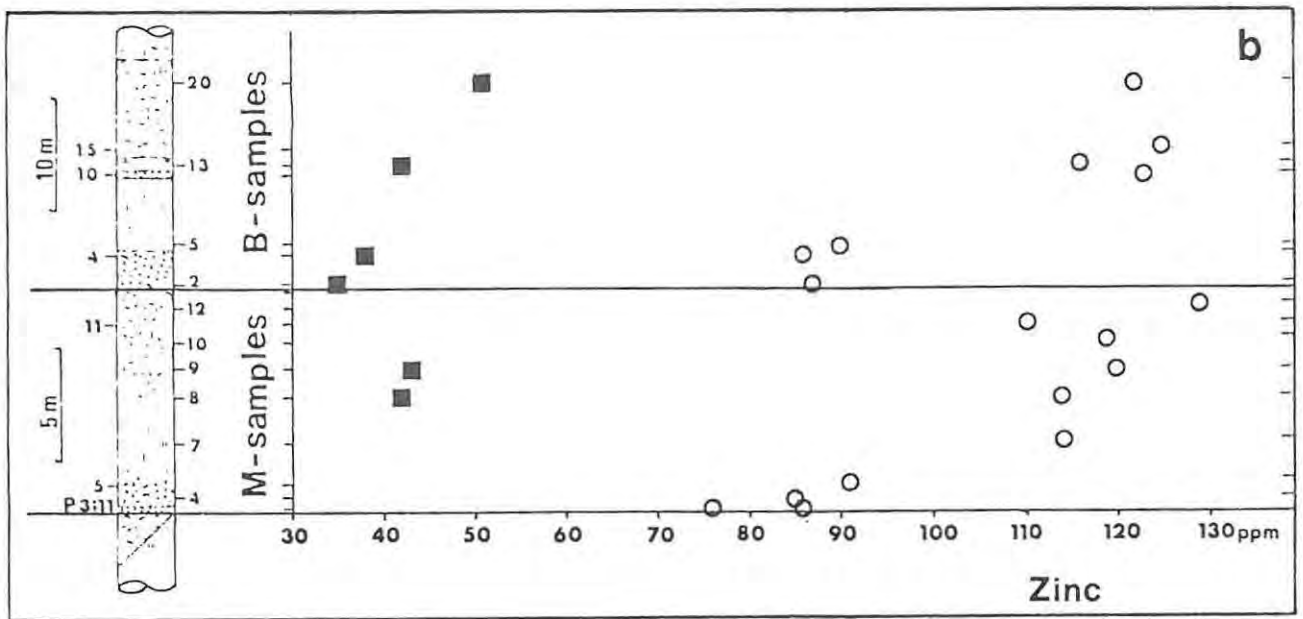
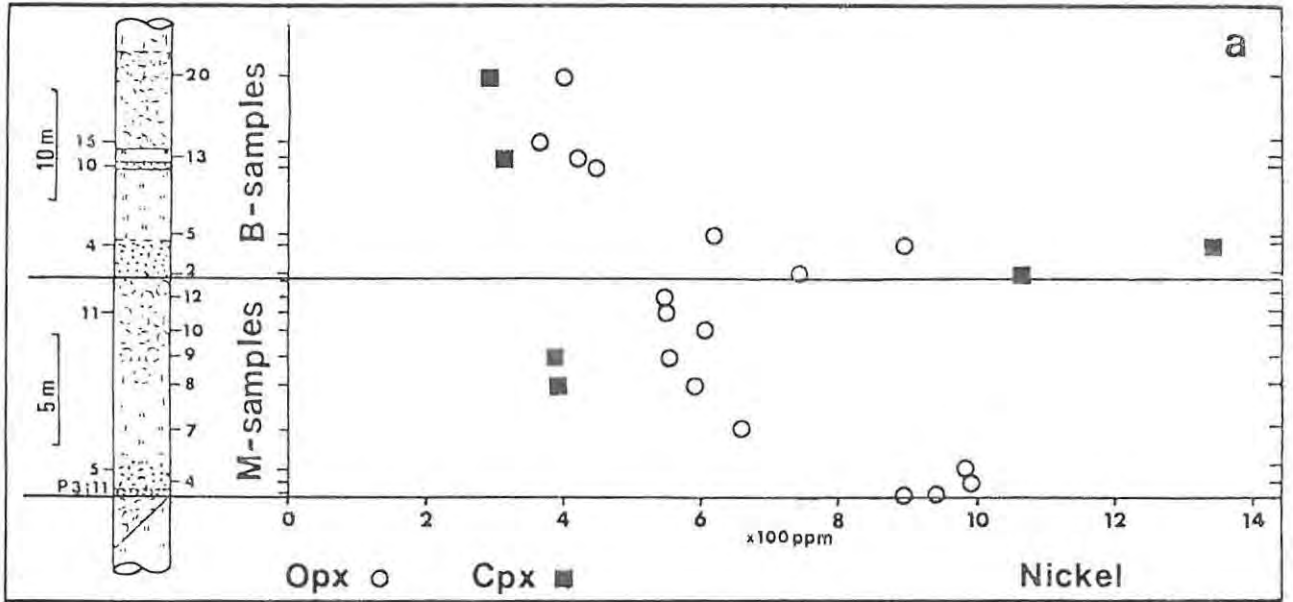
Crystal chemical considerations suggest that the concentrations of the elements Zn, Cu, Ni, Co, Cr and V in plagioclase should be very low. Thus the sometimes significant concentrations recorded probably partly reflect contamination of the separates by very small amounts of mafic silicates (Zn, Ni, Co, Cr, V) and microscopic sulphide inclusions (Cu, Ni, Co).

Chemistry of the Pyroxene Separates

The analytical results for orthopyroxene and clinopyroxene are presented in Table 2:4a and Table 2:4b respectively. The variation in the concentrations of some of the elements in the orthopyroxenes with respect to height are illustrated in Fig. 2:8. In view of the possible inhomogeneity of minor elements in the orthopyroxenes discussed above and in the following section, the concentrations of the trace elements recorded and discussed here may represent averages of zoned crystals in some cases. The concentrations recorded here should thus not be viewed as representing the liquidus primocryst orthopyroxene compositions.

The concentrations of Ni, Zn, V, Co, and Sc in orthopyroxene from the Merensky cyclic unit and the lower part of the Bastard cyclic unit (up to sample B-20) display cohesive trends with respect to height in the succession. Data from the Footwall unit are too sparse to draw any far reaching conclusions, and is omitted from the diagrams. This is also true of the two samples from above B-20 in the Bastard unit for which pyroxene separates are available, as these may belong to a separate cyclic unit.

The clinopyroxene separates from the lower part of the Bastard cyclic unit also display cohesive trends, and these are also included in the discussion. Only two clinopyroxene separates are available from the Merensky cyclic unit and thus no trends can be defined. These are included



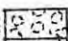
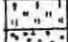

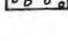
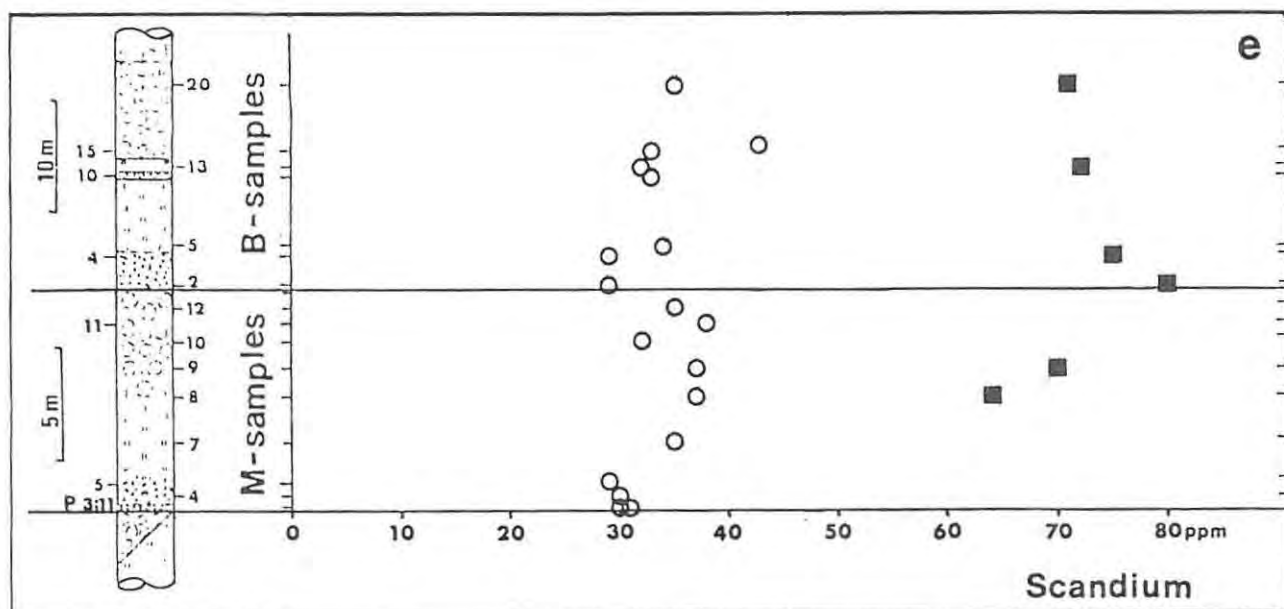
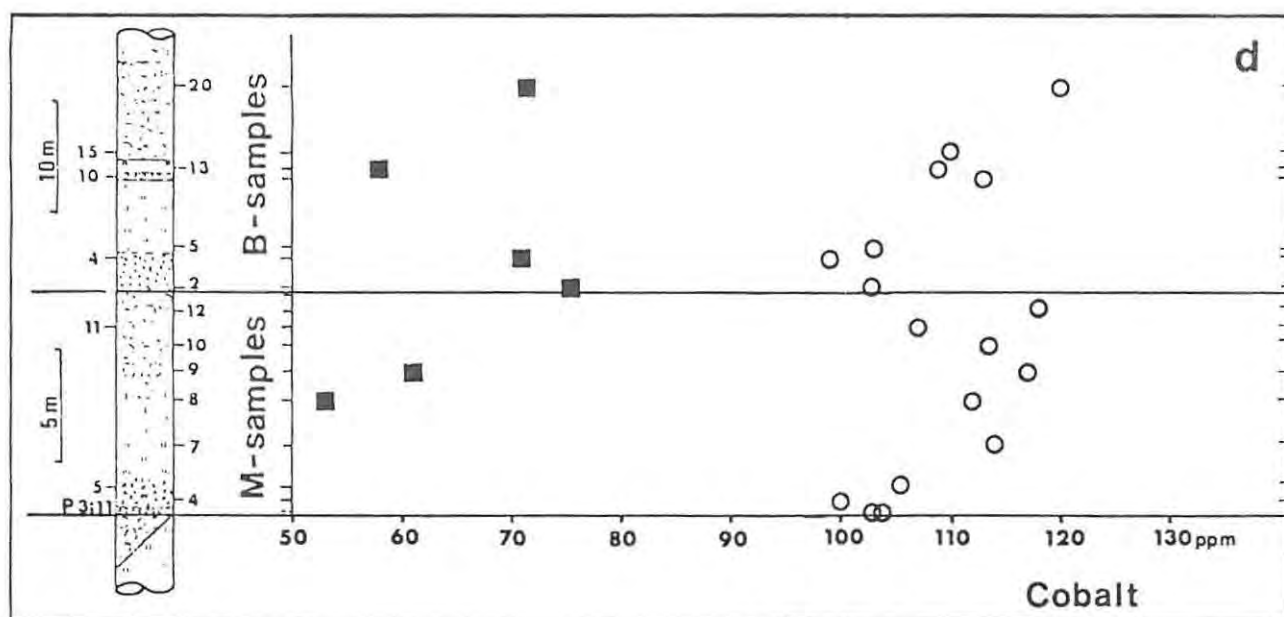
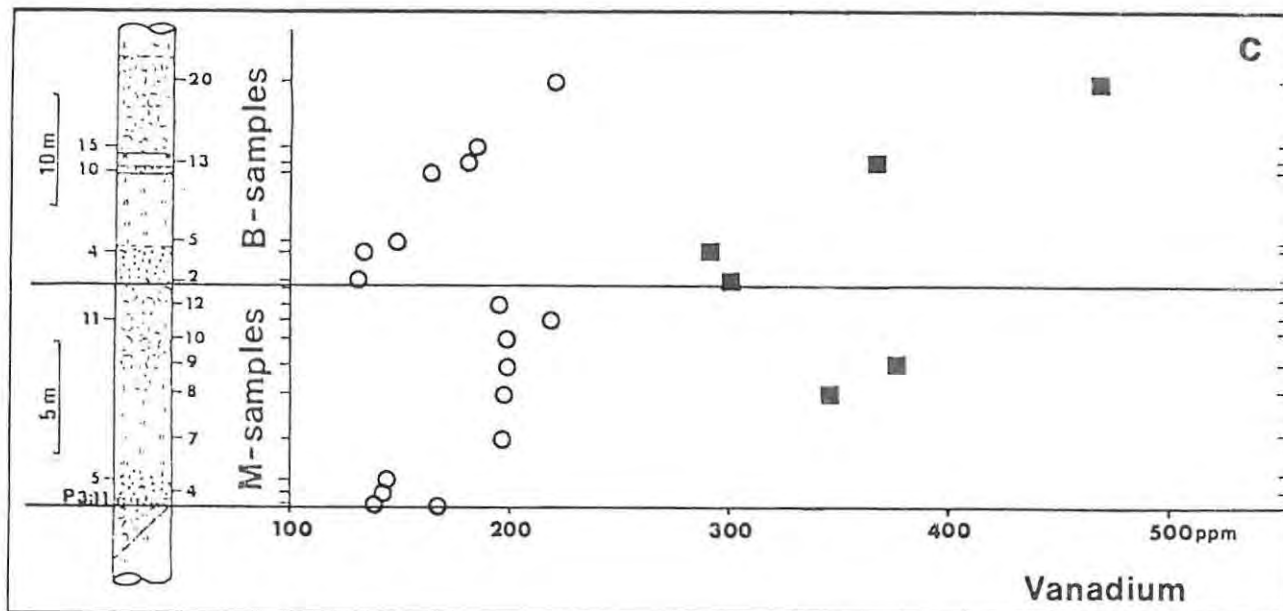
Anorthosite 
 Norite 
 Pyroxenite 
 Pegmatoid 

Fig. 2:8 The variation with respect to height of the concentrations of the trace elements Ni (a), Zn (b), V (c), Co (d) and Sc (e) in orthopyroxene and clinopyroxene separates from the Merensky cyclic unit and the lower part of the Bastard unit. Parts (c, d & e) on following page. For detailed discussion see text. Open circles = orthopyroxene; filled squares = clinopyroxene. Precision (1 sigma) usually falls within the symbol.



on the diagrams for comparison with the coexisting orthopyroxene.

The Nickel concentrations of the Pyroxenes (Fig. 2:8a)

Within the Merensky cyclic unit there is a marked decrease in the concentration of Ni in the orthopyroxene upward in the stratigraphic succession. This does not include orthopyroxene from the Merensky pegmatoid. The Ni concentrations in the orthopyroxenes of the Bastard cyclic unit display a very similar distribution to those of the Merensky cyclic unit, except that the concentrations are generally lower in the orthopyroxenes of the former unit at equivalent stratigraphic positions. However, the orthopyroxene of sample B-1 of the Bastard cyclic unit (stratigraphically roughly equivalent to the Merensky pegmatoid in the Merensky cyclic unit) does have a lower Ni concentration than the orthopyroxene from the sample immediately above (B-4). The Ni concentration of orthopyroxene from B-2 falls between that of orthopyroxenes from samples B-4 and M-12. The latter sample is from the top of the Merensky mottled anorthosite. This "switch-back" anomaly is mimicked by some other trace elements, and by the MMF ratio of the orthopyroxene as determined by microanalysis.

The Ni concentration of clinopyroxene is expected from crystal chemical considerations to be less than that of the coexisting orthopyroxene. The higher concentrations recorded for samples B-2 and B-4 are probably the result of contamination of the clinopyroxene by co-existing interstitial sulphides which are present in the rock.

The Zinc concentrations of the Pyroxenes (Fig. 2:8b)

The variation of Zn concentrations of the pyroxenes with respect to height in the succession in both the Merensky and bastard cyclic units is the opposite to that of Ni. There is an upward increase in the Zn concentration of the orthopyroxenes from the base to the top of each cyclic unit. However, this increase is not smooth. The Zn concentration of orthopyroxene from sample B-2 displays the "switchback" noted for Ni above, but this is not mimicked by the clinopyroxene Zn concentration.

The Vanadium concentrations of the Pyroxenes (Fig. 2:8c)

In the Bastard cyclic unit the concentration of V in the orthopyroxene steadily increases with stratigraphic height from the base of the unit (B-2) to the top (B-20). This steady increase is reflected by the data for clinopyroxene, except that the V concentration of clinopyroxene

displays the "switchback" effect, but the data for orthopyroxene does not. In the Merensky cyclic unit the V concentration of the orthopyroxene does not increase smoothly with respect to height. The orthopyroxene separates from the Merensky pyroxenite (M-4 & M-5) have a V concentration of about 140ppm but the orthopyroxene from the Merensky norite and mottled anorthosite have a constant V concentration of roughly 200ppm. Thus there is an increase in the V concentration with respect to height, but it is not as smooth as in the Bastard cyclic unit.

The Cobalt concentrations of the Pyroxenes (Fig. 2:8d)

The concentration of Co in orthopyroxene increases with height in both the Merensky and Bastard cyclic units. However, there is considerable scatter in the data. The data on the Co concentrations of the clinopyroxene is inconclusive.

The Scandium concentrations of the Pyroxenes (Fig. 2:8e)

In the Merensky cyclic unit the Sc concentrations of orthopyroxene appear to increase with respect to height in the succession, but there is considerable scatter in the data. The Sc concentrations of orthopyroxene from the Bastard cyclic unit have a more consistent increase upward in the stratigraphic succession. However, the Sc concentrations of clinopyroxene from the Bastard unit decrease upward in the succession. The reason for this is unclear.

The Zr, Rb, Sr, Y and Cr concentrations of the Pyroxenes

Some of the elements determined (Zr, Rb and Sr) display irregular variations in their concentrations in the pyroxenes with respect to height. This probably reflects minor contamination with phases such as zircon, mica and plagioclase in some cases and are thus difficult to interpret. Yttrium concentrations of orthopyroxenes from the whole of the study section lie between 5ppm and 10ppm, and display no systematic variation with respect to height. The concentrations of Cr in the Merensky and Bastard pyroxenites are unreliable due to the possibility of contamination by chromite.

Trace Element distributions between Orthopyroxene and Clinopyroxene

Analyses of the mineral separates prepared for this work indicate that there is an equilibrium with respect to some of the trace elements

determined despite the presence of zoning with respect to some of the minor elements. This is indicated by a consistency of the distribution coefficients obtained for orthopyroxene and clinopyroxene pairs separated from pyroxenites, norites and anorthosites (Table 2:5).

Table 2:5. Weight ratios of various elements in orthopyroxene relative to clinopyroxene [opx]/[cpx].

	Zn	Cu	Ni	Co	V	Y	Zr	Sc	Sr
B-20 $\frac{3}{4}$	2.4	0.93	1.4	1.7	0.47	0.25	0.11	0.49	0.02
B-13#	2.8	0.60	1.4	1.9	0.49	0.22	0.25	0.44	0.08
B-4 ζ	2.3	0.23*	0.7*	1.4*	0.46	0.25	0.22	0.39	0.16
B-2 ζ	2.5	0.13*	0.7*	1.4*	0.44	0.23	0.29	0.36	0.06
M-9 $\frac{3}{4}$	2.8	0.98	1.4	1.9	0.53	0.28	0.20	0.53	0.14
M-8 $\frac{3}{4}$	2.7	0.60	1.5	2.1	0.57	0.28	0.19	0.58	0.18
F-13#	2.7	0.62	1.4	1.7	0.54	0.23	0.15	0.48	0.07
AVER	2.6	0.75	1.4	1.9	0.50	0.25	0.20	0.46	0.10
COV%	7.9	26	3.9	9.2	9.6	9.7	30	18	57

Mottled anorthosite $\frac{3}{4}$, norite #, pyroxenite ζ . Some ratios (*) are excluded from the calculation of the average as the ratio is influenced by possible fine sulphide or chromite contamination. COV is the coefficient of variation in percent. The great variation in Sr coefficients is probably a result of minor plagioclase contamination, but does serve to illustrate the much greater affinity of Sr for clinopyroxene in contrast to the orthopyroxene.

A Qualitative Assessment of Equilibria and an Evaluation of Selected Samples in the Study Section

General Discussion

The approach to equilibrium of the mineral assemblage within a rock sample is dependent on two factors. These are the rate of reaction and the rate of cooling. The former is a function of the diffusion of ionic species from one mineral to the other as demanded for equilibrium, and the latter is a function of the cooling process of the intrusion and is dependent on a large number of factors. A brief discussion of this is presented in Chapter Three. Reaction does not often proceed to isothermal

equilibrium, as the temperature is continuously changing, and earlier high temperature equilibria are not quenched in, as the cooling rate is relatively slow. Most rocks in the layered sequence therefore consist of disequilibrium assemblages. Furthermore, different ions have different rates of diffusion in minerals and melts (see Freer, 1981 and Hofmann, 1980). Thus there may be a closer approach to equilibrium at a particular temperature by some ionic species relative to others. Many studies have been carried out on layered rocks emphasizing aspects of the subsolidus relationships of pyroxenes (inter alia Nwe, 1975; Nwe & Copley, 1975; von Gruenewaldt, 1970; Coleman, 1978 and Buchanan, 1979). The brief evaluation above indicates that there may be considerable complexity in material from adjacent samples, especially in the interstitial phases. Thus very careful investigation is required to unravel the history of the rocks.

Exsolved pyroxenes present other difficulties as partial separation of the lamellae from the host may occur, but this depends on the fineness of the intergrowths. Assuming that the separates are pure and that perfect separation is achieved with all the exsolution products intact, the possibility of reaction and exchange between adjacent grains still exists, but is probably limited. The mineral separate would thus ideally represent equilibria close to the solidus, but not the liquidus as at high temperatures in the presence of liquid reaction rates are relatively rapid. Zoning is present in some of the samples studied, for some elements at least (see below). The presence of zoning could invalidate the use of mineral separates in an geothermometric application, as the analyses obtained are averages and not necessarily an equilibrium composition specific to any single temperature.

Studies of the Bushveld pyroxene analyses of Atkins (1969) by Wood & Banno (1973), Wells (1977) and Kretz (1982) indicated that relatively consistent temperatures were obtained, although each formulation produced different absolute temperatures. The work of Kretz shows that an average solidus temperature for the Bushveld layered rocks (norites and gabbros) was in the region of 1020°C to 1050°C but that Mg/Fe exchange continued to slightly lower temperatures ($\pm 980^\circ\text{C}$). These relatively consistent results indicate that there is an approach to equilibrium at a similar temperature (solidus?) for all the rocks. The Atkins (1969) analyses were of mineral separates and thus host and any fine exsolution lamellae were analysed together, and any zoning was not detected.

The rate of cooling of the Bushveld Complex was very slow due to the very large size of this body, and thus in some cases reactions could continue at relatively low temperatures. For instance, the coexisting orthopyroxene and clinopyroxene pairs of the Bushveld complex have features intermediate between those of metamorphic environments and other layered intrusions (Fleet, 1974). Chromite/olivine pairs from layered rocks have been shown by Roeder et al. (1979) to equilibrate very rapidly in the solid state at temperatures well below the solidus, and Wilson (1982) has shown that in the Great Dyke, re-equilibration of chromite with orthopyroxene and olivine hosts is dependent on the rate of diffusion in the silicate phase and may be very rapid at high temperatures.

Similar effects to the above have been noted in all the samples containing chromite used in this study. This Mg/Fe exchange reaction at the subsolidus stage has been used by Wilson (1982) to trace the cooling history of the Great 'Dyke' of Zimbabwe. For further detailed work on the subsolidus relationships of chromite in mafic layered intrusions the reader is referred to the work of Irvine (1975), Cameron (1975 & 1977), Henderson & Suddaby (1971), Henderson (1975), Roeder et al. (1979), Henderson & Wood (1981), Bevan (1982) and Eales & Marsh (in press) among others.

Petrographic observations of rocks of the Bastard cyclic unit, suggest that exsolution phenomena are due to the presence of a fluid phase. This is indicated by an association of hydrous phases with abundant exsolved clinopyroxene lamellae in the orthopyroxene. Samples where there are no hydrous phases have clear unexsolved orthopyroxenes. This phenomenon of a fluid catalyst in the exsolution of minerals has not been afforded much attention in studies of layered rocks.

Zoning, exsolution and partial re-equilibration of the minerals within layered rocks presents many problems in the interpretation of the mineral chemistry and petrography of the rocks. The examples and qualitative reasoning which follow serve to clarify the possible factors that need to be considered during interpretation. Considerable chemical heterogeneity of the minerals on a micro-scale is revealed by microanalyses and petrography. This heterogeneity is due to three principal factors: (i) zoning relict from the subliquidus stage, (ii) exsolution phenomena and (iii) partial exchange reactions between different mineral species.

In Chapter Four it will be shown that many of the pyroxenes cooled as total equilibrium systems at least with respect to their MMF ratios, and that much zoning was eliminated as cooling proceeded. This is borne out by the fact that in general no significant zoning of Fe and Mg attributable to liquidus or subliquidus processes has been found within the pyroxenes analysed in this study, apart from some interstitial pyroxenes surrounded by plagioclase in mottled anorthosite and leuconorite. However, zoning with respect to minor elements (Cr, Al and Ti) is sometimes preserved. Plagioclase on the other hand is extensively zoned and complete homogenization obviously did not occur at the subliquidus or liquidus stage.

Exsolution in the pyroxenes occurs on several scales, ranging from large blebs to extremely fine lamellae which give the mineral a striated appearance. Large lamellae and blebs can be avoided in analysis of the host pyroxene, but in some cases the very fine lamellae cannot be avoided by the electron beam and a composite analyses results. In the latter case the orientation of the crystal with respect to the thin section is important as the lamellae can be oriented in any direction varying from parallel to normal to the plane of the section. A detailed investigation of exsolved pyroxenes has been carried out by Buchanan (1979), who showed that focussed beam analyses gave poorly reproducible results on single crystals, but that this was influenced by the density of exsolution lamellae. The data in the present work were all gathered with a focussed beam, with the result that the heterogeneity in the samples is somewhat emphasized. The larger exsolution bodies (~10 microns) and their hosts were analysed separately and represent a lower temperature assemblage than the composite analyses discussed above. The presence of larger exsolution bodies presents severe problems in the derivation of a bulk composition from the exsolved mineral, and great care has to be exercised in using analyses from exsolved mineral phases.

Partial reaction between adjacent mineral species (chromite/olivine and chromite/pyroxene for example) may introduce strong chemical gradients near the interfaces between phases. This effect is especially pronounced in the case of the two pairs quoted above as chromite re-equilibrates very rapidly at high temperatures and zoning within chromite crystals is not marked (Roeder et al., 1979), but may be very marked in the host mineral

(Wilson, 1982). A similar, but less readily detectable, zonation probably exists in the case of other mineral pairs (e.g. Opx/Cpx, Px/Plag and Ol/Px).

A selection of samples with different features are discussed here to illustrate the different variations that can occur. In most cases the samples show little variation of composition as indicated by the variation in the MMF ratio and minor elements in orthopyroxene. The samples have largely re-equilibrated and the crystals are not usually as markedly zoned as shown here. Sample F-13 indicates a nom.

M-8: Zoning of Orthopyroxene (Plate 2:1d)

Strong zoning of some elements is present in orthopyroxene grains in this leuconorite sample. The primocryst orthopyroxene grains are surrounded by a zone of small plagioclase primocrysts set in interstitial orthopyroxene in optical continuity with the primocryst orthopyroxene. This is in turn surrounded by areas of pure plagioclase. The impression is that orthopyroxene nucleated and grew, and incorporated the small plagioclase primocrysts after some growth.

The orthopyroxene is strongly zoned with respect to Cr_2O_3 concentrations from core (0.56%) to rim (0.31%) and where the orthopyroxene is interstitial (0.22%). This is also true of Al_2O_3 concentrations which are 1.63%, 1.04% and 0.93% respectively. However, the ionic Al/Cr ratio increases outwards from the core, from 4.34 to 6.30 reflecting the fact that Cr_2O_3 decreases more rapidly than Al_2O_3 .

The TiO_2 concentration increases strongly from the core (0.12%) to the rim (0.23) of the orthopyroxene. The interstitial orthopyroxene contains 0.32% TiO_2 .

In contrast to the above zoning effects which are relict from the subliquidus and liquidus stage, the MMF ratio of the orthopyroxene shows very subdued zoning from .745 to .725 reflecting a very gentle outward decrease of only 2%. There was thus probably considerable re-equilibration of Mg and Fe. CaO decreases outward from 1.9-3.1% in the core to 1.0-1.2% in the interstitial material. The decrease is not very smooth and probably reflects heterogeneity produced by exsolution, although this is uncertain. The decrease in the Al_2O_3 and CaO contents towards the rim of the orthopyroxene, may reflect the depletion of these two components in the liquid as a result of the nucleation and growth of plagioclase in the liquid.

F-13 & F-15: Disequilibrium and Equilibrium (Pl. 2:1c and e)

Sample F-13 is a norite containing relict olivine surrounded by orthopyroxene and it also contains relatively abundant interstitial hydrous phases (mica and amphibole) as well as magnetite. Most of the orthopyroxene primocrysts differ little in appearance from those of other rock samples except for a greater amount of interstitial magnetite and a very slightly "clouded" appearance due to very fine dusty inclusions or exsolved opaque material. Both the relict olivine and the replacing orthopyroxene have an MMF ratio of .80. The associated primocryst orthopyroxene has a MMF ratio of .76, and the interstitial pyroxene a MMF ratio of .74.

These observations imply considerable disequilibrium in the Mg/Fe ratio between the various types of orthopyroxene in the rock and between the olivine and the replacing orthopyroxene. For instance, using the equation of Morse (1979b) it can be shown that olivine with an MMF ratio of .80 should be in equilibrium with an orthopyroxene with an MMF ratio of .83.

The MMF ratio is not the only disequilibrium feature. The Al/Cr ratios and the Cr, Mn and Ti concentrations of the pyroxenes also display a range of values (Fig. 2:9). The Al/Cr ratios of the orthopyroxenes vary between 4.5 for the primocryst pyroxene, 8.9 for the interstitial pyroxene and 13.5 for the pyroxene replacing olivine. The primocrysts have the highest Cr concentration (0.53%) and the interstitial and replacement orthopyroxenes have the lowest (0.17%). This suggests that the primocryst pyroxenes crystallized early, thus depleting the liquid in Cr, and were then followed by the other two types. This is consistent with the petrography of the rock.

Most of these disequilibrium features appear to be inherited from the subliquidus stage (very near the solidus). However, the subsolidus processes could not eliminate heterogeneity in spite of the temperature remaining high for a relatively long time in the presence of a fluid phase. The presence of relatively unzoned primocryst pyroxenes of constant composition suggest that they crystallized at near equilibrium conditions, but only in parts of the rock, and that the region surrounding the olivine was closed to the remainder of the rock. This sample serves to illustrate that disequilibrium can exist on a very small scale in layered rocks.

In contrast to sample F-13 above, near equilibrium relationships in the pyroxenes are demonstrated by sample F-15. The rock has a similar

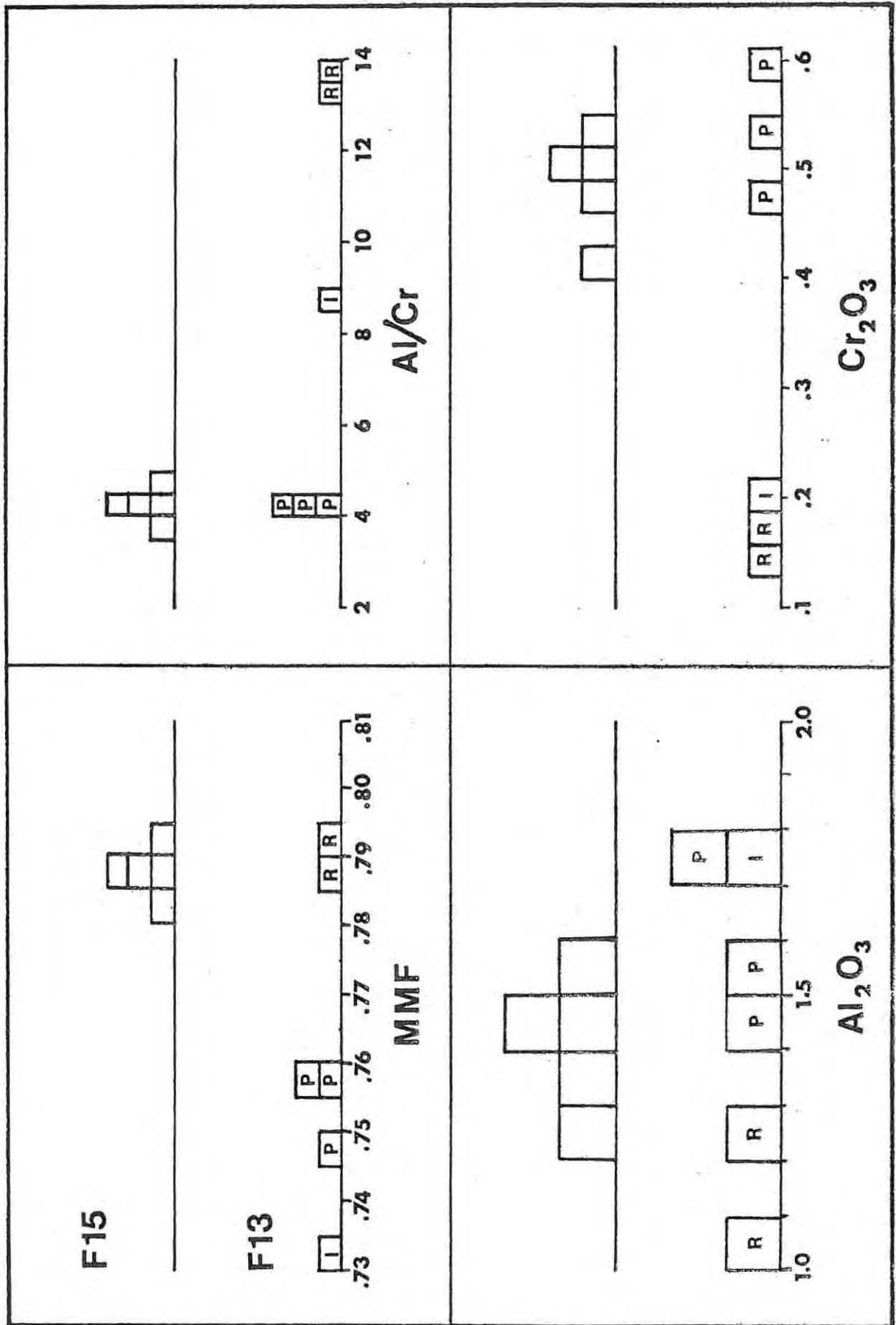


Fig. 2:9 Histograms illustrating the differences between analyses from F13 and F15. Note the spread of values displayed by F13 in contrast to F15. The concentrations of MnO, TiO₂ and CaO display a spread in both samples.

texture to F-13 and also contains minor mica and magnetite or ilmenite. The orthopyroxene (primocryst and interstitial) has an average MMF of .80 with a coefficient of variation (COV) of only 0.4% for five analyses. This constancy is also reflected in the Al/Cr ratio which averages 4.3 and the COV is 4.7%. The five clinopyroxene analyses are also closely similar (Average MMF = .84, COV 0.5%) even though some grains occur as apparently isolated interstitial blebs surrounded by plagioclase.

The compositional relationships in this rock were clearly very different to those in F-13 at the late subliquidus and solidus and subsolidus stages. The pyroxenes are unexsolved resulting in very close correspondence between analyses, but this does not account for the wide variation in F-13 as those pyroxenes are also relatively unexsolved. The contrast between these samples is illustrated by Fig. 2:9.

B-15: Disequilibrium or Isolation of Interstitial Minerals and Liquids

There is a considerable amount of late stage interstitial green and red biotite in this sample and, in addition, the pyroxenes exhibit exsolution. The green and red biotite differ significantly only in their TiO₂, FeO and Cr₂O₃ concentrations (Table 2:6). This indicates short range disequilibrium at the subliquidus stage close to the solidus for these three components. This also implies that during the final stages of crystallization different parts of the same rock had interstitial liquids of differing compositions and that these could not mix or equilibrate. This may be attributed to infiltration metasomatic effects at the subliquidus stage, or to isolation of different "pockets" of interstitial liquid from each other, and that these pockets followed different final crystallization paths. These relict effects have been preserved during the subsolidus cooling of the rock. Further subsolidus exsolution effects were imposed on the pyroxenes in some places. This sample is illustrated in Plate 2:1a and b.

Table 2:6. Analyses of Green and Red Biotite from B-15 anorthosite. Volatiles not determined.

	SiO ₂	TiO ₂	Al ₂ O ₃	FeO	MnO	MgO	K ₂ O	Cr ₂ O ₃	Total
Green	38.0	0.39	14.6	15.1	.10	16.9	9.36	0.03	94.4
Red	38.3	2.28	14.0	13.8	.05	17.3	9.59	0.24	95.5

The heterogeneity of the interstitial orthopyroxene of this sample extends to the MMF ratio of the orthopyroxenes which range from .68 to

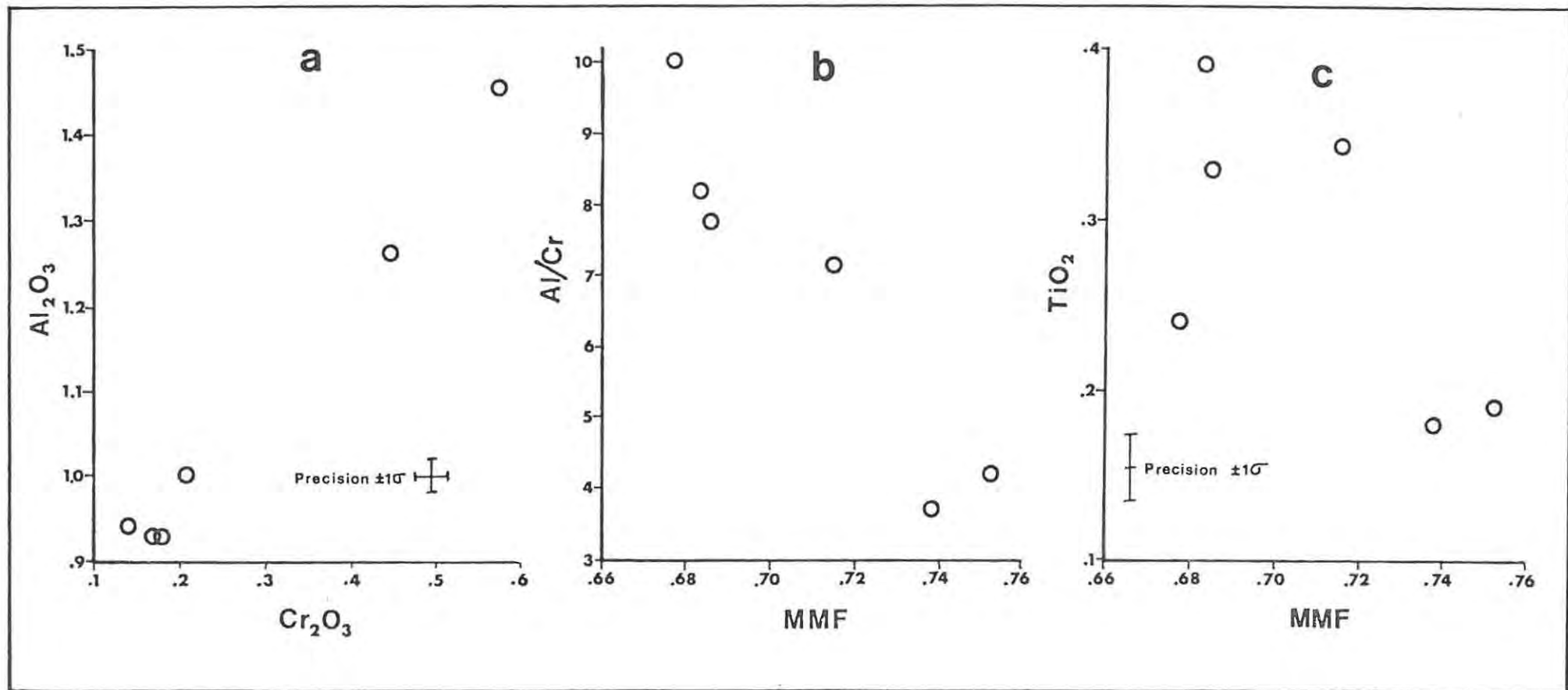


Fig. 2:10 Chemical variation displayed by the orthopyroxene analyses of B15. Note the positive correlation between Al_2O_3 and Cr_2O_3 shown in a, the decrease in the Al/Cr (ionic ratio) with increasing MMF in b and the decrease (not clearly defined) of TiO_2 with increasing MMF. For further discussion see text.

.75. There is a linear relationship between Cr and Al in the orthopyroxenes, (Fig 2:10a) but not a constant Al/Cr ratio. The latter decreases with an increasing MMF ratio (Fig 2:10b) as does the amount of Ti (Fig 2:10c) although this is not well defined due to the poor precision in the determination of Ti at low levels. These features imply fractionation effects during the crystallization of the interstitial pyroxene. Earlier crystallizing pyroxene (high MMF) is enriched in Cr and depleted in Ti, but that crystallizing later near the edge of the large sieve-like poikilophitic pyroxene grains has the reverse relationship. These features are thus relict relationships from the subliquidus stage and subsolidus re-equilibration has not homogenized the pyroxenes in this rock.

B-26 & B-30: Disequilibrium with Exsolution (Pl.2:1g and h)

These two samples have very similar textural features in that a pre-existing orthopyroxene is overgrown and replaced by later orthopyroxene. However, B-26 has clear unexsolved orthopyroxene cores (MMF = .66) surrounded by strongly exsolved zone (MMF = .61). In contrast the cores and overgrowths of B-30 are well equilibrated and have a very similar MMF (.59 to .60) even though there has been some exsolution of large clinopyroxene blebs. In B-30 both interstitial and exsolved lamellae of clinopyroxene have the same MMF ratio (.67 - .68) but interstitial clinopyroxene towards the edge of the large sieve like crystals have progressively lower MMF ratios (.65 and .64) probably reflecting earlier subliquidus fractionation.

Summary and Conclusion

The rocks of the study section are considered in this work to straddle the boundary between two major subdivisions of the Bushveld Complex. The Footwall unit falls in the Critical Zone and the Merensky and Bastard units in the Main Zone. This boundary (at the base of the Merensky cyclic unit) is marked by a disconformity and a major Sr-isotopic discontinuity indicating a new addition of magma or large scale contamination of the residual magma in the chamber.

The rocks of the Footwall unit have a variety of textures and

chemical features that require intensive study of very closely spaced samples not available for this work. Many of the features described above such as the presence of zoning in plagioclase, disequilibrium textures such as those of samples F-13, F-27 and the Boulder Bed require much more detailed work. The Boulder Bed shows a large difference in the composition of the pyroxene from the top and the bottom (Fig. 2:3a) and more detailed studies of this unit are required to investigate the nature of the compositional variation in this layer.

Within the Merensky Cyclic unit the rocks follow a clearly defined sequence from pyroxenite at the base to a mottled anorthosite at the top. This unit also has coherent chemical trends in the rocks and minerals. The decrease in the MMF ratio of the orthopyroxenes from between .80 and .84 at the base to .69 at the top is particularly striking.

The Bastard cyclic unit has similar characteristics to the Merensky cyclic unit, but there are additional complications. The Bastard mottled anorthosite has an additional layer of leuconorite which may represent the base of a new cyclic unit, although this is uncertain at present and needs more work to establish the lateral continuity of this layer. If it is confirmed that this is a cyclic unit, the upper boundary of the Bastard cyclic unit should be placed at the base of the leuconorite layer.

There is considerable heterogeneity within some of the samples studied in this work. These chemical variations have to be borne in mind when evaluating the subliquidus and liquidus processes. The properties of each sample are the result of a complex series of interactions between coexisting minerals, and between minerals and liquid or fluid. Each sample can be studied to some degree in isolation, but its setting within the succession is important for a full evaluation.

CHAPTER THREE: Physical Processes

Introduction

Several factors influence the gross cooling of an intrusion such as the Bushveld Complex. These are the shape of the intrusion, its volume, the direction of the heat flux, the nature and thickness of the enclosing rocks (Jaeger, 1968), circulation of meteoric water in the enclosing rocks (e.g. Norton & Knight, 1977; Norton & Taylor, 1979) and the number and volume of magmatic influxes to the chamber (Usselman & Hodge, 1978).

The Rustenburg Layered Suite was emplaced as a sill-like body (e.g. von Gruenewaldt, 1979), and cooling to the Curie point ($\pm 600^{\circ}\text{C}$) was accomplished while the layering was still horizontal (Gough & van Niekerk, 1959). The intrusion has a great lateral extent compared to its thickness (Cousins, 1959). The mafic layered part has the shape of a flattened torus or "doughnut". Cooling can thus be assumed to have occurred mainly from the top and bottom. Furthermore, the Rustenburg Layered Suite crystallized from a series of magma inputs (inter alia, this work; Hamilton, 1977; Sharpe, 1981a; Kruger & Marsh, 1982) and thus at any time during the accumulation of the rocks, the column of magma from which crystallization was proceeding was relatively thin. Gray (1978) has shown that due to the accumulation of crystals at the base of a convecting sill-like intrusion, heat removal occurs almost exclusively through the roof, while the crystal pile can, in some cases, contribute heat to the convecting region. The heat flux must therefore have been vertically upward during the crystallization of the major part of the Rustenburg Layered Suite. The average rate of accumulation of the layered rocks is to some extent conjectural as widely differing estimates of the time to solidify have been made (cf. Irvine, 1970a and McCarthy & Cawthorn, 1980). Much of the basis of the latter authors' estimate is refuted in the present work and that of the former appears more plausible. Irvine calculated that the layered rocks took some 200,000 years to crystallize which implies an average rate of accumulation of about 5cm per year.

The superincumbent blanket of rocks overlying the Bushveld Complex magma chamber at the time of intrusion, consisted mainly of the Rooiberg Group which has a thickness between 3570m and 4610m (SACS). A calculation of the cover thickness using the chordal model of von Gruenewaldt (1979)

for the Rustenburg Layered Suite gives a thickness of between 2.8km and 4.9km, in good agreement with the values taken from SACS. This mass of rock could thus exert a pressure of 1.2kb on the underlying Rustenburg Layered Suite magma chamber. The column of rock above the level of the Merensky cyclic unit as deduced from the stratigraphic column of SACS is 5000m in the Western Bushveld Complex. As the magma was introduced in pulses the thickness of liquid above this level was probably much less during the crystallization of the unit and the pressure correspondingly lower. Assuming a density of 2.6gm cm^{-3} for the liquid taken to be a basalt similar to that quoted in Bottinga & Weill (1970), the maximum possible pressure that could have been exerted at the Merensky cyclic unit level by the liquid was 1.3kb and thus the maximum total pressure was 2.5kb, which is considerably lower than the 4kb postulated by Cawthorn (1977) for a similar level in the Rustenburg Layered Suite of the Eastern Bushveld Complex.

Physical Processes of Magmatic Differentiation

Introduction

Various physical processes have been proposed to account for rhythmic and cryptic layering in layered intrusions. These are crystal settling from the main body of magma, density currents transporting crystals to the floor of the magma chamber, and crystal settling in isolated volumes of magma near the floor of the chamber. The alternative model is in situ crystallization with very limited, if any, crystal settling. Multiple intrusion has also been proposed as a mechanism to account for the layering. This section concentrates on aspects of possible importance in the study section and the rest of the Bushveld Complex.

Crystal Settling

Until recently it has been widely accepted that when layered intrusions crystallize, the crystals accumulate on the floor of the magma chamber, either by a process of crystal settling through the magma, or by mineral grains settling out of dense, crystal-charged currents originating near the roof of the intrusion where cooling takes place. (cf. Hess, 1960; Wager, 1968; Wager & Brown, 1968; Irvine, 1970a & 1980a).

Irvine (1970a), in an analysis of the thermal evolution of sills, assumed a convection cell which encompassed the whole of the liquid. In this model an increment of magma on the liquidus at the base of the liquid column rises up and becomes superheated, loses heat at the top of the intrusion and on descent becomes supercooled and starts to crystallize, the resulting crystals settling on the floor of the intrusion under the influence of gravity. This hypothesis relies on the contrast in the adiabatic and melting point gradients within a magma chamber (see Jackson, 1961 for a full explanation).

Jackson (1961, 1970) developed an alternative theory involving bottom crystallization of static layers of liquid at the base of the intrusion, each layer crystallizing a cyclic sequence of minerals. Repetition of the cycles was brought about by an intermittent convective overturn of the liquid above the crystallizing layer, introducing fresh magma to the crystallizing region. The minerals were assumed to crystallize from the static magma and settle to the base of the intrusion, thus recording the liquidus history of the magma batch in the primocryst mineralogy and chemistry. Incomplete or beheaded cycles were attributed to the intermittent convective overturn removing the evolving magma above the crystal mush and restarting the sequence. This incomplete fractionation of the cyclic units also accounted for the gradual evolution of the overlying rest liquid which mixed with the residue from the fractionation of each cyclic unit. The process is controlled by diffusion as only the lower static portion of the magma contributes material to the crystal pile, the overlying rest liquid being in effect isolated due to low diffusivity of components into the crystallizing region. Crystal settling was inferred to have occurred only in the basal crystallizing layer which could be quite thick.

More recently, the crystal settling and density current hypotheses have come under closer scrutiny and it has been found that many features of layered intrusions appear to be in conflict with these hypotheses. The main contradiction or paradox is that plagioclase, normally one of the most abundant minerals in mafic layered intrusions, would float in the liquids from which it crystallized (Bottinga & Weill, 1970; Campbell et al., 1978; McBirney & Noyes, 1979; Morse, 1979a; Irvine, 1979, 1980a & 1980b). Various hypotheses have been proposed to account for this paradox. For example, Irvine (1980a) proposed that the plagioclase may have been dragged down in a density current and then prevented from floating upward

by the yield strength of the liquid, and burial by denser phases. Morse (1979a) proposed that plagioclase nucleation and growth only started when the density current had reached the floor of the chamber.

McClay & Campbell (1976) have described the layering within the Jimberlana intrusion which is vertical on the side walls, and this feature was interpreted by Campbell (1978) as being due to in situ crystallization. Murase & McBirney (1973) have shown experimentally that magmas have an appreciable yield strength that has to be overcome before floating or settling of crystals can occur and that this property would have prevented all but the largest crystals from moving. Furthermore, Shaw (1969) and Murase & McBirney have also shown that the viscosity of a quiescent magma increases with time at constant pressure and temperature conditions and thus an initially more fluid moving magma would become viscid once movement stops. These non-Newtonian and thixotropic properties would appear to make the process of efficient crystal settling or floating highly unlikely. For further discussion with respect to the data gathered for this work see the discussion on page 60.

In Situ Crystallization and Double-Diffusive Convection

The apparent difficulties in substantiating a crystal settling or density current hypothesis, as outlined above, leaves the alternative of in situ nucleation and crystallization as a viable model. The hypothesis of Jackson (1961), although invoking some crystal settling, has many of the features of in situ crystallization models as crystallization was inferred to be very close to the floor of the magma chamber and the settling distance relatively short. Similar models of bottom crystallization have been described by Sharkov (1972), and Campbell (1978).

Recently the phenomenon of double-diffusive convection has come to the fore as a possible process that could occur in magma chambers. The theoretical background to this process is given by Turner (1973 & 1974) and a suggestion was made by Turner & Gustafson (1978) that this process could be relevant to magma chambers such as that of the Bushveld Complex. This and related processes have subsequently been invoked to explain many features of layered intrusions (cf. McBirney & Noyes, 1979; Irvine, 1980a & b, 1981; Rice, 1981). Each of these authors, however, presents a somewhat different interpretation of the process and the resulting fractionation of the magma and deposition of layered rocks.

In the McBirney & Noyes scenario, based on data and observations of the Skaergaard intrusion, two types of crystallization are identified and

these have different origins. The first process envisaged by McBirney & Noyes is that the liquid within the chamber becomes stratified. Due to opposing influence of temperature and composition on the density of the liquid and the difference in the diffusivity of heat (fast) and components (slow), the liquid stratifies into strongly convecting layers. This is the process of double-diffusive convection. In the case envisaged by these authors the basal (boundary) convecting layer becomes stagnant due to the steady rise in stratigraphic height of the position of highest temperature. The stagnant layer then crystallizes in situ by the oscillatory nucleation mechanism described below. While the liquid was convecting some crystal growth may have occurred in parts of the layers and these crystals could be moved between and within layers before stagnation occurred.

Bearing in mind that crystallization occurred in a static boundary layer, the second process invokes oscillatory nucleation and growth in the boundary layer controlled by the diffusion of components within that layer. This has similar origins to Liesegang phenomena. An analogue in the Bushveld Complex would be the banding of mottled anorthosites due to periodic nucleation of interstitial pyroxene. Such banding can be seen in the Bastard mottled anorthosite (Cousins, 1969), and the "strepies" horizon in the footwall beneath the Merensky unit at Northam (De Klerk, 1982) is of similar ilk.

A different model for the crystallization of the Skaergaard intrusion invoking similar processes to those envisaged by McBirney & Noyes (op. cit.) has been advanced by Rice (1981). In the case of Skaergaard the rhythmic banding associated with the Border Groups is inferred to be the same as solute banding (Hurle, 1972). This process is a disequilibrium one in which gravity and heat flux are in opposing directions. Removal of heat through the walls and roof of the intrusion causes vigorous convection. The magma sweeping past the cooling roof and walls, which are growing downward and inward, is quenched onto these temporary walls and roof of the intrusion. The quenched layer is then modified by the continuing flow of magma. One phase may be partially resorbed and this could lead to the formation of nearly monomineralic layers. Layers of magma which are quenched on to the walls subsequently could have a different phase resorbed. The mechanism is dependent on disequilibrium compositional changes across a cotectic. This process should produce pronounced fractionation effects in the direction of flow of the magma.

Rice also notes that the whole of the magma may start to crystallize and convection could continue with up to 50% crystals in suspension. Exsolution of volatiles at this stage may cause almost instantaneous gelling due to a very sharp increase in the viscosity of the magma. However, this latter process can be excluded in the study section as the layering could not have been formed by instantaneous gelling of a crystal slush strongly convecting in layers, as this cannot produce graded cyclic units of great lateral extent, or the chemical fractionation observed.

The extraction (due to the formation of cyclic bands on the roof and walls of the magma chamber) of dense, high melting-point phases from the magma may cause a chemical zonation in the underlying liquid, the light fractionated liquid floating on denser, hotter unfractionated magma. This stratified magma is what is reflected by the cryptic variation recorded in the Skaergaard intrusion (Rice, 1981). The opposed effects of temperature and density lead to the formation of double-diffusive convective layers. The freezing of the chamber records these double-diffusive layers as "zebra banding" in the Skaergaard intrusion. Later re-equilibration tends to make the boundaries very diffuse. In this model the opposing temperature and density gradients were imposed on the magma by the earlier crystallization of the Border Groups before the formation of the double-diffusive layers. The layers were frozen in with little further differentiation. This is analogous to the model of McBirney & Noyes (1979) described above, but the freezing process is not clear.

Solute banding may have occurred to produce the Merensky cyclic unit as the heat flux and gravity were probably opposed. However it is an unlikely process in view of the smooth upward decrease of MMF in the pyroxenes and apparent lack of marked lateral fractionation effects.

Irvine (1980a & b) provides a detailed model for the development of cyclic layering in the Muskox intrusion which is different to the models of McBirney & Noyes (1979) and Rice (1981). He deals only with the "diffusive" case of the double-diffusive convection process (Turner, 1973). The formation of marginal border groups is not considered. The model described by Irvine (1980b) depends on influxes of hotter, denser magma which flow to the base of the chamber. The upward flux of heat from this magma causes the liquid portion of the magma chamber to stratify into a number of vigorously convecting layers, leading to a stepped temperature and com-

positional profile in the liquid. Within each convecting layer the rising liquid is hotter than that which is descending. At the base of the magma chamber where crystallization is taking place, the temperature profile intersects the liquidus profile. Crystallization therefore takes place from the bottom up and the temperature and compositional effects are transmitted up and down, as appropriate, by the double-diffusive convection process. Irvine (1980b) terms this process double-diffusive fractional crystallization. At the very base of the magma chamber crystallization of primocrysts occurs on, or within centimetres of, the floor. Each increment of crystals removed from the overlying liquid causes a change in the composition which is transmitted up into the liquid column step by step. Irvine (1980b) states:

"....The fact that the cyclic units are individually so exceptionally well differentiated, implies that, as each unit evolved, its parental liquid was, in effect at least, "thoroughly homogenized." The impression is that, each time a layer increment of crystals was fractionated from the liquid, the compositional changes resulting from its removal were rapidly transmitted through the whole of the residual liquid, as would be expected if this liquid was undergoing double-diffusive convection.

The fact that the layered (rock) series of the intrusion terminates against the Marginal Zones instead of lapping up over them would seem to be explained if lateral circulation in the convecting liquid layers acted to remove cooled liquid from the bounding walls of the magma body and transfer it in toward the axial region.

As for the vertical olivine, it is envisaged as forming in circumstances such that the bottom contact of the lowest convection layer is essentially coincident with the top of the cumulate pile and is the junction between the main body of magma and the intercumulus liquid oozing from below. The olivine crystals grow in the diffusive interface, together with minor chromite, on nuclei carried out of the cumulate pile by the intercumulus liquid; the constituents for their growth are drawn from the overlying liquid, which has been supercooled by the convection process. As the latter liquid is depleted in the components of the minerals, its density decreases, both because of the

compositional changes and because of warming by the latent heat of crystallization; consequently, it streams upward to be mixed into the convecting layer while other, less fractionated, supercooled liquid moves down to take its place. Meanwhile, the compositional effects of bottom crystallization (most notably, the Mg/Fe decrease) are being transmitted step-by-step upward through the liquid column by the diffusion-convection process, and effects of interaction and contamination with older magma layers and roof-rock melt (i.e. effects such as silica enrichment) are similarly being transmitted downward. These chemical transfers result in the apparent "thorough homogenization" of the liquid column indicated by the differentiation of the cyclic units. In reality the liquid is not homogenized; a whole range of compositions is present at any given time, and the stepwise variations are continuously adjusting to the effects of the crystallization and other interactions. The result however, is much the same as if the liquid was entirely well mixed."

And he later states:

"...because the compositional effects of double-diffusive fractional crystallization depend on a balance between heat and chemical transfer by the diffusion-convection system, it is possible that, even in the case of perfect fractionation of crystals and liquid at the local site of crystallization along the floor of an intrusion, if chemical transfer to the site was slow, the overall compositional variations developed in the rock would be small. Differences in this type of balance might explain why some layered intrusions show very little mineralogical variation through thousands of meters of section, whereas others are almost perfectly differentiated through units only a few tens of meters thick."

In the present author's opinion there is a paradox in the model above. This description of the process implies that the compositional effects of each deposited increment are transmitted to the whole residual liquid in the magma chamber, which clearly could not then account for the marked chemical variation within a single cyclic unit. It is not clear if the parental liquid encompasses the whole residual magma or only that within the basal convecting layer.

Bearing in mind that within the basal (and other) convecting layers strong mixing occurs and chemical transfer within the layer is rapid, the following discussion refers to the transmission across diffusive boundaries from the bulk of the overlying magma. In cases where the chemical transfer is slow relative to the rate of crystallization much more marked differentiation of the cyclic units should occur as the chemical components are drawn from a smaller volume of magma. This in turn will lead to a less marked differentiation in a gross sense, as the chemical fractionation effects of crystallization are not transmitted to the overlying magma.

One extreme example would be if the bottom layer was a totally closed system. The process would then lead to complete fractionation of that layer of liquid from olivine-rich rock at the base to a quartz-rich residuum at the top. The following layer would be identical. The other extreme would be if the whole of the intrusion equilibrated each time a layer increment of crystals fractionated. In this case there would be a very gradual decrease in parameters such as the Mg/Fe ratio of mafic minerals and An content of plagioclase, there would also be a gradual addition of new phases through the whole crystal pile. No marked contrasting layers would form and no reversals would ever occur but complete differentiation would take place in a gross sense.

The account by Irvine (1980b) is clearly very different to the models of Rice (1981) and McBirney & Noyes (1979), in that the process of bottom crystallization affects the overlying liquid to a varying degree, and the convecting layers are not simply imposed on a pre-existing temperature and composition gradient and then freeze one by one from the bottom up. Crystallization is at the base of an actively convecting layer according to Irvine and the significance of a static boundary layer is underplayed.

Irvine (1981) modified and extended the model outlined above in a further report on the Muskox intrusion. In this extended model the effects of lateral cooling and circulation (Turner & Chen, 1974) and crystallization (Chen & Turner, 1980) were taken into account. Double-diffusive layers were envisaged as crystallizing inward from the margin of the intrusion and thus producing a stacked sequence of cyclic units. The convecting liquid layers would precipitate a series of mineral species (depending on the liquidus relationships in the layer) on the very gently inward-dipping temporary wall of the intrusion, thus producing the

layering which grew inward from the walls. This process should produce marked lateral fractionation effects within a single cyclic unit. This may account for the lateral fractionation observed by McBirney & Noyes (1979) in individual layers of the Skaergaard intrusion.

The latter model of Irvine is difficult to apply to the Bushveld Complex for two reasons. Firstly, the model demands lateral cooling which would probably not have been a significant factor in the Rustenburg Layered Suite due to its great lateral extent compared to its thickness. And, secondly, the process may impose a dip on the growing layers which was clearly not the case in the Rustenburg Layered Suite (Gough & Van Niekerk, 1959). Furthermore, not enough data is available to test for lateral fractionation in individual layers.

Interrelationships Between Liquidus, Subliquidus and Solidus Stages

It is opportune at this point to briefly outline the possible interrelationships and processes occurring in the overlying liquid, the crystal mush and the solid rock below. These will then be dealt with in detail in subsequent chapters. At any one time there is a downward progression within the magma chamber from a liquid magma to a solid rock. This progression can be subdivided into three zones where different processes are occurring. These are:

The Liquidus Zone:

This zone comprises the liquid part of the magma. The base of this zone is the horizon of active primocryst accumulation, which is continually moving upward as the liquid is converted to a crystal mush on the temporary floor (or walls and roof) of the magma chamber.

The Subliquidus Zone:

The crystal mush below the horizon of active crystal accumulation comprises the subliquidus zone. It consists, at the top, of an open framework of crystals but grading downward into an area with a more closed network and finally into solid rock.

The Solidus Zone:

This zone consists of solid but still hot rock which slowly cools with further reaction by coexisting phases to ambient temperatures.

As demonstrated by Irvine (1980a & b) infiltration metasomatism is a common process in ultramafic layered rocks. Active upward movement of interstitial liquid displaces that which originally coexisted with the solid phases. While this process occurs continual reaction and re-equilibration changes both the composition of the primocryst phases and the moving metasomatizing liquid. Each layer of rock is thus the product of processes in each of the above zones at different stages in its evolution. These stages have been adapted from the work of Cameron (1969) to the bottom crystallization scheme adopted here.

The Liquidus Stage:

This is the stage where active accumulation and growth of crystals occurs on the temporary floor of the magma chamber, and corresponds to chemical subsystems 1 and 2 of Cameron (op. cit.). This active accumulation is dominated largely by processes occurring in the liquidus zone described above, but it is influenced by processes, such as the extrusion of interstitial liquid, from the subliquidus zone.

The Subliquidus Stage:

This corresponds to chemical subsystem 3 of Cameron. This stage encompasses the interaction of the primocryst phases with the possibly mobile interstitial liquids and fluid in the subliquidus zone, from when the crystal mush becomes isolated from the overlying liquid, until the rock becomes solid. This is the most complex chemical system to deal with as many factors, including the original interstitial liquid composition, primocryst compositions, modal proportions of crystals and liquid, liquid movement, and the possible formation of a fluid phase have to be considered.

The Solidus and Subsolidus Stage:

This is the fourth subsystem envisaged by Cameron. At this stage the rock is solid (the solidus zone) and all further reactions are down temperature re-equilibration reactions of crystalline phases with any fluid confined only to grain boundaries. These reactions proceed to different blocking temperatures and at different rates.

Replenishment of a Differentiating Intrusion

Many layered intrusions show evidence of multiple intrusion and replenishment, Skaergaard being a notable exception. Indeed, in the case of

the Bushveld Complex, the relative roles of multiple intrusion and fractionation have been hotly debated (see Chapter One for a brief review).

A number of experiments have been conducted on the intrusion and mixing of fluids of differing physical properties such as temperature, density and composition (see Germeles, 1975; Turner & Gustafson, 1978; Turner, 1978). In addition Huppert & Sparks (1980), Huppert & Turner (1981), Keays & Campbell (1981), Campbell (1977) and Irvine (1981) have suggested processes whereby mixing can occur in magma chambers.

When a new magma of contrasting composition, temperature and density flows into a magma chamber with residual liquid still present, a number of processes may be initiated. Firstly, if the rest liquid within the chamber is stratified (smoothly or in steps brought about by double-diffusive convection) this will influence the nature of the intrusive and mixing process. Secondly, the volume, rate and site of intrusion of the new magma with respect to the rest liquid has a marked effect on the mixing process in the chamber. Germeles (1975) has shown that introduction of significant amounts of less dense new liquid with respect to the rest liquid leads to convective mixing of the two liquids and strong circulation within the chamber as a whole. This is different from the situation where a small amount of new liquid is introduced which has a minimal effect on the rest liquid as a result of the intrusive process. If the liquid introduced from below is more dense than the rest liquid it may spread out over the base of the containing chamber and not immediately mix convectively (Germeles, 1975).

The latter case has been investigated by Huppert & Sparks (1980) and Huppert & Turner (1981) who envisage a hot, dense, ultramafic liquid intruded under a cooler less dense fractionated liquid. The layer of new liquid thus formed is of limited thickness and convects in a turbulent manner losing heat, through a non-turbulent interface, to the overlying rest liquid which also convects. This process continues while the lower layer crystallizes olivine and convects as a crystal slush (cf. the proposal of Rice, 1981). When the temperature equalizes the layers become quiescent and the olivine sinks to the bottom to form a layer of crystals. The two liquids may then mix or continue as separate layers, depending on their density. The model outlined above was applied by Huppert & Sparks to layered intrusions, and while the model may account for features of the Rhum intrusion, it does not work for the Merensky cyclic unit (as the MMF ratio of the Merensky pyroxenite changes with height), or the Muskox and

Stillwater intrusions for similar reasons. Irvine (1980a & b, 1981) has advocated a similar process of intrusion for the Muskox complex, but in his model the new layer of liquid has a significant vertical extent and it stratifies into double-diffusive convective layers due to cooling at the top, and only crystallizes at the bottom.

The process discussed above is an extreme case where the new liquid is denser than the whole of the rest liquid. Turner (1978) and Turner & Gustafson (1978) have investigated the process occurring when a liquid is intruded into a density gradient (as would be expected in a magma chamber undergoing double diffusive convection). In this case the liquid would rise to its own density level and then spread out laterally.

The following discussion is speculation on the part of this author, as no direct experimental data are available. In view of the processes of entrainment and mixing discussed by Germeles (1975), if a buoyant plume of magma is intruded into a stratified rest liquid, mixing of the new liquid with the lower portion of the rest liquid may occur, up to the density level where the rest liquid is less dense than the intruding liquid. If no entrainment occurred the new magma would simply spread out at its own density level (Turner & Gustafson, 1978).

The temperature of the intruding magma is crucial to the processes occurring next. It is extremely unlikely that a new intruding liquid of roughly similar composition would be cooler than the rest liquid which has been fractionating in a high-level magma chamber for some time. If it were, it would become superheated when it spread out at its own density level. The effect on the underlying magma would be to induce copious precipitation of crystals from the cooled magma below (and possibly above), which should become more markedly stratified and convect more vigorously. The lower boundary would have a "diffusive"* interface inhibiting mixing and the upper boundary a "fingers"* interface promoting mixing (see Turner, 1978).

A more likely situation would be if the temperature of the intruding magma was higher than that of the rest liquid. In this case the magma would rise to its own density level as before, but in this case the upper boundary would have a "diffusive" interface inhibiting mixing, but the

* See Kantha (1980) and Turner (1973 or 1974) for a description.

lower boundary would have a "fingers" interface promoting mixing. This process is clearly illustrated by Turner (1978). The above mechanism coupled with entrainment of the rest liquid by the intruding magma (Germeles, 1975) would result in a thorough mixing of the new magma with at least the lower portion of that previously present. Crystallization would cease as the new and mixed magma would be superheated, and possibly some resorption of the pre-existing crystal pile would occur. Once mixing was complete the liquid would stabilize, start to cool from the top and then again stratify into double-diffusive layers. Crystallization would then resume as proposed by Irvine (1980a & b) for a dense, hot replenishment.

Wallrock Assimilation and Contamination

The possibility of country rock assimilation by the magma of layered intrusions has received considerable attention. In general, only a restricted amount of assimilation can occur, as it is a self-limiting process (Morse, 1980). For a general background to the problem Carmichael et al. (1974) give a brief resume, and McBirney (1979) a detailed review.

The analysis of Irvine (1970a) and more recent work by Rice (1981) do, however, suggest a possible mechanism for large-scale contamination of the basaltic liquid in a magma chamber by melted liquid derived from the roof rocks. The process envisaged here is more correctly termed magma mixing even though the second silicic contaminating liquid is derived by roof-rock melting due to heating by the cooling mafic magma. Irvine (1970a) has shown that considerable roof-rock melting can occur, but that it does not necessarily mix with or become assimilated by the mafic magma, but floats on top. Irvine (1970b) has suggested that periodic mixing of this magma with the basic magma of the layered intrusion could occur. He later showed that this could induce copious precipitation of chromite to form chromitite layers (Irvine, 1975). But he later rejected the model (Irvine, 1977) as improbable due to the very large amounts of contamination necessary, but later re-introduced it (Irvine, 1980b).

Rice (1981) has shown that hot basic magma underlying cooler, less dense, acid magma could eventually lead by multi-diffusive convection and mixing to a process termed "rollover", in which the basic and acid magmas homogenize, exsolve volatiles and initiate explosive volcanism of hybrid (andesitic) rocks. In view of the probable existence of this configuration

(rhyolitic roof melt over basalt magma) in layered intrusions this process deserves consideration.

Trace Element and Isotopic Mixing and Diffusion

Within a double-diffusive convecting system the mixing of new magma influxes and other possible liquids is governed by the temperature, density and composition gradients established by temperature and major element composition. The mixing by diffusion of trace elements and resulting changes in their ratios is governed by a further consideration of the chemical potential of that element with respect to the two mixing magmas.

In the case of a "fingers" mixing situation the process of mixing is relatively thorough. However in the "diffusive" case two possibilities can be visualized. Consider a situation where a dense hot magma underlies a cooler less dense magma and the system develops a series of double-diffusive layers. If a particular trace element in the dense hot magma has a higher chemical potential than that element in the overlying cooler magma, the element will move upward across the diffusive boundary into the overlying magma and thus progressively deplete the underlying layer of that component. Conversely, if an element in the overlying cooler magma has a higher chemical potential it will move downward across the diffusive interface enriching the denser hotter magma in that component. The rate of movement (diffusion) is determined by the relative chemical potential (concentration) and the diffusivity of the element.

Thus the diffusion and mixing of trace elements may be independent of the diffusion of heat and major elements which drive the double-diffusive processes. This may lead to different chemical and isotopic profiles in the convecting magma which may be recorded in the crystallizing products.

Addition of Fluid Phases from Below

The intrusion of hot basic magma into the sediments of the Transvaal Supergroup has metamorphosed the latter to varying degrees. Most progressive metamorphic changes in sedimentary rocks involve dehydration, decarbonation and the production of a fluid phase (Winkler, 1974). Part of this fluid may have been consumed by the hydration of the pre-Bushveld Complex sills within the Transvaal sediments. These sills have suffered some metamorphism to medium grade (Frick, 1973). Nevertheless, a substantial portion of the fluid liberated by metamorphism of the sediments must have migrated upward and interacted with the layered rocks of the Bushveld Complex.

Irregularities such as domes and basins in the floor of the complex would have served to concentrate these supercritical volatiles in different areas along the generally flat floor of the Rustenburg Layered Suite. Lateral migration and escape at the edges of this large blanket-like intrusion would have been restricted. Any faulting or jointing in the floor-rocks and layers already solidified at the base of the intrusion would allow access of the fluid to the magma chamber possibly in restricted areas associated with structural disturbances (De Waal, 1977). This ingress may well have been episodic and associated with new influxes of magma and adjustment of the floor of the chamber to the load imposed by introduction of new liquid.

The concentration of gaseous constituents within the magma is thus influenced by four processes: introductions of new (dry?) magma, enrichment by crystal fractionation of anhydrous phases, introduction of fluids from below and loss of volatiles from the magma due to volcanism initiated in the roof of the complex.

Physical Processes in the Bushveld Complex Magma Chamber Recorded in the Study Section

Introduction

The layered rocks in the study section may have originated through a variety of processes, some of them not well understood. Evidence presented below and in Chapter Two shows that there is a distinct break in the accumulation of the layered rocks at the top of the Footwall unit and that a large new influx of magma occurred at this point. The rocks of the Footwall unit and the overlying Merensky and Bastard cyclic units are thus part of different but related magmatic systems and are treated separately.

Data gathered during this study (Fig. 2:3 in Chapter Two) refute the theory of crystal settling or deposition from density currents in a large body of magma (i.e. the whole of the overlying volume of liquid). The MMF ratio of orthopyroxene in the Merensky cyclic unit changes from ± 0.85 at the base to ± 0.77 where orthopyroxene ceases to be a primocryst phase, some 6m above the base of the unit. This marked differentiation within a few metres in a cyclic unit cannot be attributed to crystal settling from the whole of the overlying magma, as the composition of the crystals should

then be much more uniform as the overlying volume (thickness) of liquid (probably several hundred metres) could not be significantly changed by the crystallization of such a small amount of crystals. The volume of liquid that can account for the chemical variation observed is less than 20m (see Chapter Five). The alternative model involving a density current from the roof of the intrusion also fails to explain the observed variation as there should be no systematic compositional variation in a well-mixed, turbid density current. Similar chemically graded layers have been noted elsewhere by Jackson (1970), Irvine (1980b) and McBirney & Noyes (1979). McBirney & Noyes also reject crystal settling as a significant process in magma chambers on this evidence. Density currents and crystal settling from a large magma volume are thus not tenable in the context of the Merensky cyclic unit and other persistent chemically graded units in the Bushveld Complex.

On the other hand, crystal settling from a limited layer (crystallizing in isolation from the main body of magma) is a possible mechanism for the generation of the Merensky cyclic unit, but special conditions have to be proposed. Nucleation of any crop of orthopyroxene crystals must be followed by their growth and sinking to the floor of the magma chamber. The crystals that nucleated at the base of the liquid would be the smallest and most Mg-rich; crystals nucleated at a slightly higher level would have further to settle and thus more time to grow and react becoming larger and more Fe-rich (Jackson, 1961). The residual magma in the crystallizing layer, depleted of dense pyroxene component would become less dense, it would then nucleate an additional phase (plagioclase) or mix with the overlying main volume of magma, thus contributing to the gross differentiation of the intrusion. This scenario is very similar to that presented by Jackson (1961) for major units in the Stillwater intrusion. However, as indicated in Chapter Two, the crystal size decreases upwards in the Merensky cyclic unit and this tends to refute the model outlined above. Furthermore, the occurrence of the thin chromitite layer at the base of the Merensky cyclic unit, sometimes in an "upside down" position on the sometimes "overhanging" walls of potholes indicates that this unit must have crystallized in situ (for a description and possible explanation for potholes, see Chapters Two and Four respectively). The data of Murase & McBirney (1973) and McBirney & Noyes (1979) on yield strength and viscosity of magmas also suggest any form of crystal settling in the magma is unlikely.

Strontium Isotope Data and the Identification of a New Magma Influx

$^{87}\text{Sr}/^{86}\text{Sr}$ initial ratios were determined on a suite of samples from the whole of the study section (Table 2:1). These are mainly primocryst plagioclase separates but a few whole-rock data from the Merensky cyclic unit are included (see Chapter Two). Much of the following discussion and conclusions in this section are reworked from a published report by the author and J.S. Marsh (Kruger & Marsh, 1982).

The variation of the initial ratios with height (Fig. 3:1) indicates a step like pattern which confirms, in general, the findings of Hamilton (1977). His work indicated that the rocks from the lower 3m of the Merensky cyclic unit and the top of the underlying Critical Zone (grouped by Hamilton as the "Merensky Reef Interval") have a constant initial ratio, whereas samples from the overlying Main Zone have higher but variable initial ratios. All but one of Hamilton's samples from this "Merensky Reef Interval" are from the Eastern Bushveld Complex and have initial ratios identical to the present author's feldspar separates (Table 2:1) from the Footwall unit. Four of Hamilton's Main Zone samples are from the Western Bushveld Complex, but accurate details of their stratigraphic positions are not available and this limits comparison with the data presented here. Hamilton found that three whole-rock samples extending to 3m above the Merensky pegmatoid had similar initial $^{87}\text{Sr}/^{86}\text{Sr}$ ratios to the rocks from below the Merensky cyclic unit. One of these samples is from the Western Bushveld, and the other two from separate localities in the Eastern Bushveld.

The data reported by Kruger & Marsh (1982) (and reproduced in Table 3:1) show that there is a dramatic increase in the initial ratio of the samples within the Merensky cyclic unit itself from 0.70637 ± 2 at the base of the unit (which is identical within error to the Footwall unit samples), to 0.70740 ± 3 at the top. The latter value is similar to the values characteristic of the overlying Bastard cyclic unit (Fig. 3:1). The data from the Bastard unit are much more uniform than those of the Merensky unit but there is some scatter with a slight tendency for the ratio to increase with height in the unit. Hamilton (1977) also commented on the scatter of ratios, from a much larger vertical interval in the Main Zone in the Eastern Bushveld Complex, but gives little information on any systematic trends. The sudden increase in the initial $^{87}\text{Sr}/^{86}\text{Sr}$ ratios

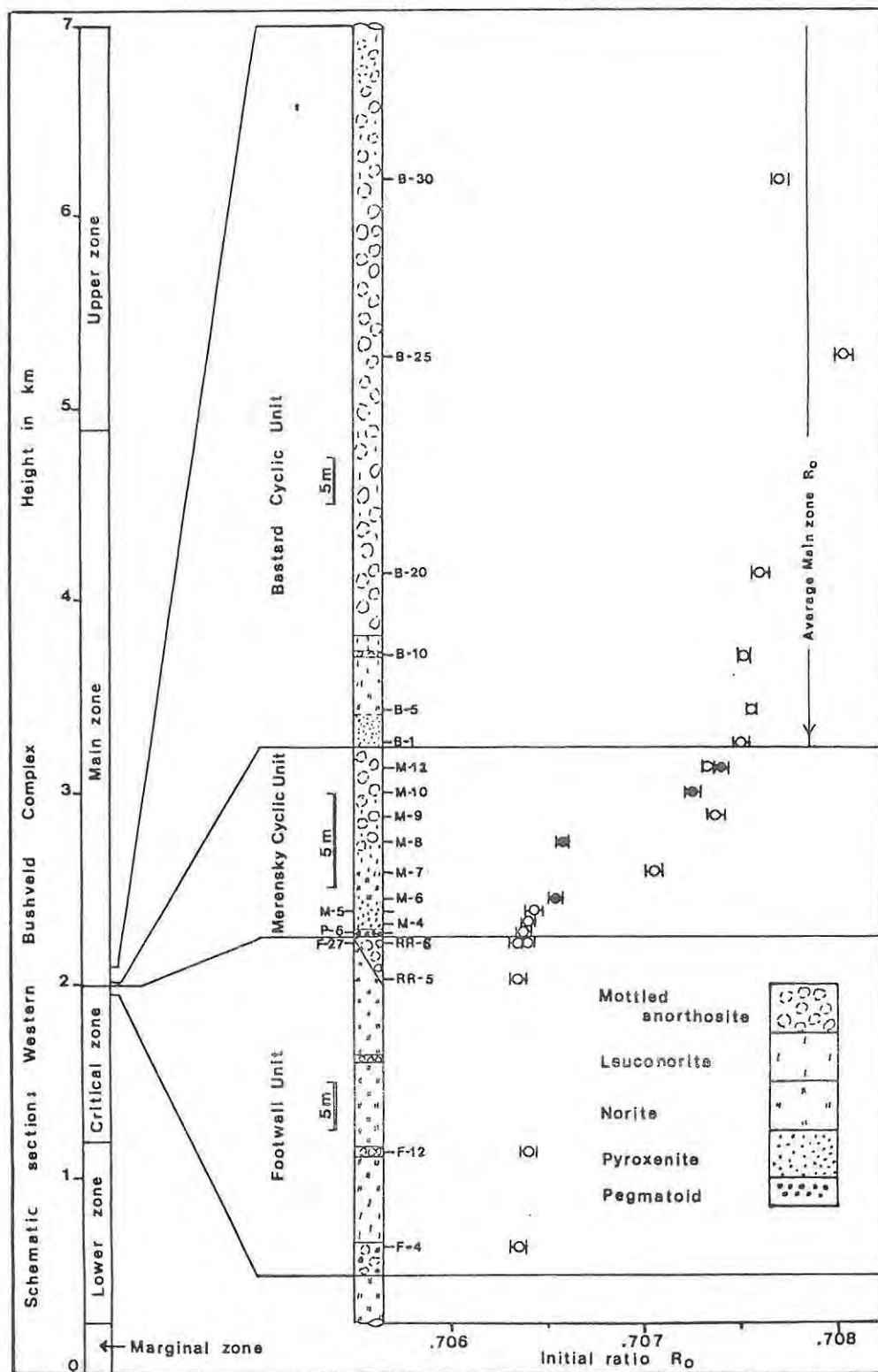


Fig. 3:1 The initial $^{87}\text{Sr}/^{86}\text{Sr}$ ratios, stratigraphic positions and lithology of samples on which Sr-isotope ratios were determined. Note the difference in vertical scale between the Footwall, Merensky and Bastard units. The average Main Zone initial ratio (R_0) is from this work and that of Hamilton (1977). Plagioclase separate \circ , Whole rock \bullet .

in the Merensky cyclic unit correlates with evidence for a marked hiatus in the accumulation of the crystal pile at this point, such as the presence of a lateral disconformity and abundant potholes, described in Chapter Two. Significantly, it also correlates with the stratigraphic level of the PGE-rich Merensky pegmatoid and pyroxenite layers. This situation is probably not fortuitous as the PGE-rich UG2 chromitite layer is also probably associated with a step-like increase in the initial $^{87}\text{Sr}/^{86}\text{Sr}$ ratio (Hamilton, 1977).

The pattern of variation in the initial $^{87}\text{Sr}/^{86}\text{Sr}$ ratios (Fig. 3:1) can help to constrain ideas on the types of processes occurring at this level during the accumulation of the Rustenburg Layered Suite. In general three main models can be envisaged, the main features of which have been described in the above section on physical processes. Firstly, the increase in initial $^{87}\text{Sr}/^{86}\text{Sr}$ through the Merensky cyclic unit and the high values (for mafic rocks) for Main Zone samples might reflect in situ contamination of the existing magma by assimilation of its wall rocks. Secondly, contamination and mixing of melted roof rock material as a result of a "rollover" process (Rice, 1981) might be considered. This process would result in mixing of a large amount of liquid accumulated from a long melting history of the roof rocks. Thirdly, the lower part of the Main Zone rocks could have crystallized from an influx of new magma having a $^{87}\text{Sr}/^{86}\text{Sr}$ ratio of 0.7075, or from a mixture of the magma already there and a new magma with a $^{87}\text{Sr}/^{86}\text{Sr}$ ratio of more than 0.7075.

Crucial to the understanding of the crystallization history of the study section are the causes for the general upward increase of the initial ratio within the Merensky cyclic unit itself. Two possibilities exist. Either the variation records processes occurring during the accumulation of the primocryst phases in the Merensky unit and hence processes in the magma chamber, or the variation (a type of "smoothing" process) was subsequently imposed on an initially sharp step-like discontinuity at the base of the Merensky cyclic unit.

Facts having a bearing on this problem are that the ratios determined on the basal portion of the Merensky cyclic unit relate to interstitial plagioclase and do not necessarily represent the ratios of the primocryst orthopyroxene of the Merensky pegmatoid or pyroxenite. There is also a significant proportion of interstitial plagioclase in the overlying Meren-

sky norite. The plagioclase separates of the Merensky mottled anorthosite consist dominantly of primocryst plagioclase. Furthermore, the whole rock sample M-8 has an initial ratio considerably lower than the primocryst plagioclase separates M-7 and M-9 which bracket this sample (Table 2:1). These observations strongly suggest that the initial ratios determined in the Merensky cyclic unit are a function of the proportions of primocryst and interstitial phases, and since the plagioclase contains almost all the Sr in the rocks, this phase has the dominant influence on the initial ratio. The interstitial phases may thus have dominantly "Critical Zone characteristics" and the primocryst phases "Main Zone characteristics". However, this postulated mixed isotopic character has not been determined on a single rock sample. This suggestion may throw light on the observation made by Hamilton (1977) that an abrupt increase in the initial ratio occurs some 3m above the base of the Merensky cyclic unit, as it is at this point that primocryst plagioclase becomes the dominant Sr-bearing phase. Further circumstantial evidence for an initial step-like discontinuity is provided in the following discussion.

The observed rapid increase in the initial ratio could conceivably be ascribed to assimilation and thorough mixing with roof rock material (Rooiberg felsite?) with a high initial ratio, concomitantly with the crystallization of the Merensky cyclic unit. However, the Merensky unit is very thin (0,34% to 3,4% of the Main Zone) and assimilation would have to have ceased by the time the base of the Bastard cyclic unit accumulated. Aside from questions as to why assimilation should suddenly start and end as required by this model, heat budget considerations would allow only a volume of felsite roughly equivalent to the volume of the Merensky cyclic unit to be assimilated. The felsite has a Sr content of about 70ppm (Lenthall & Hunter, 1977) but no Sr-isotope data is available. Assuming the magma before the postulated assimilation event had 250ppm Sr (calculated from a distribution coefficient of 1.9 (Irving, 1978) and the plagioclase primocryst Sr concentrations of the Footwall unit listed in Table 2:1) and that there was 5% contamination, the contaminant would have to have had an $^{87}\text{Sr}/^{86}\text{Sr}$ ratio of greater than 0.78. This ratio is high for felsite with Rb/Sr ± 2.5 that predate the Bushveld Complex, and whose crustal or mantle precursors had very much lower Rb/Sr ratios. Contamination by assimilation of roof-rock felsite is thus not a viable model. Contamination by any of the Transvaal Supergroup sediments would

not provide a solution either as these have low $^{87}\text{Sr}/^{86}\text{Sr}$ ratios and generally low Sr concentrations (Davies et al., 1970).

A model involving the gradual introduction of fresh basic magma with a high $^{87}\text{Sr}/^{86}\text{Sr}$ ratio (>0.7075 to >0.7086), which thoroughly mixed with the residual liquid as it was introduced, could also be invoked. In this case crystallization of the Merensky cyclic unit would occur as the magma was introduced to account for the upward increase in the initial ratio within the Merensky cyclic unit. This model is refuted by the upward decrease in the MMF ratio of primocryst orthopyroxene in the Merensky cyclic unit, as the model requires very thorough mixing of each increment of new magma, which would have to be reflected in very constant MMF ratio unless the new magma was very much more Fe-rich than the residual magma already present there. This could not have been so as the base of the overlying Bastard pyroxenite is also characterized by primocryst orthopyroxene with a MMF ratio similar to the MMF ratio of pyroxenes at the base of the Merensky pyroxenite. A slow influx of new magma coupled with mixing and crystallization is thus also not a viable hypothesis.

From available data and the above discussion, it can be concluded that the initial ratios of the primocryst minerals of the Merensky cyclic unit had Main Zone characteristics and that there was initially a sharp step-like discontinuity at the base of the Merensky cyclic unit. This may not include the Merensky pegmatoid but discussion of this point is reserved for Chapter Four. The upward increase of the initial ratio within the Merensky cyclic unit is attributed to upward diffusion of Sr, or infiltration metasomatic addition of interstitial liquid (as proposed by Irvine (1980a)) with Critical Zone characteristics from the Footwall unit.

Three further alternatives, each of which could explain the initial step-like increase in the initial ratio of the primocryst phases deduced above, are discussed here. The first model again involves the incorporation and mixing of roof rock material but this is mixed in as a pre-melted liquid floating on top of the basic magma due to density differences. In this case no heat budget constraints are involved as the liquid would have been melted over a large time interval due to heat escaping through the roof of the intrusion. Indeed, Irvine (1970a) predicted considerable melting of the roof rock of the Rustenburg Layered Suite and suggested that the Rашoop Granophyre Suite (SACS) may represent this melt. Mixing of the residual basic magma which crystallized the Footwall unit with the felsic roof melt may have occurred by the "rollover" process

as envisaged by Rice (1981). This would involve sudden and complete homogenization of the roof melt and the underlying mafic magma. Small volumes of contaminating material (<5%) are not viable as indicated in the discussion on assimilation above. However, larger volumes of felsite contaminant would require lower Sr-isotope ratios. Contamination by large volumes of felsite melt (10-30%) should have a marked influence on the major element composition of the magma, and hence on its liquidus phase compositions and phase relations. However, this has not occurred. Firstly, the phase compositions of the major phases of the Merensky and Bastard cyclic units have not been significantly changed from those of the Footwall unit relative to the amount of contamination (e.g. plagioclase should have been markedly less calcic but is not (Fig. 2:3). Secondly, mixing of a very large proportion of very silicic magma should induce copious precipitation of chromite (Irvine, 1975) which has not occurred, there being only a relatively minute quantity at the stratigraphic level under consideration. In all, it appears that the incorporation of roof-rock melt (in situ contamination) is an implausible mechanism to explain the change in the initial $^{87}\text{Sr}/^{86}\text{Sr}$ ratio, or the mineralogy and chemistry of the Merensky and Bastard cyclic units and the rest of the Main Zone.

The two remaining possibilities, both involve an influx of new basic magma similar in composition (apart from Sr-isotopes and some trace elements) to that already in the magma chamber. The only difference in the two models is the possible mixing behaviour of the new magma pulse. In both cases the introduction of the new magma was rapid and crystallization was arrested while magma addition occurred. These models were discussed in detail earlier in this chapter and are applied here to the study section. The first of these models involves the introduction of a denser superheated magma with a $^{87}\text{Sr}/^{86}\text{Sr}$ ratio equal to that of the Bastard cyclic unit. This would then be cooled through a diffusive interface at the top, stratify into double-diffusive convecting layers and start crystallizing at the base. However, this model is not favoured by the available $^{87}\text{Sr}/^{86}\text{Sr}$ ratio determinations (Hamilton, 1977) from above the Bastard cyclic unit (Fig. 3:2). These indicate that the initial ratio is variable but generally higher (except for one point) than that of the Bastard cyclic unit and the model requires that the initial ratio decreases with height reflecting mixing of the new magma with the old at its top interface.

The most plausible model considering the available data is one in which the new magma influx was less dense than that already present. This magma would rise up into the overlying liquid as a buoyant plume (Germeles, 1975) entraining part of the rest liquid. The mixing process that ensued probably involved the whole of the rest liquid in the magma chamber, as the same difficulties as with the alternative model would arise if only the lower portion of the rest liquid was involved and was separated from the upper less dense portion by a diffusive interface. Mixing would take place by turbulent convection and by efficient "fingers" regime homogenization. The new magma was probably slightly more primitive than the rest liquid and less dense only because it was hotter. The magmas would thus have been easily miscible.

The initial ratio of the new magma influx must have been considerably higher than the value recorded in the Bastard unit, and this contention is supported by the high values obtained by Hamilton (1977) for some samples in the Main Zone. The high initial ratios recorded by Hamilton for the Main Zone could be due to small additions of magma after the main influx which did not mix completely. The highest initial ratio recorded (assumed to be very close to that of the new magma), the average Main Zone initial ratio and the initial ratio of the original magma in the chamber (recorded by the Footwall unit), can be used to infer an approximate proportion for the new magma influx, using a binary mixing model. This model also rests on the assumption that the concentrations of Sr in the plagioclase separates from the Footwall and Bastard units imply real and proportional differences in the Sr concentrations of the Footwall and Bastard unit magmas respectively (a constant distribution coefficient is assumed). The calculation shows that the magma from which the Bastard and Merensky cyclic units crystallized probably consisted of a minimum of 30% residual magma and a maximum of 70% new magma.

The above analysis rests on several assumptions and should be considered speculative and only applicable to the lower Main Zone, as only two Sr isotope determinations (Hamilton, 1977) with a wide spread are available from upper Main Zone (Fig. 3:2) and there is a strong possibility of a further magma influx higher in the Main Zone (Mitchell, research in progress). Furthermore the Sr concentrations of the mixing magmas have to be known with greater certainty for the estimate of the magma volumes to

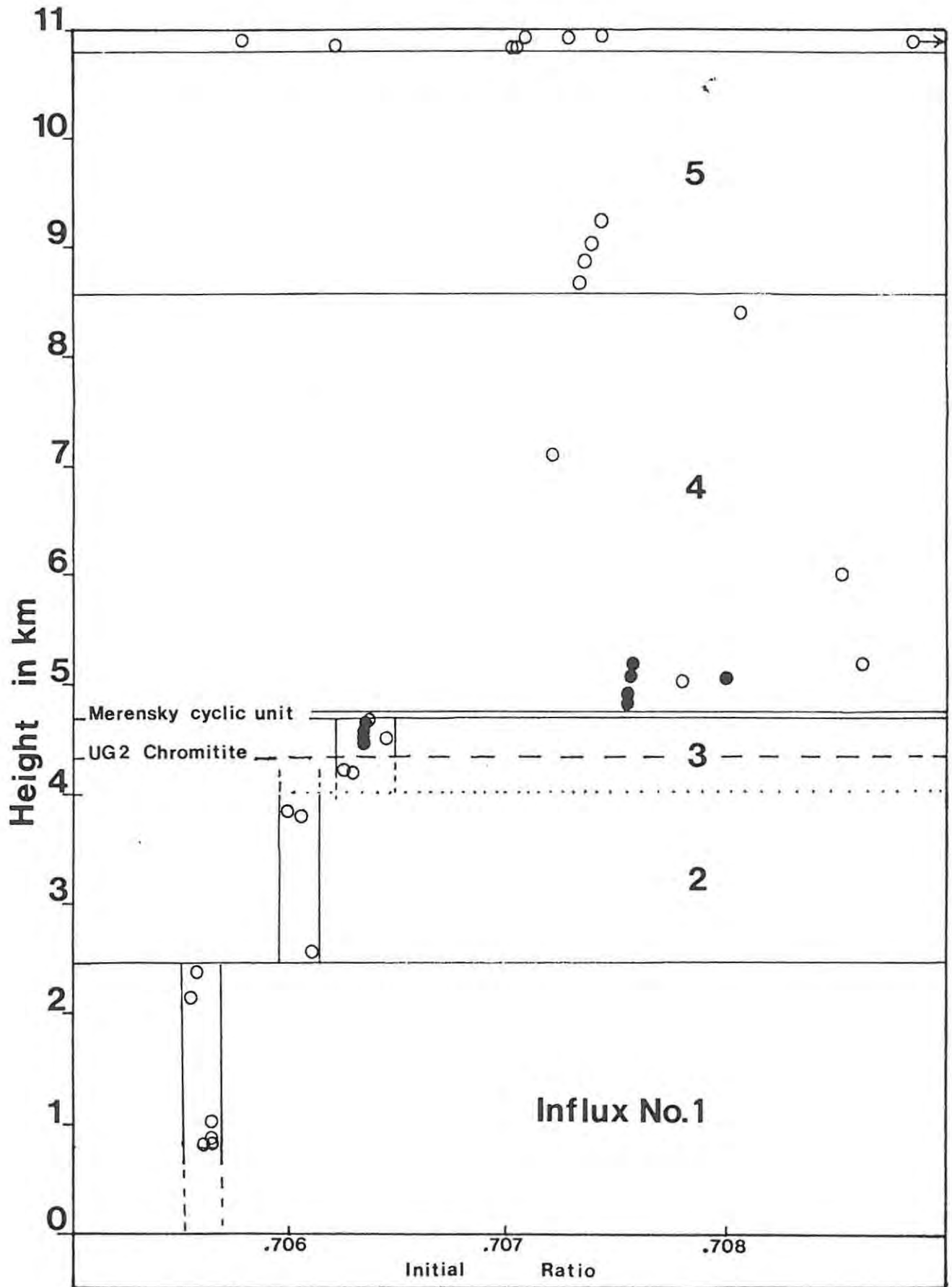


Fig. 3:2 This diagram summarizes all the $^{87}\text{Sr}/^{86}\text{Sr}$ initial ratios available for the mafic layered rocks of the Bushveld Complex (Hamilton, 1977 ○ and Kruger & Marsh, 1982 ●). The stratigraphic positions are the best available and are purely relative. no distinction is made between samples from the Eastern and Western Bushveld Complex. Note the step-like changes upward in the sequence up to the Main Zone and the irregular scatter of points in and above the Main Zone. Possible magma influxes are indicated.

be accurate. The approach adopted here and the data available can only give approximate relative volumes of the new and residual magma and not the absolute amounts.

Other Magma Influxes into the Rustenburg Layered Suite Magma Chamber

As demonstrated in this work and the work of Hamilton (1977), summarized in Fig. 3:2, there are step-like changes in the Sr-isotope initial ratios of the layered rocks below and within the succession studied here. If in situ contamination is excluded, this implies that at least two primary magmas with different initial $^{87}\text{Sr}/^{86}\text{Sr}$ ratios are involved in the evolution of the Rustenburg Layered Suite. These initial ratios span a documented range of 0.7056 to 0.7086 (Hamilton, 1977), and the ratios within this range could be a result of mixing between the two primary end-member compositions. The first magma would have had a low $^{87}\text{Sr}/^{86}\text{Sr}$ ratio and the second magma the reverse. Obviously, this is not proven and a range of primary magmas with increasing $^{87}\text{Sr}/^{86}\text{Sr}$ ratios could also produce the pattern now seen.

These observations go some way to resolving the conflicting views of Sharpe (1981a) and others who postulate several magma impulses of different composition, and the proposal of McCarthy & Cawthorn (1980) and others who postulate only two major magma influxes. The magmas recognized in the marginal sills (Sharpe, 1981a) could be regarded as mixed magmas extruded from the Bushveld magma chamber and not as primary magmas intruded into the magma chamber. A complete resolution of the conflicting views awaits very detailed Sr-isotope and chemical work on the marginal sills and more work on the layered rocks of the complex. Clearly if the introduction of new magmas was episodic, with significant crystallization between pulses, each new impulse of magma would produce a shift in the $^{87}\text{Sr}/^{86}\text{Sr}$ initial ratios recorded in the layered rocks unless the unlikely situation arose where the $^{87}\text{Sr}/^{86}\text{Sr}$ ratio of the inflowing magma was identical to the mixed magma in the chamber. The exact nature of the changes would be a function of the mixing and double-diffusive convective processes outlined in the previous sections.

The data presented here and those of Hamilton (1977) suggest that at least four magma impulses occurred either as influxes coupled with mixing of two original primary magma types as outlined above, or as separate magma types. Furthermore, Sharpe postulated that his third major influx

occurred above the Bastard unit and not at the top of the Footwall unit as shown here. Sharpe's hypothesis that further influxes may have occurred higher up in the Main Zone is supported here.

The model postulated by McCarthy & Cawthorn (1980) is refuted by the data presented in this work (Table 2:1 and Fig. 2:1) and by the data of Hamilton (1977) (Fig. 3:2) on which their model is based. As shown in Figs. 3:1 & 3:2, there is no evidence for a smooth increase in the $^{87}\text{Sr}/^{86}\text{Sr}$ initial ratio as required by the McCarthy-Cawthorn model, which also requires an excessively long cooling time (10-20Ma) for the Lower and Critical Zones and an additional 20-40Ma for the Main and Upper Zones. Furthermore, their model requires that the postulated second large magma influx above the Merensky cyclic unit had a low initial $^{87}\text{Sr}/^{86}\text{Sr}$ ratio relative to that of the Footwall unit, contrary to the observed increase in the initial ratio. The only evidence of a low initial ratio at this level is sample No. SA 1087 of Hamilton which is not from the layered rocks of the Main Zone at all, but is from a metamorphosed chill which may have suffered isotopic exchange with, or been contaminated by, the floor rocks with which it is in contact. The difficulties with the interpretation of this sample have been pointed out by Hamilton (1977), and need not be repeated here. Furthermore, Davies et al. (1980) recorded a range of possible $^{87}\text{Sr}/^{86}\text{Sr}$ initial ratios (0.7037 to 0.7098) from a thin sill in the floor rocks of the Bushveld Complex, indicating that severe problems could be encountered in using isolated determinations of Sr-isotopes of samples close to, or in contact with, the host rocks.

The data presented here also imply that the Merensky cyclic unit was the first unit to crystallize from a mixture of a new influx of magma and the residual magma left after formation of the Footwall unit, and not one of the last units to form from the residual magma after an extensive fractionation process of Lower and Critical Zone magmas as proposed by McCarthy & Cawthorn (1980), Vermaak (1976a), Sharpe (1981a) and others.

Mineralization at the Base of the Merensky Cyclic Unit

The isotope data presented here suggest two possible origins for the PGE, Ni and Cu sulphide mineralization at the base of the Merensky cyclic unit. Either the mineralization is associated with the initial step-like increase in the initial ratio and the economically important elements were precipitated as immiscible sulphide droplets from the overlying magma, or

it is associated with later infiltration metasomatic processes as first proposed by Lauder (1970).

Recently Keays & Campbell (1981) have outlined a model accounting for PGM, Cu and Ni sulphide mineralization in the Jimberlana layered intrusion in Western Australia involving the mixing of magmas by processes similar to the processes described here. They extend their model to account for the formation of the Merensky mineralization. Their magma mixing model is similar to the model outlined above, except for some details of the mixing process which are uncertain in any case. For example, they advocate convective overturn of the new magma influx whereas I prefer a "fingers" type mixing to account for the observed chemistry of the Merensky and Bastard cyclic units. Both this author's model and the Keays & Campbell model fit the PGE data of Page et al. (1981). Thus, in this author's opinion the base metal sulphide and PGM mineralization was derived from the overlying mixed magma and not from the infiltration metasomatic process. However the latter process may have altered and redistributed the pre-existing sulphides and PGE as suggested by Brynard et al. (1976).

Summary

The behaviour and crystallization of magma within the magma chamber of a layered intrusion is controversial. However, it does appear that the crystal settling theory does not explain the observed features of many layered intrusions. Bottom crystallization of a magma undergoing double-diffusive convection more successfully explains some features of layered intrusions, but at this stage there is still no agreement as to the exact role of the double-diffusive process, and there are widely divergent hypotheses that invoke the process.

Strontium isotope and chemical data presented in this work indicate that there was a major new impulse of basic magma into the Bushveld Complex magma chamber after the formation of the Footwall unit. This new magma mixed with that already present in the chamber and the Merensky cyclic unit and subsequent layers were precipitated from the blended magmas. The mixing of a new, more primitive, magma with that already in the magma chamber may have resulted in the precipitation of immiscible sulphide droplets rich in PGE which accumulated at the base of the magma chamber before or during the formation of the Merensky pyroxenite, thus accounting for the mineralization associated with this unit.

After the postulated intrusion and mixing of magmas recorded in the study section, the magma stratified into double-diffusive layers which then crystallized, from the bottom up, as partially closed systems to form the cyclic units. Subsequent or contemporaneous infiltration metasomatism from the Footwall unit modified the isotope chemistry of the lower part of the Merensky cyclic unit.

CHAPTER FOUR: The Subliquidus Stage

Introduction

The compositional changes and physical behaviour of the interstitial liquid during crystallization of the crystal mush is examined in this chapter. The subliquidus stage commences when the crystal mush consisting of primocrysts and interstitial liquid is covered and prevented from equilibrating with the overlying convecting magma. The mixing of interstitial liquid flowing out of the crystal mush with the overlying convecting magma (Irvine, 1980b), is not precluded. The subliquidus stage is characterized by the presence of a liquid or which may be saturated with volatiles. Thus the subliquidus stage terminates when the rock becomes solid.

Fractional crystallization at the liquidus stage produces chemical gradients with respect to height in both the solid phases and the interstitial liquid with which the solid phases are in equilibrium (see Chapter Five). The changes in the primocryst phase assemblages with height in the succession are also accounted for by this liquidus stage crystallization. The composition of the interstitial liquid and the primocryst phases are thus intimately related. However, the proportion of interstitial liquid is not constant, but may vary as a function of the crystallization rate at the liquidus stage (Cameron, 1969). In the absence of adcumulus growth or expulsion of the interstitial liquid, the proportion of connate interstitial liquid usually falls between 20% and 50% (e.g. Wager & Deer, 1939; Brown, 1956; Wager et al., 1960; Wager, 1963; Henderson, 1968; Wager & Brown, 1968; Cameron, 1969; Eales, 1980).

Crystallization of the interstitial liquid usually proceeds from the base of the crystal pile upward. Thus in general the solidus zone is followed upward by the subliquidus zone. However, where very little interstitial liquid is trapped, or it is expelled, the mush may become nearly solid. Consequently slab-like layers of essentially solid rock may be present within the crystal mush. This is especially true of near-monomineralic layers such as some mottled anorthosites, chromitites and pyroxenites (Morse, 1980). Such layers could form barriers to moving interstitial liquid or volatile components.

The Initial Interstitial Liquid and Primocrysts: A Qualitative Discussion

In a highly idealized situation, bottom crystallization of a thin layer of magma at the base of the magma chamber that is relatively isolated from the main magma volume, leads to changes in the residual liquid composition of the basal magma layer, induced by crystallization of each increment of crystals (Fig. 4:1). This liquid is also interstitial to, and in equilibrium with, the phases which crystallized from it. Thus in any cyclic unit the composition of the interstitial liquid is variable with height in the succession and is directly related to the composition of the primocryst phases present. For example, in the Merensky cyclic unit the interstitial liquid of the Merensky pyroxenite primocrysts was in the pyroxene phase field, that of the Merensky norite on a cotectic and that of the Merensky anorthosite in the plagioclase field. Furthermore, the changes in the composition of the orthopyroxene with height within the Merensky pyroxenite implies variation in the composition of the primocrysts and original interstitial liquid with height (Fig. 4:1). This applies to both the Irvine (1980b) and McBirney & Noyes (1979) models for the crystallization of layered rocks discussed in Chapter Three.

These two models for the in situ formation of layers should however produce contrasting trace element distributions in the initial connate interstitial liquids. The process advocated by Irvine (1980b) involves fractional crystallization, from the base upward, of a strongly convecting basal liquid layer separated from the layers above by a "diffusive" interface. There is strong convective mixing of the residual liquid in this crystallizing basal layer after the deposition of each increment of crystals. The concentrations of trace elements in this residual liquid and thus of the interstitial liquid in the crystal mush are controlled by the distribution coefficients of the various elements and the Rayleigh fractionation law. In this case the incompatible elements (with respect to all crystal phases) should be enriched in the interstitial liquid towards the top of each cyclic unit. Conversely, compatible elements would be depleted upwards in each cyclic unit (Fig. 4:1).

The alternative mechanism advocated by McBirney & Noyes (1979), in which a double-diffusive layer stagnates and then crystallizes will produce a different pattern of trace element concentrations dependent on how the liquid in the layer crystallizes. In general, if the layer stopped

Increment No.	1	2	3	4	etc
Well mixed liquid in equilibrium with the crystal mush increment.					
Increment of crystals plus coexisting liquid					

Fig. 4:1 Schematic illustration of the extraction by bottom crystallization of small increments of crystals and coexisting liquid. The residual liquid is in total equilibrium only with the crystals of each infinitely small increment and is also interstitial to the crystals. This is equivalent to surface equilibrium on a large scale (the whole layer). There is no re-equilibration with the underlying increments of crystals and interstitial liquid. The composition of each increment is fixed at the time of deposition. Thus the composition of A is different to that of B etc. Components with a $D_{bulk} < 1$ the concentration in $A < B < C < D$ etc. Those components with $D_{bulk} > 1$ the concentrations in $A > B > C > D$ etc.

convecting and then froze in situ without any fractional crystallization on the scale of the layer thickness, the whole layer would have a constant modal and chemical composition. However, if it crystallized from the bottom up with no convection (or crystal settling), the vertical chemical variation in the layer would be controlled by diffusion within the static liquid or crystal mush to where the crystallization is taking place.

The Merensky and Bastard cyclic units are considered to conform to the model proposed by Irvine and adapted for this work, discussed above and in Chapters Three and Five.

Processes Occurring in the Interstitial Liquid: A Qualitative Assessment

Crystallization of the crystal mush generated by the liquidus fractionation briefly described above as a closed system is the simplest process that can be envisaged. This assumption of a closed system is not always justified as various processes can occur which move or modify the liquid before crystallization is complete (e.g. Eales, 1980 and Irvine, 1981a).

Infiltration metasomation from below due to compaction of the crystal mush (Irvine, 1981a) is a common process in some intrusions. The infiltrating liquid continually reacts and modifies the primocrysts with which it comes into contact while moving through the mush. Furthermore, the compaction due to sintering (see discussion below) that occurs reduces the pore space of the rock and thus reduces the total amount of interstitial liquid. This process may be important in the formation of chromite and magnetite layers and some near monomineralic silicate layers such as mottled anorthosite.

Contrasting effects on the chemical and mineralogical composition of the layered rocks will be produced by these processes. The possible effects are examined below.

The Determination of the Composition of the Liquidus Primocrysts and Associated Parental Liquids which Crystallized as a Closed System

Introduction

The whole rock composition can be used to derive the composition of the interstitial liquid by subtraction of an appropriate amount of the

appropriate primocryst composition (e.g. Brown, 1956; Wager, 1960). In estimating the composition and proportion of the interstitial liquid the procedure adopted here is based on the assumption of total equilibrium between the initial primocrysts and the initial connate interstitial liquid of each layer increment of crystal mush at the liquidus stage. The crystal mush subsequently crystallized isochemically.

Accepting the model based on that of Irvine (1981b) and outlined in Chapter Three, the crystals that precipitated in situ from the convecting basal liquid layer, at the liquidus stage, are in equilibrium with their connate interstitial liquid. This interstitial liquid is identical to the rest liquid in the layer at the time of crystallization. Thus the changing composition of the interstitial liquid and the coexisting primocrysts record the evolution of the crystallizing liquid layer (see Chapter Five).

Once the layer increment of primocrysts and liquid becomes isolated from the rest liquid and cooling proceeds, a number of processes take place which modify both the primocrysts and the interstitial liquid. Therefore the primocryst compositions now observed are not necessarily the original liquidus primocryst compositions. Furthermore, the crystal mush may not be a closed system, for instance, Cameron (1969) and Henderson (1970), discuss some processes that could modify the composition of both the interstitial liquid and the primocryst grains. However, this complication is ignored in the treatment below and closed system behavior is assumed.

It has commonly been assumed or inferred that the observed compositions of primocrysts represent or approximate the liquidus compositions as a result of adcumulus growth (Brown, 1956; Wager et al., 1960; Wager, 1963; Brown & Vincent, 1963; Wager & Brown, 1968; Atkins, 1969; Ferguson, 1969; Nwe, 1975; Markgraaf, 1976). However, G.B. Hess (1972) has shown that interaction of primocrysts in the crystal pile with the overlying liquid cannot be a significant process, and thus adcumulus growth cannot be significant. Consequently, the primocrysts only interact with the interstitial liquid and liquid infiltrating from below, and mutual alteration occurs with cooling.

Ferguson (1969) and Nwe (1975) amongst others have shown that interstitial ferro-magnesian phases are more iron-rich than primocrysts from closely associated rocks. In both these studies, however, the primocryst phases were still assumed to be approximately equal to the initial

liquidus compositions and thus subliquidus changes to primocryst compositions were assumed to be of minor importance. Re-equilibration of chromite with silicates, thus changing the primocryst compositions, has been recognised by inter alia Cameron (1975) and Roeder et al. (1979). The importance of subliquidus re-equilibration and resorption of silicates has also been recognized (Keith et al., 1981; Campbell, 1977; Ford, 1981) but not investigated in detail except by Paster et al., (1974) and Irvine (1979).

Selection of Samples for the Determination of Initial Primocryst and Liquid Compositions

The method outlined here for the calculation from a whole rock analysis, of the original primocryst and interstitial liquid compositions of that rock, rests on the assumption that the crystal mush crystallized as a closed system. As noted above this assumption is not always justified, and discretion must be exercised in applying the method, especially in the selection of suitable rock specimens. Several criteria can be applied to recognize suitable material:

- a) A high concentration of incompatible elements, which indicates trapped interstitial liquid (orthocumulate texture). (Wager, 1963; Henderson, 1968 & 1970; Henderson et al., 1971; Campbell, 1977). However, some rocks may have had secondary enrichment (Eales, 1980) of incompatible elements and other components, and these must also be avoided.
- b) The rock should not be very close to being monomineralic as this indicates expulsion of interstitial liquid.
- c) The composition (major and trace elements) and mineralogy derived by the calculations must be "reasonable" and not just "possible". This is subjective in the case of a single primocryst phase, but is increasingly constrained by additional primocryst phases. The derived liquid must be capable of crystallizing the coexisting derived solid under the conditions specified by phase diagrams and models for predicting liquidus phases (e.g. Nathan & van Kirk, 1978).
- d) A "reasonable" proportion of interstitial liquid must result from the calculation. This is also subjective, but many studies indicate that between 20% and 50% of interstitial liquid is reasonable (inter alia Eales, 1980; Wager et al., 1960; Wager & Brown, 1968).

The process of selecting suitable rocks is one of trial and error, but some rocks, such as the feldspathic pyroxenites and norites, are more obvious candidates. The least suitable are anorthosites, chromitites and rocks such as pegmatoids in which obvious secondary processes have operated. Inability to produce "reasonable" coexisting primocryst and liquid pairs in feasible proportions indicates that the rock was not a closed system and is thus unsuitable for the derivation of original compositions.

Selection and Use of Major Component Distribution Coefficients

The distribution coefficient (K_D) equation of Irvine (1979) can be used to determine possible compositions of coexisting solids and liquids from the whole rock composition. Although the equations have been developed for Mg/Fe fractionation by olivine, they can be extended to include other components and phases. The general form of the equation relating K_D to the compositions of the coexisting phases is:

$$K_D = (X_{E1}/X_{E2})_{Liq} / (X_{E1}/X_{E2})_{Solid}$$

Where E_1 & E_2 refer to the element pair under consideration.

Now:

$$X_{E1} = E_1 / (E_1 + E_2) \quad \text{in cation fractions}$$

$$X_{E2} = E_2 / (E_2 + E_1) \quad "$$

and:

$$X_{E1} = 1 - X_{E2} \quad "$$

The value of K_D must be known a priori for the element pair under consideration. For most element pairs of interest experimental values are known or can be derived.

K_D for olivine is well known and lies between 0.30 and 0.36 and a value of 0.32 is a suitable value for haplo-basaltic systems that are not very iron-rich (Roeder & Emslie, 1970; Longhi & Walker, 1975; Irvine,

1979). This coefficient is independent of pressure and temperature in the case of olivine (see Irvine (1979) for a discussion).

A K_D value for orthopyroxene can be derived from that of olivine using the equation of Morse (1979b):

$$MMF_{\text{opx}} = 0.85MMF_{\text{ol}} + 0.15$$

which is equivalent to the following:

$$X_{\text{Mg opx}} = .85X_{\text{Mg ol}} + 0.15$$

Now:

$$K_{D \text{ ol}} = (X_{\text{Mg}/X_{\text{Fe}}})_{\text{liq}} / (X_{\text{Mg}/X_{\text{Fe}}})_{\text{ol}}$$

and

$$K_{D \text{ opx}} = (X_{\text{Mg}/X_{\text{Fe}}})_{\text{liq}} / (X_{\text{Mg}/X_{\text{Fe}}})_{\text{opx}}$$

Combining and simplifying the last three equations results in the K_D of orthopyroxene expressed in terms of an arbitrary olivine composition.

$$K_{D \text{ opx}} = [(0.85 - 0.85X) * K_{D \text{ ol}}(X/(1-X))]/(0.85X + 0.15)$$

Where $X = X_{\text{Mg ol}}$

This function is relatively insensitive to a changing hypothetical olivine composition and hence liquid composition. Assuming a K_D for olivine of 0.32, the K_D of orthopyroxene only varies between 0.24 and 0.27 for changing olivine composition from F_{50} to F_{90} . An appropriate value for the rocks studied in this work is 0.26.

Besides orthopyroxene, plagioclase is the only other primocryst phase in the study section as clinopyroxene and pigeonite do not occur as primocryst phases, and olivine is of very restricted occurrence. Unfortunately, plagioclase/melt equilibria are very sensitive to temperature

and fluid pressure (e.g. Kudo & Weill, 1970; Drake, 1976) and consequently these have to be known a priori before a distribution coefficient can be calculated. Furthermore, the An content of plagioclase coexisting with a liquid can only be calculated with a precision of $\pm 12\%$ (Drake, 1976). For these reasons the calculations are restricted to pyroxenites in this work.

Determination of the Major Element Composition and Proportions of the Phases

The procedure used to determine the major element composition of the connate interstitial liquid (and hence the magma composition), is one of trial and error. A possible orthopyroxene composition (more Mg-rich than those present in the rock) is selected and incrementally extracted from the whole rock assuming mass balance (Fig. 4:2). This produces a series of hypothetical liquid compositions and proportions. A K_D is calculated for each pair of liquid and solid. The concentrations of the components in the residual (interstitial) liquid (C_1) and the apparent K_D 's are plotted against the fraction of residual liquid (F). The correct K_D (known a priori) then gives the composition and proportion of the residual liquid coexisting with that particular orthopyroxene composition (Fig 4:2).

This procedure is repeated with a number of different orthopyroxene compositions spanning a range of possible MMF ratios. The determined liquid compositions and proportions are then plotted against the MMF ratios of the orthopyroxenes and a possible range of interstitial liquids are selected (Fig 4:3).

The two main weaknesses of this approach are firstly, the subjective nature of the liquid composition derived when only one primocryst phase is present, and secondly, the possibility that the primocryst phases may have been compositionally zoned at the liquidus stage. The latter problem is particularly important in the case of plagioclase as the plagioclase of the study section and the remainder of the Rustenberg Layered Suite shows considerable compositional zoning (See Chapter Two, Fig. 2:3). This further complicates the use of plagioclase for the derivation of liquid compositions.

Only SiO_2 , Al_2O_3 , Fe_2O_3 , FeO , MgO , CaO and Na_2O are taken into account in the calculations as the other components collectively constitute only about 1% of most samples. These minor components are treated with the trace elements.

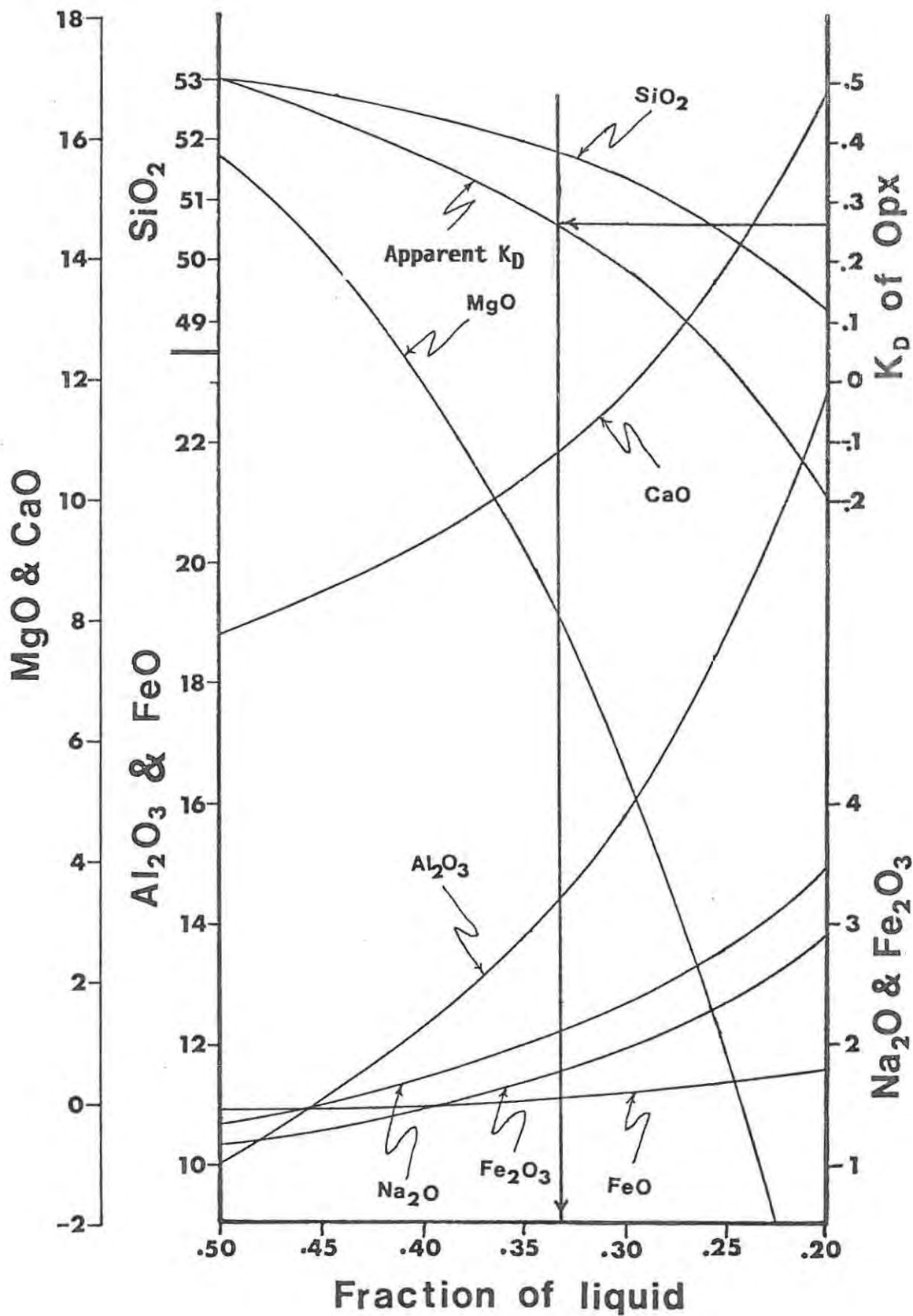


Fig. 4:2 Extraction of an orthopyroxene (MMF = .84) from M4 WR. The Mg/Fe ratio of the "residual liquid" continually changes as does the apparent K_D . The only liquid that can coexist with the given orthopyroxene ($K_D = .26$) is given by the vertical arrow which also indicates the fraction of liquid.

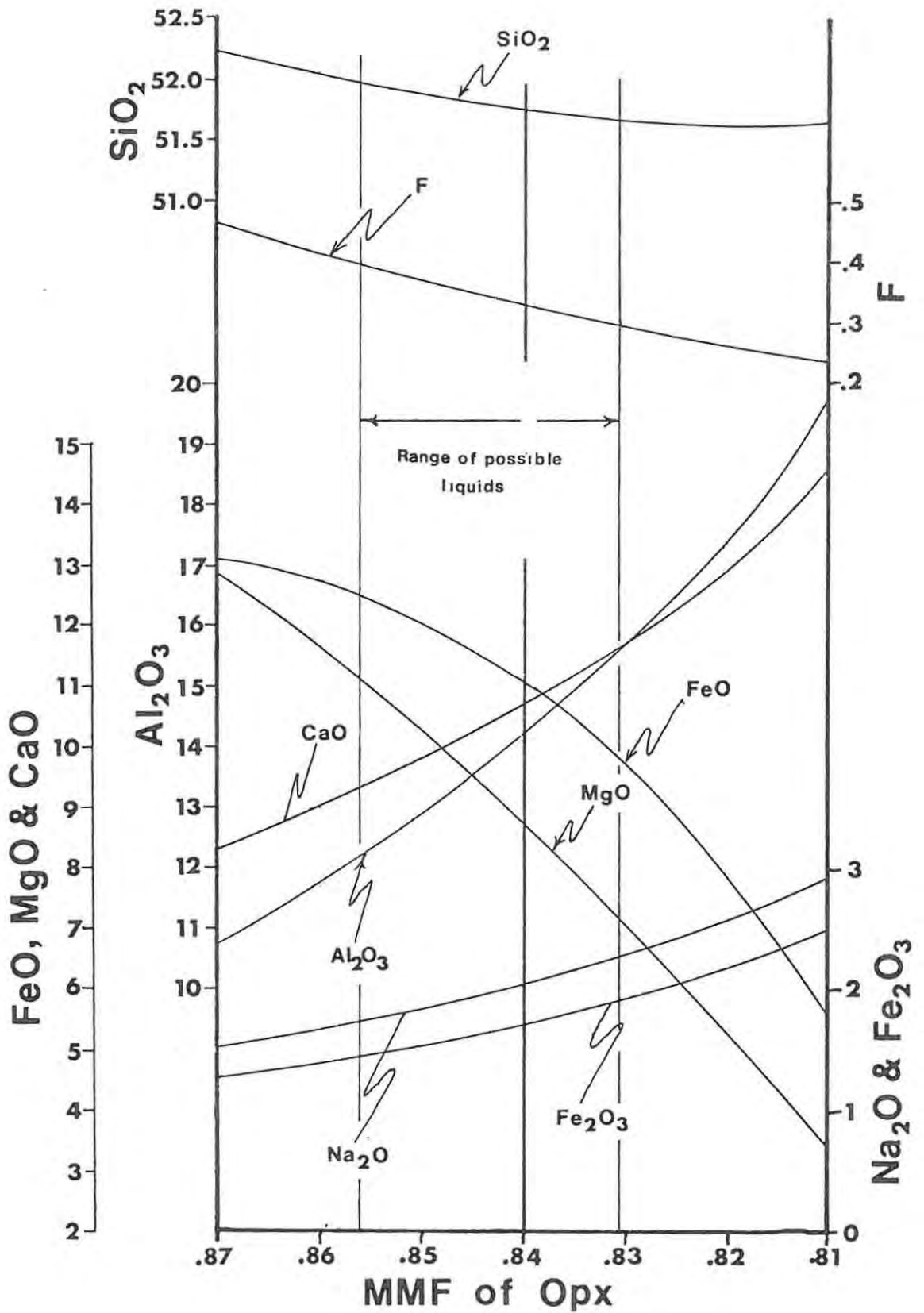


Fig. 4:3 Each composition and fraction as determined (see Fig. 4:2) is plotted to give a continuum of possible liquid compositions from which a initial interstitial liquid composition or range of possible compositions is selected (the thick vertical line corresponds to the composition derived from Fig. 4:2). See text for further discussion.

Trace Element Partitioning Between Phases

Calculation of the proportions and compositions of liquidus primocrysts and the original interstitial liquid, allows the allocation of the whole rock minor and trace elements to the various phases according to the Nernst distribution coefficients for those components. In the case of the minor and trace elements, the concentration in the liquid (again assuming isochemical crystallization) is dependent on the concentration of the element in the whole rock, the distribution coefficient (D) and the fraction of liquid and are related as follows assuming total equilibrium between the primocrysts and liquid (Arth, 1976):

$$C_l = C_r / (D - DF + F)$$

where $D \ll 1$ this simplifies to:

$$C_l = C_r / F$$

where:

C_l = Concentration in the interstitial liquid.

C_r = Concentration in the whole rock (crystal mush).

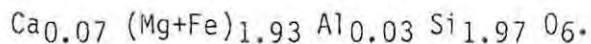
F = Fraction of interstitial liquid.

The values of F are derived from the liquid fraction calculated using the major element technique described above or an independent estimate of the fraction of liquid.

Application to the Merensky Cyclic Unit

The only whole rock pyroxenite sample fulfilling most the criteria for estimating the liquid composition is M-4WR, but some assumptions have to be made. The sample contains chromite and sulphides as additional liquidus phases, and thus Fe (expressed as FeO) is enriched in the sample as well as Cr, Ni, Cu and Co. The sulphide may have been added as Cu, Ni and PGE-rich immiscible sulphide droplets as outlined in Chapter Three. Iron (as FeO) is crucial to the application of the method outlined above and thus the amount contained in the chromite and sulphide has to be

estimated. This quantity is estimated to be between 1 and 2 percent, and the latter value is subtracted from the whole rock FeO concentration and the analysis is recalculated to 100% after also eliminating the minor elements. Fe₂O₃ was set at 0.56% for convenience as this gives a Fe₂O₃/FeO ratio of about 0.15 for the derived interstitial liquid. Correction of FeO for the presence of sulphide and chromite and the estimation of a oxidation ratio for iron does not change the conclusions reached. The coexisting liquids were then calculated using orthopyroxenes with a variable Mg/Fe ratio having the following formula:



The Ca and Al were estimated from probe analyses (Appendix Two). Errors in the estimation of Ca and Al do not greatly affect the result as the concentrations in the pyroxenes are low. Sodium and Fe³⁺ are assumed to be excluded from the orthopyroxene. As the Na and Fe³⁺ concentrations of the orthopyroxenes are very low, this assumption also does not materially affect the conclusions. The results for the major elements using different pyroxene compositions are presented in Fig. 4:3. The curves indicate the compositions and fractions (F) of interstitial liquids which could coexist with pyroxenes with a variable MMF ratio.

Examination of Fig. 4:3 shows that a range of derived liquids are possible, but that liquids coexisting with orthopyroxenes with a MMF ratio of ~0.84 are unlikely to have been the original interstitial liquid as the high concentrations of Al₂O₃, CaO and Na₂O and the low concentrations of FeO and MgO would favour the existence of plagioclase as a primocryst phase, which was not the case. The average MMF of the pyroxenes in M-4 (probe data) is 0.775 to 0.790 and these clearly could not have coexisted in equilibrium with any initial interstitial liquid with the composition of normal basic igneous liquids.

The amount of interstitial liquid coexisting with the orthopyroxene (MMF = 0.85) is ±30% which is not an unreasonable amount. Taking the upper limit as 40% (a subjective assessment) the coexisting orthopyroxene would have a MMF of 0.88. These results are summarized in Table 4:1a.

If no FeO is subtracted from the analysis of M-4 to compensate for the presence of chromite and sulphide the liquids derived are somewhat different and Table 4:1b illustrates this.

Table 4:1a. Interstitial liquids to M-4 WR (-2%FeO).

F	MMFopx	SiO ₂	Al ₂ O ₃	Fe ₂ O ₃	FeO	MgO	CaO	Na ₂ O	MMFliq
.40	.88	54.3	12.2	1.4	10.0	11.0	9.4	1.7	.66
.30	.85	54.7	16.6	2.0	6.2	5.5	12.5	2.4	.61

Table 4:1b. Interstitial liquids to M-4 WR.

F	MMFopx	SiO ₂	Al ₂ O ₃	Fe ₂ O ₃	FeO	MgO	CaO	Na ₂ O	MMFliq
.40	.86	52.1	11.7	1.4	12.7	11.6	9.0	1.7	.62
.30	.83	51.7	15.7	1.9	9.7	6.9	11.8	2.3	.56

All the liquids estimated using the approach used here appear to be normal tholeiitic basalt compositions. For comparative purposes several different liquid compositions proposed as primary magmas for the Bushveld Complex are presented in Table 4:2.

Table 4:2. A selection of magma compositions reported in the literature that have been proposed as "parental" to the mafic layered rocks of the Bushveld Complex. Compositions excluding minor elements reported by the authors. Analyses normalized to 100%.

Reference.		SiO ₂	Al ₂ O ₃	Fe ₂ O ₃	FeO	MgO	CaO	Na ₂ O
Cawthorn et al. (1981)		56.4	12.9	1.1	7.9	12.6	7.0	2.0
	ditto	51.2	15.8	2.8	10.3	6.0	11.0	2.9
Sharpe (1981)	No. 10	53.6	11.4	---	10.8	15.0	7.5	1.6
	ditto	12	49.3	16.8	---	12.6	7.7	2.2
	ditto	13	51.3	16.2	---	9.3	9.3	2.6

Conclusions

This analysis has indicated that fairly extensive changes to the liquidus primocryst compositions can occur as a result of subliquidus re-equilibration even if the crystal mush crystallized as a closed system. The analysis rests on the assumption of an idealized closed system which

is not entirely justified as infiltration metasomatism has occurred. Therefore the compositions of the primocrysts and interstitial liquids derived are not absolute or definitive of the liquids from which the Merensky unit crystallized. The trace elements are not dealt with as their concentrations are subject to even greater uncertainty as there is chromite and sulphide in the rock investigated, and the incompatible elements may have been enriched by infiltration metasomatic processes.

Sintering and Infiltration Metasomatism.

Introduction and Discussion of Irvine's Model

Infiltration metasomatic effects in mafic layered rocks due to upward streaming of interstitial liquid were first invoked by Irvine (1978) and he has subsequently developed and refined the model (Irvine, 1980a). Irvine's model was developed to explain the apparent upward movement of interstitial liquid in the ultramafic layers of the Muscox intrusion which are rich in olivine and pyroxene, with no primocryst plagioclase. He invokes a mechanism for expulsion of the interstitial liquid due to the gravitational compaction of the primocrysts.

While gravitational compaction is feasible for the ultramafic rocks, it is less efficient for rocks containing substantial amounts of primocryst plagioclase such as norites, leuconorites and anorthosites. The reason for this is the lack of density contrast between crystal assemblages containing abundant plagioclase and the interstitial liquid, due to plagioclase being less dense than the liquid (Campbell et al., 1978; McBirney & Noyes, 1979). A more efficient mechanism for compaction of the crystal mush is the process of sintering used in many metallurgical and ceramic processes which does not rely on gravity as the driving force, in combination with gravitational compaction.

Sintering as a Petrological Process

Many detailed works are available dealing with the theoretical and experimental aspects of sintering with applications to industrial processes (e.g. Harker & Parker, 1945; Smith, 1948 & 1964; Kingery, 1959; Kingery & Narasimhan, 1959; Coble, 1961; Coble & Burke, 1963; and Thummler & Thomma, 1967). The last named is a very detailed review, and the work of

Kingery and Kingery & Narasimhan deals specifically with sintering in the presence of a liquid phase, and is thus of particular relevance to layered rocks.

Sintering is the process whereby crystalline fine grained materials with a high surface energy, that are loosely packed with much pore space, tend to coalesce, compact, and structurally readjust to reduce the pore space. This is accomplished below the melting point of the material. Sintering occurs due to the tendency for the crystalline phase to reduce its total surface area and thus the total surface energy. The minimum surface energy results when the grains are all in contact with no pore space, and equilibrium angles between phases meeting at a triple point are attained, at which stage the process stops. In a single phase system the equilibrium angle is 120° . In the sintering process some grains tend to enlarge at the expense of others as the surface energy of a large grain is less than that of smaller grains. Sintering produces polygonal grains with straight boundaries, 120° triple point contacts and a considerable coarsening of the texture.

Processes analogous to sintering have often been invoked to account for textures in metamorphic rocks and some sulphide ores have been attributed to processes analogous to sintering (De Vore, 1959; Voll, 1960; Stanton, 1964; Stanton & Gorman, 1968; Vernon, 1970 & 1975). Resumés of the process as applied to metamorphic rocks and ores are given by Spry (1969) and Stanton (1972) respectively.

References to sintering as an igneous process are few but Voll (1960), Weedon (1965), Vernon (1970), Moore (1973) and Reynolds (1978, 1979 & 1980) do invoke the mechanism to explain textures of igneous (mainly layered) rocks. The "resolution" process envisaged by Cameron (1969) and von Gruenewaldt (1979) is analogous to sintering. Vernon, Moore and Reynolds suggest that the mechanism of sintering leads to expulsion of interstitial liquid and a reduction in the volume of the crystal pile, especially if only one primocryst phase is present. The process of sintering aided by gravitational compaction can therefore be viewed as a type of "magmatic pump" for the connate interstitial liquid, and the driving force behind the infiltration metasomatic processes.

In layered rocks the process of sintering would start as soon as the crystals accumulate at the base of the magma chamber, and continue until the rock becomes solid. In practice sintering would proceed concomitantly

with further growth of the grains from the interstitial liquid and thus it will be interrelated with the processes described before. Thus the expulsion of the interstitial liquid from the crystal pile will be accompanied by a change in the composition of the expelled liquid. Expulsion of material would initially be rapid, but then slow as the pore volume and the total surface area of the grains are reduced. There is thus a continual flow of interstitial material from lower parts of the sintering layer through the crystal pile and this can be viewed as a process of auto-metasomatism (as envisaged by Irvine (1978)). The liquid flowing past a layer of crystals would be continually changing in composition and decreasing in volume until movement ceased. The composition of the liquid would be buffered by the primocryst crystals and thus the major element composition would not vary very dramatically except where a phase change occurs (e.g. where a boundary between anorthosite and pyroxenite is crossed).

The changes in the chemistry of the interstitial liquid is due only to the crystallization of the interstitial liquid concomitantly with sintering and not due to the sintering process per se, as sintering is a process of recrystallization only and the total volume and composition of the crystals is not being changed.

Sintering and Infiltration Metasomatism in the Study Section

Textures of pyroxenites and anorthosites in the study section (see Chapter Two) bear a striking resemblance to the textures described and illustrated by the authors quoted above. The mottled anorthosites in particular have features that can be attributed to this mechanism. These are:

- a) The marked difference in the size of the plagioclase crystals included in the pyroxene mottles compared to those in areas of pure plagioclase. The latter are very much larger.
- b) The plagioclase included in the mottles is euhedral to subhedral and tabular, while that in areas of pure plagioclase is subhedral to anhedral, with curved and straight boundaries not necessarily related to any crystallographic direction. The triple junctions of grains suggest an approach to equilibrium conditions. The texture has the "foam-like" appearance described in many of the references quoted in the above sections.

The trace element composition of the anorthosites indicates that a considerable amount interstitial liquid has been expelled as they are low in incompatible elements and are almost monomineralic. Compositional characteristics of the Bastard pyroxenite may also present evidence of infiltration of interstitial material expelled from elsewhere. The orthopyroxene at the very base of the Bastard pyroxenite is depleted in Ni, and enriched in other elements such as Zn (Fig. 2:8). The orthopyroxene at the base of the pyroxenite is also slightly more iron-rich than that immediately above (see Fig. 2:3). This could be explained if the pyroxenes in this layer equilibrated with Fe-rich and Ni-poor liquid possibly infiltrating upwards from the underlying Merensky mottled anorthosite.

The Footwall unit characteristics of the $^{87}\text{Sr}/^{86}\text{Sr}$ initial ratio of the Merensky cyclic unit can be attributed to mixing of interstitial liquids infiltrating from the Footwall unit due to sintering processes. This upward migrating liquid would displace or mix with that in the Merensky unit, and the proportion of Sr with the Footwall unit isotopic characteristics would decrease with height in the crystal pile. The $^{87}\text{Sr}/^{86}\text{Sr}$ of the interstitial material would therefore vary with the proportion of Sr introduced from the footwall, and the upward increasing initial ratios depicted in Fig. 3:1 would result. This could have occurred during the accumulation of the Merensky cyclic unit or as a post depositional process. The former alternative is presently favoured by me as expulsion of liquid must have been occurring continually and flowing through the crystal pile while deposition was occurring at the liquidus stage. The final liquids to be expelled from the Footwall unit could have contributed to the Merensky pegmatoid in a similar way to that suggested for the base of the Bastard pyroxenite. The Merensky pegmatoid may thus be a product of many processes as suggested previously.

Zoning is very common in the plagioclase of the mottled anorthosites as illustrated by the great variations in the determined compositions from a single thin section. Zoning is present in large crystals that could have grown during sintering process outlined here. Thus the zoning might have been acquired during the sintering process. This may be the result of changing liquid compositions during sintering and reaction of adjacent grains with each other and with the changing interstitial liquid. The mechanisms whereby this can occur are unclear at present and await a very detailed study of the zoning and growth patterns of the plagioclase.

The Behavior of Volatile Components in the Crystal Mush

Introduction

As the crystal mush normally crystallizes from the bottom up, incompatible volatile components could conceivably be enriched ahead of the upward moving interface between the solidus and subliquidus zones. This enrichment could be aided by these components being trapped beneath slab-like layers of rock such as chromitite horizons possibly produced by sintering as outlined above.

The Merensky Pegmatoid

The genesis of the Merensky pegmatoid (and other pegmatoidal layers and lenses in the Rustenburg Layered Suite) can be at least partially explained by invoking volatile (H_2O & CO_2) enrichment due to trapping below more or less impervious layers. It is, however probably seldom that volatiles reach high enough concentrations in the interstitial liquid to form a separate fluid phase without the aid of impervious layers. This is due to the high concentrations of water required to saturate the interstitial liquid ($\pm 5-6\%$ in a basaltic liquid at 2-3Kb (Burnham, 1979)). Basaltic liquids probably have $\pm 0.25\%$ water (Carmichael et al., 1974) and this or a slightly higher concentration may be typical of interstitial liquids. However, as is suggested above, the presence of impervious blocking layers allows an increase in the concentration of volatile components in the final interstitial liquids below these layers. Saturation may have been achieved at sites such as the Merensky pegmatoid, the Pothole marker and the lower contacts of chromitite layers.

The high concentration of volatiles would considerably lower the freezing point of the crystal mush which would then be much less viscous and remain partially liquid fairly long after the associated layers have solidified. This hydrothermal activity could explain the textural features of the pegmatoid and the associated unusually high concentrations of As, Bi, Te and other elements (Vermaak, 1976a) associated with hydrothermal ore deposits (Stanton, 1972).

This dual origin for the pegmatoid and the PGE, Ni and Cu mineralization is further supported by the fact that often the PGE, Ni and Cu are not directly associated with the pegmatoid but are in the Merensky pyroxenite, the pegmatoid being relatively barren (von Gruenewaldt, 1979). Where the pegmatoid and the PGE mineralization coincide there is often

evidence for a two stage origin for the sulphides. This idea has also been supported in part by Brynard et al. (1976) who invoke late stage hydrothermal redistribution of the sulphide.

The volatile enrichment and trapping at the base of the Merensky pyroxenite is considered to have been late in the development of the Merensky cyclic unit, some time after the normal infiltration metasomatism referred to earlier. The Merensky pyroxenite must have formed an effective vapour seal.

The Origin of Potholes

The enrichment and trapping of volatiles below impervious layers and the possible generation of a separate fluid phase in the not yet totally solidified footwall rocks also offers a possible mechanism for the generation of potholes. A fluid trapped below an impervious layer will migrate laterally until a weakness or opening allows further upward migration. Any fluids trapped below layers such as the chromitite horizons would tend to be released along zones of weakness where structural re-adjustment of the magma chamber occurs in response to changing conditions and additions of magma. These zones of weakness are very likely to be associated with faulting and jointing in the floor rocks of the complex. Weaknesses such as this may possibly also allow the influx of CO₂ and H₂O from the floor rocks as envisaged by De Waal (1977) and described in Chapter Three. This may add to the volatiles trapped below impervious layers.

The fluid which is concentrated as "plumes" in the crystal mush due to the structural control would rise up and excavate a pothole in the crystal pile at the interface between the liquidus and solidus zones. The fluid would tend to lower the freezing temperature of the crystal mush in the vicinity of the the fluid plume causing some dissolution of primocrysts. This would weaken the structure of the crystal "network", and this coupled with a lower density and reduced viscosity of the interstitial liquid could enable the fluid to excavate the potholes at the interface between the liquidus and subliquidus zones. The material excavated from the pothole would be swept up into the convecting portion of the magma thus explaining the "missing" material.

The pits excavated in the footwall crystal pile would subsequently be filled by the in situ crystallization of the Merensky cyclic unit. Renewed

fluid streaming from below in the same site after the formation of the Merensky cyclic unit, would result in this unit also being potholed and then subsequently filled with Bastard cyclic unit material. This would result in "stacked" potholes. The volatiles invoked here considerably predate those invoked to account for the Merensky pegmatoid as the potholes predate the pegmatoid.

This mechanism for the generation of potholes appears to overcome many of the problems that have invalidated some of the other proposals as outlined in Chapter Two.

The Origin of the Ultramafic Pegmatites

The ultramafic pegmatites which are often associated with potholes may result from the continuation of the process that generated the latter. The following discussion is mainly speculative in nature with little direct evidence.

The ultramafic pegmatites are rich in the clinopyroxene components and in FeO as well as being somewhat deficient in SiO₂ (see sample FEP3 as described in Chapter Two). They have considerable petrographic evidence for late stage fluid activity. They are also partly magmatic and partly metasomatic in character (R.N.Scoon, personal communication). Ultramafic pegmatites are also concentrated in structurally favourable areas and are not randomly distributed.

All the components of the ultramafic pegmatites can be derived from the layered rocks. The high water content of the last liquids may have caused them to become extremely mobile. These final liquids which would be rich in the components of clinopyroxene, which is the last important interstitial phase to crystallize in the layered rocks. These water-rich ultramafic liquids could then be expelled from the consolidating rock and concentrate in zones of weakness. Due to their high water pressure, the density of this liquid may be relatively low and it would then intrude upward through the zones of weakness. This liquid would be very reactive due to its extreme composition and high fluid content and could thus intrude as well as react with, consume and replace the wall rocks.

Similar ideas to the above have been advanced by Cameron & Desborough (1964) to account for large pipe-like bodies such as Onverwacht. The Ni-rich sulphide pipes of Vlakfontein (Vermaak, 1976b) could also have a similar origin.

Conclusion

Volatile activity has been invoked here to account for three features of the study section: potholes, concordant pegmatoid and cross-cutting ultramafic pegmatites. If these hypotheses are correct, volatile activity of different types spanned a long time interval in the development of these rocks (liquidus to near solidus).

Summary

The above discussions have emphasised the changes to the primocryst and interstitial liquid compositions that can occur during the subliquidus stage. The chemistry and texture of the rock and minerals is a product of all these processes, and thus cannot be viewed as the result of liquidus processes only. A large amount of data is required to unravel the complexities in the chemistry of layered rocks.

Relatively marked changes to the MMF ratio of primocryst orthopyroxenes can occur during solidification of the crystal mush as a closed system. The compositions of the orthopyroxenes are therefore not liquidus compositions and allowances have to be made for this. Sintering and concomitant infiltration metasomatism can also change the composition of the rocks and thus the assumption of closed system behavior of the crystal mush is not always justified. Volatile activity may have occurred over a long period in the crystal mush, and may have had several roles including the generation of potholes, the formation of pegmatoids and the evolution of the ultramafic pegmatites.

CHAPTER FIVE: The Liquidus Stage

Introduction

In Chapter Three it was established that a major new influx of magma occurred immediately after the deposition of the Footwall unit, mixed with the rest liquid and then crystallized the primocryst phases of the Merensky and then the Bastard cyclic units. If this is valid then the Footwall unit represents a different magmatic system to the Merensky and Bastard cyclic units.

The Footwall unit was derived from a magma with a considerable history of crystallization and fractionation. It may also have crystallized from layers within a compositionally stratified liquid. Furthermore, a number of subliquidus processes may have modified the chemistry of the rocks in this unit, and as pointed out in Chapter Two the available data is not extensive enough to clearly delimit compositional breaks or trends. Thus no attempt is made here to model this unit.

The Merensky and Bastard cyclic units have been considerably modified by subliquidus and subsolidus processes, but the coherent chemistry and extensive sampling do allow a more quantitative approach in attempts to explain features of these units. In Chapter Three it was pointed out that the crystal settling or density current hypotheses (e.g. Hess, 1960; Wager & Brown, 1968) fail to explain the chemical and mineralogical variation of the Merensky and Bastard units, and these models are thus disregarded in the following work. It was also pointed out that the chemistry was consistent with bottom crystallization from a limited volume of liquid, as suggested by the model of Irvine (1980a & b). The following discussion is based on that model as modified and set out in Chapters Three, Four and below.

Fractional Crystallization in Layered Rocks: General Principles

The General Principles

As suggested by Irvine (1980b) and discussed in Chapter Three, the magma in the convecting crystallizing layer is undergoing almost perfect fractional crystallization, and this is reflected in the chemistry of the primocryst phases and interstitial liquid. In simple systems fractional crystallization can be described in terms of the instantaneous solid

composition (ISC) and the instantaneous liquid composition (ILC) (Morse, 1980). However, the fractional crystallization of layered rocks involves a variable amount of interstitial liquid as outlined in Chapter Four. The instantaneous fractional extract (IFE), (equivalent to the ISC in simple systems) thus consists of a mixture of crystals and interstitial liquid (Fig. 5:1) . As the interstitial liquid is the same composition as the overlying residual liquid it is equivalent to the ILC. The ISC (initial primocrysts) are, however, not equivalent to the extract of simple systems, but do represent the liquidus ISC before any subliquidus re-equilibration.

In the case where subliquidus crystallization occurred as a closed system (Chapter Four), the whole rock (crystal mush) represents the IFE, from the overlying convecting basal layer. The interstitial liquid represents the ILC, and the liquidus primocrysts represent the ISC. The whole of the extracted portion (in the cyclic unit or the whole intrusion depending on the boundaries of the system) could be termed the total fractional extract (TFE), and is the summation of all the IFE increments. Work on the Kiglapait intrusion by Morse and his co-workers, (e.g. Morse, 1979a & c, 1981a & b, 1982 and references therein) involves the determination of the TFE at any point and the subtraction of this from the original bulk composition (BC) of the magma to determine the path of fractional crystallization of the magma (the ILC path). There may be problems with this approach, however, as the calculations are only correct in a gross sense as the model assumption is that each IFE increment was from the whole residual magma volume, and does not take the possibility of a compositionally stratified magma into consideration.

The approach adopted here differs from that of Morse in that the continuous variation of the IFE, ISC and ILC with respect to "height" is used to determine the volume of the fractionating system, and hence in the case of cyclic units the thickness of the basal convecting layer of magma contributing to crystallization of the rocks. As a first approximation it is assumed that diffusion of material across double-diffusive boundaries is negligible and that the layer undergoing fractional crystallization is well mixed by convection after each IFE increment of crystallization. This approach is in contrast to the mechanism invoked by Cawthorn & McCarthy (1980 & 1981) to explain the chemical variations with respect to height in the magnetitite layers of the Bushveld Complex. In their model they

attribute the variation in Cr content of magnetite to diffusion in the liquid above the crystallizing magnetite layer coupled with periodic convective overturn of the liquid to account for reversals.

Estimating the Thickness of Double-Diffusive Convection Layers

The Raleigh fractionation law (Arth, 1976) for layered rocks is as follows (Fig. 5:1):

$$C_r/C_{r0} = F(D-1)$$

rearrangement gives:

$$F = e^{[\ln(C_r/C_{r0})/(D-1)]}$$

Where:

F = Fractionation of liquid remaining in the basal crystallizing layer.

D = Bulk distribution coefficient between the IFE (crystal mush) and ILC (liquid in the remaining convecting portion of the layer).

C_r = Concentration (or concentration ratio) of the components in the crystal mush (rock).

C_{r0} = Concentration in the initial crystal mush.

The exponent in square brackets [] is given the symbol x in the following derivation and the last equation above simplifies to:

$$F = e^x$$

Now consider a column of liquid initially of thickness t crystallizing from below (Fig 5:1). The accumulation of crystals is of thickness a and the "residual liquid" is of thickness f so that:

$$t = a+f$$

$$f = t-a$$

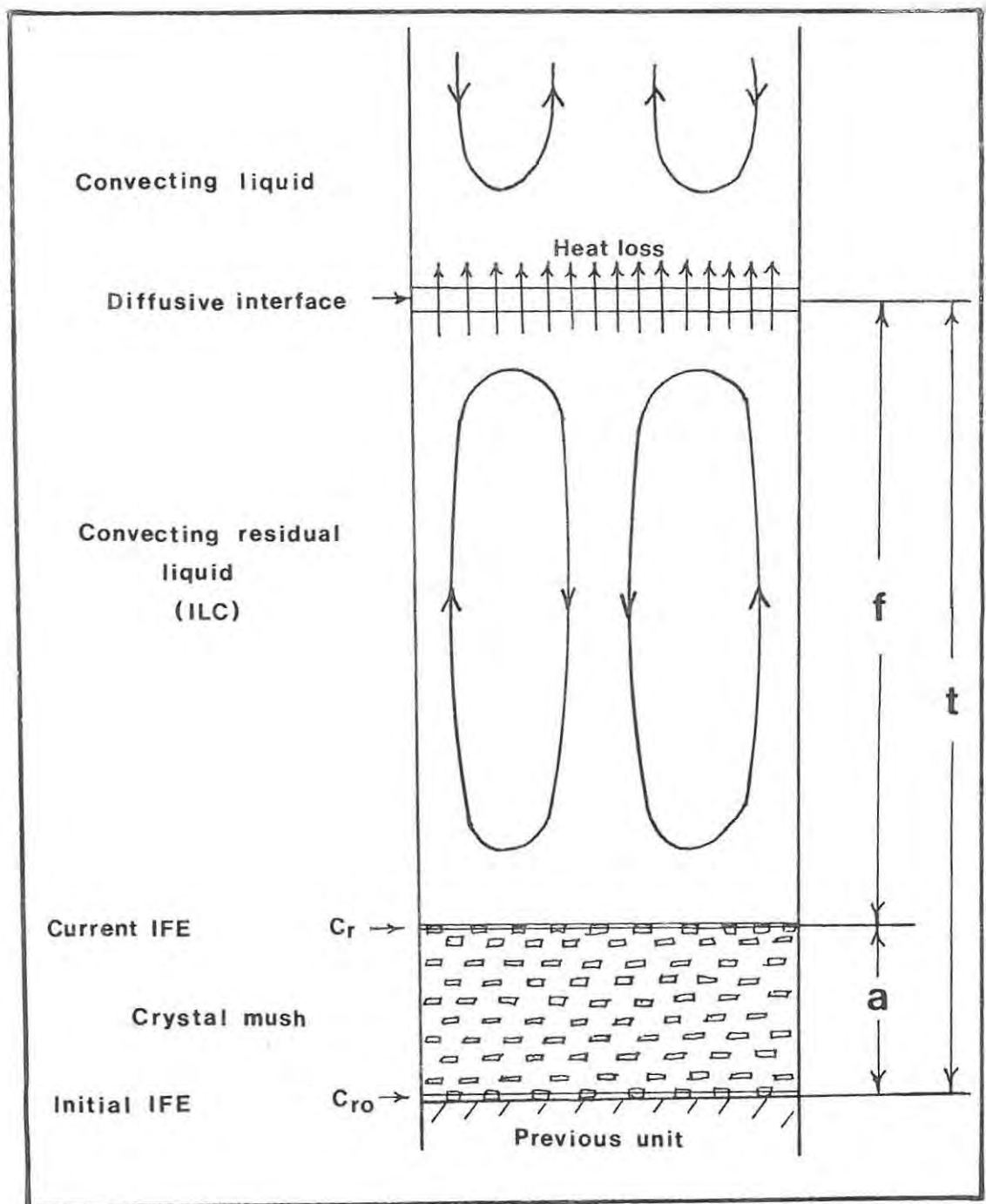


Fig. 5:1 A schematic physical model of the crystallization of a cyclic unit from the basal layer of a magma stratified into convecting liquid layers separated by "diffusive" interfaces. The basal layer is crystallizing from the bottom upward and is "closed" by a diffusive interface from the layer above.

but the fraction of liquid (F) is f/t , therefore:

$$F = (t-a)/t$$

and thus:

$$e^x = (t-a)/t$$

rearrangement and recalling the expression for x results in:

$$t = a / (1 - e^{[\ln(C_r/C_{r0}) / (D-1)]}).$$

This equation can be used to calculate the thickness of liquid from which a particular cyclic unit crystallized. Ideally, all that is required is the concentrations of any component in two samples (C_{r0} and C_r) separated by a known vertical distance and an accurate knowledge of the bulk distribution coefficient of that component or component ratio. However, a combination of elements with different D 's in a number of vertically separated samples should be used to give independent estimates of the thickness, from which a combined assessment can be made. It is important to note that the thickness of the cyclic unit above C_{r0} is determined, and the distance below C_{r0} to the base of the unit has to be added if C_{r0} is not from the very base of the unit.

Fractional Crystallization with Interstitial Liquid

As pointed out in the previous chapter, subliquidus processes can change the composition of the primocrysts as crystallization takes place. Thus assumptions have to be made, or the influence of these processes has to be assessed using the techniques outlined in Chapter Four or other published methods.

In Fig 5:2 the chemical profiles that would result if an assemblage of crystals and interstitial liquid are extracted from a certain volume of liquid by Rayleigh fractionation. Curves for components with high and low distribution coefficients (D_{xtals}) for the crystalline phases are illustrated ($D_{xtals} = 10$ and 0.5). In all cases the interstitial liquid extracted with the crystals has a D of 1. The bulk distribution

coefficient (D_{bulk}) of the mixture of crystals and liquid is thus significantly dependent on the proportion of interstitial liquid as the bulk D is calculated according to the following equation:

$$D_{\text{bulk}} = D_{\text{xtals}} * X_{\text{xtals}} + 1 * X_{\text{liq}}$$

where:

$$X_{\text{xtals}} + X_{\text{liq}} = 1$$

The diagrams (Fig. 5:2) illustrate the variation in concentration that could be expected if there was 50% or 20% of interstitial liquid extracted with the crystals during Rayleigh fractionation. Inspection of Fig 5:2 reveals that the composition of the whole rock (crystal mush), at any point during fractionation, is dependent on the proportion of primocrysts and interstitial liquid.

On cooling as a closed system at the subliquidus stage, re-equilibration of the primocrysts with a shrinking volume of interstitial liquid, will change both the compositions of the primocrysts and the interstitial liquid. In practice the composition of the re-equilibrated primocryst phases would fall in the shaded areas in Fig. 5:2, i.e. the process reduces the concentration of the compatible elements in the primocrysts relative to the liquidus composition, and increases the incompatible element concentration in the primocrysts relative to the liquidus. This depends on the nature of the other interstitial phases which may crystallize.

Where sintering and immediate expulsion of interstitial liquid occurs as the crystal pile is being deposited, the extreme situation would be if all the interstitial liquid is expelled before any reaction occurs. This would result in a monomineralic rock, but the primocrysts would have liquidus compositions. In any event the interstitial liquid would be reduced and this is also illustrated in Fig 5:2 where the difference between the graphs of 50% and 20% interstitial liquid illustrate the effect. In situ crystallization and sintering thus have opposing effects on the composition of the primocrysts, whole rock and liquid.

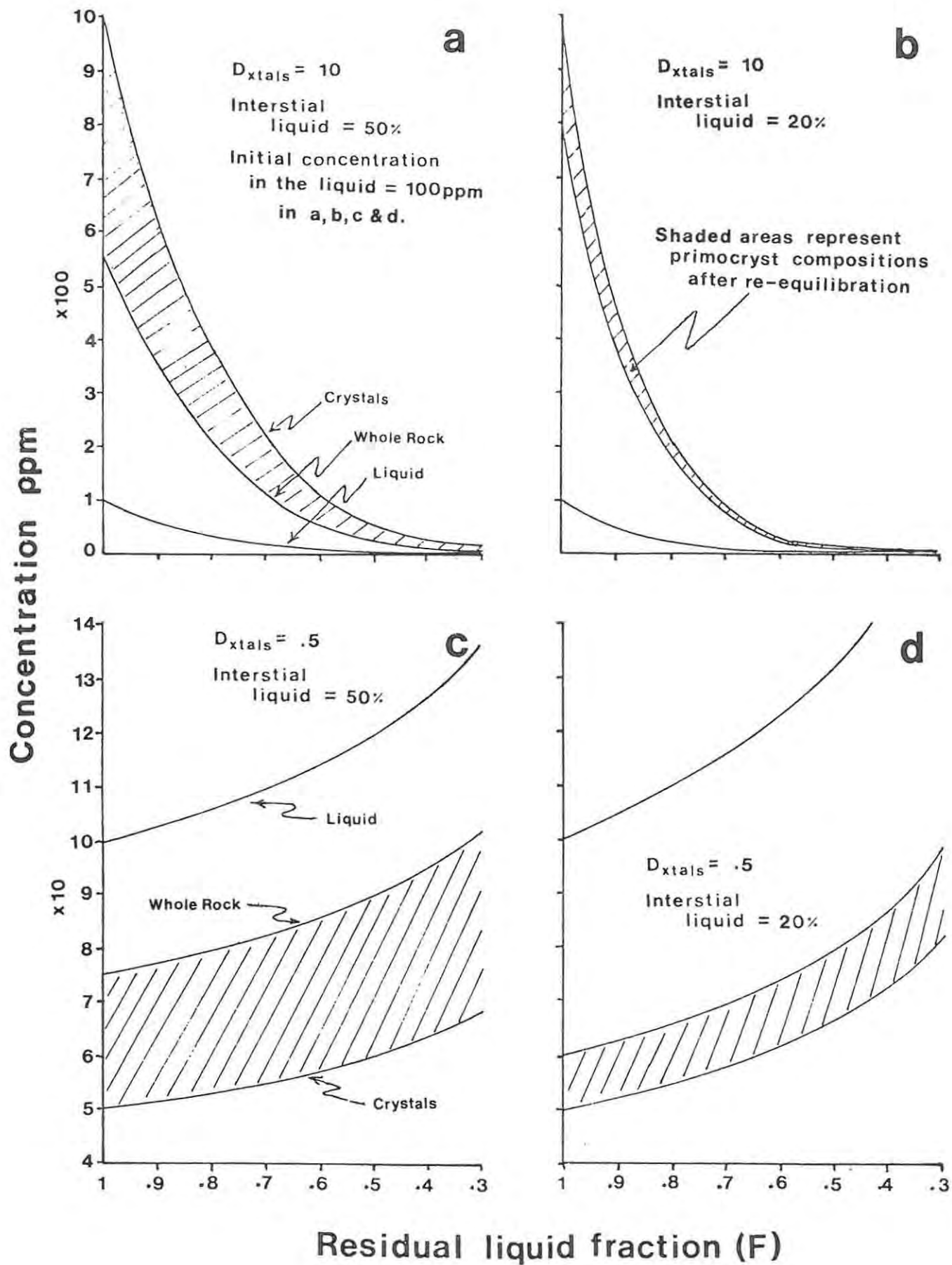


Fig. 5:2 Rayleigh fractionation of a finite volume of liquid by extraction of crystals plus interstitial liquid. The interstitial liquid is considered to be an additional phase with a distribution coefficient of 1. The D_{bulk} is thus dependant on the D_{xtals} and the proportion of interstitial liquid.

Applications to the Study Section.

Notwithstanding the extensive complexities and changes that can occur to the chemistry of primocryst phases as a result of subliquidus processes as outlined in Chapter Four, the chemistry of the rocks and orthopyroxene primocrysts from the lower part of the Merensky unit (the Merensky pyroxenite and the lower portion of the norite) can be used to estimate the thickness of the magma from which the Merensky cyclic unit crystallized, and hence the thickness of the basal convecting layer. Although the approach adopted can be fully quantitative, a large amount of data on a very closely sampled section is needed, and the problems and processes outlined in the previous two chapters need to be evaluated. This could not be done in detail, and thus the conclusions reached here are subject to considerable uncertainty, but nevertheless serve to place limits on the volume of magma the Merensky cyclic unit crystallized from. This may give an indication of the size or thickness of the crystallizing basal convecting layer in the double-diffusive system.

In the case of the orthopyroxene/liquid system dealt with here, the trace elements Zn, Mn and Ni behave in a coherent manner, even though the last named is influenced by the presence of sulphide. The MMF ratio of the pyroxene can also be used. All the other components determined in this work give inconclusive results for a variety of reasons such as the presence of additional phases such as sulphide, chromite, mica and interstitial plagioclase, and a lack of adequate precision in determination. The concentrations of the more incompatible elements, including Zn and Mn ($D < 1$), have probably also been changed by infiltration metasomatic processes.

The Merensky Cyclic Unit

The assumption made here is that the unit crystallized in situ and that for some elements at least their concentrations in the orthopyroxene can be related to the concentrations at the liquidus stage. The liquidus stage concentrations were controlled by Rayleigh fractionation of a convecting layer of magma as outlined above. To account for variations in the amount of interstitial liquid two sets of calculations are made assuming 30% and 40% of interstitial liquid. These are believed to bracket the true value (Chapter Four) and would also account for some of the error introduced by the assumptions made.

Only the lower part of the Merensky cyclic unit is used to estimate the thicknesses as significant fractionation of two primocryst phases would change C_r such that it would no longer relate in a simple way to the C_{r0} at the base of the pyroxenite, as D_{xtals} and thus D_{bulk} changes. The most comprehensive data available is on the MMF ratio of the orthopyroxene, which as this is the dominant mafic phase to crystallize, reflects the Mg# of the bulk rock. Orthopyroxene is also the dominant liquidus phase. For the purposes of the calculations the inverse of the K_D (.26) is used for D_{xtals} (3.85) as the K_D was originally defined as $K_D = X_{liq}/X_{solid}$ (Chapter Four, Irvine, 1979). In Fig. 5:3 the variation in the $(MMF/1-MMF)_{opx}$ (see Irvine, 1979) of the lower part of the Merensky cyclic unit is illustrated. Two extreme curves (A and B) within an envelope that includes all $(MMF/1-MMF)_{opx}$ values determined on the probe from directly above the Merensky pegmatoid are also illustrated. Curves A and B were calculated using the extreme ends (a & b) and (a' & b') as C_{r0} and C_r respectively. The thickness of the fractionating unit was calculated using the values of C_r and C_{r0} shown on Fig. 5:3. The D_{bulk} was calculated assuming a model with 30% and 40% interstitial liquid. The results are listed in Table 5:1.

Table 5:1. Thickness of magma crystallizing the lower part of the Merensky Cyclic unit assuming two extreme models (A & B in Fig 5:3) and 30% and 40% interstitial liquid.

	D_{opx}	$D_{30\%}$	$D_{40\%}$	a	C_r/C_{r0}	t _{30%}	t _{40%}
A	3.85	2.99	2.71	2.7m	0.47	8.6m	7.6m
B	3.85	2.99	2.71	2.7m	0.79	24.2m	21.0m

This layer of magma (7 to 24m thick) brackets the thickness of the Merensky cyclic unit ($\pm 10m$), and the thickness of the cyclic unit could thus represent the approximate thickness of the original convecting layer. Although there is a considerable margin of error in the calculations due to factors outlined previously and summarized below, and a lack of very comprehensive data, the model outlined here does indicate that if the Merensky cyclic unit fractionally crystallized from an "isolated" basal layer of magma, that layer of magma was roughly the same thickness as the

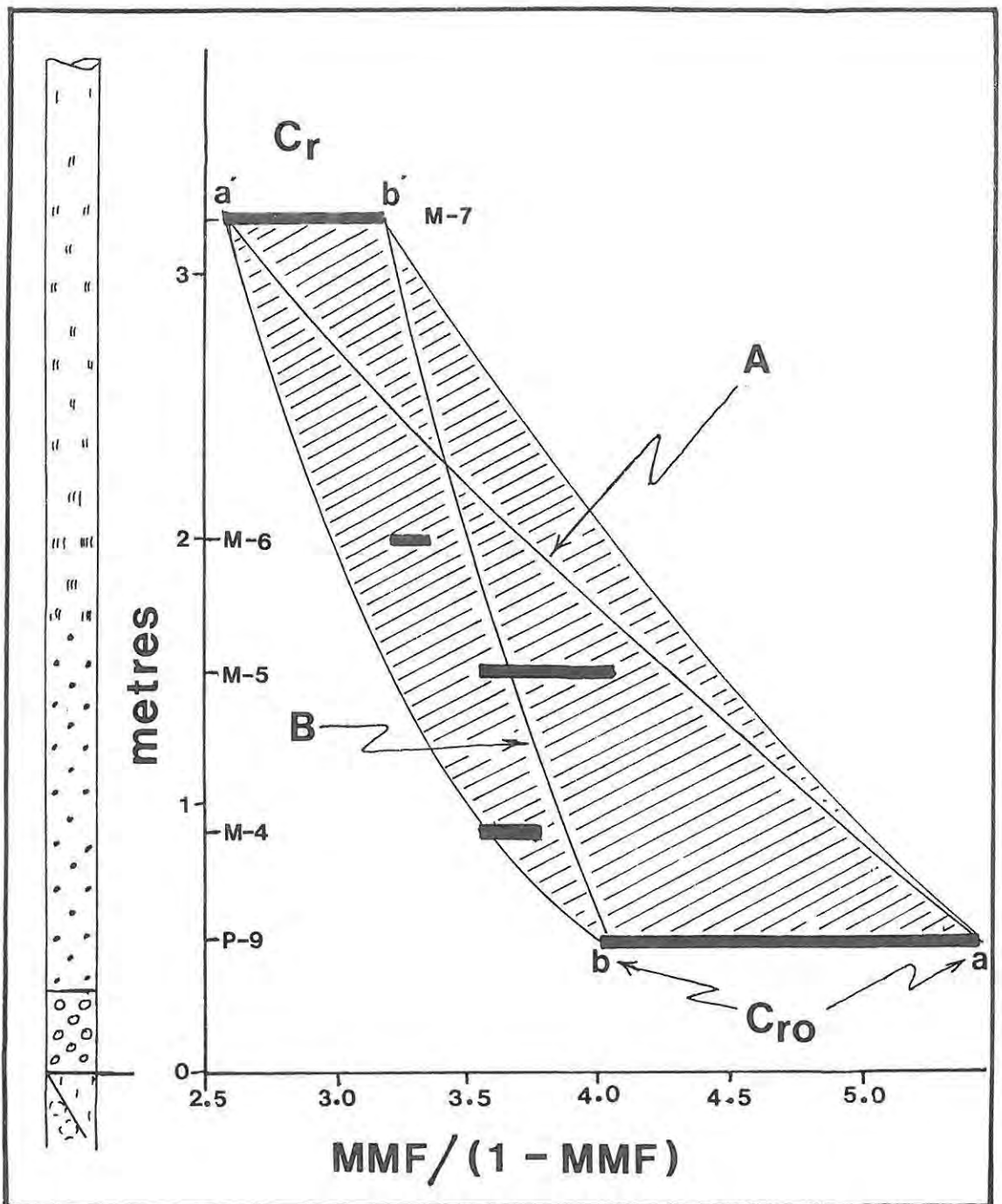


Fig. 5:3 This shows the variation of the $(MMF)/(1-MMF)$ ratio of the primocryst orthopyroxenes of the lower part of the Merensky cyclic unit. The range in compositions from individual samples is indicated by the horizontal black bars, and the shaded area indicates a possible overall range. The curves A and B are the extreme fractionation curves referred to in the text. Other symbols are also referred to in the text.

cyclic unit itself. This is subject to the correctness of the model adopted and the assumptions made.

As a further test of the model some trace and minor elements (Mn, Ni and Zn) can be used. In the case of Mn much data is available, but it shows a wide scatter with a general upward increase in concentration (see Chapter Two). The distribution coefficient D_{opx} is ± 0.7 (Irving, 1978) but the bulk distribution coefficient D_{bulk} is between 0.79 and 0.82. As pointed out above, greater precision is needed as D_{bulk} approaches 1, the scatter of data thus makes calculation of a thickness very imprecise. The thicknesses calculated are very variable depending on the data points selected and averages used, and vary between $\pm 2\text{m}$ and 17m , the latter figure being an absolute maximum, the other values clustering between 3 and 5 metres. The upward increase in Mn is a poor test for the model but does indicate that a relatively thin layer of magma was involved in the generation of the rocks.

Few data are available for the concentrations of Ni and the published distribution coefficients have a wide range (1.1 to 10 (Irving, 1978)). To test the model, a different approach is adopted. The thicknesses calculated using the Mg/Fe ratio (Table 5:1) are used to calculate two apparent distribution coefficients for Ni and these should then correspond to the published values after correction for the interstitial liquid. The two concentrations selected were of M-5 and M-7, as M-4 contains significant sulphide. No other data are available in this section. The distribution coefficients calculated are 3.3 and 8.5 for the minimum and maximum thicknesses respectively, and these fall within the range of published values. This also indicates that the true thickness of the convecting layer was probably close to the minimum determined using the Mg/Fe variation, i.e. similar to the Merensky Cyclic unit in thickness.

Virtually no data are available on the distribution coefficients of Zn for orthopyroxene. The data in this work suggest a very low value ($D_{\text{opx}} \ll 1$). A D_{bulk} value of 0.22 to 0.25 was calculated using the approach above, but this is inconsistent with the probable amount of interstitial liquid. The explanation for the anomalous but consistent behaviour of this element in orthopyroxene probably lies in the sub-liquidus processes, especially infiltration metasomatism and variations in the fraction of interstitial liquid. Much more data on closely spaced samples are needed to fully evaluate the roles of different processes in the distribution of Zn and many other elements.

The Bastard Cyclic Unit

The MMF ratios of primocryst orthopyroxenes in the Bastard cyclic unit are not as consistent as those of the Merensky cyclic unit (see Chapter Two). Only three samples are available from the Bastard pyroxenite and the lower part of this unit has been affected by infiltration metasomatism from the Merensky mottled anorthosite (see Chapter Five).

The Bastard norite and anorthosite also have inconsistent variations in the MMF ratio of the orthopyroxene. The trace elements on the other hand appear to be more consistent in their behaviour, but fewer data points are available. The chemical and mineralogical variation of the Bastard cyclic unit broadly resembles that of the Merensky cyclic unit suggesting similar process in operation, but detailed precise modelling is not possible without more extensive data on more closely spaced samples (especially in the Bastard pyroxenite). Precise data on the amount of interstitial liquid within the norite and the modes of the primocrysts before reaction with the interstitial liquid is needed. The resemblance to the Merensky cyclic unit suggests that the Bastard cyclic unit also crystallizes from a convecting layer of limited thickness.

Limitations and Problems

There are several interrelated factors which can affect the use of the above approach to determine the thickness of the convecting layer and the course of crystallization. Some of these have been explicitly dealt with above or in other chapters, or implicitly assumed to be invariant. These are:

- a) Variations in the fraction of interstitial liquid.
- b) Variations in the composition of the interstitial liquid.
- c) Changes in the mineral distribution coefficient used as a function of the composition of liquid and solid.
- d) Diffusion across double-diffusive interfaces.
- e) Imperfect fractional crystallization.
- f) Subliquidus, solidus and subsolidus processes.
- g) Precision of the abundance data.

These factors weaken the simple model adopted here to calculate the thickness of the crystallizing basal double-diffusive layer. Nevertheless,

many of the data are explained using the simple model developed above, but refinement of the model is not justified by the data available. The hypothesis advanced could be further tested with more closely spaced data points and by assessing and correcting for each of the above factors.

Summary and Conclusion

In this chapter the data available for the Merensky cyclic unit is shown to be consistent with the hypothesis of double-diffusive fractional crystallization as outlined by Irvine (1980b) and adapted to this work. The thickness of magma from which the Merensky unit crystallized (the basal double-diffusive layer of the new magmatic system) appears to be similar in thickness to the cyclic unit itself.

The Bastard cyclic unit has generally similar chemical and mineralogical variations to the Merensky unit, but significant subliquidus processes obscure this general picture to some extent, and thus this unit cannot be interpreted quantitatively with the data available. The similarities to the Merensky unit do however suggest a very similar origin.

Data on the Footwall unit is not comprehensive enough to pronounce positively in favour of a model similar to that adopted here for the Merensky unit or for the model as outlined by McBirney & Noyes (1979). A further detailed study of the Footwall unit is thus a pre-requisite for complete understanding of this magmatic system.

CHAPTER SIX: Summary and Conclusions

Introduction

In this work the data gathered on the study section was interpreted using the concepts of bottom crystallization and double-diffusive convection coupled to the older idea of multiple intrusion. This interpretation reconciles many of the apparently divergent views of different workers on the Bushveld Complex.

The Evolution of the Study Section: a Resumé

The Physical Processes

The physical model that at present most successfully explains the features observed in the Merensky cyclic unit is one of bottom crystallization of a stratified convecting magma. It was argued using Sr-isotope and other evidence in Chapter Three that a large new influx of magma occurred after the deposition of the Footwall unit, mixed with the residual magma and then crystallized the Merensky and Bastard cyclic units from convecting layers at the base of the magma chamber. The convecting layers formed due to opposing heat (upward) and mass (downward) fluxes and are known as double-diffusive convective layers. The model adopted is based on that of Irvine (1980b).

The Liquidus Processes

The chemical variation within the study section is explained by the model outlined in Chapters Three, Four and Five. The chemical and mineralogical data can be used to quantify the thicknesses of the magma layer from which the Merensky cyclic unit crystallized. It was assumed that the lower part of the Merensky cyclic unit fractionated from a finite thickness of magma and that the Rayleigh fractionation law governed the chemical evolution. From the changes in the Mg/Fe ratio of the orthopyroxenes with respect to height in the Merensky pyroxenite and norite, it was deduced that the layer of magma from which the cyclic unit crystallized was similar in thickness to the thickness of the cyclic unit itself ($\pm 10\text{m}$ in the study area).

The Subliquidus Processes

A number of processes can occur during the subliquidus crystallization of the crystal mush (primocrysts plus interstitial liquid). These are in situ crystallization of the crystal mush as a closed system, infiltration metasomatism and expulsion of interstitial liquid due to sintering or compaction of the primocryst phases.

In situ crystallization is the most easily modelled. During crystallization the bulk composition of the rock does not change, but that of the primocrysts and interstitial liquid does as a result of fractionation of the solid and liquid phases. In most pyroxenites the in situ crystallization proceeded as a total equilibrium system (with respect to the MMF ratio) resulting in relatively unzoned grains in the final rock, but in the norites and anorthosites surface equilibrium fractionation effects (such as zoning of some elements) relict from the subliquidus stage are still apparent. These have been briefly examined in Chapter Two.

Sintering and compaction on the one hand and infiltration metasomatism on the other, are complimentary processes as the liquid expelled from one rock infiltrates and reacts with the rock above, unless the sintering process is occurring at the interface between the magma and the crystal pile. Infiltration metasomatism can account for some of the Sr-isotope results of the Merensky cyclic unit as outlined in Chapters Three and Four. Sintering and compaction may produce "solid" impervious monomineralic layers in the crystal mush which may form barriers to upward moving volatile components and expelled liquid. These may then be trapped to form pegmatoidal layers such as the Merensky pegmatoid, or migrate laterally to zones of weakness, move upward through the crystal mush and excavate potholes at the interface between the liquidus and subliquidus zones. The late stage volatile rich liquids may also concentrate in zones of weakness and intrude upward to form the ultramafic pegmatites.

It is important to note that in a single "rock" several of the above processes may operate simultaneously or in sequence. For instance, a crystal mush when deposited may start to sinter expelling liquid, but the mush below may also do this simultaneously, injecting the expelled liquid into the rock above where it partially replaces the interstitial liquid remaining (e.g. the Merensky cyclic unit). The sintering may then cease and the rock proceed to crystallize as a closed system from then on. This goes a long way to explain the great complexities that are sometimes encountered in layered rocks.

Solidus and Subsolidus Processes

At the solidus and subsolidus stages there is continued reaction involving mutual exchange reactions between adjacent minerals and also exsolution of the pyroxenes. These processes may be aided by the presence of an intergranular fluid phase. Considerable disequilibrium may be present in rocks, which is not always eliminated or masked by subsolidus processes. These factors make the interpretation of mineral separates and probe analyses problematic in some instances.

Conclusion

This brief outline illustrates some possible processes that can occur in the generation of the present (observable) rock. A large number of factors have to be considered when interpreting the data on a single rock or suite of samples, and this increases the degree of uncertainty in any conclusions drawn. The only remedy is very closely spaced sampling and detailed evaluation of each sample with respect to its intensive properties (chemistry, texture, mineralogy etc.) and with respect to its position in the succession as a whole.

The Formation of the Bushveld Complex: Unification of Models

The review in Chapter One indicated that two main hypotheses have been invoked to account for the Bushveld Complex: multiple intrusions and in situ differentiation with or without magma additions. More recently these opposing views have become partly reconciled as the multiple intrusion with subordinate in situ differentiation (Coertze, 1974) school on the one hand and the multiple magma addition with marked in situ differentiation school of thought, on the other. The former school of thought does not consider that magma mixing within the magma chamber is a major process, while the latter does. Controversy still exists within the latter school as to the number, timing and volume of the magma additions. The new ideas invoking double-diffusive convection in, and multiple magma additions to, evolving magma chambers provide a unified framework of physical processes within magma chambers. Double-diffusive convection and multiple magma additions can also be philosophically unifying concepts between the various schools of thought discussed above.

The process of double-diffusive convection results in a stratified layer of magma with slightly different compositions stacked one above the other. In the model outlined by McBirney & Noyes (1979) these layers can gel and crystallize in situ. The layers are to a greater or lesser extent closed systems and can thus be viewed as "independent" entities and are in some ways similar to multiple intrusions. Magma additions to an evolving residual liquid in a magma chamber can behave in different ways and need not necessarily mix efficiently with the residual magma (see Chapter Three) and in some cases may form an independent layer within the liquid. The magma addition may thus have many of the characteristics of a independent intrusion. Fractionation on a large scale and on the scale of individual layers may occur thus changing the composition of the residual liquid within layers, or the whole of the intrusion. This discussion emphasizes the similarities between the different points of view that have hitherto been adopted.

The Compositions and Origins of Bushveld Complex Magmas.

Introduction

The composition of the magmas that gave rise to Rustenberg Layered Suite is the subject of much dispute (see Sharpe (1981a) for a brief review). In view of the above discussion and the possibilities of multiple magma additions in a double-diffusive system the approaches adopted by various authors to estimate the parental magma compositions for the Rustenberg Layered Suite must be viewed with reservations.

The approach of estimating the modal proportions and the volumes of the various zones (Vermaak, 1976a; Cameron, 1978 & 1980) cannot give the magma composition from which a specific horizon crystallized by subtraction of the material below that horizon from the total, because any layer is a result of the complex interplay of the physical processes in the magma chamber and addition and mixing of new magma influxes. This approach is only valid if a single magma introduced as a single event differentiates as a closed system (Morse, 1979a).

The approach of Frick (1973), Davies et al. (1980), Cawthorn et al. (1981) and Sharpe (1981a) of investigating the nature of the sills in the floor rocks of the complex and from these selecting likely parental magmas to the layered suite is also fraught with difficulties as the sills may

not represent true samples of undifferentiated primary magma and may in fact represent mixed or partly mixed magmas instead (Sharpe, 1981a; Davies et al., 1980). They may also represent different fractions of a compositionally stratified liquid and may thus be unrepresentative of any initial or final liquid composition. The approach of Sharpe (1981a) of equating the MMF of orthopyroxene from the layered rocks with that inferred to crystallize from the Marginal Zone sills is also simplistic, as the primocrysts of the layered rocks are not necessarily liquidus compositions, as shown in Chapter Four.

The experimental approach of McBirney (1975) who partially melted rocks of the Skaergaard intrusion to determine the composition of the interstitial liquid holds some promise but is only applicable to the norites, gabbros and some feldspathic pyroxenites as the monomineralic rocks may have had metasomatic addition or subtraction of components (von Gruenewaldt, 1979; Chapter Four and M.J. Botha, work in progress). The approach outlined in Chapter Four has similar restrictions to the approach of McBirney (op. cit.).

In this work (Chapters Three and Four) the magmas from which the rocks of the study section were derived are considered to be average tholeiitic basalts. In situ contamination was rejected as a possible explanation for the change in the $^{87}\text{Sr}/^{86}\text{Sr}$ initial ratio at the level of the Merensky cyclic unit. Contamination or assimilation before introduction to the chamber was not considered.

The Composition of the Primary Magmas

Extensive controversy exists as to the roles of mantle heterogeneity and crustal contamination in producing the diversity in isotopic and chemical characteristics of basaltic magmas (see e.g. Erlank et al., 1980; O'Hara, 1980; Moorbath & Thompson, 1980; Carlson et al., 1981; Thompson et al., 1982) and it is outside the scope of this work to deal with the various proposals and models that have been published.

Assuming that there was negligible in situ crustal contamination of the magmas that crystallized the layered rocks (Hamilton, 1977; Kruger & Marsh, 1982), the initial $^{87}\text{Sr}/^{86}\text{Sr}$ ratios recorded are anomalously high (Hamilton, 1977). This implies that the mantle from which the magmas were derived were anomalously enriched in radiogenic Sr and had a high Rb/Sr ratio of ± 0.25 , or there was a crustal component in the magmas.

These considerations and light rare earth enriched REE patterns led Hamilton to suggest that the mantle from which the magmas were derived was enriched metasomatically by a fluid with kimberlitic or potassic affinities. This suggestion of "kimberlitic" affinities for the Bushveld Complex magmas was also made by Vermaak (1976a) and others. Various models for the generation of the magmas are discussed by Hamilton, but a review of these is beyond the scope of this work.

The minimum and maximum $^{87}\text{Sr}/^{86}\text{Sr}$ ratios recorded from the layered sequence are 0.70556 and 0.70853 respectively (Hamilton, 1977). These two values thus represent possible end member initial $^{87}\text{Sr}/^{86}\text{Sr}$ ratios of a two primary magma system as envisaged by Davies et al. (1980) and Cawthorn et al. (1981). They could also represent the two extremes of a series of magmas with different and sequentially increasing ratios (Hamilton, 1977).

The PGE have received a growing amount of attention but has centred mainly on the mineralized horizons in the complex and some of the layered rocks (see Cousins & Vermaak, 1976; Vermaak & Hendriks, 1976; and Page et al., 1981). Sharpe (1981b) has presented PGE analyses of the marginal rocks of the Bushveld complex and reports concentrations that are considerably higher than those reported in chilled margins of other layered intrusions, and at least in order of magnitude greater than mid ocean ridge basalt. The Bushveld magmas are therefore considered by Sharpe to be derived from a PGE-enriched mantle or were evolved before emplacement. The latter suggestion was also made by Allegre & Luck (1980) in interpreting a single anomalous $^{187}\text{Os}/^{186}\text{Os}$ ratio of Merensky "reef" laurite.

There is some consensus that the early magmas of the Bushveld Complex were both magnesian and silicic and thus of unusual composition while later influxes were more "normal" tholeiitic compositions (inter alia Vermaak, 1976a; Hamilton, 1977; Cameron, 1978; von Gruenewaldt, 1979; Davies et al., 1980; Cawthorn et al., 1981; Sharpe, 1981a). The magmas intruded at later stages (parental to the Critical, Main and Upper Zones) are considered to be tholeiitic in composition (inter alia this work; von Gruenewaldt, 1973; Vermaak, 1976a; Cawthorn et al., 1980; Sharpe, 1981a; Cawthorn & Davies, 1982). There may therefore be two main magma types parental to the layered suite, but this is a very broad definition and no certainty as to actual volumes and compositions or ranges of composition exists. Furthermore, it is unknown if there are differences between the

compositions of magmas intruded into different lobes of the Bushveld Complex although it is assumed that the lobes are broadly similar, at least in the upper parts. There is some evidence that the lobes were interconnected at the level of the Merensky Cyclic unit (e.g. Kruger & Marsh, 1982).

Chromium is relatively insoluble in mafic magmas but the solubility is strongly dependent on the composition and inversely dependent the oxygen fugacity of the liquid (Hill & Roeder, 1974). The work of Hill & Roeder (op. cit.) indicates that the maximum solubility of Cr is less than 1000ppm unless very low oxygen fugacities are indicated (Fisk & Bence, 1980). The very high Cr concentrations indicated by Davies et al., (1980) and Sharpe (1981a) (970ppm and 915 to 1497ppm respectively) for the earlier magmas may thus indicate that the magmas had unusually low oxygen fugacities or that there was enrichment with Cr bearing phases (chromite and pyroxene). Cameron (1978) also suggests a high Cr content for the early Bushveld magmas.

The magmas that intruded into the Bushveld Complex magma chamber appear to be of two main types or end members. An early magnesian and possibly silicic magma with a high chromium content and relatively low initial Sr-isotope ratio, was followed by later influxes (at least four) of magmas with more tholeiitic affinities and relatively high initial Sr-isotope ratios. The magmas may have been derived from a metasomatically enriched mantle with anomalously high Rb, LREE and possibly PGE.

REFERENCES

- Albee, A.L. & Ray, L. (1970) Correction factors for electron probe micro-analysis of silicates, oxides, carbonates, phosphates and sulfates. *Anal. Chem.* 42, 1408-1414.
- Allegre, C.J. & Luck, J-M. (1980) Osmium isotopes as petrogenetic and geological tracers. *Earth Planet. Sci. Lett.* 48, 148-154.
- Arth, J.G. (1976) Behavior of trace elements during magmatic processes - a summary of theoretical models and their applications. *J. Res. U. S. Geol. Sur.* 4, 41-47.
- Atkins, F.B. (1969) Pyroxenes of the Bushveld intrusion, South Africa. *J. Petrol.* 10, 222-249.
- Bence, A.E. & Albee, A.L. (1968) Empirical correction factors for the electron microanalysis of silicates and oxides. *J. Geol.* 76, 382-403.
- Bevan, J.C. (1982) Reaction rims of orthopyroxene and plagioclase around chrome spinels in olivine from Skye and Rhum. *Contrib. Mineral. Petrol.* 79, 124-129.
- Bottinga, Y. & Weill, D.F. (1970) Densities of liquid silicate systems calculated from partial molar volumes of oxide components. *Amer. J. Sci.* 269, 169-182.
- & ----- (1972) Viscosity of magmatic silicate liquids: a model for calculation. *Amer. J. Sci.* 272, 438-475.
- Brown, G.M. (1956) The layered ultrabasic rocks of Rhum, Inner Hebrides. *Phil. Trans. Roy. Soc. Lond. Series B* 240, 1-56.
- & Vincent, E.A. (1963) Pyroxenes from the late stages of fractionation of the skaergaard intrusion, East Greenland. *J. Petrol.* 4, 175-197.
- Brynard, H.J. (1976) Die mineralogie en petrografie van die Merenskyrif in die Western Platinum-myn, naby Marikana. Unpub. MSc. thesis, Rand Afrikaans Universiteit.
- , De Villiers, J.P.R. & Viljoen, E.A. (1976) A mineralogical investigation of the Merensky Reef at the Western Platinum mine, near Marikana, South Africa. *Econ. Geol.* 71, 1299-1307.
- Buchanan, D.L. (1979) A combined transmission electron microscope and electron microprobe study of the Bushveld pyroxenes from the Bethal area. *J. Petrol.* 20, 327-354.
- Burnham, C.W. (1979) The importance of volatile constituents. In: *Evolution of the Igneous Rocks: Fiftieth Anniversary Perspectives*. H.S. Yoder ed. Princeton. Chapter 16. 439-482.

- Cameron, E.N. (1969) Postcumulus changes in the Eastern Bushveld Complex. *Amer. Mineral.* 54, 754-779.
- (1975) Postcumulus and subsolidus equilibration of chromite and co-existing silicates in the Eastern Bushveld Complex. *Geochim. Cosmochim. Acta* 39, 1021-1033.
- (1977) Chromite in the Central Sector of the Eastern Bushveld Complex, South Africa. *Amer. Mineral.* 62, 1080-1096.
- (1978) The Lower Zone of the Eastern Bushveld Complex in the Olifants river trough. *J. Petrol.* 19, 437-462.
- (1980) Evolution of the Lower Critical Zone, Central Sector, Eastern Bushveld Complex and its chromite deposits. *Econ. Geol.* 75, 845-871.
- & Desborough, G.A. (1964) Origin of certain magnetite-bearing pegmatites in the eastern part of the Bushveld Complex, South Africa. *Econ. Geol.* 59, 197-225.
- Campbell, I.H. (1977) A study of macro-rhythmic layering and cumulate processes in the Jimberlana intrusion, Western Australia: Part I: Upper Layered Series. *J. Petrol.* 18, 183-215.
- (1978) Some problems with the cumulus theory. *Lithos* 11, 311-323.
- , Roeder, P.L. & Dixon, J.M. (1978) Plagioclase buoyancy in basaltic liquids as determined with a centrifuge furnace. *Contrib. Mineral. Petrol.* 67, 369-377.
- Carlson, R.W., Lugmair, G.W. & MacDougall, J.D. (1981) Columbia River Volcanism: the question of mantle heterogeneity or crustal contamination. *Geochim. Cosmochim. Acta* 45, 2483-2499.
- Carmichael, I.S.E., Turner, F.J. & Verhoogen, J. (1974) *Igneous Petrology* McGraw-Hill. 739pp.
- Cawthorn, R.G. (1977) Pyroxene compositions, reaction relations and the lack of silica enrichment in the Eastern Bushveld Complex. *Trans. Geol. Soc. S. Afr.* 80, 139-144.
- & Davies, G. (1982) Possible komatiitic affinity of the Bushveld Complex, South Africa. In: *Komatiites*. N.T. Arndt & E.G. Nisbet eds., George Allen & Unwin, Lond. pp91-96.
- , -----, Chubley-Armstrong, A. & McCarthy, T.S. (1981) Sills associated with the Bushveld Complex, South Africa: an estimate of parental magma composition. *Lithos* 14, 1-15.

- Cawthorn, R.G. & McCarthy, T.S. (1980) Variations in Cr content of magnetite from the Upper Zone of the Bushveld Complex - Evidence for heterogeneity and convection currents in magma chambers. *Earth Planet. Sci. Lett.* 46, 335-343.
- & McCarthy, T.S. (1981) Bottom crystallization and diffusion control in layered complexes: evidence from Cr distribution in magnetite from the Bushveld Complex. *Trans. Geol. Soc. S. Afr.* 84, 41-50.
- Chen, C.F. & Turner, J.S. (1980) Crystallization in a double-diffusive system. *J. Geophys. Res.* 85, 2573-2593.
- Coble, R.L. (1961) Sintering crystalline solids I. Immediate and final state diffusion models. *J. Appl. Phys.* 32, 787-792.
- & Burke, J.E. (1963) Sintering in ceramics. In: *Progress in Ceramic Science* 3, J.E. Burke ed. Pergamon Press, Lond. Chapter 4, 194-251.
- Coertze, F.J. (1958) Intrusive relationships and ore deposits in the western part of the Bushveld Igneous Complex. *Trans. Geol. Soc. S. Afr.* 61, 387-400.
- (1959) Discussion of "The Geological succession in a portion of the north-western Bushveld (Union Section) and its interpretation" by G.Feringa. *Trans. Geol. Soc. S. Afr.* 62, 233.
- (1960a) Anorthosite emplaced in a shear-zone in gabbro of the Bushveld Igneous Complex. *Trans. Geol. Soc. S. Afr.* 63, 75-81.
- (1960b) Reply to discussion by C.A. Cousins of "Anorthosite emplaced in a shear-zone in gabbro of the Bushveld Igneous Complex." *Trans. Geol. Soc. S. Afr.* 63, 84-85.
- (1962a) The Rustenburg fault as a controlling factor of ore deposition south-west of Pilanesberg. *Trans. Geol. Soc. S. Afr.* 65, 253-262.
- (1962b) The relationship between the Pretoria Series and the Bushveld Igneous Complex north-east of Pretoria. *Annals. Geol. Surv. S. Afr.* 1, 67-70.
- (1963) Structures in the Merensky Reef in the Rustenburg Platinum Mine. *Annals. Geol. Surv. S. Afr.* 2, 69-77.
- (1966) The genesis and geological environment of the Bushveld magnetite in the area south-west of the Leolo Mountains. *Bull. Geol. Surv. S. Afr.* 47, 57pp.
- (1970) The geology of the western part of the Bushveld Igneous Complex. *Geol. Soc. S. Afr. Spec. Publ.* 1, 5-22.
- (1974) The geology of the Basic portion of the Western Bushveld Igneous Complex. *Geol. Surv. S. Afr. Mem.* 66, 148pp.

- Cousins, C.A. (1959) The structure of the mafic portion of the Bushveld Igneous Complex. (With discussions and replies). *Trans. Geol. Soc. S. Afr.* 62, 179-201.
- (1964) The platinum deposits of the Merensky Reef. In: *The Geology of Some Ore Deposits in Southern Africa*. S.H. Haughton ed. *Geol. Soc. S. Afr. Vol 2*, 225-237.
- (1969) The Merensky Reef of the Bushveld Igneous Complex. *Econ. Geol. Monograph 4*, 239-251.
- & Vermaak, C.F. (1976) The contribution of South African ore deposits to the geochemistry of the platinum group metals. *Econ. Geol.* 71, 287-305.
- Coleman, L.C. (1978) Solidus and subsolidus compositional relationships of some co-existing Skaergaard Pyroxenes. *Contrib. Mineral. Petrol.* 66, 221-227.
- Daly, (1928) Bushveld Igneous Complex of the Transvaal. *Bull Geol. Soc. Amer.* 30, 703-768.
- Daly, R.A. & Molengraaf, G.A.E (1924) Structural relations of the Bushveld Igneous Complex of the Transvaal. *J. Geol.* 32, 1-35.
- Darwin, C. (1844) Geological observations on the Volcanic Islands visited during the voyage of H.M.S. Beagle, together with some brief notices on the geology of Australia and the Cape of Good Hope. Being the second part of the geology of the voyage of the Beagle under the command of Capt. Fitzroy, R.N., during the years 1882-1836. Smith Elder. Lond. 175pp.
- Davies, G., Cawthorn, R.G., Barton, J.M.Jr. & Morton, M. (1980) Parental magma to the Bushveld Complex. *Nature* 287, 33-35.
- Davies, R.D., Allsopp, H.L., Erlank, A.J. & Manton, W.I. (1970) Sr-isotopic studies on various layered mafic intrusions in Southern Africa. *Geol. Soc. S. Afr. Spec. Publ.* 1, 576-593.
- De Klerk, W.J. (1982) The geology, geochemistry and silicate mineralogy of the Upper Critical Zone of the North-western Bushveld Complex, at Rustenburg Platinum Mines, Union Section. Unpub. MSc. thesis. Rhodes University.
- De Vore, G.W. (1959) Role of minimum interfacial free energy in determining the macroscopic features of mineral assemblages I. The Model. *J. Geol.* 67, 211-227.
- De Waal, S.A. (1977) Carbon dioxide and water from metamorphic reactions as agents for sulphide and spinel precipitation. *Trans. Geol. Soc. S. Afr.* 80, 193-196.
- Dietz, R.S. (1963) Vredefort Ring - Bushveld Complex impact event and lunar maria (abstr). *Geol. Soc. Amer., Spec. Pap.* 73, 35.

- Drake, M.J. (1976) Plagioclase-melt equilibria. *Geochim. Cosmochim. Acta.* 40, 457-465.
- Eales, H.V. (1980) Contrasted trace-element variations in two Karroo cumulus complexes. *Chem. Geol.* 29, 39-48.
- & ----- (in press) Al/Cr ratios of coexisting orthopyroxenes and spinellids in some ultramafic rocks. *Chem. Geol.* in press.
- Erlank, A.J., Allsopp, H.L., Duncan, A.R. & Bristow, J.W. (1980) Mantle heterogeneity beneath Southern Africa: evidence from the volcanic record. *Phil. Trans. Roy. Soc. Lond. Series A* 297, 295-307.
- Ferguson, J. (1969) Compositional variation in minerals from mafic rocks of the Bushveld Complex. *Trans. Geol. Soc. S. Afr.* 72, 61-78.
- & Botha, E. (1963) Some aspects of igneous layering in the basic zones of the Bushveld Complex. *Trans. Geol. Soc. S. Afr.* 66, 259-278.
- & McCarthy, T.S. (1970) Origin of an ultramafic pegmatoid in the eastern part of the Bushveld Complex. *Geol. Soc. S. Afr. Spec. Publ.* 1, 74-79.
- Feringa, G (1959) The geological succession in a portion of the North-western Bushveld (Union Section) and its interpretation. *Trans. Geol. Soc. S. Afr.* 62, 219-233.
- Fisk, M.R. & Bence, A.E. (1980) Experimental crystallization of chrome spinel in FAMOUS basalt. *Earth Planet. Sci. Lett.* 48, 111-123.
- Flanagan, F.J. (1973) 1972 values for international geological reference samples. *Geochim. Cosmochim. Acta* 38, 1731-1744.
- Fleet, M.E. (1974) Partitioning of major and minor elements and equilibration in coexisting pyroxenes. *Contrib. Mineral. Petrol.* 44, 259-274.
- Ford, C.E. (1981) Parental liquids of the Skaergaard intrusion cumulates. *Nature* 291, 21-25.
- Freer, R. (1981) Diffusion in silicate minerals and glasses: A data digest and guide to the literature. *Contrib. Mineral. Petrol.* 76, 440-454.
- Frick, C. (1973) The "Sill Phase" and the "Chill Zone" of the Bushveld Igneous Complex. *Trans. Geol. Soc. S. Afr.* 76, 7-14.
- Geikie, A. (1894) On the relations of the basic and acid rocks of the Tertiary Volcanic series of the Inner Hebrides. *Quart. J. Geol. Soc. Lond.* 50, 212-229.

- Geikie, A. & Teall, J.J.H. (1894) On the banded structure of some Tertiary gabbros in the Isle of Skye. *Quart. J. Geol. Soc. Lond.* 1, 645-659.
- Germeles, A.E. (1975) Forced plumes and mixing of liquids in tanks. *J. Fluid Mech.* 71, 601-623.
- Gijbels, R.H., Millard, H.T., Desborough, G.A. & Bartel, A.J. (1974) Osmium, ruthenium, iridium and uranium in silicates and chromite from the eastern Bushveld Complex, South Africa. *Geochim. Cosmochim. Acta* 38, 319-337.
- Gough, D.I. & Van Niekerk, C.B. (1959) A Study of the paleomagnetism in the Bushveld Complex. *Phil. Mag.* 4, 126-136.
- Gray, N.H. (1978) Cooling of a convecting intrusive sheet. *Mathl. Geol.* 10, 301-310.
- Hall, A.L. (1932) The Bushveld Igneous Complex of the central Transvaal. *Geol. Surv. S. Afr. Mem.* 28, 560pp.
- Hamilton, J. (1977) Sr-isotope and trace element studies of the Great Dyke and Bushveld mafic phase and their relation to early Proterozoic magma genesis in Southern Africa. *J. Petrol.* 18, 24-52.
- Hamilton, W. (1970) Bushveld Complex - Product of impacts? *Geol. Soc. S. Afr. Spec. Publ.* 1, 367-374.
- Harker, A. (1904) The Tertiary igneous rocks of Skye. *Mem. Geol. Surv. Scotland.*
- Harker, D. & Parker, E.R. (1945) Grain shape and grain growth. *Trans. Amer. Soc. Metals.* 34, 156-195.
- Heinrich, K.F.J. (1966) X-ray absorption uncertainty. In: *The Electron Microprobe*. McKinley, T.D., Heinrich, K.F.J. & Wittry, D.B. eds., J. Wiley & Sons, New York. p269-377.
- Henderson, P. (1968) The distribution of phosphorus in the early and middle stages of fractionation of some layered intrusions. *Geochim. Cosmochim. Acta* 32, 897-911.
- (1970) The significance of the mesostasis of basic layered igneous rocks. *J. Petrol.* 11, 463-473.
- (1975) Reaction trends shown by spinels of the Rhum layered intrusion. *Geochim. Cosmochim. Acta* 39, 1035-1044.
- Henderson, P. & Suddaby, P. (1971) The nature and origin of the chrome spinel of the Rhum layered intrusion. *Contrib. Mineral. Petrol.* 33, 21-31.
- , MacKinnon, A. & Gale, N.H. (1971) The distribution of uranium in some basic igneous cumulates and its petrological significance. *Geochim. Cosmochim. Acta* 35, 917-925.

- & Wood, R.J. (1981) Reaction relationships of chrome spinels in igneous rocks and further evidence from the layered intrusions of Mull and Rhum, Inner Hebrides, Scotland. *Contrib. Mineral. Petrol.* 78, 225-229.
- Hess, G.B. (1972) Heat and mass transport during crystallization of the Stillwater Igneous Complex. *Geol. Soc. Amer. Mem.* 132, 503-520.
- Hess, H.H. (1960) Stillwater Igneous Complex Montana: A quantitative mineralogical study. *Geol. Soc. Amer. Mem.* 80, 230pp.
- Hill, R. & Roeder, P.L. (1974) The crystallization of spinel from basaltic liquid as a function of oxygen fugacity. *J. Geol.* 82, 709-729.
- Hofmann, A.W. (1980) Diffusion in natural silicate melts: a critical review. In: *Physics of Magmatic Processes*. R.B. Hargraves ed. Princeton. Chapter 9, 385-417.
- Hunter, D.R. & Hamilton, P.J. (1978) The Bushveld Complex. In: *Evolution of the Earth's Crust*. D.H. Tarling ed. Academic Press, Lond. Chapter 4, 107-173.
- Huppert, H.E. & Sparks, R.S.J. (1980) The fluid dynamics of a basaltic magma chamber replenished by influx of hot, dense ultrabasic magma. *Contrib. Mineral. Petrol.* 75, 279-289.
- & Turner, J.S. (1981) A laboratory model for a replenished magma chamber. *Earth Planet. Sci. Lett.* 54, 144-152.
- Hurle, D.J.J. (1972) Hydrodynamics, convection and crystal growth. *J. Crystal Growth* 13/14, 39-43.
- Irvine, T.N. (1967) The Duke Island ultramafic complex, Southeastern Alaska. In: *Ultramafic and Related Rocks*. P.J. Wyllie ed. J. Wiley & Sons. New York. Chapter 4, 84-97.
- (1970a) Heat transfer during solidification of layered intrusions I. Sheets and sills. *Canad. J. Earth Sci.* 7, 1031-1061.
- (1970b) Crystallization sequences in the Muskox intrusion and other layered intrusions I. olivine-pyroxene-plagioclase relations. *Geol. Soc. S. Afr. Spec. Publ.* 1, 441-476.
- Irvine, T.N. (1975) Crystallization sequences in the Muskox intrusion and other layered intrusions II. Origin of chromitite layers and similar deposits of other magmatic ores. *Geochim. Cosmochim. Acta* 39, 991-1020.
- (1977) The origin of chromitite layers in the Muskox intrusion and other stratiform intrusions: a new interpretation. *Geology* 5, 273-277.

- (1978) Infiltration metasomatism, adcumulus growth and secondary differentiation in the Muskox intrusion. *Carnegie Inst. Wash. Yb.* 77, 743-751.
- Irvine, T.N. (1979) Rocks whose composition is determined by crystal accumulation and sorting. In: *Evolution of the Igneous rocks: Fiftieth Anniversary Perspectives*. H.S. Yoder ed. Princeton. Chapter 9, 245-306.
- (1980a) Magmatic density currents and cumulus processes. *Amer. J. Sci.* 280A, 1-58.
- (1980b) Magmatic infiltration metasomatism, double-diffusive fractional crystallization and adcumulus growth in the Muskox intrusion and other layered intrusions. In: *Physics of Magmatic Processes*. R.B. Hargraves ed. Princeton. Chapter 8, 325-383.
- (1981) A liquid-density controlled model for chromitite formation in the Muskox intrusion. *Carnegie Inst. Wash. Yb.* 80, 317-324.
- (1982) Terminology for layered intrusions. *J. Petrol.* 23, 127-162.
- Irving, A.J. (1978) A review of experimental studies of crystal/liquid trace element partitioning. *Geochim. Cosmochim. Acta* 42, 743-770.
- Jackson, E.D. (1961) Primary textures and mineral associations in the ultramafic zone of the Stillwater Complex, Montana. *U.S. Geol. Surv. Prof. Pap.* 358, 106pp.
- (1970) The cyclic unit in layered intrusions: a comparison of repetitive stratigraphy in the ultramafic parts of the Stillwater, Muskox, Great Dyke and Bushveld Complexes. *Geol. Soc. S. Afr. Spec. Publ.* 1, 391-424.
- Jaeger, J.C. (1968) Cooling and solidification of igneous rocks. In: *Basalts. The Poldervaart Treatise on Rocks of Basaltic Composition*. H.H. Hess & Arie Poldervaart eds. Interscience, New York. Vol. 2, 503-536.
- Jones, J.P. (1976) Pegmatoidal nodules in the layered rocks of the Bafokeng leasehold area. *Trans. Geol. Soc. S. Afr.* 79, 312-320.
- Kantha, L (1980) A note on the effect of viscosity on double-diffusive processes. *J. Geophys. Res.* 85, 4398-4404.
- Keys, R.R. & Campbell, I.H. (1981) Precious metals in the Jimberlana intrusion, Western Australia: implications for the genesis of platiniferous ores in layered intrusions. *Econ. Geol.* 76, 1118-1141.

- Keith, D.W., Todd, S.G., Schissel, D.J. & Irvine, T.N. (1981) The J-M platinum-palladium reef of the Stillwater Complex: II. Petrologic Relationships. (Abstr). Soc. Econ. Geol. & Geol. Soc. S. Afr. Third Int. Platinum Symp. Abstr. of Pap. p20-21.
- Kingery, W.D. (1959) Densification during sintering in the presence of a liquid phase. I. Theory. J. Appl. Phys. 30, 301-306.
- & Narasimhan, M.D. (1959) Densification during sintering in the presence of a liquid phase. II. Experimental. J. Appl. Phys. 30, 307-310.
- Kretz, R. (1982) Transfer and exchange equilibria in a portion of the pyroxene quadrilateral as deduced from natural and experimental data. Geochim. Cosmochim. Acta 46, 411-421.
- Kruger, F.J. & Marsh, J.S. (1982) The significance of $^{87}\text{Sr}/^{86}\text{Sr}$ ratios in the Merensky cyclic unit of the Bushveld Complex. Nature 298, 53-55.
- Kudo, A.M. & Weill, D.F. (1970) An igneous plagioclase thermometer. Contrib. Mineral. Petrol. 25, 52-65.
- Lauder, W.R. (1970) Origin of the Merensky Reef. Nature 227, 365-366.
- Lee, C.A. (1981) Post-deposition structures in the Bushveld Complex mafic sequence. J. Geol. Soc. 138, 327-341.
- & Sharpe, M.R. (1980) Further examples of silicate liquid immiscibility and spherical aggregation in the Bushveld Complex. Earth Planet. Sci. Lett. 48, 131-147.
- Lenthall, D.H. & Hunter, D.R. (1977) The geochemistry of the Bushveld Granites in the Potgietersrus tin-field. Precambrian Res. 5, 359-400.
- Lombaard, B.V. (1934) On the differentiation and relationships of the rocks of the Bushveld Igneous Complex. Trans. Geol. Soc. S. Afr. 37, 5-52.
- Longhi, J., Walker, D. & Hays, J.F. (1978) The distribution of Fe and Mg between olivine and Lunar basaltic liquids. Geochim. Cosmochim. Acta 42, 1545-1558.
- Maaløe, S. (1978) The origin of rhythmic layering. Mineral. Mag. 42, 337-346.
- McBirney, A.R. (1975) Differentiation of the Skaergaard intrusion. Nature 253, 691-694.
- (1979) Effects of assimilation. In: The Evolution of the Igneous Rocks. H.S. Yoder ed. Princeton. Chapter 10, 307-338.
- & Noyes, R.M. (1979) Crystallization and layering of the Skaergaard Intrusion. J. Petrol. 20, 487-554.

- McCarthy, T.S. & Cawthorn, R.G. (1980) Changes in initial $^{87}\text{Sr}/^{86}\text{Sr}$ ratio during protracted fractionation in Igneous Complexes. *J. Petrol.* 21, 245-264.
- McClay, K.R. & Campbell, I.H. (1976) The structure and shape of the Kimberlana Intrusion, Western Australia as indicated by an investigation of the Bronzite Complex. *Geol. Mag.* 113, 129-139.
- Markgraaf, J. (1976) Pyroxenes of the Western Bushveld Complex, South Africa. *Trans. Geol. Soc. S. Afr.* 79, 217-224.
- Marsh, J.S. (1979) A manual for X-ray fluorescence determination of major and trace elements in natural silicate rock materials. Unpub. Manual, Rhodes University. 41pp.
- Meyer, G. (1969) Some petrological aspects of mafic rocks from four borehole sections between the Merensky Reef and the Main-Zone gabbro in the Western and Eastern Bushveld Complex. Unpub. MSc. thesis. Potchefstroom University for C.H.E.
- Molengraaf, G.A.F. (1901) Geology de la Republique Sud Africaine du Transvaal. *Bull. Soc. Geolog. de France.* 4 Ser, Tome 1, 13-92.
- (1905) Inter-Colonial Irrigation Commission. Pretoria, 90pp.
- Moorbath, S & Thompson, R.N. (1980) Strontium isotope geochemistry and petrogenesis of the early Tertiary lava pile of the Isle of Skye, Scotland and other basic rocks of the British Tertiary Province: an example of magma-crust interaction. *J. Petrol.* 21, 295-321.
- Moore, A.C. (1973) Studies of igneous and tectonic textures and layering in the rocks of the Gosse-Pile intrusion, Central Australia. *J. Petrol.* 14, 49-79.
- Morse, S.A. (1979a) Kiglapait Geochemistry I: Systematics, sampling and density. *J. Petrol.* 20, 555-590.
- (1979b) Reaction constants for En-Fo-Sil equilibria: an adjustment and some applications. *Amer. J. Sci.* 279, 1060-1069.
- (1979c) Kiglapait geochemistry II: Petrography. *J. Petrol.* 20, 591-624.
- (1980) Basalts and Phase Diagrams: An Introduction to the Quantitative Use of Phase Diagrams in Igneous Petrology. Springer-Verlag, New York. 493pp.
- (1981a) Kiglapait geochemistry III: Potassium and rubidium. *Geochim. Cosmochim. Acta* 45, 163-180.
- (1981b) Kiglapait geochemistry IV: The major elements. *Geochim. Cosmochim. Acta* 45, 461-479.
- (1982) Kiglapait geochemistry V: Strontium *Geochim. Cosmochim. Acta* 46, 223-234.

- Murase, T. & McBirney, A.R. (1973) Properties of some common igneous rocks and their melts at high temperatures. *Geol. Soc. Amer. Bull.* 84, 3563-3592.
- Myers, J.S. (1978) Pipes of mafic pegmatite in the stratiform Fiskenaasset Anorthositic Complex, S.W. Greenland. *Lithos* 11, 277-282.
- Nathan, H.P. & van Kirk, C.K. (1978) A model for magmatic crystallization. *J. Petrol.* 19, 66-94.
- Nesbitt, R.W., Mastins, H., Stolz, G.W. & Bruce, D.R. (1976) Matrix corrections in trace element analyses by X-ray fluorescence: an extension of the Compton scattering technique to long wavelengths. *Chem. Geol.* 18, 203-213.
- Norrish, K & Hutton, J.T. (1969) An accurate X-ray spectrographic method for analysis of a wide range of geological samples. *Geochim. Cosmochim. Acta* 33, 431-453.
- Norton, D. & Knight, J. (1977) Transport phenomena in hydrothermal systems: cooling plutons. *Amer. J. Sci.* 277, 937-981.
- & Taylor, H.P. (1979) Quantitative simulation of the hydrothermal systems of crystallizing magmas on the basis of transport theory and oxygen isotope data: an analysis of the Skaergaard intrusion. *J. Petrol.* 20, 421-486.
- Nwe, Y.Y. (1975) Two different pyroxene crystallization trends in the Trough Bands of the Skaergaard intrusion, East Greenland. *Contrib. Mineral. Petrol.* 49, 285-300.
- & Copley, P.A. (1975) Chemistry, subsolidus relations and electron petrography of pyroxenes from the late ferrodiorites of the Skaergaard intrusion, East Greenland. *Contrib. Mineral. Petrol.* 53, 37-54.
- O'Hara, M.J. (1980) Nonlinear nature of the unavoidable long-lived isotopic, trace and major element contamination of a developing magma chamber. *Phil. Trans. Roy. Soc. Lond. Series A* 297, 215-227.
- Page, N.J., von Gruenewaldt, G., Haffty, J. & Aruscavage, P.J. (1981) Comparison of certain Platinum-Group Element distributions in some layered intrusions with special reference to the late differentiates of the Bushveld Complex. *Inst. Geol. Res. Bushveld Complex, University of Pretoria. Report* 29, 25pp.
- Paster, T.P., Schauwecker, D.S. & Haskin, L.A. (1974) The behaviour of some trace elements during solidification of the Skaergaard layered series. *Geochim. Cosmochim. Acta* 38, 1549-1577.
- Reuning, E. (1927) Verbandsverhältnisse und Chemismus der gesteine des "Bushveld Igneous Complex" Transvaals und des problem seiner entstehung. *Neuen Jb. Mineral. Geol. Paläont. Beilage-Band.* 57, Abt. A, 631-664.

- Reynolds, I.M. (1978) A mineralogical investigation of coexisting iron-titanium oxides from various igneous rocks, with special reference to some South African titaniferous iron ores. Unpub. PhD. thesis. Rhodes University, 632pp.
- (1979) Grain boundary relationships in some Bushveld titaniferous magnetite cumulates (Abstr). Geol. Soc. S. Afr. 18th Congr. Proc., Extended Abstr. 297-299.
- (1980) Ore petrography and mineralogy of the vanadium bearing titaniferous magnetite layer of the Kafferskraal intrusion, Heidelberg District, Transvaal. Trans. Geol. Soc. S. Afr. 83, 221-230.
- Reynolds, R.C. (1967) Estimation of mass absorption coefficients by Compton scattering: Improvements and extensions of the method. Amer. Mineral. 52, 1493-1502.
- Rhodes, R.C. (1975) Bushveld granophyre in the Stavoren tin district, Transvaal. Trans. Geol. Soc. S. Afr. 78, 71-75.
- Rice, A. (1981) Convective fractionation: A mechanism to provide cryptic zoning (macrosegregation), layering, crescumulates, banded tuffs and explosive volcanism in igneous processes. J. Geophys. Res. 86, 405-417.
- Roeder, P.L. & Emslie, R.F. (1970) Olivine-liquid equilibria. Contrib. Mineral. Petrol. 29, 275-289.
- , Campbell, I.H. & Jamieson, H.E. (1979) A re-evaluation of the olivine-spinel geothermometer. Contrib. Mineral. Petrol. 68, 325-334.
- Sampson, E. (1970) Discussion: Stillwater, Montana chromite deposits. Geol. Soc. S. Afr. Spec. Publ. 1, 72-75.
- Sandberg, C.G.S. (1926) On the probable origin of the members of the Bushveld Igneous Complex (Transvaal). Geol. Mag. 63, 210-219.
- Schmidt, E.R. (1952) The structure and composition of the Merensky reef and associated rocks on the Rustenburg Platinum mine. Trans. Geol. Soc. S. Afr. 55, 233-279.
- Schwellnus, J.S.I. (1956) The basal portion of the Bushveld Igneous Complex and the adjoining metamorphosed sediments in the Northeastern Transvaal. Unpub. DSc. thesis. University of Pretoria.
- Shaw, H.R. (1969) Rheology of basalt in the melting range. J. Petrol. 10, 510-535.
- Sharkov, Y.E. (1972) Rhythmic stratification in layered intrusions and its origin. Int. Geol. Rev. 14, 592-598.

- Sharpe, M.R. (1981a) The chronology of magma influxes to the eastern compartment of the Bushveld Complex as exemplified by its marginal border groups. *J. Geol. Soc. Lond.* 138, 307-326.
- (1981b) Noble metals in the marginal rocks of the Bushveld Complex. *Inst. Geol. Res. Bushveld Complex. University of Pretoria. Report 30*. 24pp.
- & Snyman, J.A. (1980) A model for the emplacement of the eastern compartment of the Bushveld Complex. *Tectonophysics* 65, 58-110.
- Sinclair, A.J. (1976) Applications of probability graphs in mineral exploration. *Assn. Expl. Geochem. Spec. Vol. 4*, 95pp.
- Smith, C.S. (1948) Grains, phases and interfaces: an interpretation of microstructure. *Trans. Amer. Inst. Min. Metall. Engrs.* 175, 15-51.
- (1964) Some elementary principles of polycrystalline microstructure. *Metall. Rev.* 9, 1-48.
- South African Committee for Stratigraphy (SACS), (1980) Stratigraphy of South Africa. Part 1. (Comp. L.E. Kent). Lithostratigraphy of the Republic of South Africa, South West Africa/Namibia, and the Republics of Bophuthatswana, Transkei and Venda. *Handbk. Geol. Surv. S. Afr.* 8, 223-241.
- Spry, A. (1969) *Metamorphic Textures*. Pergamon Press. Lond. 350pp.
- Stanton, R.L. (1964) Mineral interfaces in stratiform ores. *Trans. Inst. Min. and Metall.* 74, 45-79.
- (1972) *Ore Petrology*. McGraw-Hill, New York. 713pp.
- & Gorman, H. (1968) A phenomenological study of grain boundary migration in some common sulphides. *Econ. Geol.* 63, 907-923.
- Streckeisen, A.L. (1973) Plutonic rocks: Classification and nomenclature recommended by the IUGS Subcommittee on the systematics of igneous rocks. *Geotimes*, Oct.1973, 26-30.
- Thompson, R.N., Dicken, A.P., Gibson, I.L. & Morrison, M.A. (1982) Elemental fingerprints of isotopic contamination of Hebridean Paleocene mantle derived magmas by Archean sial. *Contrib. Mineral. Petrol.* 79, 159-168.
- Thümmel, F. & Thomma, W. (1967) The sintering process. *Metall. Rev.* 12, 69-108.
- Truter, F.C. (1955) Modern concepts of the Bushveld Igneous Complex. *C.C.T.A. South Reg. Comm. Geol.* 1, 77-92.

- Turner, J.S. (1973) Buoyancy Effects in Fluids. Cambridge University Press. p251-287.
- (1974) Double diffusive phenomena. *Ann. Rev. Fluid Mech.* 6, 37-56.
- (1978) Double diffusive intrusions into a density gradient. *J. Geophys. Res.* 83, 2887-2901.
- & Chen, C.F. (1974) Two dimensional effects in double-diffusive convection. *J. Fluid. Mech.* 63, 577-592.
- & Gustafson, L.B. (1978) The flow of hot active solution from vents in the sea floor - some implications for exhalative sulfide and other ore deposits. *Econ. Geol.* 73, 1082-1100.
- Usselman, T.M. & Hodge, D.S. (1978) Thermal control of low-pressure fractionation processes. *J. Volc. Geotherm. Res.* 4, 265-281.
- Van Biljon, S. (1949) Transformation of the Pretoria Series in the Bushveld Complex. *Trans. Geol. Soc. S. Afr.* 52, 1-172.
- (1955) L'Origine des structures rubanees dans la partie basique du Complex du Bushveld. *Publn. C.N.R.S. Colloque*, 68, 131-150.
- (1963) Structures in the Basic Belt of the Bushveld Complex. *Trans. Geol. Soc. S. Afr.* 66, 11-32.
- (1974) Transformation and deformation of the Pretoria Series in the South-western part of the Bushveld Complex. *Trans. Geol. Soc. S. Afr.* 52, 1-172.
- Van Zyl, J.P. (1960) Die petrologie van die Merenskyrif en geassosieerde gesteentes in 'n aantal boorgat en mynprofiele op Swartklip 988, Rustenburg. Unpub. MSc. thesis. Potchefstroom University for C.H.E.
- (1970) The petrology of the Merensky reef and associated rocks on Swartklip 988, Rustenburg district. *Geol. Soc. S. Afr. Publ.* 1, 80-107.
- Vermaak, C.F. (1976a) The Merensky Reef - thoughts on its environment and genesis. *Econ. Geol.* 71, 1270-1298.
- (1976b) The nickel pipes of Vlakfontein and vicinity, Western Transvaal. *Econ. Geol.* 71, 261-286.
- & Hendricks, L.P. (1976) A review of the mineralogy of the Merensky Reef with special reference to new data on the precious metal mineralogy. *Econ. Geol.* 71, 1244-1269.
- Vernon, R.H. (1970) Comparative grain-boundary studies of some basic and ultrabasic granulites, nodules and cumulates. *Scott. J. Geol.* 6, 337-351.

- Vernon, R.H. (1975) *Metamorphic Processes: Reactions and Microstructure Development*. Halsted Press. New York. 247pp.
- Voll, G. (1960) New work on petrofabrics. *Lpool. Manchr. Geol. J.* 2, 503-567.
- Von Gruenewaldt, G. (1970) On the phase change orthopyroxene-pigeonite and the resulting textures in the Main and Upper Zones of the Bushveld Complex in the Eastern Transvaal. *Geol. Soc. S. Afr. Spec. Publ.* 1, 67-73.
- (1973) The Main and Upper Zones of the Bushveld Complex in the Roossenekal area, Eastern Transvaal. *Trans. Geol. Soc. S. Afr.* 76, 207-227.
- (1979) A review of some recent concepts of the Bushveld Complex, with particular reference to sulfide mineralization. *Canad. Mineral.* 17, 233-256.
- Wager, L.R. (1960) The major element variation of the layered series of the Skaergaard intrusion and a re-estimation of the average composition of the hidden layered series and of the successive residual magmas. *J. Petrol.* 1, 364-398.
- (1963) The mechanism of adcumulus growth in the layered series of the Skaergaard intrusion. *Mineral. Soc. Amer. Spec. Pap.* 1, 1-9.
- (1968) Rhythmic and cryptic layering in mafic and ultramafic plutons. In: *Basalts: The Poldervaart Treatise on Rocks of Basaltic Composition*. H.H. Hess & A. Poldervaart eds. Interscience, New York. Vol. 2, 573-622.
- & Brown, G.M. (1968) *Layered Igneous Rocks*. Oliver & Boyd. Lond. 588pp.
- , ----- & Wadsworth, W.J. (1960) Types of igneous cumulates. *J. Petrol.* 1, 73-85.
- & Deer, W.A. (1939) Geological investigation in East Greenland Part III. The petrology of the Skaergaard intrusion, Kangerdlugssuaq, East Greenland. *Meddelelser om Grønland Bd.* 105. No. 4. 343 pp.
- Wagner, P.A. (1929) *The Platinum Deposits and Mines of South Africa*. Oliver & Boyd. Edinburgh. 326pp.
- Weedon, D.S. (1965) The layered ultrabasic rocks of Sgurr Dubh, Isle of Skye. *Scott. J. Geol.* 1, 41-68.
- Wells, P.R.A. (1977) Pyroxene thermometry in simple and complex systems. *Contrib. Mineral. Petrol.* 62, 129-139.
- Whittaker, E.J.W. & Muntus, R. (1970) Ionic radii for use in geochemistry *Geochim. Cosmochim. Acta* 34, 945-956.

- Willemse, J. (1964) A brief outline of the geology of the Bushveld Igneous Complex. In: The Geology of Some Ore Deposits in Southern Africa. S.H. Haughton ed. Geol. Soc. S. Afr. Vol. 2, 91-128.
- (1969) The geology of the Bushveld Igneous Complex, the largest repository of magmatic ore deposits in the world. Econ. Geol. Mono. 4, 1-22.
- Wilson, A.H. (1982) The geology of the Great 'Dyke', Zimbabwe: The ultramafic rocks. J. Petrol. 23, 240-292.
- Winkler, H.G.F. (1974) Petrogenesis of the Metamorphic Rocks. 3rd ed. Springer-Verlag. New York. 320pp.
- Wood, B.J. & Banno, S. (1973) Garnet-orthopyroxene and orthopyroxene-clinopyroxene relationships in simple and complex systems. Contrib. Mineral. Petrol. 42, 109-124.

APPENDIX ONE: Electron Microprobe Analyses

A Cambridge Instruments Microscan V instrument utilizing wave length dispersive crystal spectrometers was used for all the microprobe analyses. Data collection and reduction was on line using a Bence-Albee reduction routine (Bence & Albee, 1968) on a South-West Technical Products Corp. 6800 micro-processor.

A variety of mineral standards were used for analyses. These were:

<u>Standard</u>	<u>Institution or Individual</u>
St. John's Island Olivine.	Dr. J.V.P. Long, Cambridge.
Kakanui Hornblende	Dr. E. Gasparrini
Orthoclase PSU-Or-1A	Dr. C.O. Ingamells.
Synthetic Spinel	University of Cape Town.
Nickel Magnetite	Dr. L.J. Cabri.
Ilmenite	Dr. C. Frick, Geol. Surv. S. Afr.
Rhodonite	University of Cape Town.
Chromite (53-In-8)	Dr. L.J. Cabri.
Wollastonite	Dr. J.V.P. Long, Cambridge.
Pyroxene (PSU 5-182)	Dr. C.O. Ingamells.
Pyroxene (PSU-Px 1)	Dr. C.O. Ingamells.
Jadeite	Dr. J.V.P. Long, Cambridge.

Counts were collected on peaks and backgrounds using series of up to seven 10 sec counting times. Aberrant counts were rejected before data reduction.

The electron beam spot diameter was between one and three microns, and the specimen current was set at 30nA and the accelerating voltage was set at 20kV.

APPENDIX TWO: Electron Probe Analyses of Minerals

All the data gathered using the electron probe are listed here. The analyses are grouped together under the appropriate mineral names. The first number refers to the sample (e.g. B15, M4 or F27) while the second is a serial number.

In the computer listing 0.00 refers to an element that was not determined.

NUMBER	SiO2	Al2O3	FeO	CaO	Na2O	K2O	TOTAL
RR6 0001	49.78	31.40	0.37	15.12	2.46	0.15	99.28
RR6 0002	49.94	31.32	0.34	15.20	2.68	0.19	99.67
RR6 0003	49.93	31.59	0.37	15.98	2.57	0.14	100.58
RR6 0004	49.53	31.41	0.45	15.88	2.55	0.16	99.98
RR6 0005	49.55	31.83	0.48	16.39	2.40	0.16	100.81
RR6 0006	48.87	31.80	0.42	16.64	2.15	0.11	99.99
RR6 0007	48.83	31.60	0.46	16.61	2.41	0.15	100.06
RR6 0008	49.17	32.05	0.43	16.21	2.69	0.13	100.68
RR6 0009	48.28	32.14	0.42	16.16	2.45	0.14	99.59
RR6 0010	49.69	31.61	0.45	15.73	2.75	0.01	100.22
RR6 0011	47.96	32.09	0.48	16.46	2.40	0.10	99.49
RR6 0012	49.23	32.00	0.43	15.90	2.75	0.14	100.45
RR6 0013	49.82	31.66	0.43	15.79	2.78	0.18	100.66
RR6 0014	48.88	31.23	0.39	15.85	2.87	0.15	99.37
RR6 0015	49.66	31.89	0.45	16.35	2.38	0.13	100.86
RR6 0017	48.99	31.87	0.38	15.50	2.69	0.12	99.55
RR6 0018	48.93	31.64	0.40	15.52	2.77	0.14	99.40
RR6 0019	50.34	31.06	0.32	15.87	2.95	0.09	100.63
RR6 0020	50.14	31.03	0.37	15.75	2.72	0.12	100.13
RR6 0021	49.18	31.49	0.38	16.33	2.44	0.16	99.98
RR6 0022	48.27	31.88	0.41	15.91	2.23	0.13	98.63
RR6 0023	47.72	32.38	0.41	16.31	2.19	0.13	99.14
RR6 0024	47.28	32.29	0.41	16.36	2.20	0.12	98.60
F27 0041	50.58	30.60	0.38	15.96	2.32	0.19	100.03
F27 0042	50.78	30.22	0.41	16.00	2.39	0.17	99.97
F27 0043	50.89	30.66	0.35	15.74	2.39	0.20	100.23
F27 0044	49.42	31.97	0.39	17.54	1.69	0.11	101.12
F27 0045	49.88	31.08	0.26	16.38	1.97	0.16	99.73
F27 0047	49.58	29.78	0.23	15.85	2.16	0.15	97.75
F27 0048	49.73	30.60	0.29	16.10	2.23	0.18	99.13
M4 0065	51.14	30.50	0.24	14.94	2.95	0.22	99.99
M4 0066	50.97	31.06	0.22	15.06	3.13	0.20	100.64
M4 0067	51.37	30.71	0.24	14.75	3.19	0.24	100.50
M4 0068	54.23	28.99	0.38	12.64	4.28	0.37	100.89
M4 0069	50.51	30.55	0.25	15.06	3.15	0.25	99.77
M4 0070	51.48	31.19	0.24	15.37	3.12	0.23	101.63
M4 0071	50.52	30.95	0.25	15.46	3.01	0.21	100.40
M4 0072	51.06	30.78	0.22	14.82	2.99	0.18	100.05

NUMBER	SI02	AL2O3	FE0	CA0	NA2O	K2O	TOTAL
M5 0115	50.36	30.58	0.25	14.73	4.47	0.30	100.69
M5 0116	51.33	30.29	0.29	14.50	4.48	0.31	101.00
M5 0117	50.19	30.32	0.23	14.63	4.36	0.25	99.98
M5 0118	50.51	30.37	0.23	14.43	4.35	0.26	100.15
M5 0119	50.68	30.28	0.25	14.51	4.28	0.28	100.28
M5 0120	50.64	30.37	0.28	14.74	4.29	0.30	100.62
M8 0146	49.05	31.54	0.32	15.97	3.20	0.13	100.21
M8 0147	49.29	31.34	0.42	15.83	2.99	0.34	100.21
M8 0148	48.78	31.76	0.38	16.50	2.98	0.12	100.32
M8 0149	49.49	31.19	0.38	15.53	3.40	0.15	100.14
M8 0150	49.58	31.31	0.40	15.76	3.29	0.17	100.51
M8 0151	48.82	31.23	0.43	15.97	3.09	0.14	99.68
M8 0152	49.82	31.12	0.44	15.35	3.69	0.13	100.55
M8 0153	49.43	31.02	0.63	15.53	3.31	0.34	100.26
M8 0154	49.63	30.52	0.39	14.86	4.02	0.19	99.61
M8 0155	50.79	30.70	0.46	14.87	3.95	0.19	100.96
M8 0156	49.96	31.72	0.43	15.75	3.47	0.15	101.48
M8 0157	50.20	31.75	0.43	16.07	3.22	0.16	101.83
M8 0158	48.41	31.27	0.50	15.64	3.48	0.16	99.48
M8 0159	49.30	30.20	1.17	14.26	3.72	0.19	98.84
M8 0160	50.38	31.06	0.43	15.05	4.05	0.21	101.18
M8 0161	48.73	31.94	0.32	16.79	2.50	0.09	100.37
M9 0162	48.06	31.98	0.00	15.82	2.71	0.00	98.57
M9 0163	48.64	32.04	0.00	16.04	2.53	0.00	99.25
M9 0164	48.76	32.27	0.00	15.98	2.66	0.00	99.67
M9 0165	50.37	31.56	0.00	15.08	3.24	0.00	100.25
M9 0166	48.70	32.30	0.00	15.97	2.68	0.00	99.65
M9 0167	47.20	32.34	0.00	16.16	2.40	0.00	98.10
M9 0168	48.11	31.64	0.00	15.47	2.78	0.00	98.00
M9 0169	48.40	32.00	0.00	15.65	2.70	0.00	98.75
M10 0186	50.17	31.75	0.30	15.40	3.01	0.17	100.80
M10 0187	49.22	32.61	0.29	16.40	2.56	0.17	101.25
M10 0188	49.81	32.02	0.27	15.77	2.70	0.14	100.71
M10 0189	50.00	31.97	0.31	15.64	3.08	0.19	101.19
M10 0190	50.14	32.18	0.24	15.61	2.89	0.14	101.20
M10 0191	48.59	32.60	0.30	16.49	2.58	0.13	100.49
M10 0192	49.66	32.93	0.36	15.94	2.54	0.14	101.57
M10 0203	48.92	32.51	0.38	15.57	2.77	0.12	100.27

NUMBER	SiO2	Al2O3	FeO	CaO	Na2O	K2O	TOTAL
M10 0204	47.89	32.94	0.32	16.28	2.29	0.13	99.85
M10 0205	47.72	32.89	0.33	16.22	2.34	0.14	99.64
M10 0206	48.22	32.62	0.32	15.74	2.59	0.11	99.60
M10 0207	47.75	33.03	0.33	16.22	2.21	0.09	99.63
M10 0208	47.79	32.77	0.31	16.15	2.51	0.11	99.64
M10 0209	48.93	31.88	0.34	15.06	2.94	0.17	99.32
M10 0210	48.18	32.75	0.37	16.37	2.45	0.17	100.29
M10 0211	49.11	32.38	0.35	15.45	2.74	0.18	100.21
M10 0212	48.12	32.17	0.37	15.50	2.44	0.16	98.76
M10 0213	50.17	31.75	0.30	15.40	3.01	0.17	100.80
M10 0214	49.05	33.74	0.36	16.33	2.49	0.15	102.12
M10 0215	49.16	33.02	0.35	16.43	2.57	0.14	101.67
M10 0216	48.24	31.68	0.36	15.81	2.72	0.12	98.93
M10 0217	48.24	32.71	0.40	16.40	2.43	0.12	100.30
M10 0218	48.72	33.02	0.37	16.28	2.50	0.17	101.06
M10 0219	48.45	32.17	0.34	16.03	2.66	0.15	99.80
M10 0220	49.55	32.69	0.34	16.10	2.77	0.00	101.45
M10 0221	49.37	32.49	0.36	16.05	2.97	0.11	101.35
M10 0222	48.47	32.73	0.35	16.30	2.45	0.12	100.42
M10 0223	48.96	33.36	0.34	16.38	2.56	0.15	101.75
M10 0224	48.37	32.76	0.33	16.46	2.47	0.11	100.50
M10 0225	48.38	32.58	0.34	15.88	2.60	0.16	99.94
M11 0226	50.85	32.78	0.00	15.71	2.72	0.00	102.06
M11 0227	50.63	32.61	0.00	15.59	2.65	0.00	101.48
M11 0228	50.35	32.40	0.00	15.65	2.58	0.00	100.98
M11 0229	50.78	32.37	0.00	15.43	2.69	0.00	101.27
M11 0230	50.21	32.17	0.00	15.47	2.67	0.00	100.52
M11 0231	49.37	32.20	0.00	15.84	2.36	0.00	99.77
M11 0232	49.36	32.45	0.00	15.91	2.54	0.00	100.26
M11 0233	50.17	31.96	0.00	15.40	2.69	0.00	100.22
R1 0234	50.11	30.06	0.21	14.70	3.23	0.20	98.51
R1 0235	50.95	30.88	0.21	14.75	3.40	0.13	100.32
R1 0236	51.36	30.61	0.23	14.59	3.32	0.24	100.35
R1 0237	51.01	31.03	0.23	15.01	3.10	0.18	100.61
R1 0238	50.80	30.42	0.22	14.54	3.36	0.20	99.54
R1 0239	48.54	31.92	0.21	16.25	2.50	0.12	99.54
R1 0240	49.42	31.81	0.24	16.10	2.45	0.10	100.12
R1 0241	50.80	30.00	0.31	14.33	3.24	0.16	98.84

NUMBER	SiO2	Al2O3	FeO	CaO	Na2O	K2O	TOTAL
R2 0242	50.39	31.12	0.19	15.13	3.04	0.15	100.02
R2 0243	50.46	31.44	0.19	15.67	2.94	0.15	100.85
R2 0244	50.60	30.77	0.16	14.81	3.28	0.20	99.82
R2 0245	50.85	31.00	0.18	14.52	3.46	0.20	100.21
R2 0246	51.18	30.50	0.23	14.22	3.52	0.20	99.85
R2 0247	51.34	30.37	0.23	14.45	3.51	0.24	100.14
R2 0248	51.73	30.36	0.23	14.66	3.49	0.21	100.68
R2 0249	51.05	30.43	0.22	14.53	3.79	0.20	100.22
R3 0250	50.87	30.54	0.27	14.65	3.05	0.22	99.60
R3 0251	51.35	30.16	0.19	13.96	3.34	0.23	99.23
R3 0252	52.24	29.68	0.25	13.43	3.62	0.26	99.48
R3 0253	51.95	29.73	0.24	13.57	3.67	0.27	99.43
R3 0254	52.24	29.64	0.28	13.03	3.43	0.29	98.91
R3 0255	51.35	30.29	0.24	13.54	3.38	0.26	99.06
R3 0256	51.00	30.41	0.16	14.21	3.00	0.20	98.98
R3 0257	50.91	30.37	0.27	14.30	3.07	0.22	99.14
M14 0258	48.56	31.81	0.00	16.05	2.17	0.00	98.59
M14 0259	48.65	31.44	0.00	15.91	2.33	0.00	98.33
M14 0260	49.16	31.32	0.00	15.54	2.54	0.00	98.56
M14 0261	48.70	31.61	0.00	15.82	2.40	0.00	98.53
M14 0262	48.44	31.54	0.00	15.87	2.38	0.00	98.23
M14 0263	48.29	31.94	0.00	16.25	2.23	0.00	98.71
M14 0264	48.95	31.12	0.00	15.56	2.59	0.00	98.22
M14 0265	48.48	31.36	0.00	15.94	2.41	0.00	98.19
P9B 0266	50.79	31.03	0.22	14.86	2.95	0.26	100.11
P9B 0267	50.87	30.13	0.21	14.17	3.32	0.24	98.94
P9B 0268	50.09	31.36	0.22	15.31	2.68	0.16	100.02
P9B 0269	50.68	30.88	0.22	14.56	3.03	0.11	99.48
P9B 0270	49.78	30.88	0.19	15.29	3.00	0.13	99.27
P9B 0271	49.56	30.75	0.19	15.26	2.68	0.09	98.73
P9B 0272	47.68	32.28	0.15	16.70	2.11	0.05	98.97
P9B 0273	47.94	32.09	0.12	16.47	2.16	0.04	98.82
P9B 0314	49.84	31.54	0.21	15.48	2.77	0.13	99.97
P9B 0315	49.78	32.26	0.22	15.67	2.64	0.07	100.64
P9B 0316	50.72	31.64	0.17	15.16	3.02	0.14	100.85
P9B 0317	50.27	32.17	0.18	15.39	2.71	0.10	100.82
P9B 0318	51.12	31.64	0.14	14.51	3.12	0.12	100.65
P9B 0319	51.66	30.93	0.18	14.56	3.41	0.13	100.67

APPENDIX TWO *** A *** ALL PLAGIOCLASE ANALYSES. PAGE: 5

NUMBER	SI02	AL2O3	FFO	CAO	NA2O	K2O	TOTAL
P9B 0320	50.47	31.83	0.15	15.34	2.68	0.11	100.58
P9B 0321	51.28	31.37	0.16	14.22	3.41	0.17	100.61
M12 0330	50.36	31.53	0.38	15.30	2.97	0.21	100.75
M12 0331	50.09	31.71	0.41	15.38	2.88	0.22	100.69
M12 0332	49.63	32.03	0.39	15.86	2.65	0.16	100.72
M12 0333	49.01	32.03	0.34	16.06	2.53	0.16	100.13
M12 0334	48.47	32.38	0.46	15.85	2.44	0.14	99.74
M12 0335	48.34	31.73	0.46	15.96	2.74	0.17	99.40
M12 0336	48.24	32.10	0.46	16.29	2.37	0.15	99.61
M12 0337	48.21	32.29	0.43	16.10	3.09	0.13	100.25
B10 0346	48.60	31.84	0.37	17.06	2.23	0.14	100.24
B10 0347	48.81	32.28	0.31	16.75	2.30	0.13	100.58
B10 0348	49.36	32.06	0.33	16.39	2.51	0.16	100.81
B10 0349	48.61	31.53	0.33	16.52	2.29	0.12	99.40
B10 0350	49.32	31.95	0.34	16.36	2.58	0.11	100.66
B10 0351	49.45	31.84	0.33	16.31	2.46	0.17	100.56
B10 0352	48.84	32.13	0.34	16.42	2.31	0.11	100.15
B10 0353	49.51	32.10	0.34	15.96	2.67	0.08	100.66
M14 0354	48.49	32.32	0.61	16.50	2.43	0.15	100.50
M14 0355	49.05	31.72	0.61	15.61	2.93	0.18	100.10
M14 0356	49.50	31.34	0.49	15.65	2.29	0.18	99.45
M14 0357	48.70	31.89	0.56	15.88	2.58	0.14	99.75
M14 0358	48.48	32.08	0.56	16.21	2.36	0.16	99.85
M14 0359	48.53	31.55	0.57	16.21	2.47	0.16	99.49
M14 0360	49.14	32.20	0.49	15.77	2.24	0.19	100.03
M14 0361	49.17	32.35	0.56	16.03	2.47	0.16	100.74
M14 0362	49.44	31.65	0.56	15.50	2.68	0.21	100.04
M14 0363	49.44	32.19	0.52	15.62	2.62	0.14	100.53
B3 0372	55.18	28.19	0.19	11.44	5.01	0.33	100.34
B3 0373	55.02	28.74	0.16	11.53	5.01	0.28	100.74
B3 0374	52.44	29.91	0.21	13.62	3.84	0.35	100.37
B3 0375	52.72	29.95	0.22	13.13	3.92	0.30	100.24
B3 0376	54.10	28.19	0.16	11.81	4.95	0.29	99.50
B3 0377	65.90	18.05	0.15	0.04	1.17	15.36	100.67
B3 0378	52.22	30.52	0.24	13.48	3.79	0.29	100.54
B3 0379	52.26	29.78	0.22	13.23	3.73	0.24	99.46
P11 0402	50.15	31.47	0.36	16.04	2.61	0.21	100.84
P11 0403	50.09	30.79	0.41	15.38	2.90	0.27	99.84

NUMBER	S102	AL203	FE0	CA0	NA2O	K2O	TOTAL
P11 0404	50.54	30.71	0.46	15.60	2.91	0.28	100.50
P11 0405	49.68	31.57	0.48	15.92	2.62	0.22	100.29
P11 0406	49.04	32.23	0.46	17.08	2.08	0.12	101.01
P11 0407	49.87	30.57	0.46	15.02	2.97	0.29	98.98
P11 0408	48.42	31.30	1.18	15.73	2.47	0.11	99.21
P11 0409	46.42	32.43	0.78	17.94	1.55	0.09	99.21
P11 0410	48.67	31.70	0.28	16.03	2.54	0.19	99.41
P11 0411	49.29	31.84	0.36	16.08	2.65	0.19	100.41
P11 0412	49.64	30.96	0.37	15.53	2.64	0.20	99.54
P11 0413	48.67	31.69	0.34	16.08	2.44	0.20	99.42
P11 0414	49.73	31.13	0.24	15.51	2.65	0.20	99.46
P11 0415	48.43	31.96	0.35	16.53	2.33	0.17	99.75
P11 0416	49.00	31.76	0.28	16.28	2.54	0.17	100.03
P11 0417	48.82	31.46	0.31	15.95	2.53	0.18	99.25
B5A 0418	49.19	32.09	0.29	16.00	2.59	0.19	100.35
B5A 0419	48.95	32.10	0.29	15.99	2.67	0.15	100.15
B5A 0420	49.29	31.83	0.26	15.50	3.03	0.20	100.11
B5A 0421	49.20	32.23	0.30	15.77	2.64	0.17	100.51
B5A 0422	48.34	32.27	0.28	16.22	2.49	0.17	99.77
B5A 0423	50.15	31.47	0.32	15.55	3.01	0.22	100.52
B5A 0424	49.63	32.15	0.31	15.89	2.80	0.16	100.94
B5A 0425	48.34	32.34	0.35	16.13	2.55	0.15	99.82
F24 0434	48.83	31.92	0.29	15.50	2.93	0.25	99.72
F24 0435	48.29	32.75	0.34	16.20	2.55	0.17	100.31
F24 0436	48.72	32.28	0.31	15.85	2.64	0.21	100.01
F24 0437	48.13	32.56	0.32	16.15	2.42	0.13	99.69
F24 0438	49.22	32.41	0.25	15.74	2.86	0.16	100.66
F24 0439	48.19	32.58	0.30	15.96	2.75	0.18	99.96
F24 0440	48.14	32.58	0.33	16.03	2.59	0.17	99.84
F24 0441	48.90	32.30	0.29	15.45	3.12	0.18	100.24
F1 0468	49.34	31.36	0.29	15.95	2.32	0.14	99.40
F1 0469	48.97	32.00	0.32	15.92	2.38	0.11	99.70
F1 0470	49.28	31.60	0.30	15.60	2.46	0.18	99.42
F1 0471	49.11	32.09	0.36	15.81	2.23	0.14	99.65
F1 0472	49.86	31.19	0.37	15.09	2.67	0.21	99.59
F1 0473	49.29	31.70	0.38	15.75	2.55	0.16	99.81
F1 0474	49.29	31.39	0.39	15.56	2.41	0.19	99.03
F1 0475	49.26	31.57	0.36	15.46	2.41	0.17	99.25

NUMBER	SI02	AL2O3	FeO	CaO	Na2O	K2O	TOTAL
F13 0489	49.47	31.21	0.28	15.52	2.83	0.16	99.47
F13 0490	49.39	31.52	0.38	15.99	2.48	0.17	99.93
F13 0491	49.45	31.58	0.34	15.68	2.75	0.16	99.96
F13 0492	49.85	31.27	0.35	15.41	2.93	0.21	100.02
F13 0493	48.78	31.71	0.38	15.65	2.57	0.19	99.28
F13 0494	50.11	31.13	0.33	14.97	3.29	0.13	99.96
F13 0495	49.34	31.23	0.34	15.20	2.97	0.16	99.24
F13 0496	49.25	31.41	0.38	15.64	2.78	0.20	99.66
F13 0497	49.25	31.49	0.37	15.57	2.85	0.14	99.47
M7 0530	50.05	32.09	0.32	15.71	2.57	0.22	100.96
M7 0531	50.18	31.70	0.32	15.48	2.85	0.19	100.72
M7 0532	50.35	31.39	0.29	15.78	2.42	0.09	100.32
M7 0533	51.25	30.55	0.38	15.18	2.70	0.20	100.26
M7 0534	49.97	31.12	0.34	14.91	3.03	0.25	99.62
M7 0535	49.55	31.62	0.37	16.02	2.71	0.17	100.44
M7 0536	49.54	31.57	0.35	16.43	2.42	0.19	100.50
M7 0537	49.82	30.66	0.35	15.67	2.60	0.23	99.33
M6 0546	49.09	32.52	0.29	15.71	2.49	0.11	100.21
M6 0547	50.24	31.49	0.27	15.36	2.98	0.24	100.53
M6 0548	50.83	31.09	0.31	14.77	3.34	0.21	100.55
M6 0549	48.60	31.96	0.33	16.16	2.74	0.19	99.98
M6 0550	48.82	32.35	0.33	16.62	2.57	0.18	100.87
M6 0551	50.10	31.84	0.32	15.58	2.80	0.23	100.87
M6 0552	48.73	32.63	0.30	16.44	2.39	0.16	100.65
M6 0553	49.89	31.64	0.28	14.75	3.00	0.23	99.79
B23 0563	48.99	32.07	0.32	15.56	2.61	0.15	99.70
B23 0564	49.81	31.65	0.30	14.77	2.91	0.21	99.65
B23 0565	49.92	31.80	0.28	14.99	2.76	0.16	99.91
B23 0566	49.96	32.09	0.33	15.27	2.77	0.16	100.58
B23 0567	49.29	32.51	0.29	15.51	2.66	0.13	100.39
B23 0568	50.18	31.63	0.32	14.64	2.94	0.21	99.92
B23 0569	49.53	32.36	0.33	15.55	2.57	0.16	100.52
B23 0570	50.32	31.74	0.31	14.66	2.93	0.16	100.14
B13 0579	48.76	32.17	0.33	15.54	2.46	0.13	99.39
B13 0580	48.74	32.43	0.23	15.92	2.32	0.11	99.75
B13 0581	49.52	31.69	0.41	14.99	2.81	0.19	99.61
B13 0582	49.32	32.20	0.31	15.56	2.55	0.16	100.10
B13 0583	48.92	32.15	0.37	15.52	2.46	0.14	99.56

NUMBER	SI02	AL203	FE0	CA0	NA20	K20	TOTAL
B13 0584	48.32	32.41	0.30	15.99	2.22	0.14	99.38
B13 0585	48.74	32.56	0.31	15.79	2.52	0.15	100.07
B13 0586	48.99	32.01	0.31	15.71	2.46	0.17	99.65
B28 0587	49.93	31.46	0.39	14.92	2.88	0.22	99.80
B28 0588	51.44	30.65	0.38	13.89	3.55	0.25	100.16
B28 0589	50.44	31.35	0.36	14.61	3.10	0.23	100.10
B28 0590	51.63	30.26	0.37	13.36	3.70	0.26	99.58
B28 0591	51.31	30.96	0.30	13.93	3.44	0.20	100.14
B28 0592	50.32	31.55	0.34	14.66	3.16	0.15	100.18
B28 0593	51.50	30.48	0.37	13.60	3.59	0.32	99.86
B28 0594	50.97	30.93	0.35	14.06	3.34	0.29	99.94
B28 0595	51.45	30.76	0.35	13.86	3.43	0.18	100.03
B28 0596	50.76	31.07	0.38	14.33	3.17	0.21	99.92
B28 0597	51.68	30.54	0.33	13.50	3.76	0.24	100.05
B30 0605	49.48	31.85	0.38	14.93	2.69	0.17	99.50
B30 0606	51.02	30.97	0.35	14.14	3.18	0.27	99.93
B30 0607	50.01	31.47	0.37	14.44	3.05	0.21	99.55
B30 0608	51.42	30.37	0.39	13.38	3.74	0.27	99.57
B30 0609	50.84	31.12	0.32	13.95	3.27	0.25	99.75
B30 0610	52.19	30.25	0.35	13.16	3.86	0.24	100.05
B30 0611	51.63	30.61	0.33	13.24	3.61	0.30	99.72
B30 0612	49.84	31.75	0.34	14.46	2.90	0.21	99.50
B30 0613	49.90	31.66	0.35	14.42	2.86	0.19	99.38
B30 0614	51.32	30.59	0.32	13.62	3.39	0.25	99.49
B30 0615	51.40	30.99	0.26	13.69	3.44	0.20	99.98
B3 634	51.77	30.50	0.18	12.96	3.72	0.23	99.36
B3 635	52.12	30.69	0.19	13.05	3.50	0.26	99.81
B3 636	51.34	30.49	0.24	13.60	3.21	0.24	99.12
B3 637	49.77	31.75	0.23	14.06	2.92	0.23	98.96
B3 638	50.14	31.27	0.21	13.98	3.13	0.19	98.92
B3 639	54.05	29.39	0.19	11.19	4.39	0.23	99.44
B3 640	49.87	32.15	0.24	15.30	2.64	0.13	100.33
B3 641	51.18	31.26	0.20	14.22	3.27	0.22	100.35
B20 650	56.56	31.96	0.39	14.96	2.71	0.18	106.76
B20 651	49.97	32.03	0.39	15.04	2.55	0.20	100.18
B20 652	50.97	31.03	0.53	14.36	2.88	0.50	100.27
B20 653	51.12	31.90	0.35	14.91	2.72	0.19	101.19
B20 654	51.15	30.27	0.30	14.66	2.98	0.17	99.53

NUMBER	SI02	AL2O3	FeO	CAO	NA2O	K2O	TOTAL
B20 655	51.31	31.44	0.35	14.59	2.91	0.20	100.80
B20 656	52.32	31.03	0.48	14.21	2.71	0.20	100.95
B20 657	49.28	31.15	0.39	16.08	2.71	0.24	99.85
B25 667	49.10	32.15	0.27	15.04	2.71	0.18	99.45
B25 668	48.48	31.88	0.24	15.21	2.50	0.13	98.44
B25 669	50.47	31.24	0.27	14.37	3.09	0.24	99.70
B25 670	49.31	31.94	0.28	15.04	2.60	0.17	99.34
B25 671	50.18	31.30	0.25	14.22	3.22	0.24	99.41
B25 672	49.85	31.11	0.28	14.12	3.22	0.19	98.77
B25 673	49.06	32.25	0.31	15.41	2.50	0.16	99.69
B25 674	50.04	31.37	0.28	14.43	3.07	0.20	99.39
B9 687	47.66	33.00	0.30	16.25	2.17	0.11	99.49
B9 688	48.24	32.59	0.30	15.83	2.30	0.14	99.40
B9 689	47.97	33.00	0.38	15.88	2.22	0.11	99.56
B9 690	47.92	32.88	0.38	16.11	2.33	0.13	99.75
B9 691	48.45	32.88	0.35	16.21	2.22	0.20	100.31
B9 692	48.74	32.57	0.32	15.70	2.39	0.14	99.86
B9 693	47.39	33.17	0.41	16.47	1.98	0.16	99.58
B9 694	47.68	32.99	0.40	16.57	1.93	0.10	99.67
B15 707	49.51	31.72	0.37	15.09	2.59	0.13	99.41
B15 708	48.94	32.05	0.38	15.71	2.69	0.13	99.90
B15 709	48.93	31.84	0.35	15.50	2.71	0.13	99.46
B15 710	48.46	31.85	0.40	15.87	2.44	0.14	99.16
B15 711	48.29	32.36	0.39	16.00	2.31	0.12	99.47
B15 712	48.42	31.95	0.37	15.59	2.62	0.14	99.09
B15 713	48.08	32.37	0.38	16.18	2.19	0.11	99.31
B15 714	48.54	32.50	0.33	16.16	2.40	0.10	100.05
RR1 723	50.08	31.51	0.34	15.17	3.00	0.19	100.29
RR1 724	49.99	31.39	0.34	14.93	2.90	0.23	99.78
RR1 725	50.09	31.50	0.35	14.94	3.01	0.18	100.07
RR1 726	49.33	31.63	0.34	15.21	2.71	0.14	99.36
RR1 727	49.68	31.80	0.32	15.17	2.72	0.18	99.87
RR1 728	50.67	31.12	0.40	14.33	3.27	0.17	99.96
RR1 729	50.19	31.23	0.40	14.81	3.00	0.21	99.84
RR1 730	48.76	32.20	0.39	15.91	2.53	0.18	99.97
RR1 731	50.69	30.71	0.35	14.48	3.24	0.19	99.66
RR1 732	49.39	32.15	0.39	15.71	2.59	0.13	100.36
RR1 733	49.93	31.64	0.38	14.99	2.92	0.20	100.06

NUMBRER	SI02	AL2O3	FFO	CAO	NA2O	K2O	TOTAL
F7 742	50.21	31.86	0.34	14.82	2.90	0.13	100.26
F7 743	49.19	32.30	0.39	15.50	2.62	0.17	100.26
F7 744	50.38	31.57	0.34	14.76	3.30	0.14	100.49
F7 745	49.70	31.76	0.36	15.15	2.84	0.15	99.96
F7 746	49.62	32.11	0.45	15.19	2.77	0.14	100.28
F7 747	50.08	31.74	0.33	14.90	2.71	0.21	99.99
F7 748	49.69	32.32	0.36	15.37	2.82	0.15	100.71
F7 749	49.65	31.57	0.33	15.15	2.93	0.12	99.75
F15 760	49.54	31.58	0.31	15.36	2.66	0.22	99.67
F15 761	49.28	31.91	0.31	15.34	2.72	0.21	99.77
F15 762	50.14	31.26	0.33	14.60	2.95	0.32	99.60
F15 763	49.29	31.97	0.32	15.41	2.60	0.21	99.80
F15 764	50.34	31.21	0.31	14.71	3.07	0.24	99.88
F15 765	50.03	31.41	0.25	14.64	3.06	0.21	99.60
F15 766	49.35	31.63	0.29	15.09	2.68	0.18	99.22
F15 767	49.32	31.32	0.31	15.06	2.86	0.19	99.06
F15 768	48.76	31.16	0.28	14.86	2.93	0.24	98.23
F15 769	50.21	31.25	0.37	14.55	3.16	0.16	99.70
F8 779	49.71	31.91	0.36	14.96	2.90	0.16	100.00
F8 780	49.68	32.06	0.37	15.15	2.91	0.16	100.35
F8 781	49.65	31.87	0.40	14.81	3.03	0.16	100.12
F8 782	50.18	31.61	0.33	14.61	3.18	0.21	100.12
F8 783	49.01	32.38	0.31	15.37	2.67	0.12	99.86
F8 784	49.33	32.23	0.35	15.29	2.74	0.14	100.08
F8 785	49.71	31.81	0.34	14.64	2.95	0.18	99.63
F8 786	49.58	32.09	0.37	15.07	2.91	0.13	100.15
B4 787	53.05	30.13	0.17	12.47	4.54	0.24	100.60
B4 788	50.18	32.25	0.19	14.90	3.07	0.19	100.78
B4 789	52.61	30.33	0.25	12.62	4.28	0.35	100.44
B4 790	53.24	29.91	0.23	12.05	4.74	0.22	100.39
B4 791	50.12	31.75	0.25	14.60	3.21	0.23	100.16
B4 792	48.89	32.37	0.33	15.26	2.62	0.15	99.82
B4 793	49.83	31.65	0.32	14.33	3.13	0.21	99.47
B4 794	52.20	30.33	0.25	12.67	4.00	0.32	99.77
B7 815	48.87	32.53	0.26	15.24	2.36	0.07	99.33
B7 816	49.04	31.76	0.31	15.12	2.47	0.14	98.84
B7 817	48.40	31.83	0.32	15.33	2.48	0.16	98.52
B7 818	47.63	32.41	0.29	15.88	2.17	0.13	98.51

NUMBER	SI02	AL2O3	FFO	CAO	NA2O	K2O	TOTAL
B7 819	48.99	31.85	0.29	15.05	2.37	0.11	98.66
B7 820	49.17	31.90	0.32	15.05	2.38	0.15	98.97
B7 821	48.68	32.26	0.30	15.46	2.23	0.14	99.07
B7 822	49.26	32.04	0.29	14.92	2.47	0.13	99.11
B7 823	48.81	32.03	0.22	15.20	2.52	0.14	98.92
B26 832	49.69	31.59	0.26	14.75	2.82	0.12	99.23
B26 833	49.60	31.61	0.36	15.00	2.85	0.14	99.56
B26 834	50.25	31.04	0.34	14.48	3.11	0.19	99.41
B26 835	49.47	31.62	0.31	15.05	2.75	0.14	99.34
B26 836	50.97	30.57	0.36	13.87	3.40	0.21	99.38
B26 837	48.54	32.32	0.33	15.31	2.77	0.09	99.36
B26 838	49.07	31.68	0.33	15.29	2.60	0.19	99.16
B26 839	51.03	30.54	0.31	13.67	3.55	0.20	99.30
B21 853	49.12	31.43	0.34	14.69	2.87	0.18	98.63
B21 854	48.31	31.81	0.36	14.96	2.58	0.15	98.17
B21 855	49.82	31.17	0.35	14.15	3.16	0.21	98.86
B21 856	48.77	31.50	0.31	15.16	2.64	0.22	98.60
B21 857	49.26	31.26	0.37	14.79	2.77	0.24	98.69
B21 858	47.95	32.42	0.31	16.00	2.24	0.13	99.05
B21 859	48.10	32.28	0.26	15.84	2.36	0.12	98.96
B21 860	49.31	31.45	0.31	14.65	2.89	0.17	98.78
B21 861	48.32	31.97	0.30	15.64	2.46	0.14	98.83
B22 871	48.71	32.10	0.28	15.50	2.48	0.14	99.21
B22 872	49.06	31.76	0.28	15.00	2.81	0.15	99.06
B22 873	48.39	32.07	0.30	15.50	2.45	0.15	98.86
B22 874	49.71	31.42	0.35	14.56	2.97	0.18	99.19
B22 875	49.28	31.55	0.38	14.92	2.94	0.11	99.18
B22 876	49.41	31.21	0.34	14.79	2.87	0.21	98.83
B22 877	49.59	31.35	0.27	14.42	2.82	0.17	98.62
B22 878	49.12	32.00	0.28	15.35	2.56	0.15	99.46
B19 887	50.91	30.59	0.34	13.63	3.57	0.16	99.20
B19 888	49.59	31.73	0.37	14.43	2.93	0.12	99.17
B19 889	48.82	32.30	0.39	15.54	2.69	0.08	99.82
B19 890	50.12	31.33	0.32	13.93	3.16	0.20	99.06
B19 891	49.08	32.04	0.32	15.70	2.70	0.20	100.04
B19 892	47.47	32.95	0.36	16.26	2.03	0.10	99.17
B19 893	49.85	31.36	0.29	14.72	3.14	0.19	99.55
B19 894	50.09	31.42	0.34	14.07	3.17	0.17	99.26

NUMBER	SI02	AL2O3	FE0	CA0	NA2O	K2O	TOTAL
F4 904	48.68	31.75	0.34	16.81	2.85	0.14	100.57
F4 905	48.73	31.93	0.38	15.24	2.55	0.16	98.99
F4 906	49.18	31.48	0.34	16.53	2.94	0.12	100.39
F4 907	49.08	31.78	0.29	15.29	2.74	0.13	99.31
F4 908	47.61	31.93	0.35	16.05	2.73	0.09	98.76
F4 909	49.61	31.94	0.37	15.02	2.65	0.15	99.74
F4 910	49.84	31.71	0.34	14.52	2.67	0.14	99.02
F4 911	49.26	31.94	0.32	15.16	2.74	0.11	99.53
F4 912	50.08	31.61	0.40	14.26	2.75	0.14	99.24
F4 913	48.67	31.91	0.30	15.05	2.77	0.11	98.81
P9C 938	49.51	31.50	0.19	14.95	2.98	0.11	99.24
P9C 939	48.69	32.54	0.22	15.44	2.53	0.09	99.51
P9C 940	49.89	31.61	0.19	14.40	3.00	0.15	99.24
P9C 941	49.52	31.20	0.30	14.82	2.84	0.14	98.82
P9C 942	49.95	31.50	0.15	14.59	3.11	0.15	99.45
P9C 943	50.83	30.52	0.23	13.52	3.43	0.21	98.74
P9C 944	50.44	30.83	0.20	13.60	3.24	0.20	98.51
P9C 945	50.73	30.30	0.18	13.51	3.51	0.25	98.48

APPENDIX TWO *** R *** ALL ORTHOPYROXENE ANALYSES. ----- PAGE: 13

NUMBER		SI02	TI02	AL2O3	FE0	MNO	RGO	CAO	NA2O	CR2O3	NI0	TOTAL
F27	35	54.99	0.33	1.54	12.89	0.25	28.97	0.81	0.00	0.19	0.11	100.08
F27	36	54.53	0.27	1.70	13.04	0.22	29.88	0.73	0.00	0.23	0.13	100.73
M4	81	54.30	0.21	0.97	13.74	0.26	27.27	1.98	0.00	0.39	0.00	99.12
M4	82	55.35	0.13	0.47	14.28	0.30	27.79	0.75	0.00	0.18	0.00	99.25
M4	83	54.84	0.05	1.13	12.97	0.27	26.82	2.34	0.00	0.51	0.00	98.93
M4	84	55.43	0.07	1.15	13.84	0.27	27.65	1.01	0.00	0.50	0.00	99.92
M4	85	54.78	0.13	1.10	13.74	0.29	28.05	1.18	0.00	0.47	0.00	99.74
M4	86	54.73	0.17	1.08	13.58	0.25	28.17	0.96	0.00	0.45	0.00	99.39
M4	87	55.23	0.29	0.89	13.76	0.35	27.93	1.01	0.00	0.43	0.00	99.87
M4	88	55.26	0.16	1.06	13.18	0.26	27.77	1.81	0.00	0.44	0.00	99.94
M5	97	55.39	0.13	1.58	13.15	0.26	28.01	0.95	0.00	0.00	0.00	99.47
M5	98	55.25	0.09	1.51	13.42	0.26	28.00	0.83	0.00	0.00	0.00	99.36
M5	99	55.08	0.14	1.56	12.50	0.25	26.77	2.71	0.00	0.00	0.00	99.01
M5	100	55.28	0.13	1.58	13.20	0.28	27.95	2.25	0.00	0.42	0.00	101.09
M5	101	54.80	0.17	1.42	14.15	0.27	28.32	0.90	0.00	0.40	0.00	100.43
M5	102	55.38	0.12	1.48	12.90	0.22	28.14	2.21	0.00	0.44	0.00	100.89
M5	104	54.82	0.13	1.61	14.17	0.25	28.39	1.57	0.00	0.43	0.00	101.37
M5	105	55.19	0.17	1.18	13.44	0.26	28.64	2.25	0.00	0.42	0.00	101.55
M5	106	54.80	0.29	1.16	14.19	0.25	29.62	1.05	0.00	0.28	0.00	101.62
M5	107	54.91	0.16	1.47	13.01	0.24	27.11	2.82	0.17	0.44	0.00	100.33
M5	108	55.01	0.17	1.34	13.66	0.25	29.44	0.90	0.00	0.45	0.00	101.22
M5	111	55.11	0.13	1.58	12.58	0.22	27.67	1.54	0.00	0.52	0.00	99.35
M5	112	54.90	0.12	1.95	13.87	0.24	28.99	2.35	0.03	0.42	0.00	102.87
M5	121	55.74	0.25	1.40	12.84	0.28	28.09	0.76	0.00	0.39	0.00	99.75

APPENDIX TWO *** B *** ALL ORTHOPYROXENE ANALYSES. PAGE: 14

NUMBER	SI02	TIO2	AL2O3	FE0	MNO	MGO	CAO	NA2O	CR2O3	NIO	TOTAL
M5 122	56.00	0.24	1.26	12.78	0.27	28.37	1.06	0.00	0.43	0.00	100.41
M5 123	55.14	0.19	1.49	12.71	0.25	28.18	1.49	0.00	0.50	0.00	99.93
M5 124	54.67	0.22	1.57	11.94	0.26	27.34	3.40	0.00	0.55	0.00	99.95
M5 125	54.93	0.13	1.49	12.95	0.30	28.32	0.84	0.00	0.46	0.00	99.42
M5 126	54.94	0.15	1.81	11.64	0.20	26.41	3.83	0.00	0.52	0.00	99.50
M5 127	54.82	0.13	1.68	13.00	0.33	28.37	1.19	0.00	0.49	0.00	100.01
M5 128	55.07	0.13	1.69	12.41	0.29	27.78	1.81	0.00	0.49	0.00	99.67
M8 130	54.66	0.12	1.63	15.55	0.33	25.20	3.06	0.00	0.56	0.00	100.91
M8 131	54.64	0.14	1.52	16.36	0.31	25.49	1.94	0.00	0.49	0.00	100.89
M8 132	55.35	0.23	1.04	16.84	0.37	25.82	1.47	0.00	0.31	0.00	101.43
M8 133	55.64	0.30	0.96	16.89	0.36	25.50	1.03	0.00	0.26	0.00	100.94
M8 134	55.34	0.32	0.93	17.52	0.34	25.60	1.17	0.00	0.22	0.00	101.24
M8 135	55.34	0.21	1.23	17.12	0.35	25.96	1.04	0.00	0.44	0.00	101.69
M8 136	55.63	0.29	0.89	17.23	0.32	26.00	1.18	0.00	0.24	0.00	101.78
M8 137	55.81	0.30	0.95	17.16	0.35	25.75	0.95	0.00	0.25	0.00	101.52
M8 138	54.41	0.15	1.45	17.59	0.35	26.27	0.87	0.00	0.47	0.00	101.34
M8 139	54.22	0.11	1.68	16.43	0.30	25.50	2.49	0.00	0.57	0.00	101.30
M8 140	54.32	0.11	1.73	17.57	0.31	26.10	0.93	0.00	0.55	0.00	101.42
M8 141	54.37	0.24	1.30	17.29	0.32	25.47	1.84	0.00	0.42	0.00	101.25
M8 142	54.61	0.25	0.90	17.32	0.32	25.90	1.14	0.00	0.28	0.00	100.72
M8 143	54.77	0.39	0.82	17.84	0.36	25.97	0.86	0.00	0.22	0.00	101.23
M8 144	54.75	0.29	0.91	17.85	0.35	25.89	1.01	0.00	0.21	0.00	101.26
M8 145	54.24	0.29	0.92	17.80	0.30	25.64	1.26	0.00	0.24	0.00	100.69
M9 170	53.41	0.17	1.55	16.68	0.34	26.01	1.29	0.01	0.32	0.03	99.81

APPENDIX TWO *** B *** ALL ORTHOPYROXENE ANALYSES. PAGE: 15

NUMBER	SI02	TI02	AL203	FE0	MNO	MGO	CA0	NA2O	CR2O3	NI0	TOTAL
M9 174	52.57	0.14	1.62	16.85	0.34	25.84	0.91	0.03	0.40	0.06	98.76
M9 175	52.39	0.18	1.41	16.45	0.38	25.49	1.73	0.02	0.35	0.03	98.43
R3 178	55.91	0.20	1.16	10.82	0.25	30.65	1.08	0.00	0.45	0.00	100.52
R3 179	56.35	0.11	1.99	9.98	0.24	29.92	2.02	0.00	0.57	0.00	101.16
R3 180	56.31	0.13	1.70	10.39	0.25	30.02	0.82	0.00	0.51	0.00	100.13
R3 181	56.68	0.21	1.13	10.40	0.24	30.10	0.99	0.00	0.44	0.00	100.19
R3 182	56.40	0.00	1.37	10.49	0.27	29.59	1.26	0.00	0.46	0.00	99.84
R3 183	56.90	0.14	1.16	10.12	0.24	30.71	0.82	0.00	0.46	0.00	100.53
R3 184	55.94	0.11	2.02	10.09	0.24	29.65	1.46	0.00	0.58	0.00	100.09
R3 185	56.18	0.16	1.41	10.42	0.26	29.21	1.83	0.00	0.49	0.00	99.96
M10 194	50.97	0.30	1.13	18.40	0.36	25.88	1.19	0.14	0.00	0.00	98.37
M10 195	53.63	0.11	1.65	17.09	0.24	26.61	1.85	0.06	0.00	0.00	101.22
M10 198	54.28	0.28	0.85	19.07	0.43	26.64	1.03	0.05	0.00	0.00	102.63
M10 199	53.75	0.32	1.02	18.40	0.39	26.78	1.14	0.09	0.00	0.00	101.89
M10 200	53.58	0.29	1.12	18.28	0.38	26.72	0.96	0.09	0.00	0.00	101.42
M10 201	53.71	0.13	1.62	16.37	0.33	26.11	1.93	0.06	0.00	0.00	100.26
M10 202	53.80	0.31	1.08	18.98	0.39	26.41	0.91	0.09	0.00	0.00	101.97
P9B 274	54.71	0.09	1.36	10.60	0.22	31.95	0.89	0.00	0.33	0.00	100.15
P9B 275	55.60	0.11	1.72	10.24	0.24	29.52	2.97	0.00	0.50	0.00	100.88
P9B 276	55.11	0.27	1.18	12.25	0.27	29.99	0.98	0.00	0.33	0.00	100.38
P9B 277	54.92	0.12	1.71	10.02	0.24	29.55	3.05	0.00	0.54	0.00	100.15
P9B 278	55.56	0.16	1.44	11.30	0.26	30.16	1.26	0.00	0.42	0.00	100.56
P9B 279	55.61	0.19	1.32	11.58	0.26	29.89	1.15	0.00	0.45	0.00	100.45
P9B 280	55.42	0.24	1.40	11.70	0.27	29.88	0.91	0.00	0.44	0.00	100.26

APPENDIX TWO *** R *** ALL ORTHOPYROXENE ANALYSES PAGE: 16

NUMBER	SI02	TI02	AL2O3	FE0	MNO	MGO	CAO	NA2O	CR2O3	NI0	TOTAL
P9B 281	55.38	0.14	1.65	11.12	0.24	30.08	0.96	0.00	0.48	0.00	100.05
P9B 282	55.88	0.11	1.71	11.49	0.27	29.13	0.90	0.00	0.55	0.11	100.15
P9B 283	56.39	0.12	1.42	10.83	0.25	30.29	0.71	0.00	0.41	0.13	100.53
P9B 284	55.52	0.15	1.40	11.43	0.24	28.42	2.20	0.00	0.53	0.09	99.98
P9B 285	55.31	0.13	1.60	11.22	0.26	29.57	1.76	0.00	0.57	0.11	100.53
P9B 286	55.02	0.13	1.89	10.67	0.22	27.08	3.43	0.00	0.61	0.09	99.14
P9B 287	55.39	0.12	1.65	10.64	0.24	29.55	2.14	0.00	0.56	0.08	100.37
P9B 288	55.38	0.12	1.76	11.80	0.26	27.86	1.39	0.00	0.44	0.13	99.16
P9B 289	54.94	0.18	1.45	11.53	0.26	28.38	1.99	0.00	0.52	0.11	99.16
M12 323	53.90	0.26	0.84	19.28	0.44	24.21	1.04	0.06	0.27	0.08	100.38
M12 325	53.86	0.29	0.91	19.15	0.43	24.25	1.19	0.02	0.15	0.04	100.29
M12 326	54.17	0.26	0.83	18.58	0.43	24.84	1.37	0.05	0.14	0.06	100.73
M12 329	54.15	0.22	0.83	18.88	0.40	24.47	0.92	0.00	0.11	0.10	100.08
B10 338	55.57	0.21	1.08	14.93	0.32	27.40	1.09	0.00	0.28	0.07	100.95
B10 340	55.27	0.21	1.10	15.09	0.35	27.08	1.02	0.00	0.35	0.05	100.52
B10 341	54.71	0.25	1.02	15.28	0.32	27.32	0.88	0.00	0.33	0.04	100.15
B10 342	54.82	0.17	1.11	14.98	0.30	28.10	0.93	0.00	0.29	0.06	100.76
B10 344	53.85	0.27	1.13	15.84	0.32	26.53	1.13	0.00	0.37	0.06	99.50
B10 345	54.10	0.28	1.02	15.85	0.35	26.94	1.20	0.00	0.30	0.06	100.10
B2 366	55.24	0.21	1.26	13.02	0.27	29.30	1.02	0.00	0.39	0.09	100.80
B2 367	55.28	0.12	1.34	12.53	0.27	29.15	1.48	0.00	0.43	0.07	100.47
B2 368	54.98	0.21	1.47	12.08	0.31	27.82	2.65	0.00	0.43	0.09	100.04
B2 369	55.27	0.13	1.52	12.56	0.24	28.40	2.30	0.00	0.47	0.07	100.76
B2 370	55.00	0.14	1.34	12.68	0.28	28.83	1.55	0.00	0.46	0.10	100.38

APPENDIX TWO *** B *** ALL ORTHOPYROXENE ANALYSES PAGE: 17

NUMBER	SI02	TIO2	AL2O3	FE0	MNO	MGO	CAO	NA2O	CR2O3	NIO	TOTAL
P-11 395	54.94	0.11	1.37	12.15	0.24	30.14	0.89	0.00	0.25	0.10	100.19
P-11 396	54.53	0.14	1.57	12.20	0.24	30.02	1.15	0.00	0.39	0.09	100.33
P-11 397	54.86	0.18	1.55	12.26	0.27	28.86	1.02	0.00	0.39	0.09	99.48
P-11 398	54.82	0.15	1.49	12.52	0.25	29.09	0.75	0.00	0.23	0.09	99.39
P-11 399	54.68	0.09	1.78	11.65	0.24	29.34	2.11	0.00	0.55	0.10	100.54
P-11 400	54.37	0.19	1.36	12.47	0.25	29.69	0.89	0.00	0.40	0.14	99.76
P-11 401	54.65	0.17	1.60	11.86	0.25	29.32	1.26	0.00	0.40	0.11	99.62
B-5 426	54.88	0.18	1.32	12.59	0.30	28.28	1.22	0.00	0.46	0.12	99.35
B-5 429	54.98	0.21	1.28	12.01	0.28	28.96	1.01	0.00	0.51	0.08	99.32
B-5 430	54.96	0.14	1.41	12.60	0.27	30.10	0.89	0.00	0.45	0.08	100.90
B-5 431	54.93	0.15	1.52	12.60	0.25	28.67	1.79	0.00	0.45	0.09	100.43
B-5 435	55.06	0.20	1.34	12.11	0.27	28.23	2.28	0.00	0.43	0.07	99.99
F-24 442	55.53	0.16	1.43	11.86	0.25	28.75	1.73	0.00	0.47	0.09	100.27
F-24 445	54.92	0.21	1.42	12.03	0.27	27.69	2.14	0.00	0.45	0.11	99.24
F-24 446	54.92	0.16	1.55	11.92	0.27	29.38	2.09	0.00	0.55	0.11	100.95
F-24 449	55.17	0.23	1.29	12.67	0.30	29.03	1.02	0.00	0.45	0.08	100.24
F-1 452	55.37	0.13	1.63	11.60	0.27	30.26	1.50	0.00	0.52	0.08	101.36
F-1 453	55.25	0.09	1.51	11.99	0.25	30.03	1.34	0.00	0.57	0.04	101.05
F-1 454	55.01	0.14	1.39	12.58	0.25	29.51	1.40	0.00	0.53	0.09	100.90
F-1 455	55.07	0.22	1.30	12.55	0.27	29.84	1.29	0.00	0.47	0.07	101.08
F-1 456	55.15	0.25	1.22	13.26	0.28	30.06	1.04	0.00	0.44	0.09	101.79
F-1 457	55.32	0.26	1.11	13.03	0.30	29.80	1.21	0.00	0.40	0.10	101.53
F-1 458	55.22	0.24	1.29	12.52	0.24	29.37	2.02	0.00	0.45	0.11	101.46
F-1 459	55.41	0.17	1.56	10.93	0.26	30.52	2.28	0.00	0.38	0.06	101.57

APPENDIX TWO *** B *** ALL ORTHOPYROXENE ANALYSES. PAGE: 18

NUMBER	SI02	TI02	AL203	FE0	MNO	MGO	CA0	NA2O	CR203	NIO	TOTAL
F-13 479	55.28	0.18	1.74	13.58	0.25	29.93	0.67	0.00	0.19	0.07	101.87
F-13 480	55.50	0.19	1.26	13.21	0.27	30.26	0.82	0.00	0.14	0.09	101.74
F-13 482	54.36	0.16	1.70	14.66	0.28	27.28	2.95	0.00	0.59	0.05	102.03
F-13 483	54.55	0.20	1.42	15.18	0.30	28.27	1.36	0.00	0.48	0.06	101.82
F-13 484	54.43	0.15	1.59	15.75	0.30	27.72	1.69	0.00	0.53	0.09	102.25
F-13 486	54.54	0.36	1.02	16.85	0.30	26.98	1.10	0.00	0.17	0.05	101.37
MBC 516	55.28	0.12	1.52	9.46	0.09	31.46	1.02	0.00	0.48	0.11	99.54
MBC 517	55.74	0.17	1.52	8.54	0.21	32.67	0.57	0.00	0.45	0.09	99.96
M7 522	54.35	0.24	1.04	16.20	0.32	27.69	0.43	0.00	0.31	0.11	100.69
M7 523	54.13	0.12	1.62	15.26	0.32	26.67	1.06	0.00	0.56	0.10	99.84
M7 524	53.99	0.13	1.47	15.55	0.28	27.16	1.27	0.00	0.50	0.09	100.44
M7 525	54.02	0.22	1.08	15.80	0.29	27.07	1.78	0.00	0.41	0.08	100.75
M7 529	53.41	0.28	0.91	16.22	0.35	26.10	1.72	0.00	0.24	0.09	99.30
M6 538	52.58	0.13	1.48	15.01	0.35	27.72	1.72	0.00	0.39	0.12	99.48
M6 539	54.02	0.10	1.74	15.16	0.35	26.43	1.68	0.00	0.49	0.14	100.09
M6 540	53.70	0.20	1.36	14.87	0.35	27.64	1.38	0.00	0.41	0.11	100.00
M6 541	54.06	0.27	1.09	15.27	0.31	27.83	0.94	0.00	0.30	0.07	100.14
M6 543	54.41	0.19	1.34	14.76	0.30	27.97	1.13	0.00	0.39	0.14	100.63
M6 545	54.11	0.34	0.88	15.10	0.32	27.54	0.90	0.00	0.31	0.10	99.60
B23 555	52.55	0.19	1.07	18.41	0.38	25.07	2.00	0.00	0.20	0.06	99.93
B23 556	52.73	0.31	0.83	18.87	0.30	24.87	1.54	0.00	0.11	0.04	99.66
B23 558	53.72	0.26	0.96	17.91	0.38	24.67	2.09	0.00	0.22	0.02	100.23
B23 559	53.17	0.19	0.88	18.35	0.30	24.79	1.42	0.00	0.12	0.07	99.35
B23 560	53.26	0.16	1.08	18.06	0.37	24.67	1.94	0.00	0.30	0.05	99.89

APPENDIX TWO *** a *** ALL ORTHOPYROXENE ANALYSES PAGE: 19

NUMBER	SI02	TI02	AL2O3	FE0	MNO	HGO	CAO	NA2O	CR2O3	NIO	TOTAL
B23 561	53.01	0.32	0.86	18.96	0.36	24.52	1.14	0.00	0.13	0.06	99.36
B13 571	54.58	0.24	1.10	15.57	0.33	27.34	1.59	0.00	0.35	0.10	101.20
B13 572	54.57	0.26	1.13	15.44	0.32	27.37	1.31	0.00	0.34	0.04	100.78
B13 573	54.55	0.22	1.09	15.39	0.32	26.98	1.50	0.00	0.34	0.06	100.45
B13 574	54.31	0.26	1.11	15.54	0.34	27.25	1.14	0.00	0.32	0.08	100.35
B13 577	54.49	0.24	0.97	15.69	0.35	27.13	1.32	0.00	0.27	0.06	100.52
B28 598	52.50	0.28	0.80	23.97	0.44	21.10	1.36	0.00	0.10	0.02	100.57
B28 599	52.67	0.26	0.78	24.53	0.44	20.81	1.10	0.00	0.10	0.05	100.74
B28 601	52.28	0.21	1.10	24.01	0.47	20.90	1.60	0.00	0.08	0.09	100.74
B28 603	52.16	0.24	0.78	25.03	0.51	20.97	0.99	0.00	0.08	0.04	100.80
B30 616	52.28	0.19	0.81	24.66	0.47	20.73	1.37	0.00	0.09	0.06	100.66
B30 617	52.23	0.27	0.76	24.87	0.45	19.85	1.44	0.00	0.07	0.04	99.98
B30 622	51.50	0.30	0.78	24.85	0.46	20.23	1.31	0.00	0.07	0.04	99.54
B30 623	51.95	0.27	0.82	24.10	0.44	19.34	2.39	0.00	0.11	0.06	99.48
B3 624	53.96	0.10	1.48	12.05	0.27	30.40	1.33	0.00	0.48	0.12	100.19
B3 625	54.61	0.13	1.73	11.91	0.24	29.80	1.55	0.00	0.51	0.12	100.60
B3 626	54.20	0.23	1.28	12.13	0.26	29.54	1.35	0.00	0.41	0.13	99.53
B3 627	54.81	0.24	1.59	11.94	0.27	29.65	1.84	0.00	0.40	0.10	100.84
B3 628	54.34	0.23	1.28	12.19	0.25	29.54	1.73	0.00	0.37	0.09	100.02
B3 631	54.70	0.00	1.25	12.04	0.25	30.54	1.13	0.00	0.41	0.09	100.41
B20 644	52.95	0.25	0.86	21.88	0.47	22.37	0.90	0.00	0.06	0.04	99.78
B20 645	53.12	0.19	0.70	21.88	0.46	22.42	0.80	0.00	0.03	0.05	99.65
B20 647	52.77	0.21	0.91	22.50	0.47	23.09	0.89	0.00	0.15	0.04	100.83
B20 649	52.82	0.23	1.36	21.08	0.50	22.95	0.92	0.00	0.05	0.05	99.96

APPENDIX TWO *** R *** ALL ORTHOPYROXENE ANALYSES PAGE: 20

NUMBER	SI02	TI02	AL2O3	FE0	MNO	MGO	CAO	NA2O	CR2O3	NIO	TOTAL
B25 659	53.54	0.17	1.11	17.35	0.35	25.32	1.37	0.00	0.35	0.06	99.62
B25 660	53.24	0.27	0.84	18.95	0.39	25.24	1.20	0.00	0.10	0.05	100.28
B25 662	53.79	0.17	0.98	16.50	0.32	25.78	2.18	0.00	0.27	0.04	100.03
B25 664	53.11	0.18	0.99	18.27	0.37	24.93	1.95	0.00	0.24	0.03	100.07
B9 675	53.25	0.10	1.68	15.52	0.31	27.67	0.81	0.00	0.51	0.06	99.91
B9 676	53.14	0.18	1.30	15.22	0.32	27.95	1.29	0.00	0.38	0.05	99.83
B9 678	53.66	0.18	1.18	14.73	0.35	27.15	1.43	0.00	0.39	0.06	99.11
B9 680	53.73	0.21	1.13	16.14	0.37	26.75	0.78	0.00	0.38	0.08	99.57
B9 685	53.95	0.22	1.16	14.77	0.29	26.99	1.82	0.00	0.35	0.06	99.61
B9 684	53.89	0.27	0.99	15.24	0.35	27.08	1.23	0.00	0.26	0.03	99.32
B9 686	54.25	0.18	1.28	14.84	0.35	27.34	1.66	0.00	0.38	0.07	100.33
B15 695	53.61	0.18	1.45	16.22	0.35	25.62	2.78	0.00	0.58	0.06	100.83
B15 696	55.16	0.34	1.00	17.97	0.39	25.29	1.27	0.00	0.21	0.02	101.65
B15 700	52.93	0.24	0.94	20.67	0.42	24.27	0.93	0.00	0.14	0.06	100.60
B15 701	52.62	0.39	0.93	20.26	0.38	24.47	1.21	0.00	0.17	0.06	100.49
B15 702	53.50	0.19	1.26	15.51	0.31	26.33	2.88	0.00	0.45	0.06	100.49
B15 705	52.35	0.33	0.93	20.14	0.40	24.62	0.99	0.00	0.18	0.06	100.00
RR1 715	54.55	0.23	1.37	13.79	0.30	28.00	1.62	0.00	0.39	0.09	100.34
RR1 716	54.75	0.25	1.36	15.03	0.30	28.55	0.65	0.00	0.32	0.08	101.29
RR1 721	54.76	0.31	1.01	14.74	0.35	28.28	0.87	0.00	0.20	0.04	100.54
RR1 722	54.59	0.29	1.23	14.29	0.29	28.49	0.85	0.00	0.35	0.07	100.45
F7 734	53.77	0.26	1.31	16.01	0.34	26.19	1.41	0.00	0.39	0.08	99.76
F7 735	53.22	0.20	1.51	15.46	0.31	25.85	1.76	0.00	0.53	0.07	98.91
F7 B735	54.09	0.20	1.51	15.46	0.31	26.31	1.76	0.00	0.53	0.07	100.24

APPENDIX TWO *** R *** ALL ORTHOPYROXENE ANALYSES PAGE: 21

NUMBER	SI02	TI02	AL2O3	FE0	MNO	MGO	CAO	NA2O	CR2O3	NIO	TOTAL
F7 C735	53.46	0.20	1.51	15.46	0.31	26.59	1.76	0.00	0.53	0.07	99.89
F7 736	53.87	0.14	1.72	15.08	0.31	27.30	2.11	0.00	0.59	0.06	101.18
F7 737	53.86	0.15	1.50	15.14	0.29	25.94	2.12	0.00	0.56	0.11	99.67
F7 739	54.68	0.29	1.02	16.77	0.34	27.03	0.89	0.00	0.26	0.06	101.34
F7 740	54.61	0.34	1.17	15.90	0.35	27.09	1.63	0.00	0.50	0.09	101.66
F7 741	54.84	0.34	1.02	16.20	0.35	27.27	1.06	0.00	0.31	0.08	101.45
F15 750	55.17	0.16	1.54	12.71	0.29	28.52	1.49	0.00	0.52	0.06	100.46
F15 751	55.93	0.17	1.45	12.69	0.27	28.38	1.98	0.00	0.50	0.08	101.45
F15 752	54.48	0.15	1.41	12.63	0.24	28.36	1.72	0.00	0.48	0.10	99.57
F15 755	55.36	0.27	1.21	12.95	0.28	28.35	0.95	0.00	0.40	0.08	99.85
F15 756	55.07	0.18	1.36	12.95	0.24	27.87	1.36	0.00	0.51	0.10	99.64
F8 770	53.71	0.15	1.47	15.79	0.31	27.16	1.88	0.00	0.45	0.08	101.00
F8 771	54.01	0.21	1.49	15.64	0.32	27.10	2.27	0.00	0.51	0.06	101.61
F8 772	53.82	0.16	1.56	16.01	0.31	27.65	1.27	0.00	0.56	0.05	101.39
F8 773	53.62	0.29	1.11	16.41	0.35	27.44	1.10	0.00	0.32	0.05	100.67
F8 775	53.62	0.35	1.16	16.80	0.32	27.70	1.00	0.00	0.32	0.09	101.36
B4 795	54.62	0.11	1.56	11.64	0.27	30.00	1.59	0.00	0.50	0.11	100.40
B4 796	54.14	0.13	1.59	11.36	0.26	29.69	2.04	0.00	0.53	0.12	99.86
B4 797	55.28	0.28	1.23	12.07	0.25	30.89	0.84	0.00	0.44	0.11	101.39
B4 798	55.17	0.14	1.62	11.75	0.25	30.51	1.90	0.00	0.49	0.10	101.91
B4 800	55.04	0.17	1.73	12.09	0.25	30.96	0.79	0.00	0.48	0.13	101.64
B4 802	55.17	0.24	1.08	12.56	0.26	31.07	0.84	0.00	0.31	0.10	101.63
B7 803	54.81	0.14	1.60	11.48	0.24	28.99	1.95	0.00	0.54	0.07	99.82
B7 805	55.24	0.21	1.21	11.78	0.27	29.33	1.03	0.00	0.48	0.09	99.64

APPENDIX TWO *** R *** ALL ORTHOPYROXENE ANALYSES. PAGE: 22

NUMBER	SI02	TI02	AL2O3	FE0	MNU	MGO	CA0	NA2O	CR2O3	NIO	TOTAL
B7 806	55.39	0.20	1.22	11.66	0.25	29.43	1.02	0.00	0.46	0.08	99.69
B7 807	54.86	0.20	1.26	11.57	0.26	29.43	1.05	0.00	0.43	0.08	99.14
B7 809	54.05	0.20	1.38	11.43	0.26	29.25	1.07	0.00	0.51	0.07	98.22
B7 811	54.24	0.18	1.03	12.57	0.26	29.60	1.09	0.00	0.33	0.08	99.18
B26 824	52.71	0.16	1.31	20.75	0.39	22.90	1.72	0.00	0.32	0.02	100.28
B26 825	53.34	0.15	1.16	20.72	0.37	22.89	1.62	0.00	0.30	0.07	100.62
B26 826	51.92	0.33	1.08	24.09	0.48	21.04	1.02	0.00	0.11	0.02	100.09
B26 827	52.36	0.23	0.94	22.51	0.41	19.43	4.53	0.00	0.10	0.04	100.55
B26 828	51.75	0.38	0.71	25.01	0.48	20.06	1.25	0.00	0.08	0.03	99.75
B26 829	52.01	0.32	0.75	24.76	0.48	20.11	1.20	0.00	0.04	0.06	99.73
B26 830	51.51	0.23	0.73	26.10	0.48	19.73	0.84	0.00	0.04	0.06	99.72
B26 831	52.01	0.24	0.91	22.17	0.41	19.30	4.37	0.00	0.07	0.02	99.50
B26 843	51.59	0.24	0.78	25.82	0.51	18.95	2.25	0.00	0.02	0.04	100.20
B21 844	53.70	0.18	1.15	16.57	0.33	26.12	1.68	0.00	0.29	0.06	100.08
B21 845	54.01	0.12	1.31	16.11	0.34	26.08	2.34	0.00	0.34	0.06	100.71
B21 847	53.82	0.18	1.10	16.98	0.34	26.40	1.29	0.00	0.28	0.05	100.44
B21 849	53.75	0.17	1.10	16.67	0.34	25.20	1.69	0.00	0.31	0.07	99.28
B21 850	53.69	0.14	1.29	16.50	0.34	26.13	1.94	0.00	0.35	0.08	100.44
B22 862	54.49	0.17	1.12	17.15	0.34	25.10	2.31	0.00	0.28	0.06	101.02
B22 863	54.21	0.30	0.83	18.14	0.37	26.08	1.17	0.00	0.12	0.07	101.29
B22 864	53.87	0.31	0.93	18.06	0.36	25.14	1.27	0.00	0.08	0.07	100.09
B22 866	54.23	0.12	1.39	16.19	0.33	26.63	1.65	0.00	0.40	0.06	101.00
B19 879	53.31	0.19	1.51	17.50	0.33	25.70	1.60	0.00	0.30	0.06	100.50
B19 880	53.38	0.17	1.12	17.20	0.35	25.53	1.52	0.00	0.28	0.06	99.61

APPENDIX TWO *** B *** ALL ORTHOPYROXENE ANALYSES. PAGE: 23

NUMBER	SI02	TI02	AL203	FE0	MNU	MGO	CA0	NA20	CR203	NIO	TOTAL
B19 881	53.55	0.16	1.07	16.57	0.35	26.10	1.53	0.00	0.24	0.07	99.64
B19 886	53.12	0.31	0.96	19.52	0.39	23.71	1.42	0.00	0.16	0.05	99.64
F4 899	52.42	0.35	0.98	22.37	0.45	21.66	1.18	0.00	0.06	0.05	99.52
F4 900	52.62	0.25	0.84	22.47	0.45	21.93	1.01	0.00	0.05	0.03	99.65
F4 901	52.87	0.25	0.92	22.28	0.45	22.14	0.97	0.00	0.10	0.04	100.02
F4 902	52.31	0.35	0.92	22.16	0.45	21.48	1.33	0.00	0.07	0.02	99.09
P9C 930	54.33	0.10	1.85	11.97	0.25	29.97	0.89	0.00	0.51	0.09	99.92
P9C 931	54.80	0.12	1.72	11.52	0.25	29.79	1.32	0.00	0.53	0.11	100.16
P9C 932	54.31	0.17	1.60	11.26	0.23	27.25	5.62	0.00	0.57	0.09	101.10
P9C 933	55.08	0.09	1.79	10.92	0.24	30.84	1.00	0.00	0.48	0.14	100.58
P9C 934	55.19	0.11	1.89	10.82	0.24	29.69	1.67	0.00	0.48	0.09	100.18
P9C 935	54.86	0.11	1.99	11.57	0.25	29.87	1.33	0.00	0.58	0.11	100.45
P9C 936	55.11	0.13	1.87	11.68	0.26	29.36	1.62	0.00	0.52	0.14	100.69
P9C 937	55.90	0.19	1.56	10.02	0.25	31.50	0.80	0.00	0.39	0.12	100.71

APPENDIX TWO *** C *** ALL CLINOPYROXENE ANALYSES. PAGE: 24

NUMBER	SI02	TI02	AL203	FE0	MNO	HGO	CA0	NA2O	CR203	NIO	TOTAL
RR6 25	51.62	1.09	1.47	8.34	0.00	14.93	20.78	0.11	0.10	0.04	98.48
RR6 26	50.75	1.56	1.65	8.45	0.10	14.85	20.52	0.34	0.14	0.04	98.48
RR6 27	50.92	1.48	1.68	7.94	0.19	15.28	20.80	0.29	0.20	0.03	98.81
RR6 29	51.55	1.20	1.46	8.27	0.19	15.45	20.47	0.21	0.19	0.03	99.02
RR6 30	51.31	1.44	1.76	8.22	0.19	14.99	20.69	0.20	0.00	0.00	98.80
F27 37	52.10	0.63	2.35	5.56	0.10	15.56	23.29	0.00	0.44	0.07	100.16
F27 38	52.10	0.60	2.14	6.33	0.10	15.16	23.06	0.00	0.57	0.05	100.17
M5 109	52.25	0.66	2.55	5.68	0.17	14.93	21.86	0.14	0.00	0.00	98.24
M5 110	52.34	0.26	4.51	6.42	0.17	20.17	11.96	0.71	0.82	0.00	97.36
M9 171	51.77	0.37	1.87	6.57	0.19	14.77	22.71	0.31	0.51	0.01	99.08
M9 172	51.45	0.29	2.17	7.03	0.21	15.34	20.62	0.21	0.54	0.02	97.88
M9 173	51.23	0.29	2.14	6.58	0.24	14.74	22.39	0.42	0.00	0.00	97.81
M9 176	51.05	0.32	2.01	6.82	0.19	15.19	22.05	0.34	0.63	0.08	98.68
M9 177	51.23	0.41	2.01	6.82	0.21	14.71	22.75	0.27	0.42	0.06	98.89
M10 196	52.56	0.51	1.70	8.26	0.24	15.80	19.96	0.28	0.00	0.00	99.29
M10 197	51.37	0.57	2.15	7.93	0.25	15.72	20.02	0.33	0.00	0.00	98.34
M12 322	52.63	0.46	1.57	8.40	0.24	14.85	22.15	0.27	0.30	0.04	100.91
M12 324	52.45	0.42	1.53	9.21	0.20	15.35	20.83	0.24	0.23	0.06	100.58
M12 327	53.12	0.40	1.60	8.93	0.22	15.71	21.75	0.24	0.26	0.05	102.28
M12 328	52.42	0.41	1.60	7.86	0.24	14.89	21.69	0.32	0.27	0.06	99.76
B10 339	51.82	0.40	1.73	6.21	0.10	15.58	23.69	0.28	0.51	0.03	100.41
B10 343	52.82	0.38	1.89	5.90	0.10	15.91	22.79	0.31	0.53	0.03	100.72
B2 364	53.08	0.70	2.10	5.58	0.10	16.21	22.08	0.44	0.72	0.06	101.13
B2 365	53.52	0.26	4.25	5.96	0.10	19.87	12.52	0.59	0.29	0.12	97.48

APPENDIX TWO *** C *** ALL CLINOPYROXENE ANALYSES PAGE: 25

NUMBER	SI02	TI02	AL2O3	FeO	MNO	MgO	CaO	Na2O	CR2O3	NiO	TOTAL
B2 371	52.61	0.61	1.90	5.59	0.14	16.20	22.08	0.37	0.60	0.07	100.17
B-5 427	52.42	0.39	2.37	5.08	0.15	15.28	22.96	0.00	0.86	0.07	99.58
B-5 428	52.41	0.41	2.33	5.07	0.14	15.76	23.35	0.00	0.86	0.03	100.36
B-5 432	52.70	0.43	2.46	4.94	0.15	15.67	22.54	0.00	0.82	0.07	99.78
F-24 443	52.30	0.52	2.35	4.94	0.15	14.90	23.34	0.00	0.81	0.02	99.33
F-24 444	52.48	0.44	2.15	4.82	0.14	15.08	23.15	0.00	0.89	0.04	99.19
F-24 447	53.29	0.34	1.48	4.53	0.10	15.67	24.32	0.00	0.61	0.02	100.36
F-24 448	52.68	0.41	2.40	4.73	0.15	15.45	23.17	0.00	0.91	0.04	99.94
F-13 481	53.02	0.34	2.13	6.65	0.15	17.88	20.18	0.00	0.42	0.05	100.85
F-13 488	52.69	0.48	1.83	6.14	0.17	15.77	23.48	0.00	0.45	0.07	101.08
MBC 515	52.00	0.33	2.34	3.78	0.12	16.91	23.36	0.00	0.94	0.05	99.83
FEP3 518	51.67	0.42	2.02	10.32	0.24	13.76	21.99	0.00	0.18	0.04	100.64
FEP3 519	52.68	0.40	1.77	9.73	0.24	13.33	22.33	0.00	0.20	0.06	100.74
FEP3 520	52.77	0.40	1.76	9.75	0.21	13.51	22.71	0.00	0.17	0.08	101.36
FEP3 521	52.97	0.40	1.86	9.97	0.20	13.83	22.04	0.00	0.15	0.04	101.52
M7 526	52.67	0.52	1.91	6.80	0.19	15.36	23.57	0.00	0.57	0.04	101.63
M7 527	52.70	0.41	1.78	6.67	0.19	15.25	23.44	0.00	0.50	0.06	101.00
M7 528	51.19	0.46	1.65	6.66	0.20	14.83	23.80	0.00	0.54	0.06	99.39
M6 542	52.49	0.56	1.50	6.39	0.17	16.17	21.58	0.00	0.20	0.07	99.13
M6 544	52.59	0.52	1.83	5.69	0.17	15.90	22.40	0.00	0.53	0.09	99.72
B23 557	52.10	0.46	1.51	8.31	0.22	14.94	20.86	0.00	0.21	0.05	98.66
B23 557	52.36	0.48	1.45	7.92	0.21	15.41	21.28	0.00	0.15	0.06	99.32
B23 562	52.07	0.48	1.37	7.02	0.17	14.95	22.24	0.00	0.22	0.07	98.59
B13 575	52.67	0.52	1.66	6.04	0.15	15.53	22.12	0.00	0.53	0.04	99.26

APPENDIX TWO *** C *** ALL CLINOPYROXENE ANALYSES PAGE: 26

NUMBER	SI02	TI02	AL2O3	FE0	MNO	MGG	CAO	NA2O	CR2O3	NIO	TOTAL
B13 576	52.92	0.46	1.67	5.85	0.16	15.72	22.04	0.00	0.51	0.03	99.36
B13 578	52.66	0.56	1.78	6.52	0.19	15.69	21.72	0.00	0.51	0.08	99.71
B28 A600	51.88	0.37	1.63	10.48	0.24	13.39	20.88	0.00	0.18	0.03	99.08
B28 B600	52.02	0.44	1.87	10.18	0.24	13.91	20.85	0.00	0.16	0.04	99.71
B28 C600	51.79	0.42	1.87	10.18	0.24	14.33	20.85	0.00	0.16	0.04	99.88
B28 602	51.04	0.26	1.71	11.77	0.26	13.18	20.71	0.00	0.07	0.03	99.03
B30 618	51.60	0.48	1.64	11.10	0.24	13.15	20.64	0.00	0.15	0.02	99.00
B30 619	51.58	0.30	1.29	11.26	0.25	12.84	21.28	0.00	0.05	0.05	98.90
B30 620	50.58	1.44	1.57	12.53	0.46	13.25	18.15	0.00	0.09	0.00	98.07
B30 621	51.47	0.38	1.60	12.79	0.27	12.66	19.41	0.00	0.10	0.05	98.73
B3 629	52.08	0.65	1.86	5.08	0.14	16.40	21.83	0.00	0.69	0.02	98.75
B3 630	51.74	0.64	2.25	5.00	0.15	15.92	22.38	0.00	0.79	0.01	98.88
B20 642	52.40	0.41	1.55	8.67	0.24	14.55	21.79	0.00	0.22	0.01	99.84
B20 646	51.99	0.39	1.46	8.13	0.21	14.84	22.56	0.00	0.27	0.00	99.85
B20 648	51.82	0.47	1.37	9.12	0.24	14.70	22.21	0.00	0.09	0.03	100.05
B25 661	52.89	0.41	1.41	7.93	0.25	15.19	22.04	0.00	0.17	0.05	100.32
B25 663	51.79	0.33	1.59	8.96	0.24	15.51	20.74	0.00	0.26	0.03	99.43
B25 665	51.33	0.30	1.47	8.78	0.21	15.49	20.74	0.00	0.28	0.03	98.63
B25 666	52.42	0.37	1.29	7.15	0.19	15.34	22.17	0.00	0.19	0.06	99.18
B9 677	52.04	0.31	1.87	6.88	0.18	15.72	20.21	0.00	0.54	0.03	97.78
B9 679	52.08	0.37	1.98	6.20	0.18	15.64	21.77	0.00	0.66	0.05	98.93
B9 681	52.04	0.39	2.00	5.93	0.21	15.42	22.21	0.00	0.63	0.05	98.88
B9 682	52.36	0.24	2.07	7.00	0.19	15.86	20.60	0.00	0.55	0.04	98.91
B9 685	52.65	0.38	1.73	5.97	0.18	15.27	22.36	0.00	0.52	0.01	99.07

APPENDIX TWO *** C *** ALL CLINOPYROXENE ANALYSES. PAGE: 27

NUMBER	SI02	TI02	AL2O3	FE0	MNU	MGO	CA0	NA2O	CR2O3	NIO	TOTAL
B15 697	53.30	0.37	1.70	8.09	0.14	14.24	22.08	0.00	0.33	0.03	100.28
B15 698	53.30	0.39	2.05	9.68	0.23	15.03	19.47	0.00	0.46	0.04	100.65
B15 699	53.69	0.47	1.84	8.16	0.24	14.32	21.84	0.00	0.36	0.04	100.94
RR1 717	52.50	0.64	2.00	5.96	0.15	16.05	21.93	0.00	0.56	0.05	99.84
RR1 718	52.94	0.51	1.80	5.40	0.15	15.76	22.75	0.00	0.50	0.04	99.83
RR1 719	52.41	0.54	1.96	6.54	0.17	15.69	22.07	0.00	0.27	0.01	99.46
RR1 720	52.57	0.56	1.82	6.51	0.21	15.80	21.51	0.00	0.27	0.02	99.27
F7 738	52.71	0.21	1.50	5.74	0.17	14.78	23.77	0.00	0.38	0.04	99.30
F15 753	52.38	0.65	2.19	5.27	0.14	15.58	22.76	0.00	0.88	0.03	99.86
F15 754	52.61	0.60	2.01	5.10	0.15	15.16	23.08	0.00	0.78	0.06	99.55
F15 757	52.46	0.43	2.09	4.99	0.14	15.18	22.61	0.00	0.90	0.04	98.84
F15 758	52.36	0.53	2.18	5.29	0.15	15.00	22.35	0.00	0.80	0.05	98.69
F15 759	53.10	0.60	2.16	5.38	0.15	15.19	22.40	0.00	0.86	0.07	99.91
F8 774	52.07	0.63	2.03	6.49	0.18	16.07	21.80	0.00	0.56	0.05	99.88
F8 776	51.60	0.64	2.07	6.61	0.14	15.72	21.90	0.00	0.60	0.06	99.34
F8 777	52.04	0.76	2.01	6.80	0.19	15.78	21.79	0.00	0.62	0.05	100.04
F8 778	51.88	0.69	2.04	7.16	0.17	15.97	20.89	0.00	0.60	0.04	99.44
B4 799	52.18	0.39	2.87	4.73	0.15	16.12	22.20	0.00	0.97	0.08	99.67
B4 801	53.40	0.44	1.34	4.89	0.13	17.24	22.20	0.00	0.43	0.08	100.15
B7 804	53.06	0.37	1.82	4.60	0.11	16.08	22.23	0.00	0.80	0.05	99.12
B7 808	52.38	0.38	1.77	4.17	0.13	15.94	21.85	0.00	0.77	0.07	97.46
B7 810	52.27	0.30	1.74	4.10	0.13	15.78	21.66	0.00	0.82	0.05	96.85
B26 841	51.50	0.57	1.47	11.67	0.27	13.04	19.63	0.00	0.11	0.07	98.33
B26 842	51.41	0.46	1.52	11.81	0.29	12.91	20.48	0.00	0.03	0.04	98.95

APPENDIX TWO *** C *** ALL CLINOPYROXENE ANALYSES. PAGE: 28

NUMBER	SI02	TIO2	AL2O3	FeO	MNO	MGO	CAO	NA2O	CR2O3	NIO	TOTAL
B21 846	52.41	0.28	1.50	6.33	0.17	15.79	22.07	0.00	0.52	0.04	99.11
B21 848	52.15	0.44	1.44	7.55	0.18	15.69	21.26	0.00	0.21	0.06	98.98
B21 851	52.67	0.43	1.48	7.14	0.20	15.31	21.67	0.00	0.30	0.06	99.26
B21 852	52.29	0.47	1.39	8.35	0.21	14.42	21.35	0.00	0.10	0.03	98.61
B22 865	52.86	0.47	1.49	7.82	0.20	15.50	20.77	0.00	0.13	0.01	99.25
B22 867	52.67	0.44	1.49	7.60	0.22	14.98	21.83	0.00	0.22	0.07	99.52
B22 868	53.22	0.48	1.44	8.43	0.24	15.16	21.03	0.00	0.21	0.04	100.25
B22 869	52.58	0.47	1.45	8.10	0.22	14.96	21.41	0.00	0.17	0.04	99.40
B22 870	52.21	0.45	1.44	7.98	0.22	14.92	21.66	0.00	0.12	0.01	99.01
B19 882	52.70	0.24	1.86	8.14	0.22	15.96	20.37	0.00	0.47	0.03	99.99
B19 883	52.63	0.25	2.05	7.69	0.19	15.36	20.25	0.00	0.57	0.04	99.03
B19 884	52.54	0.37	1.94	8.59	0.23	14.89	20.68	0.00	0.54	0.04	99.82
B19 885	52.21	0.26	2.02	9.34	0.22	14.75	19.50	0.00	0.50	0.04	98.84
F4 895	51.33	0.40	1.55	9.89	0.26	13.75	21.00	0.00	0.17	0.02	98.37
F4 896	51.94	0.36	1.43	9.51	0.27	13.28	21.35	0.00	0.13	0.03	98.30
F4 897	52.11	0.48	1.71	9.54	0.24	13.43	21.01	0.00	0.27	0.03	98.82
F4 898	51.97	0.46	1.58	9.35	0.30	13.22	21.40	0.00	0.14	0.02	98.44
F4 903	52.17	0.55	1.71	8.86	0.21	13.77	21.31	0.00	0.17	0.04	98.79

APPENDIX TWO D CHROMITE

Analysis No.	TiO ₂	Cr ₂ O ₃	Al ₂ O ₃	Fe ₂ O ₃	FeO	MgO	MnO	NiO	Total
M4 89	2.66	37.38	6.96	18.85	28.69	3.49	.54	.39	98.96
M4 90	2.41	36.76	6.96	19.65	29.17	2.98	.56	.42	98.91
M4 91	1.59	38.33	7.05	19.69	29.72	2.31	.57	.40	99.66
M4 92	2.54	35.92	7.78	19.42	29.27	3.12	.51	.43	98.99
M4 93	2.55	35.68	7.80	19.60	28.99	3.30	.53	.37	98.82
M4 94	2.48	37.64	7.74	19.10	28.37	3.93	.52	.41	100.19
M4 96	2.11	37.47	6.53	19.63	29.02	2.79	.55	.40	98.50
P9B 290	1.61	41.44	10.09	14.51	28.03	4.09	.79	N/A	100.56
P9B 291	2.17	41.47	10.09	14.69	25.60	6.10	.74	N/A	100.86
P9B 292	1.30	41.75	12.56	12.19	27.15	4.75	.78	N/A	100.48
P9B 293	1.43	43.98	11.80	10.86	25.44	5.81	.75	N/A	100.07
P9B 294	1.24	41.91	14.22	10.59	27.12	4.99	.80	N/A	100.87
P9B 295	1.53	41.12	12.67	12.80	25.33	6.05	.75	N/A	100.25
P9B 296	1.35	42.11	15.68	10.19	23.09	7.95	.44	.26	101.07
P9B 297	1.28	41.34	15.51	11.11	22.84	7.95	.46	.30	100.79
P9B 298	1.40	41.80	15.49	10.44	22.91	8.00	.45	.27	100.76
P9B 299	1.53	41.58	14.97	10.50	23.60	7.47	.46	.30	100.41
P9B 300	1.43	41.64	15.62	10.21	23.25	7.77	.44	.32	100.68
P9B 301	1.11	41.58	14.72	11.95	26.04	5.98	.51	.19	102.08
P9B 302	1.11	41.59	14.72	11.02	23.72	7.64	.49	.31	100.60
P9B 303	0.82	41.77	16.48	10.26	23.30	7.58	.46	.18	100.85
P9B 304	0.73	41.72	15.03	11.17	25.87	5.64	.51	.22	100.89
P9B 305	0.87	41.12	14.72	11.33	27.65	4.51	.54	.24	100.98
P9B 306	0.89	39.95	16.21	12.05	23.62	7.30	.45	.25	100.72
P9B 307	0.90	39.01	15.58	14.02	23.50	7.32	.48	.32	101.13
P9B 308	0.88	39.42	16.83	11.87	23.75	7.26	.49	.24	100.74
P9B 309	2.22	40.16	7.84	16.62	30.81	2.43	.59	.25	100.92
P9B 310	0.76	40.07	17.03	11.61	23.29	7.59	.50	.21	100.56
P9B 311	0.88	39.09	16.49	12.64	23.42	7.41	.48	.26	100.67
P9B 312	1.13	41.52	14.27	11.60	24.67	6.47	.49	.24	100.39
P9B 313	1.52	41.35	14.76	10.95	23.79	7.34	.49	.24	100.44
F1 460	1.31	36.21	14.23	17.10	24.19	6.92	.47	.20	100.63
F1 461	1.65	35.47	14.27	17.62	24.77	6.90	.46	.23	101.37
F1 462	1.20	35.24	14.62	18.13	24.45	6.79	.45	.27	101.15
F1 463	1.59	35.21	14.63	17.39	24.63	6.90	.48	.22	101.04
F1 464	1.72	34.92	14.60	17.10	24.77	6.79	.50	.20	100.60
F1 465	1.34	35.13	14.86	17.28	24.27	6.90	.47	.22	100.47
F1 466	1.52	34.75	14.16	17.70	25.25	6.24	.49	.22	100.33
F1 467	3.08	34.75	14.09	14.61	26.93	6.07	.48	.24	100.25
MBC 498	1.52	39.94	17.64	9.26	22.01	8.81	.33	.17	99.68
MBC 499	1.09	40.75	16.81	10.65	21.69	8.67	.49	.22	100.37
MBC 500	1.22	41.22	16.07	10.11	22.09	8.29	.47	.21	99.68
MBC 501	1.56	41.08	15.51	10.18	22.34	8.24	.48	.22	99.61
MBC 502	1.41	41.14	16.04	9.91	22.00	8.18	.43	.25	99.09
MBC 503	1.24	41.20	15.49	10.30	21.97	8.18	.48	.22	99.08
MBC 504	0.86	40.37	18.11	10.36	21.31	9.03	.44	.20	100.68
MBC 505	0.98	40.44	17.28	10.66	21.24	8.92	.47	.24	100.23
MBC 506	1.00	40.44	17.69	10.05	21.29	8.96	.45	.19	100.07
MBC 507	1.26	40.91	16.11	10.87	21.77	8.64	.44	.23	100.23
MBC 508	1.60	40.04	15.24	12.08	22.46	8.31	.47	.24	100.44

Analysis No.	TiO ₂	Cr ₂ O ₃	Al ₂ O ₃	Fe ₂ O ₃	FeO	MgO	MnO	NiO	Total
MBC 509	1.63	39.22	16.04	12.08	22.97	8.11	.50	.28	100.83
MBC 510	1.53	40.53	14.61	11.75	22.58	7.97	.46	.25	99.68
MBC 511	1.58	40.02	15.17	12.08	22.69	8.14	.46	.22	100.36
MBC 512	1.38	42.55	14.47	10.85	22.17	8.33	.44	.21	100.40
MBC 513	2.01	41.42	16.11	9.19	23.15	8.34	.46	.19	100.87
MBC 514	1.28	41.02	16.22	10.88	22.23	8.47	.46	.23	100.79
B15 704	1.05	27.41	5.99	32.14	31.72	.62	.53	.16	99.62
P9C 914	1.23	40.34	15.25	11.20	23.65	7.11	.53	.21	99.52
P9C 915	1.34	40.87	15.32	11.33	23.78	7.35	.50	.24	100.73
P9C 916	1.37	40.55	15.21	11.31	24.12	7.09	.46	.22	100.33
P9C 917	1.43	40.82	15.28	10.81	24.03	7.17	.46	.23	100.23
P9C 918	1.42	40.54	15.38	11.03	23.78	7.33	.44	.22	100.14
P9C 919	1.55	40.26	14.47	11.31	23.64	7.14	.51	.22	99.10
P9C 920	1.66	39.80	13.68	12.21	23.74	7.01	.48	.21	98.79
P9C 921	2.64	40.68	11.91	10.90	25.17	6.38	.47	.26	98.41
P9C 922	0.94	39.69	17.11	11.00	23.08	7.64	.47	.29	100.22
P9C 923	1.04	39.87	16.55	10.83	22.91	7.66	.44	.25	99.55
P9C 924	0.61	38.05	18.09	10.04	24.98	5.99	.45	.24	98.45
P9C 925	1.94	41.80	11.13	12.60	25.55	5.89	.48	.23	99.62
P9C 926	2.02	37.12	14.12	13.80	25.77	6.02	.49	.35	99.69
P9C 927	1.06	41.71	13.86	11.18	24.20	6.46	.48	.22	99.17
P9C 928	0.79	40.90	16.30	9.94	23.25	7.20	.46	.17	99.01
P9C 929	1.53	40.86	14.99	10.68	22.93	7.75	.44	.25	99.43

APPENDIX TWO E OLIVINE

Analysis No.	SiO ₂	FeO	MnO	MgO	CaO	NiO	Total
F27 33	38.58	20.28	.23	39.98	.03	.53	99.63
F27 34	38.62	20.45	.23	39.86	.05	.51	99.72
P11 387	39.06	19.15	.21	41.41	.05	.53	100.41
P11 388	38.96	19.34	.26	41.02	.05	.46	100.09
P11 389	38.97	19.75	.26	39.97	.03	.50	99.48
P11 390	38.88	19.62	.27	39.93	.04	.48	99.22
P11 391	38.57	19.72	.21	40.66	.04	.50	99.70
P11 392	38.57	19.71	.25	40.57	.02	.51	99.63
P11 393	38.62	19.47	.28	40.30	.03	.48	99.18
P11 394	38.90	19.57	.26	41.00	.04	.44	100.21
F1 450	39.07	17.84	.23	42.92	.04	.36	100.46
F1 451	39.27	17.86	.22	42.88	.06	.33	100.62
F13 476	38.93	19.10	.26	41.81	.03	.35	100.48
F13 477	39.17	18.62	.25	41.81	.01	.34	100.20
F13 478	39.01	17.90	.23	42.43	.04	.34	99.95

APPENDIX TWO F BIOTITE

Analysis No.	SiO ₂	TiO ₂	Al ₂ O ₃	FeO	MgO	CaO	K ₂ O	Cr ₂ O ₃	Total
M4 73	38.84	5.61	13.52	8.69	17.11	.14	9.34	1.30	94.55
M4 74	40.25	5.51	14.11	8.95	17.80	.09	9.01	1.36	97.08
M4 75	38.18	5.45	13.71	8.81	17.45	.14	9.46	1.43	94.63
M4 76	39.96	5.28	13.63	8.63	17.76	.15	8.96	1.34	95.71
M4 77	39.43	5.58	13.62	8.21	17.85	.14	9.23	1.19	95.25
M4 78	39.37	5.27	13.93	8.50	17.74	.14	8.99	1.35	95.29
M4 79	39.73	4.70	13.96	8.68	18.17	.10	9.14	1.30	95.78
M4 80	39.04	5.20	13.86	8.34	17.83	.12	9.23	1.41	95.03
M5 113	38.94	3.06	13.25	12.77	17.18	N/A	8.35	.92	94.47
M5 114	39.91	1.99	12.90	9.66	20.17	N/A	9.29	.69	94.61
M5 129	40.92	3.92	12.71	9.00	19.33	N/A	9.29	.71	95.88
B2 380	40.69	1.45	14.40	8.64	20.74	.10	9.76	.65	96.43
B2 381	38.83	4.70	13.94	9.16	18.47	.24	9.60	.77	95.71
B2 382	39.24	4.92	13.60	9.02	18.65	.24	10.04	.73	96.44
B2 383	39.85	3.56	14.10	9.01	19.39	.12	9.72	.59	96.34
B2 384	40.01	3.17	14.01	8.51	19.70	.14	9.64	.97	96.15
B2 385	39.02	4.92	13.70	8.77	18.43	.18	10.01	.84	95.87
B2 386	40.34	.58	14.10	7.98	21.78	.20	9.44	.55	94.97
B15 706	38.28	2.28	14.02	13.78	17.28	N/A	9.59	.24	95.51
B15 705	37.96	.39	14.62	15.07	16.90	N/A	9.36	.03	94.43
B7 813	40.01	.24	13.96	6.99	21.87	N/A	8.50	.33	91.94

APPENDIX TWO G OTHER (ILMENITE & AMPHIBOLE)

Anal No.	SiO ₂	TiO ₂	Al ₂ O ₃	FeO	MnO	MgO	CaO	Na ₂ O	K ₂ O	Cr ₂ O ₃	Tot
Ilmenite											
B20 658		46.51		48.67	2.27	0.64				.11	98.37
B28 604		48.48		47.23	3.09	0.20				.08	99.19
B26 840		46.53		48.85	0.78	0.91				.07	97.14
Amphibole											
F13 485	48.46	1.33	7.20	9.33	0.08	16.94	12.49	0.59	1.05	.37	97.84
B7 812	54.03	0.03	3.01	5.29	0.14	21.12	11.76	0.38	N/A	.16	95.92

APPENDIX TWO CONTINUED : Mineral descriptions.

In the following listing of analysis points and their descriptions, the first column is the sample name, the second is the serial number. Both these numbers occur in the listings that follow, thus identifying the analysis.

The third number refers to the analysis point recorded on photographs of the slide in the author's possession. These can be obtained from me if necessary.

The series of letters is a code briefly describing the mineral and this is as follows :

First letter: (F) Footwall unit, (M) Merensky unit, (B) Bastard unit, (P) Merensky pegmatoid, (R) Rolling reef area footwall.

Second letter: Mineral code: (H) Orthopyroxene, (C) Clinopyroxene, (S) Spinel, (P) Plagioclase, (O) Olivine, (I) Ilmenite, (M) Mica.

Third letter: (P) Primocryst/Phenocryst, (I) Interstitial.

Fourth letter: Size: (V) Very large, (L) Large, (M) Medium and (S) Small relative to the size of other grains of the same mineral.

Fifth letter: (C) Core, (R) Rim, (Z) Zonation.

RR-6A

1	1	RPPLC
"	2	RPPLC
"	3	RPPLC
"	4	RPPLC
"	5	RPPLC
"	6	RPPLC
"	7	RPPLC
"	8	RPPLC
"	9	RPPLC
"	10	RPPLC
"	11	RPPLC
"	12	RPPLC
"	13	RPPLC
"	14	RPPLC
"	15	RPPLC

NOT USED

17	17	RPPLC
"	18	RPPLZ
"	19	RPPLZ
"	20	RPPLZ
"	21	RPPLZ
"	22	RPPLZ
"	23	RPPLZ
"	24	RPPLZ/R
"	25	RCISC
"	26	RCISC
"	27	RCISC

From 17 to 24 zoned xtal core to rim

NOT USED

28	28	RCISC
"	29	RCISC

NOT USED

F-27A

30	1	FCPLR
"	2	FCPLR
"	3	FCPLR
"	4	FCPLR
"	5	FCPLR
"	6	FCPLR

NOT USED

NOT USED

41	9	FPPN2
"	10	FPPN2
"	11	FPPN2
"	12	FPPN2
"	13	FPPN2
"	14	FPPN2
"	15	FPPN2
"	16	FPPN2

No 41 to 48 core to rim in plag in ol.

to 48 are not used.

49	1	MPILC
"	2	MPILC
"	3	MPILC
"	4	MPILC
"	5	MPILC
"	6	MPILC
"	7	MPILC
"	8	MPILC
"	9	MPILC
"	10	MPILC
"	11	MPILC
"	12	MPILC
"	13	MPILC

67

3 MPILC

"	74	14	MRPSC	
"	75	15	MRISC	
"	76	16	MRILR	
"	77	17	MRPLC	
"	78	18	MRPLC	
"	79	19	MRPLC	
"	80	20	MRPLC	Same xtal as 93
"	81	21	MRPLC	
"	82	22	MRPLC	
"	83	23	MRPSC	
"	84	24	MRPLC	
"	85	25	MRPSC	
"	86	26	MRPSC	
"	87	27	MRPMC	
"	88	28	MRPLC	
"	89	29	MRPLR	
"	90	30	MRPMC	
"	91	NCT	USED	
"	92	32	MRILC	
"	93	1	MRPLC	
"	94	2	MRPMC	
"	95	3	MRPMC	
"	96	4	MRPLC	
"	97	5	MRPLC	Cf. 101 -128
"	98	6	MRPLC	
"	99	7	MRPSC	
"	100	8	MRPSC	
"	101	9	MRPSC	
"	102	10	MRPSC	
"	103	11	MRPLC	
"	104	12	MRPSC	
"	105	13	MRPSC	
"	106	14	MRPSC	
"	107	15	MRPSC	
"	108	16	MRPSC	
"	109	17	MRPSC	
"	110	18	MRPSC	
"	111	19	MRPSC	
"	112	20	MRPSC	
"	113	21	MRPSC	
"	114	22	MRPSC	
"	115	23	MRPSC	
"	116	24	MRPSC	
"	117	25	MRPSC	
"	118	26	MRPSC	
"	119	27	MRPSC	
"	120	28	MRPSC	
"	121	29	MRPSC	
"	122	30	MRPSC	
"	123	31	MRPSC	
"	124	32	MRPSC	
"	125	1	MRPSC	
"	126	2	MRPSC	
"	127	3	MRPSC	
"	128	4	MRPSC	
"	129	5	MRPSC	
"	130	6	MRPSC	
"	131	7	MRPSC	
"	132	8	MRPSC	
"	133	9	MRPSC	

"	139	10	HNPLC	
"	140	11	HNPLC	
"	141	12	HNPLC	
"	142	13	HNPLR	
"	143	14	HNILR	
"	144	15	HNILR	
"	145	16	HNILR	
"	146	17	NPPSC	
"	147	18	NPPSC	
"	148	19	NPPSC	
"	149	20	NPPSC	
"	150	21	NPPSC	
"	151	22	NPPSC	
"	152	23	NPPMC	
"	153	24	NPPMC	
"	154	25	NPPLC	
"	155	26	NPPMZ	
"	156	27	NPPMZ	
"	157	28	NPPMZ	
"	158	29	NPPMZ	
"	159	30	NPPMZ	
"	160	31	NPPMZ	
"	161	32	NPPLR	
N-9	162		162- 169 Assort of sizes (random).	
"	170	9	HNPLC	
"	171	10	NCISC	
"	172	11	NCISC	
"	173	12	NCISC	
"	174	13	HNPLC	
"	175	14	HNPLC	
"	176	15	HNPLC	
"	177	16	NCISC	
P-2 (N-3)	178	1	NPPVC	
"	179	2	NPPVZ	
"	180	3	NPPVZ	
"	181	4	NPPVZ	
"	182	5	NPPVC	
"	183	6	NPPVR	
"	184	7	HNPLC	
"	185	8	HNPLR	
N-10	186	1	NPP LZ	
"	187	2	NPP LZ	
"	188	3	NPP LZ	
"	189	4	NPP LZ	
"	190	5	NPP LZ	
"	191	6	NPP LR	
"	192		192 - 225 Marked on photo.	
-11	226	1	NPPSC	
"	227	2	NPPSC	
"	228	3	NPPSC	
"	229	4	NPPSC	
"	230	5	NPPLC	
"	231	6	NPPVC	
"	232	7	NPPLC	
N-2 (P-1)	233	8	NPISC	
"	234		NPILC	
"	235		NPILR	
"	236		NPILC	
"	237		NPILC	
"	238		NPILC	
"	239		NPILR	

"	240		MPILR	
"	241		MPILC	
P-3 (P-3)	242		MPILL	
"	243		MPILR	
"	244		MPILR	
"	245		MPILR	
"	246		MPILC	
"	247		MPILC	
"	248		MPILC	
"	249		MPILC	
P-3 (P-3)	250		MPILC	
"	251		MPILR	
"	252		MPILR	
"	253		MPILR	
"	254		MPILC	
"	255		MPILC	
"	256		MPILR	
"	257		MPILC	
L-14	258		258 -	265 flag anal 4 elements only (random)
258	259	1	MPILC	Above upper chro layer
"	267	2	MPILR	"
"	268	3	MPISC	"
"	269	4	MPISC	"
"	270	5	MPILC	"
"	271	6	MPILR	below " " "
"	272	7	MPILC	"
"	273	8	MPILC	"
"	274	9	MPPLC	
"	275	10	MPPLC	
"	276	11	MPPLC	
"	277	12	MPPLC	
"	278	13	MPPLC	
"	279	14	MPPSC	
"	280	15	MPPSC	
"	281	16	MPPLC	
"	282	17	MPPLC	
"	283	18	MPPLR	
"	284	19	MPPLR	
"	285	20	MPPLC	
"	286	21	MPPLC	
"	287	22	MPPLC	
"	288	23	MPPSR	
"	289	24	MPPLP	
"	290	25	MPSPC	
"	291	26	MPSPC	
"	292	27	MPSPC	
"	293	28	MPSPC	
"	294	29	MPSPC	
"	295	30	MPSPC	
"	296	31	MPSPC	
"	297	32	MPPLC	
"	298	33	MPSPC	
"	299	34	MPSPC	
"	300	35	MPSPC	
"	301	36	MPSPC	
"	302	37	MPSPC	
"	303	38	MPSPC	
"	304	39	MPSPC	
"	305	40	MPSPC	
"	306	41	MPSPC	
"	307	42	MPSPC	

"	307	43	NSPSC
"	309	44	NSPSC
"	310	45	NSPSC
"	311	46	NSPSC
"	312	47	NSPSC
"	313	48	NSPLC
"	314	49	NPILC
"	315	50	NPILC
"	316	51	NPILC
"	317	52	NPILC
"	318	53	NPILC
"	319	54	NPILC
"	320	55	NPILC
"	321	56	NPILC
1-12A	322	1	NCISC
"	323	2	NHISC
"	324	3	NCISC
"	325	4	NHISC
"	326	5	NHISC
"	327	6	NCISC
"	328	7	NCISC
"	329	8	NHISC
"	330	9	NPPLC
"	331	10	NPPLC
"	332	11	NPPLR
"	333	12	NPPLR
"	334	13	NPPLC
"	335	14	NPPLC
"	336	15	NPPLC
"	337	16	NPPLR
2-10A	338	1	BNINC
"	339	2	BCISC
"	340	3	BNINC
"	341	4	BNINC
"	342	5	BNINC
"	343	6	BCILC
"	344	7	BNINC
"	345	8	BNINC
"	346	9	BPPLC
"	347	10	BPPLR
"	348	11	BPPLC
"	349	12	BPPLC
"	350	13	BPPLC
"	351	14	BPPLC
"	352	15	BPPLC
"	353	16	BPPLC
"	354	1	BPPLC
"	355	2	BPPLR
"	356	3	BPPLR
"	357	4	BPPLC
"	358	5	BPPLC
"	359	6	BPPLC
"	360	7	BPPLC
"	361	8	BPPLC
"	362	9	BPPLC
"	363	10	BPPLC
"	364	1	BCILC
"	365	2	BCILC
"	366	3	BPPLC
"	367	4	BPPLC
"	368	5	BPPLR

"	369	6	EMPLC
"	370	7	EMPRC
"	371	8	BCILC
"	372	9	EPISC
"	373	10	EPISC
"	374	11	EPILC
"	375	10	EPILC
"	376	13	EPILR
"	377	14	EPISC
"	378	15	EPINC
"	379	16	EPISC
"	380	17	BMILC
"	381	18	BMILC
"	382	19	BMILC
"	383	20	BMISC
"	384	21	BMISC
"	385	22	BMILC
"	386	23	BMISC
P-11A	387	1	NOPLC
"	388	2	NOPLC
"	389	3	NOPLC
"	390	4	NOPLR
"	391	5	NOPLC
"	392	6	NOPLR
"	393	7	NOPLC
"	394	8	NOPLC
"	395	9	EMISC
"	396	10	EMPLC
"	397	11	EMPLR
"	398	12	EMISC
"	399	13	EMPLC
"	400	14	EMISC
"	401	15	EMILR
"	402	17	EMILR
"	403	18	EMILR
"	404	19	EMILC
"	405	20	EMILR
"	406	21	EMILR
"	407	22	EMILC
"	408	23	EMINR
"	409	24	EMINR
"	410	25	FPPIC
"	411	26	FPPILR
"	412	27	FPPIC
"	413	28	FPPIC
"	414	29	FPPIC
"	415	30	FPPSC
"	416	31	FPPSC
"	417	32	FPPIC
-FA	418	1	BPPSC
"	419	2	BPPSC
"	420	3	BPPSR
"	421	4	BPPIC
"	422	5	BPPILR
"	423	6	BPPIC
"	424	7	BPPILR
"	425	8	EMPRC
"	426	9	EMPLR
"	427	10	BCISC
"	428	11	BCISC
"	429	12	BCISC

WANTLE ON SULPHIDE.

F-27A

F-1

F-13

"	430	13	BNPLR
"	431	14	BNPLC
"	432	15	FCISC
"	433	16	BNPLC
"	434	1	FPPLR
"	435	2	FPPLC
"	436	3	FNPLZ
"	437	4	FPPLZ
"	438	5	FPPSC
"	439	6	FPPSC
"	440	7	FPPIC
"	441	8	FPPNR
"	442	9	FHPIC
"	443	10	FCISC
"	444	11	FCISC
"	445	12	FHPIC
"	446	13	FNPLC
"	447	14	FCISC
"	448	15	FCISC
"	449	16	FHISC
"	450	1	FOPSC
"	451	2	FOPSC
"	452	3	FNPLC
"	453	4	FNPLC
"	454	5	FNPLC
"	455	6	FNPLC
"	456	7	FNISC
"	457	8	FNISC
"	458	9	FPPSC
"	459	10	FNPLC
"	460	11	FSPSC
"	461	12	FSPIC
"	462	13	FSPIC
"	463	14	FSPIC
"	464	15	FSPSC
"	465	16	FSPSC
"	466	17	FSPSC
"	467	18	FSPIC
"	468	19	FPPIC
"	469	20	FPPNR
"	470	21	FPPSC
"	471	22	FPPIC
"	472	23	FPPIC
"	473	24	FPPNR
"	474	25	FPPSC
"	475	26	FPPNR
"	476	1	FOPIC
"	477	2	FOPIC
"	478	3	FOPSC
"	479	4	FNISC
"	480	5	FNISC
"	481	6	FNISC
"	482	7	FNPLC
"	483	8	FNPLC
"	484	9	FNPLC
"	485	10	FNISC
"	486	11	FNISC
"	487	12	MIXTURE OF X/LT SYMPLECTITE?
"	488	13	FCISC
"	489	14	FPPSC
"	490	15	FPPSC

"	491	16	FPFSC
"	492	17	FPPLR
"	493	18	FPPLZ
"	494	19	FPPLC
"	495	20	FPPLC
"	496	21	FPPLZ
"	497	22	FPPLR
IBC	498	1	NSPLC
"	499	2	NSPLC
"	500	3	NSPLC
"	510	4	NSPLC
"	502	5	NSPSC
"	503	6	NSPSC
"	504	7	NSPLC
"	505	8	NSPSC
"	506	9	NSPLC
"	507	10	NSPLC
"	508	11	NSPLC
"	509	12	NSPLC
"	510	13	NSPSC
"	511	14	NSPSC
"	512	15	NSPSC
"	513	16	NSPSC
"	514	17	NSPLC
"	515	18	NCISC
"	516	19	NPILC
"	517	20	NPILR
FEP-2	518	1	Pognatite.cpx
"	519	2	"
"	520	3	"
"	521	4	"
1-7A	522	1	NPPLR
"	523	2	NPPLC
"	524	3	NPPLR
"	525	4	NPPLC
"	526	5	NCILC
"	527	6	NCILR
"	528	7	NCISC
"	529	8	NPILC
"	530	9	NPPLC
"	531	10	NPPLC
"	532	11	NPPLC
"	533	12	NPPLZ
"	534	13	NPPLR
"	535	14	NPPLC
"	536	15	NPPLZ
"	537	16	NPPLR
1-11	538	1	NPPLC
"	539	2	NPPLC
"	540	3	NPPLC
"	541	4	NPPLC
"	542	5	NCISC
"	543	6	NPPLR
"	544	7	NCISC
"	545	8	NCISC
"	546	9	NPPLC
"	547	10	NPPLZ
"	548	11	NPPLR
"	549	12	NPPLC
"	550	13	NPPLC
"	551	14	NPPLZ

"	552	15	BPPLZ
"	553	16	BPPLR
B-23	554	17	SULPHIDE
"	555	1	BHPLC
"	556	2	BHPLR
"	557	3	LCISC
"	558	4	DNPLC
"	559	5	BHPLR
:	560	6	BHPLC
"	561	7	DNPLR
"	562	8	DCISC
"	563	9	BPPHC
"	564	10	BPPHZ
"	565	11	BPPMR
"	566	12	BPPSC
"	567	13	BPPSC
"	568	14	BPPLC
"	569	15	BPPLZ
"	570	16	BPPLR
B-13	571	1	BHPHC
"	572	2	BHPHC
"	573	3	BHPHC
"	574	4	BHPHC
"	575	5	DCISC
"	576	6	DCISC
"	577	7	BHPHC
"	578	8	DCISC
"	579	12	BPPHC
"	580	13	BPPHZ
"	581	14	BPPMR
"	582	15	BPPSC
"	583	16	BPPSC
"	584	17	BPPLC
"	585	18	BPPLZ
"	586	19	BPPLR
B-28	587	1	BPPLC
"	588	2	BPPLZ
"	589	3	BPPLZ
"	590	4	BPPLR
"	591	5	BPPSC
"	592	6	BPPSR
"	593	7	BPPLC
"	594	8	BPPLZ
"	595	9	BPPLZ
"	596	10	BPPLZ
"	597	11	BPPLR
"	598	12	BHINC
"	599	13	BHINC
"	600	14	DCINC
"	601	15	BHPLC
"	602	16	LCISC
"	603	17	BHINC
"	604	18	BHINC
B-31	605	1	BPPLC
"	606	2	BPPLZ
"	607	3	BPPLZ
"	608	4	BPPLZ
"	609	5	BPPLZ
"	610	6	BPPLR
"	611	7	BPPLC
"	612	8	BPPLC

"	613	9	BPPLC
"	614	10	BPPLZ
"	615	11	BPPLR
"	616	12	BHPIC
"	617	13	BHINC
"	618	14	BCINC
"	619	15	BCISC
"	620	16	BCINR
"	621	17	BCINC
"	622	18	BHPIC
"	623	19	BHINR
B-3	624	1	BHPLC
"	625	2	BHPLC
"	626	3	BHPLR
"	627	4	BHPNR
"	628	5	BHPIC
"	629	6	BCISC
"	630	7	BCINC
"	631	8	BHPSC
"	632	9	ODD OPAQUE
"	633	10	BSPIC
"	634	11	BPILC
"	635	12	BPILR
"	636	13	BPILC
"	637	14	BPILC
"	638	15	BPILR
"	639	16	BPILC
"	640	17	BPILR
"	641	18	BPILR
P-20	642	1	BCINC
"	643	2	BCISC
"	644	3	BHISC
"	645	4	BHISC
"	646	5	BHISC
"	647	6	BHISC
"	648	7	BHISC
"	649	8	BHISC
"	650	9	BPPLC
"	651	10	BPPLZ
"	652	11	BPPLR
"	653	12	BPPSC
"	654	13	LPPLC
"	655	14	BPPLZ
"	656	15	BPPLR
"	657	16	BPISC
"	658	17	BPILC
"	659	1	BHPLC
"	660	2	BHINC
"	661	3	BCINC
"	662	4	BHINC
"	663	5	BCINC
"	664	6	BHINC
"	665	7	BCINC
"	666	8	BPPLC
"	667	9	BPPLC
"	668	10	BPPLR
"	669	11	BPPLC
"	670	12	BPPNR
"	671	13	BPPNR
"	672	14	BPPLC
"	673	15	BPPLZ

"	674	10	BPPLR
"	675	1	BPPLC
"	676	2	BHINC
"	677	3	BCI..C
"	678	4	LMI..C
"	679	5	FCI..C
"	680	6	BHISC
"	681	7	BCI..C
"	682	8	FCI..C
"	683	9	BHINC
"	684	10	BHINC
"	685	11	BCISC
"	686	12	BPPLC
"	687	13	BPPSC
"	688	14	BPPSC
"	689	15	BPPZH
"	690	16	BPPLC
"	691	17	LPPSC
"	692	18	BPPSC
"	693	19	BPPHC
"	694	20	BPPHC
B-15	695	1	BHINC
"	696	2	BHINC
"	697	3	BCI..A
"	698	4	BCI..C
"	699	5	LCISC
"	700	6	BHISC
"	701	7	BHINC
"	702	8	BHINC
"	703	9	BHINC
"	704	10	BSPSC
"	705	11	BHISC
"	706	12	BHISC
"	707	13	BPPHC
"	708	14	BPPHZ
"	709	15	BPPHR
"	710	16	BPPLC
"	711	17	BPPLZ
"	712	18	BPPLR
"	713	19	BPPSC
"	714	20	BPPSC
B-1	715	1	FHINC
"	716	2	FHINC
"	717	3	FCISC
"	718	4	FCISC
"	719	5	FCISC
"	720	6	FCISC
"	721	7	FHISC
"	722	8	FHINC
"	723	9	FPPHC
"	724	10	FPPHC
"	725	11	FPP..A
"	726	12	FPPSC
"	727	13	FPPSC
"	728	14	FPPHC
"	729	15	FPP..A
"	730	16	FPP..A
"	731	17	FPP..C
"	732	18	FPP..Z
"	733	19	FPP..E
F-7	734	1	FPP..C

"	735	2	FHPLC
"	736	3	FHPLC
"	737	4	FHPLR
"	738	5	FCISC
"	739	6	FHISC
"	740	7	FHILC
"	741	8	FHISC
"	742	9	FPHMC
"	743	10	FPPHZ
"	744	11	FPPNR
"	745	12	FPPSC
"	746	13	FPPSR
"	747	14	FPPMC
"	748	15	FPPNR
"	749	16	FPPSC
F-15	750	1	FHPMC
"	751	2	FHPSC
"	752	3	FHPLC
"	753	4	FCISC
"	754	5	FCISC
"	755	6	FHILC
"	756	7	FHILC
"	757	8	FCINC
"	758	9	FCISC
"	759	10	FCINC
"	760	11	FPPSC
"	761	12	FPPSC
"	762	13	FPPHC
"	763	14	FPPHZ
"	764	15	FPPNR
"	765	16	FPPSR
"	766	17	FPPCR
"	767	18	FPPHC
"	768	19	FPPHZ
"	769	20	FPPLR
F-8	770	1	FHPLC
"	771	2	FHPLC
"	772	3	FHPLC
"	773	4	FHPSC
"	774	5	FCISR
"	775	6	FHISC
"	776	7	FCISC
"	777	8	FCISC
"	778	9	FCISR
"	779	10	FPPLC
"	780	11	FPPLZ
"	781	12	FPPLZ
"	782	13	FPPLR
"	783	14	FPPSC
"	784	15	FPPSC
"	785	16	FPPSC
"	786	17	FPPSC
"	787	1	EPILR
"	788	2	EPILR
"	789	3	EPILC
"	790	4	EPILF
"	791	5	EPILF
"	792	6	EPILC
"	793	7	EPILC
"	794	8	EPILR
"	795	9	EHPLR

"	795	10	BHPLC
"	797	11	BHPLR
"	798	12	BHPLC
"	799	13	BCESC
"	799	13	BCESC
"	800	14	BHPLC
"	801	15	BCISC
"	802	16	BHPLR
5-7	803	1	BHPLC
"	804	2	BCISR
"	805	3	BHPLC
"	806	4	BHPSC
"	807	5	BHPSC
"	808	6	BCISR
"	809	7	BHPIC
"	810	8	BCESC
"	811	9	BHPSC
"	812	10	BHISC
"	813	11	BHISC
"	814	12	ECISC
"	815	13	EPISC
"	816	14	BPPLC
"	817	15	BPPLZ
"	818	16	BPPLZ
"	819	17	BPPLC
"	820	18	BPPLZ
"	821	19	BPPLR
"	822	20	CIILC
"	823	21	BPPSC
5-26	824	1	BHPLC
"	825	2	LRPLC
"	826	3	BHPLR
"	827	4	BHPLR
"	828	5	BHILR
"	829	6	BHILC
"	830	7	BHILC
"	831	8	BHILC
"	832	9	BPPSC
"	833	10	EPPLC
"	834	11	BPPLR
"	835	12	BPPLC
"	836	13	BPPLZ
"	837	14	BPPLR
"	838	15	BPPLC
"	839	16	BPPLR
"	840	17	BIILC
"	841	18	BCISC
"	842	19	ECILC
"	843	20	BHILC
5-31	844	1	BHPLC
"	845	2	BHPLC
"	846	3	BCISC
"	847	4	LRPLC
"	848	5	ECILC
"	849	6	BHPLC
"	850	7	LRPLC
"	851	8	BCISC
"	852	9	BCISC
"	853	10	BPPLC
"	854	11	BPPLZ
"	855	12	BPPLZ

"	866	13	BPPLZ
"	867	14	BPPLZ
"	868	15	BPPLR
"	869	16	BPPNC
"	860	17	BPPSC
"	861	18	BPPLC
B-22	862	1	BHPLC
"	863	2	BHINC
"	864	3	BHISC
"	865	4	BCISC
"	866	5	BHPLC
"	867	6	BCINC
"	868	7	BCINC
"	869	8	BCISC
"	870	9	BCISC
"	871	10	BPPNC
"	872	11	BPPLC
"	873	12	BPPLZ
"	874	13	BPPLR
"	875	14	BPPLC
"	876	15	BPPLZ
"	877	16	BPPLR
"	878	17	BPPSC
B-19	879	1	BHILC
"	880	2	BHILC
"	881	3	BHINC
"	882	4	BCILC
"	883	5	BCILC
"	884	6	BCILC
"	885	7	BCILL
"	886	8	BHILC
"	887	9	BPPNC
"	888	10	BPPNZ
"	889	11	BPPLR
"	890	12	BPPLC
"	891	13	BPPLC
"	892	14	BPPLR
"	893	15	BPPNC
"	894	16	BPPLR
B-4	895	1	FCISC
"	896	2	FCISC
"	897	3	FCISC
"	898	4	FCISC
"	899	5	FHISC
"	900	6	FHISC
"	901	7	FHISC
"	902	8	FHILC
"	903	9	FCISC
"	904	10	FPPLC
"	905	11	FPPLZ
"	906	12	FPPLR
"	907	13	FPPNC
"	908	14	FPPNR
"	909	15	FPPLC
"	910	16	FPPLZ
"	911	17	FPPLR
"	912	18	FPPSC
"	913	19	FPPSC
B-30	914	1	NSPLC
"	915	2	NSPLR
"	916	3	NSPNC

"	917	4	NSPSP
"	918	5	NSPLC
"	919	6	NSPSC
"	920	7	NSPSC
"	921	8	NSPSC
"	922	9	NSPLC
"	923	10	NSPLC
"	924	11	NSPSC
"	925	12	NSPSC
"	926	13	NSPSC
"	927	14	NSPSC
"	928	15	NSPSC
"	929	16	NSPLC
"	930	17	NHPLC
"	931	18	NHPLC
"	932	19	NHPLC
"	933	20	NHPLC
"	934	21	NHPLC
"	935	22	NHPLC
"	936	23	NHPLC
"	937	24	NHISC
"	938	25	NPISC
"	939	26	NPISC
"	940	27	NPILC
"	941	28	NPILC
"	942	29	NPILC
"	943	30	NPILC
"	944	31	NPILC
"	945	32	NPILC

APPENDIX THREE: X-Ray Fluorescence Spectrometry

A Phillips PW 1410 semi-automatic X-ray fluorescence spectrometer was used for the determination of all major and trace elements using the standard techniques employed at Rhodes University. (Marsh, 1979). A variety of international and secondary (Rhodes) standards were used for calibration. The concentrations used were based on those recommended by Flanagan (1973).

The major elements, excluding Na, were analysed using the fusion method of Norrish & Hutton (1969). Na was analysed on pressed powder briquettes.

All the trace elements were determined on briquettes. Full corrections were made for instrumental drift, dead-time, background, tube and spectral line interferences. Matrix effects were corrected using the mass absorption coefficients calculated from the major elements using Heinrich's (1966) values. Where major elements were not available the Mo-Compton method (Reynolds, 1967 and Nesbitt et al., 1976) was used to determine the mass absorption coefficients.

Rb and Sr concentrations used to calculate initial $^{87}\text{Sr}/^{86}\text{Sr}$ ratios were determined using the Mo-tube (as it is the most efficient for exciting Rb and Sr) and extended counting times. The counting times were 400secs on the Rb peak and 200 secs on the Sr peak. The Rb backgrounds were counted for 200 secs and Sr backgrounds for 100 secs.

Typical running conditions and instrumental settings used in the laboratory are listed in Marsh (1979) and reproduced with permission below. (Tables A2:1, A2:2 & A2:3).

Table A3:1 Typical Instrumental Settings for Major Element Analyses

Element	Mn	Fe	Ti	Ca	K	Si	Al	Mg	P	
Crystal	LiF 200	-----				PET	-----		TlAP	Ge
Collimator	Coarse	Fine	F	F	F	C	C	F	C	
Angle	63.08	57.53	86.19	113.16	136.79	109.20	145.20	45.18	141.11	
Threshold	200	-----						250	380	
Window	350	-----						300	440	
Filter	In	Out	-----							
Count Time	20	20	10	10	10	40	40	200	40	

All analyses carried out using a Chromium tube energised at 50KV and 40mA.

Attenuation set at 2¹. Analyses carried out with the Vacuum ON.

Table A3:2 Sodium Analysis

KV	mA	Counter	Collimator	Crystal	E	E	Att	Peak	Background
55	40	Flow EHT=553	Fine	TlAP	150	400	2 ¹	200secs @ 55.13°	100secs @ 57.00°

Table A3:3 Standard Instrumental Settings for Trace Element Analyses

Element	Line	Tube	Holder	Crystal	Vacuum	Collimator	Counter
Nb	K _a	W	W	LiF 220	No	Fine	Scint.
Zr	"	"	"	"	"	"	"
Y	"	"	"	"	"	"	"
Sr	"	Mo, W	"	"	"	"	"
Rb	"	"	"	"	"	"	"

Zn	K _a	Mo	Al	"	Yes	"	Flow + Scint.
Cu	"	"	"	"	"	"	" " "
Ni	"	"	"	"	"	"	" " "

Co	"	W	W	"	"	"	Flow
Cr	"	"	"	"	"	"	"
V	"	"	"	"	"	"	"

Ba	L _{b2}	Cr	W	"	"	"	"

Sc	K _a	"	"	LiF 200	"	"	"
=====							

APPENDIX FOUR: Mineral Separations

The sample was prepared by crushing and sieving. The fraction between 72# and 150# was retained, washed to remove the fines, rinsed in distilled water and dried at 110°C before separation.

An electromagnetic separator was used to separate orthopyroxene, clinopyroxene and plagioclase. The technique adopted was to separate first the mineral with the highest magnetic susceptibility and then those with lower values. A trial and error approach was adopted initially to establish the optimum inclination and sideways tilt of the separator (25-30° and 10-15° respectively) and the best feed rate. The current was progressively increased so that only the pure high susceptibility fraction was removed at each stage. The optimum current was determined by inspection of the separated fraction under a binocular microscope.

Orthopyroxene: A very pure separate was easily obtained. Purity was estimated at >98% (Visual estimate).

Clinopyroxene: Less pure separates of this phase were obtained as the magnetic susceptibility is between that of orthopyroxene and that of plagioclase. Nevertheless purity was estimated at ±95% or better.

Plagioclase: Extremely pure separates (>99%) were easily obtained. The only contamination of note would be alkali feldspar and quartz, both of which may occur in very small quantities in the rocks and could not be removed.

IPL Refers to interstitial plagioclase from pyroxenite.

PL No differentiation between cumulus and intercumulus.

CPL Cumulus plagioclase derived from pyroxene mottles of mottled anorthosite. The mottled material was hand picked from coarse crushes (1cm) before final crushing and separation.

MP Non-mottle plagioclase. Pure plagioclase almost devoid of interstitial pyroxene derived from the same samples as the CPL fraction.

APPENDIX FIVE: Sampling

Sampling was carried out underground in cross-cuts, drives and stopes of the Rustenburg Platinum Mine (Rustenburg Section). All the F-samples were obtained from the Frank Shaft area (23 Y-cut ill.) sampling up from the Boulder bed to the Merensky pegmatoid. The H-samples were also obtained from the Frank Shaft area (15 level haulage), sampling upward from the Merensky pegmatoid to the Bastard pyroxenite.

The L-samples were obtained from the Paardekraal Shaft (12 level X-cut S). The RR- (Rolling Reef area) samples were obtained from "6" level of Townlands No. 1 Incline. The P-samples are from stope faces in the Frank Shaft "10" level area.

The vertical distances between samples were carefully measured with respect to laterally continuous markers as well as calculated where vertical distances could not be directly measured. The error in the vertical dimension is less than 30cm in the case of F-, RR- and H-samples and about 50cm in the case of P-samples where control markers are less well established. In the upper part of the Bastard unit (L-20 to L-30) the error could be slightly greater as the dips are low and could not be accurately measured and there was a lack of suitable markers.

Large samples, in general measuring about 20x20x20 cm. were taken and in some cases the size of the samples allowed continuous sampling with respect to height.